A Clinicopathological Study of Inclusion Body Myositis

by

Stefen Brady

Keble College, University of Oxford

A thesis submitted for the degree of Doctor of Philosophy in Clinical Neurosciences

Trinity term 2013

A Clinicopathological study of Inclusion Body Myositis

Stefen Brady, Keble College

A thesis submitted for the degree of Doctor of Philosophy, Trinity term 2013

ABSTRACT

Sporadic inclusion body myositis (IBM) is the commonest acquired myopathy in individuals aged over 50 years. Currently, diagnosis is based largely upon specific muscle biopsy findings, though these are thought to lack sensitivity. More recently, many abnormal protein aggregates have been described in IBM and some have been proposed as diagnostic markers. However, their diagnostic utility is untested and how they relate to the pathogenesis is uncertain.

The clinical characteristics, pathological findings and disease course in 67 patients with histopathologically diagnosed and clinically diagnosed IBM were compared and revealed that patients with IBM have a characteristic pattern of weakness at presentation that is independent of the pathological findings. Current diagnostic pathological features are more common in older patients and therefore may be linked to disease duration.

The pathology of IBM and the diagnostic utility of protein aggregates in IBM were studied in six clinicopathologically typical cases of IBM. Protein aggregates immunoreactive for p62, TDP-43, myotilin, α B-crystallin and ubiquitin were more abundant than the current diagnostic pathological features. The diagnostic potential of these pathological features was then assessed in pathologically typical and atypical IBM and controls. This revealed that staining for p62, MHC Class I, CD8 positive lymphocytes and mitochondrial abnormalities could support the diagnosis and should be included in diagnostic criteria for IBM.

Laser microdissection and label-free mass spectrometry were used to validate the histological findings. The presence of nuclear and aggresomal proteins in rimmed vacuoles indicated that they are derived from myonuclei. Increased protein synthesis and ER stress suggest that abnormal protein aggregates may be the result of abnormal protein production.

In conclusion, this thesis emphasises that a diagnosis of IBM can be confidently made on clinical grounds, with a supportive muscle biopsy. The histological and proteomic findings reveal that there is a spectrum of pathological features most likely associated with the disease duration and that adherence to the current pathological based diagnostic criteria may have led to some erroneous conclusions about the pathogenesis of this enigmatic disease.

PUBLICATIONS RELATED TO THIS THESIS

Chapter 3 is pre-copyedited author-produced version of an article accepted for publication in the Journal of Neurology, Neurosurgery and Psychiatry following peer review. The definitive publisher-authenticated version: Brady S., Squier W., Hilton-Jones D. (2013). Clinical assessment determines the diagnosis of inclusion body myositis independently of pathological features. Journal of Neurology Neurosurgery and Psychiatry *84*,1240-1246.

Chapters 4 and 5 are pre-copyedited author-produced version of an article accepted for publication in BMJ Open following peer review. The definitive publisher-authenticated version: Brady S., Squier W., Sewry C., Hanna M., Hilton-Jones D., Holton J.L. (2014). A retrospective cohort study identifying the principal pathological features useful in the diagnosis of inclusion body myositis. BMJ Open 4:e004552 is available online at http://bmjopen.bmj.com/content/4/4/e004552.long

TABLE OF CONTENTS

ABSTRACT ii

PUBLICATIONS RELATED TO THIS THESIS iii

TABLE OF CONTENTS iv

LIST OF TABLES x

LIST OF FIGURES xii

LIST OF ABBREVIATIONS xiv

Chapter 1

1.1 Introduction 1

1.2 Clinical features of IBM 3

1.2.1 Demographics 3

1.2.2 Disease specific pattern of weakness 3

1.2.3 Disease progression and disability 5

1.2.4 Response to treatment 6

1.3 Pathology of IBM 8

1.3.1 Diagnostic pathological features 9

1.3.2 Protein aggregates and mitochondrial changes 14

1.4 Biomarkers 22

1.5 Pathogenesis 22

1.5.1 Inflammation 23

1.5.2 Myonuclear degeneration 24

1.5.3 Autophagy 25

1.5.4 Endoplasmic reticulum stress 27

1.5.5 Ubiquitin-proteasome system 28

1.6 Diagnostic criteria 28

1.7 Patients with clinical features of IBM but non-diagnostic biopsies 30
1.7.1 Clinical features 31
1.7.2 Disease progression 33
1.7.3 Pathological features 33
1.8 Concluding remarks 34
1.9 Hypotheses 36
1.10 Aims 36

Chapter 2

2.1 General points 37
2.2 Clinical characteristics of patients 37
2.2.1 IBM Cases 37
2.2.2 Control cases 39
2.2.3 Statistical analysis 39
2.3 Pathological description of IBM 41
2.3.1 Cases 41
2.3.2 Tissue preparation and staining 41
2.3.3 Definitions and quantification 48
2.3.4 Statistical analyses 51
2.4 Assessment of pathological biomarkers in IBM and disease controls. 51
2.4.1 Cases 51
2.4.2 Tissue staining 55
2.4.3 Definitions and quantification 55
2.4.4 Statistical analysis 56
2.5 Proteomic analysis of IBM muscle 57
2.5.1 Cases 57
2.5.2 Detection of rimmed vacuoles and immunofluorescent aggregates 57

2.5.3 IF staining 57
2.5.4 Laser capture microscopy 57
2.5.5 Protein digestion 59
2.5.6 High-performance liquid chromatography and tandem mass spectrometry 59
2.5.7 Data processing 60
2.5.8 Data analysis 60

Chapter 3

3.1 Introduction 61
3.2 Hypothesis 62
3.3 Aims 62
3.4 Methods 62
3.5 Results 63
3.5.1 Demographics 63
3.5.2 Presentation and associated conditions 66
3.5.3 Pattern and distribution of weakness in IBM 66
3.5.4 Investigations 69
3.5.5 Immunosuppression 71
3.5.6 Disability 71
3.5.7 Comparison of the pattern of weakness observed in IBM and disease controls 73
3.5.8 Diagnostic criteria 81
3.6 Discussion 82
3.6.1 Previous studies 82
3.6.2 The clinical picture is sensitive and specific independently of the pathological features 84
3.6.3 Pathological features are associated with disease duration 84
3.6.4 Disease progression is independent of pathological features 85
3.6.5 Inclusion of the clinical examination in future diagnostic criteria 86

3.6.6 Study limitations 86
3.6.7 Final comments 87

Chapter 4

4.1 Introduction 88
4.2 Hypothesis 89
4.3 Aims 89
4.4 Methods 90
4.5 Results 90
4.5.1 Clinical characteristics of IBM and control patients 90
4.5.2 Optimisation of primary antibodies and conditions 92
4.5.3 Alkalinised Congo red staining and thioflavin S staining are more sensitive than crystal violet for identifying amyloid in AD 92
4.5.4 Intra-observer reliability was good 92
4.5.5 Histological and pathological findings in IBM and normal control muscle 95
4.6 Discussion 112
4.6.1 Previous studies 113
4.6.2 Protein aggregates identified with IHC are more sensitive than the current diagnostic pathological features in IBM 114
4.6.3 Congophilic deposits as opposed to amyloid are present in IBM 115
4.6.4 The inflammatory changes in IBM resemble those reported in PM 116
4.6.5 Possible disease mechanisms inferred from IHC findings 116
4.6.6 Study limitations 118
4.6.7 Final comments 119

Chapter 5

5.1 Introduction 120

5.2 Hypothesis....121
5.3 Aims....122
5.4 Methods....122
5.5 Results....123
5.5.1 Clinical characteristics....123
5.5.2 Quantitative assessment of protein aggregates and mitochondrial changes....123
5.5.3 Diagnostic utility of protein aggregates and mitochondrial changes....129
5.5.4 Qualitative assessment of protein aggregates....133
5.5.5 Immunological characteristics of IBM....138
5.5.6 Clinicopathological correlation....145
5.6 Discussion....145
5.6.1 Previous studies....146
5.6.2 Diagnostic utility of pathological features in IBM....147
5.6.3 Pathological findings in IBM+RV and IBM–RV indicate a common pathogenesis....150
5.6.4 Study limitations....151
5.6.5 Final comments....151

Chapter 6

6.1 Introduction....153
6.2 Hypothesis....154
6.3 Aims....154
6.4 Methods and technical approaches....154
6.5 Results....155
6.5.1 Clinical characteristics of IBM patients....155
6.5.2 Optimisation of PET membrane staining....155
6.5.3 Workflow....158
6.5.4 Protein composition of IBM samples is homogeneous....161

6.5.5 Greater variety of proteins are present in RV and N than ST 161
6.5.6 Markers of ER stress are up-regulated in IBM 161
6.5.7 Differentially expressed proteins between samples 163
6.5.8 GO annotations analysis of proteomics data 167
6.6 Discussion 173
6.6.1 Previous studies 174
6.6.2 Rimmed vacuoles contain nuclear membrane proteins 175
6.6.3 Increased protein expression leads to aggresome formation 177
6.6.4 Proteomic studies support IHC findings 178
6.6.5 Study limitations 179
6.6.6 Final comments 180

Chapter 7

7.1 Overview of results 182
7.2 Future directions 185
7.2.1 Elucidation of the protein composition of 'normal' fibres in IBM 186
7.2.2 Altered protein synthesis or disordered degradation 186
7.3 Concluding remarks 187

REFERENCES 188
APPENDICES 212
ACKNOWLEDGEMENTS 219

LIST OF TABLES

Table 1.1 Proteins reported in IBM 15

Table 1.2 Summary of studies characterising patients with clinical features suggestive of IBM but who lack diagnostic pathological features of IBM 32

Table 2.1 Pathological definitions 40

Table 2.2 Commercial antibodies tested 42

Table 2.3 Definitions of pathological features 50

Table 2.4 Clinical and pathological inclusion criteria 54

Table 2.5 Primary antibodies and conditions for IF staining 58

Table 3.1 Revised 2011 ENMC diagnostic criteria for IBM 64

Table 3.2 Demographic characteristics of the groups analysed 65

Table 3.3 Patterns of weakness included in current diagnostic criteria assessed at first presentation 68

Table 3.4 Serum CK and muscle biopsy findings 70

Table 3.5 Pathological features dependant on the site and strength of the muscle biopsied 72

Table 3.6 Multivariate analysis of the influence of clinical and pathological features on disability outcomes 78

Table 3.7 Clinical characteristics in IBM and control patients 79

Table 3.8 Pattern of weakness observed in IBM and control patients at first presentation 80

Table 4.1 Clinical characteristics of IBM patients and control cases 91

Table 4.2 Antibodies and optimum conditions 93

Table 4.3 Pattern of immunoreactivity in normal muscle and the cellular location of protein aggregates in IBM 97

Table 5.1 Clinical characteristics 124

Table 5.2 Comparison of the proportion of positive cases in each group 134

Table 5.3 Morphology of p62 aggregates in each group 136

Table 5.4 Patterns of MHC Class I staining in IBM, PM&DM and PAM+RV 140

Table 5.5 Location and severity of the inflammatory infiltrate assessed using the semi-quantitative score tool and the proportion of cases with fibres undergoing partial invasion 144

Table 6.1 Clinical characteristics of IBM patients 156

Table 6.2 The number of proteins common to samples from each area 162

Table 6.3 Proteins increased in RV compared to N 164

Table 6.4 Proteins increased in RV compared to ST 165

Table 6.5 Proteins increased in ST compared to N 166

LIST OF FIGURES

Figure 2.1 Depiction of stereological assessment of tissue sections using ImagePro 6.2 49

Figure 2.2 Stereological assessment of a tissue section 52

Figure 2.3 Modified inflammatory score tool 53

Figure 3.1 Distribution and severity of weakness at presentation 67

Figure 3.2 Probability of remaining independent of a walking aid over time 74

Figure 3.3 Probability of remaining independent of a wheelchair over time 76

Figure 4.1 Intra-observer agreement 96

Figure 4.2 p62 immunoreactivity 99

Figure 4.3 TDP-43 immunoreactivity 100

Figure 4.4 α B-crystallin immunoreactivity 101

Figure 4.5 Myotilin immunoreactivity 102

Figure 4.6 Ubiquitin immunoreactivity 103

Figure 4.7 Percentage of fibres containing protein aggregates and the Griggs diagnostic pathological features in IBM 104

Figure 4.8 Alkalinised Congo red staining visualised under fluorescent light 106

Figure 4.9 Emerin and lamin A/C immunoreactivity 107

Figure 4.10 MHC Class I staining in normal muscle and IBM 109

Figure 4.11 Median number of inflammatory cells in IBM and normal muscle 110

Figure 4.12 Partial invasion in IBM 111

Figure 5.1 Percentage of fibres containing protein aggregates and diagnostic pathological findings in IBM+RV 126

Figure 5.2 Percentage of fibres containing protein aggregates and COX-/SDH+ fibres in each group 127

Figure 5.3 Optimum sensitivity and specificity of rimmed vacuoles, protein aggregates and COX-/SDH+ fibres in IBM+RV compared to PAM+RV 130

Figure 5.4 Optimum sensitivity and specificity of rimmed vacuoles, protein aggregates and COX-/SDH+ fibres in IBM-RV compared to PM&DM 132
Figure 5.5 Patterns of p62 immunoreactivity observed in IBM and disease controls 135
Figure 5.6 Morphology of myotilin aggregates in IBM and disease controls 137
Figure 5.7 Fluorescent Congophilic aggregates in IBM+RV and PAM+RV 139
Figure 5.8 MHC Class I staining in normal muscle and IBM 141
Figure 5.9 Severity and distribution of the inflammatory infiltrate 143
Figure 5.10 Proposed diagnostic algorithm for IBM based on pathological findings 149
Figure 6.1 IF staining of muscle tissue on standard glass and PET membrane slides to demonstrate protein aggregates 157
Figure 6.2 Workflow applied to muscle samples 159
Figure 6.3 Up-regulated biological processes between samples 169
Figure 6.4 Over-represented biological processes between samples 171
Figure 6.5 Proposed pathogenesis of IBM and the associated pathological features 181

LIST OF ABBREVIATIONS

2DGE	Two dimensional gel electrophoresis
Aβ	β Amyloid
AD	Alzheimer's disease
AH	Ancestral haplotype
ApoE	Apolipoprotein E
APP	Amyloid precursor protein
ATP	Adenosine triphosphate
BACE 1	β-Secretase 1
BACE 2	β-Secretase 2
Bcl-2	B-cell lymphoma 2 protein
BiNGO	Biological Networks Gene Ontology
BMD	Becker muscular dystrophy
BSA	Bovine serum albumin
CBD	Corticobasal degeneration
CD	Cluster of differentiation protein
CK	Creatine kinase
COX	Cytochrome c oxidase
COX/SDH	Combined cytochrome c oxidase and succinate dehydrogenase
COX-/SDH+	Cytochrome c oxidase negative and succinate dehydrogenase positive
DAB	3,3'-Diaminobenzidine
DM	Dermatomyositis
DNA	Deoxyribonucleic acid
DMRV	Hereditary distal myopathy with rimmed vacuoles
EM	Electron microscopy
ENMC	European Neuromuscular Centre

EOR	Endoplasmic reticulum overload response
ER	Endoplasmic reticulum
FA	Formic acid
FDR	False discovery rate
FITC	Fluorescein isothiocyanate
FTLD-FUS	Frontotemporal lobar degeneration with FUS positive inclusions
FTLD-TDP	Frontotemporal lobar degeneration with TDP-43 positive inclusions
FUS	Fused in sarcoma protein
H&E	Haematoxylin and eosin
HC	Histochemical
hIBM	Hereditary inclusion body myopathy
HSP	Heat shock protein
GO	Gene ontology
Grp78	78 KDa Glucose-regulated protein
Grp94	94 KDa Glucose-regulated protein
HPLC	High performance liquid chromatography
HRP	Horseradish peroxidase
IBM	Sporadic inclusion body myositis
IBM-C	Clinically diagnosed IBM
IBM-IS	IBM patients not treated with immunosuppressive medication
IBM+IS	IBM patients treated with immunosuppressive medication
IBM-P	Pathologically diagnosed IBM
IBM-RV	IBM without rimmed vacuoles on muscle biopsy
IBM+RV	IBM with rimmed vacuoles on muscle biopsy
IBMPFD	Inclusion body myopathy with Paget’s disease and frontotemporal dementia
IF	Immunofluorescence
IHC	Immunohistochemistry

IIM	Idiopathic inflammatory myopathy
IPI	International Protein Index
κ	Cohen kappa statistic
LC3	Microtubule-associated protein 1A/1B-light chain 3
LCM	Laser capture microscopy
LR	Likelihood ratio
MFM	Myofibrillar myopathy
MHC Class I	Major histocompatibility complex class I
MND	Motor neuron disease
MRC	Medical Research Council
mRNA	Messenger ribonucleic acid
MS	Mass spectrometry
MS/MS	Tandem mass spectrometry
N	Normal muscle fibres or sarcoplasm from morphologically normal fibres
NBR1	Neighbour of BRCA 1 gene 1
NF-κB	Nuclear factor κ-light-chain-enhancer of activated B cells
NIGMS	National Institute of General Medical Sciences
OPMD	Oculopharyngeal muscular dystrophy
p62	Sequestosome 1
PAM	Protein accumulation myopathies
PAM+RV	Protein accumulation myopathies with rimmed vacuoles on muscle biopsy
PBS	Phosphate buffered saline
PD	Parkinson's disease
PERK	Protein kinase RNA-like endoplasmic reticulum kinase
PET	Polyethylene terephthalate
PFA	Paraformaldehyde
PM	Polymyositis

PM&DM	Steroid-responsive inflammatory myopathies
PrP	Prion protein
QSBB	Queen Square Brain Bank for Neurological Disorders
RNA	Ribonucleic acid
ROC	Receiver operating characteristic
ROS	Reactive oxygen species
RT	Room temperature
RV	Rimmed vacuoles, their contents and the immediate surrounding sarcoplasm
SI	Spectral index
ST	Non-vacuolated sarcoplasm from fibres containing rimmed vacuoles
TDP-43	Transactivation response DNA binding protein 43
TRIS	Tris(hydroxymethyl)aminomethane
UBB^{+1}	Mutant ubiquitin
UK	United Kingdom
UPR	Unfolded protein response
UPS	Ubiquitin-proteasome system
VCP	Valosin containing protein

Chapter 1

INTRODUCTION

1.1 Introduction

The first description of sporadic inclusion body myositis (IBM) and some of the pathological features which have become synonymous with the diagnosis was published in 1967 (Chou, 1967). Chou described a 66 year old man with a six year history of progressive proximal weakness and dysphagia. Muscle biopsy revealed 10-30 nm tubulofilaments, membranous bodies and abnormal mitochondria in addition to changes typical of polymyositis (PM). The filaments were likened to viral particles and a viral aetiology was proposed for chronic PM. Initially, IBM was not readily accepted as a disease entity by the medical community. Because of its clinical and pathological similarities to PM, namely proximal limb weakness and inflammatory infiltration on muscle biopsy it was considered to be a form of chronic PM poorly responsive to immunosuppressive treatment. In a further case report in 1971, eosinophilic inclusions were found to contain abnormal filaments on electron microscopy (EM) and led to coining of the term IBM (Yunis and Samaha, 1971). With the recognition of specific clinical and pathological features associated with the IBM it was finally accepted as a separate disorder in the late 1970s.

Clinicopathological findings in six cases of IBM confirmed that the disease shared some similarities with PM and dermatomyositis (DM) and it was proposed that it should be similarly classified as an idiopathic inflammatory myopathy (IIM). When compared to PM and DM, IBM was noted to have additional pathological features these being rimmed vacuoles, 15-18 nm tubulofilaments and amyloid. Clinical differences were also noted, with IBM pursuing a slowly progressive course often with asymmetric weakness and early weakness of the long finger flexor and knee extensor muscles; IBM also demonstrated resistance to current immunosuppressive treatment (Amato et al., 1996)(Benveniste et al., 2011). Despite these noteworthy clinical

differences between IBM and PM and DM, successive diagnostic criteria for IBM focussed on the pathological findings which were thought to be both highly specific and sensitive.

Increasingly, it is recognised that patients with the characteristic pattern of weakness associated with IBM (predominant finger flexor and knee extensor weakness) may lack the pathological features included in the diagnostic criteria. However, the diagnostic criteria have remained focussed on the pathological features and are largely responsible for the frequent initial misdiagnosis and subsequent inappropriate treatment of many patients with IBM (Sayers et al., 1992)(Badrising et al., 2000)(Felice and North, 2001)(Needham et al., 2008a)(Benveniste et al., 2011). A further consequence has been the exclusion of patients lacking the diagnostic pathological features from clinical studies. As a result, detailed clinical and research data on this group of patients is absent and conclusions drawn from studies to date about the aetiology and pathogenesis of IBM may be erroneous being solely based upon the findings in those patients with a 'full-house' of pathological features. Moreover, there is a suspicion that the diagnostic pathological features occur in advanced disease and are indicative of end-stage changes, and therefore patients without the fully developed pathological changes may be more amenable to therapeutic intervention.

Over the last two decades, accumulation of many different proteins has been reported in pathologically diagnosed IBM. Many of these, such as amyloid β (Aβ) and its precursor amyloid precursor protein (APP), α-synuclein, phosphorylated tau and prion protein (PrP), are more commonly associated with neurodegenerative diseases. These findings have led to analogies being drawn between IBM and neurodegenerative diseases such as Alzheimer's disease (AD). However, not all of these observations have been consistently and independently reproduced and therefore a clear understanding of the role of protein accumulation in the pathogenesis of IBM and their potential diagnostic role is unknown.

1.2 Clinical features of IBM

1.2.1 Demographics

IBM is a rare disorder, though it is now considered the commonest acquired myopathy in those older than 50 years of age. Its prevalence is estimated to be between 4.9 and 10.7 per million in Caucasian populations (adjusted to between 16.0 and 35.5 per million over the age of 50) (Badrising et al., 2000)(Felice and North, 2001)(Needham et al., 2008a). However, the incidence depends on the diagnostic criteria used and therefore may be significantly higher. Middle aged males are most commonly affected. The male-to-female ratio is typically two-to-one and the typical age at disease onset is in the late sixth and early seventh decades. The delay to diagnosis from symptom onset has remained unchanged over the last 25 years at approximately 5 years; 5.1 years in 1987 (Ringel et al., 1987) and 59 months in 2011 (Benveniste et al., 2011). The majority of this time is accounted for by patients delaying seeking medical advice but there is still a considerable delay from seeking medical advice until the diagnosis is reached (Badrising et al., 2000). Many patients are initially misdiagnosed. Case series have shown the rate of misdiagnosis to be between 31% and 86%. The most common alternative diagnoses are motor neuron disease, arthritis and PM.

1.2.2 Disease specific pattern of weakness

The case report that led to the disease name ironically described a patient who would not be recognised as suffering from IBM today; a 26-year-old female who had noticed weakness and muscle wasting since the age of 18. Examination revealed symmetrical wasting and weakness of the thigh adductor and abductor muscles, gluteus maximus and triceps without weakness of the quadriceps and near normal hand muscles (Yunis and Samaha, 1971). Subsequent case reports described patients that had a combination of dysphagia and limb weakness associated with a normal or moderately raised serum creatine kinase (CK) (Sato et al., 1971)(Jerusalem et al., 1972)(Hughes and Esiri, 1975)(Oteruelo, 1976). A number of different patterns of weakness were

described: generalised, quadriceps, distal weakness greater than proximal, proximal weakness greater than distal and asymmetric.

In the first case series reported (Carpenter et al., 1978), the authors commented on the marked involvement of the distal muscles. These findings were later disputed in a larger case series of 40 patients (Lotz et al., 1989). The picture was confused further by case reports of significant distal weakness in patients with PM (Sundaram and Ashenhurst, 1981)(Marconi et al., 1982). The explanation for these divergent observations was likely the reliance on the pathological features considered to be diagnostic of IBM without clinical correlation leading to the inclusion of patients without IBM and the misdiagnosis of IBM patients without a 'full-house' of pathological findings as PM. Patients with IBM can fulfil the Bohan and Peter diagnostic criteria for definite PM and therefore may have been included among these cases (Bohan and Peter, 1975a)(Bohan and Peter, 1975b). The presumed reliability of pathological features in isolation in IBM may have led to a delay in defining the characteristic pattern of weakness associated with IBM and resulted in early studies incorrectly reporting a bimodal distribution in the age at disease onset of IBM (Calabrese et al., 1987).

Knee extension weakness and the inability to make a fist in IBM were first reported by Calabrese *et al.* (Calabrese et al., 1987). Dalakas found finger flexor weakness to be an early feature of the disease; distal weakness, finger flexion and ankle dorsiflexion, was and detectable in 50% of patients at presentation (Dalakas, 1991). In a later review, Sekul and Dalakas reported that in their experience all IBM patients had distal weakness at the time of diagnosis, with weakness of the deep finger flexors of the third, fourth and fifth digits being specific and sensitive for IBM (present in 88% of patients) and asymmetric weakness occurring in a third of patients (Sekul and Dalakas, 1993). In their seminal paper, Griggs *et al.* stated that at least one of the following examination findings is necessary for a diagnosis of possible IBM: finger flexor weakness, wrist flexor weakness greater than wrist extensor or knee extensor weakness (Griggs et al., 1995). Amato *et al.*

retrospectively reviewed the pattern of weakness at presentation in 15 patients with pathologically definite IBM and other inflammatory myopathies (Amato et al., 1996). They found wrist flexor or finger flexor strength less than shoulder abductor strength and knee extensor weakness greater than hip flexor weakness was sensitive and specific for IBM. However, from ten subsequent case series only two have included any data on the pattern of weakness at presentation in IBM. These studies found finger flexor weakness to be present in 14 to 87.5% of cases and knee extensor weakness in 63 to 87.5% at presentation (Badrising et al., 2005)(Chahin and Engel, 2008). Dysphagia affects between 33 and 66% of patients (Sayers et al., 1992)(Sekul and Dalakas, 1993)(Badrising et al., 2005)(Needham et al., 2008a)(Benveniste et al., 2011). Barium swallow studies have shown the defect to be delayed initiation of swallowing and dysfunction of the lower pharyngeal muscles (Sekul and Dalakas, 1993). Facial weakness is reported in up to 41% of patients (Sekul and Dalakas, 1993)(Badrising et al., 2005)(Needham and Mastaglia, 2007); this is typically peri-orbital and mild (Badrising et al., 2005).

Although most experts believe that the pattern of weakness in IBM at presentation is highly characteristic, there is little data available to support this. A recent study reported involvement of knee extensors and deep finger flexors to be pathognomonic of IBM (Needham et al., 2008a). However, the clinical examination was not performed at presentation and the authors also reported there to be a considerable degree of phenotypic variability among patients. Two small imaging studies have confirmed the clinical findings detectable on examination but were shown to be less sensitive than the clinical examination in detecting the affected muscles (Sekul et al., 1997)(Phillips et al., 2001).

1.2.3 Disease progression and disability

Disease progression in IBM is typically slow. The first report of disease outcome described that six patients who were observed for more than 15 years all became severely incapacitated (Lotz et al., 1989). Sekul *et al.* reported that 71% of cases required a walking aid five years after symptom

onset and 60% required a wheelchair 10 years or more after symptom onset (Sekul and Dalakas, 1993). However, a further study found that only 7% of patients required a wheelchair or scooter after an average disease duration of 8.5 years (Badrising et al., 2005). Life expectancy appears to be unaffected (Badrising et al., 2000)(Benveniste et al., 2011).

Peng *et al.* were able to show that disease progression and disability are related to the age at symptom onset; patients older at disease onset required ambulatory support sooner (Peng et al., 2000a). These findings were confirmed in a separate cohort of patients (Benveniste et al., 2011). The reasons for this more rapid decline in older patients are unknown. The presence of other mobility limiting co-morbidities with increasing age or age-related sarcopenia has been suggested. Quantitative studies have shown the loss of strength to be extremely variable from 1.4% per month to 2% per year. However, these studies have examined different muscles for different lengths of time and reported individual or composite muscle scores making comparisons difficult.

1.2.4 Response to treatment

Despite its classification alongside PM and DM as an IIM it is widely accepted that IBM is poorly responsive to immunosuppressive therapy. However, some reports claim that immunosuppressive therapy may slow disease progression (Lotz et al., 1989)(Sayers et al., 1992)(Beyenburg et al., 1993)(Lindberg et al., 1994) and immunosuppressive therapy is still routinely given in some countries. How to best monitor disease progression or treatment response is uncertain. Most prospective treatment studies in IBM have been under-powered in terms of patient numbers and treatment duration.

Eleven small prospective studies using a number of immunosuppressive medications including methotrexate, azathioprine, steroids, intravenous immunoglobulin, Alemtuzumab, beta-interferon 1a and anti-T-lymphocyte globulin, have shown no or mild benefit in arresting disease progression (Leff et al., 1993)(Amato et al., 1994)(Barohn et al., 1995)(Dalakas et al., 1997)(Walter et al.,

2000)(Muscle Study Group, 2001)(Badrising et al., 2002)(Rutkove et al., 2002)(Lindberg et al., 2003)(Muscle Study Group, 2004)(Dalakas et al., 2009). Ten retrospective studies have analysed the benefit of immunosuppression in 251 patients treated with a variety of immunosuppressive agents (Lotz et al., 1989)(Sayers et al., 1992)(Beyenburg et al., 1993)(Lindberg et al., 1994)(Amato et al., 1996)(Felice and North, 2001)(Rose et al., 2001)(Badrising et al., 2005)(Chahin and Engel, 2008)(Needham et al., 2008b). In all but one study, there was disease progression in the majority of patients despite treatment and in five studies all cases progressed regardless of treatment. In a large observational study, Benveniste *et al.* looked at disease progression in 146 patients with IBM, approximately half of whom received immunosuppressive treatment, and found there to be no difference in disease progression between the two groups.

Although immunosuppressive therapies appear not to significantly affect the disease course, they have been shown to reduce the serum CK level and the inflammatory response observed on muscle biopsy. These findings have been taken as evidence for the secondary role of the inflammation in the pathogenesis of IBM. Alternative agents to standard immunosuppression therapy are being considered and trialled in disease models of IBM and patients. A transgenic mouse model of IBM which over-expresses tau was treated with lithium chloride though without clinical effect (Kitazawa et al., 2008). Arimoclomol, a compound that induces heat-shock protein expression by prolonging the activity of heat-shock factor 1 has undergone phase IIa safety and tolerability trials (UCL, Queen Square Centre for Neuromuscular Diseases website). Significant difficulties concerning treatment and evaluation of treatment efficacy exist; firstly, how best to monitor the treatment effect in a rare slowly progressive disease such as IBM. Secondly, the prolonged delay to diagnosis may mean that the muscle damage undergone is too far advanced to be ameliorated by treatment.

1.3 Pathology of IBM

Muscle biopsies from patients with IBM show several different pathological features broadly described as inflammatory or degenerative. Haematoxylin and eosin (H&E) staining reveals endomysial inflammation, invasion of morphologically normal fibres by inflammatory cells (partial invasion), necrosis, regeneration, neurogenic atrophy, rounded atrophic fibres, split fibres, rimmed vacuoles and eosinophilic inclusions. Using more specialist techniques a number of other pathological features have been described such as protein accumulation, increased major histocompatibility complex class I (MHC Class I) expression, amyloid, mitochondrial changes and tubulofilaments. Some of these features may help in distinguishing IBM from other myopathies.

Ten-30 nm tubulofilaments visualised within fibres using EM were the first pathological abnormality thought to be specific to IBM (Chou, 1986). Subsequently, rimmed vacuoles and amyloid were described in IBM and thought to be sine qua non and pathognomonic (Mendell et al., 1991). However, these abnormalities have all subsequently been documented in other myopathies. Nevertheless, in combination they are still considered to be highly specific for IBM. Despite our long-standing awareness of the presence of these pathological features in IBM, how they relate to the pathogenesis is unknown.

The classical definition of amyloid is an extracellular, proteinaceous deposit exhibiting beta-pleated sheet structure which is identified by apple-green birefringence when stained with Congo red and observed under polarised light. The discovery of amyloid deposits in muscle from IBM patients led to a search for proteins known to aggregate in a beta-pleated sheet formation. Currently, over forty proteins have been found to be accumulated in IBM. Many of these proteins were originally associated with neurodegenerative diseases. Some proteins, such as Aβ, have been reported as sensitive and specific for IBM leading to parallels being drawn between the pathogenesis of IBM and neurodegenerative diseases, particularly AD. These findings have been widely accepted throughout the scientific community and have led to the development of animal

and cellular models of IBM based on Aβ, APP and tau over-expression (Sugarman et al., 2002)(Kitazawa et al., 2008)(Terracciano et al., 2010)(Kim et al., 2011)(Rebolledo et al., 2011). Despite the general acceptance that IBM is akin to neurodegenerative disease independent groups have failed to reproduce a number of key scientific findings supporting these theories raising concerns about their validity.

1.3.1 Diagnostic pathological features

1.3.1.1 Tubulofilamentous inclusions

Chou reported the presence of intranuclear and sarcoplasmic tubulofilaments in a 66 year old male with chronic PM unresponsive to immunosuppressive treatment (Chou, 1967). EM examination revealed membranous bodies containing electron dense granules, tubulofilaments, cytomembranous whorls and structurally abnormal mitochondria. Intranuclear tubulofilaments were 10-20 nm in diameter whereas those present in the sarcoplasm were 20-30 nm in diameter. Sarcoplasmic filaments were not present in all fibres in which intranuclear filaments were found leading to the hypothesis that intranuclear tubulofilaments occurred first. Their morphological similarity to the myxovirus nucleocapsid led to viral studies which were ultimately negative (Sato et al., 1971)(Chou, 1986)(Nishino et al., 1989). A resemblance to myosin filaments was noted; however staining using immunohistochemistry (IHC) for actin and myosin was negative (Chou, 1986). A likeness to amyloid filaments was postulated and led to demonstration of amyloid (apple-green birefringent deposits visualised with polarised light) in IBM muscle stained using alkalinised Congo red dye (Mendell et al., 1991). Amyloid deposits were heterogeneous in appearance, predominantly found in vacuolated fibres and were seen in similar distribution to the tubulofilaments, adjacent to rimmed vacuoles and in perinuclear and intranuclear locations. The authors of this article went further to suggest that tubulofilaments were virtually identical to PrP since these deposits resembled amyloid filaments by EM and show apple-green birefringence when stained with Congo red and visualised under polarised light (Prusiner et al., 1983). IHC was claimed to reveal the presence of PrP in IBM. However, further studies using EM

immunochemistry found tubulofilaments were strongly positive for ubiquitin and PrP, but not Aβ (Askanas et al., 1993a) which were found to decorate amorphous material within the muscle fibre (Askanas et al., 1992a)(Askanas et al., 1993a).

Tubulofilaments have also been observed in a number of other myopathies, including sarcoidosis (Mhiri and Gherardi, 1990), oculopharyngeal muscular dystrophy (OPMD) (Villanova et al., 1993) and hereditary distal myopathy with rimmed vacuoles (DMRV) (Matsubara and Tanabe, 1982)(Mendell et al., 1991). As is seen in IBM rimmed vacuoles were also present on biopsy in these myopathies suggesting a possible link between the two pathological features. The nature of the tubulofilaments remains unknown.

1.3.1.2 Amyloid

Amyloid was first detected in IBM with Congo red staining visualised under polarised light (Mendell et al., 1991). Staining using IHC for components of systemic amyloid [human P component, transthyretin and immunoglobulin light chain] were negative (Mendell et al., 1991). Amyloid deposits correlate with the number of fibres containing rimmed vacuoles. Rimmed vacuoles may represent lysosomes (Villanova et al., 1993)(Sherriff et al., 1995)(Tsuruta et al., 2001)(Nishii et al., 2011), raising the possibility that lysosomal modification of a cellular protein makes it aggregation prone and amyloidogenic.

The association of Aβ and amyloid in AD directed investigators to search for Aβ and other proteins associated with AD in IBM (Askanas et al., 1992a)(Askanas et al., 1992b). Although Aβ was found in IBM and postulated to represent the amyloid peptide deposited, it did not co-localise with the tubulofilaments which originally led to the search for amyloid (Askanas et al., 1992a). Some fibres contained Aβ but lacked amyloid, these were thought to represent an earlier stage in the pathological process (Askanas et al., 1992a).

Amyloid deposits have been reported in other vacuolated myopathies, including the pathologically similar hereditary inclusion body myopathy (hIBM). Other staining methods have been reported to be more sensitive than traditional Congo red staining visualised under polarised light. These include Congo red visualised under fluorescent light, crystal violet and thioflavin staining. In particular, crystal violet was claimed to be specific for IBM and enable its differentiation from hIBM (Askanas et al., 1992a)(Askanas et al., 1992b)(Gayathri et al., 2000).

To date, fifteen studies have studied amyloid staining in IBM tissue (Mendell et al., 1991)(Askanas et al., 1992a)(Askanas et al., 1992b)(Askanas et al., 1993b)(Askanas et al., 1993c)(Villanova et al., 1993)(Nalbantoglu et al., 1994)(Murakami et al., 1995)(Sherriff et al., 1995)(Pruitt et al., 1996) (Banwell and Engel, 2000)(Gayathri et al., 2000)(Vattemi et al., 2003)(Temiz et al., 2009)(Vattemi et al., 2009). Fourteen of these reported amyloid staining in IBM although half of these reports were from a single group who appear to have used some of the same patients repeatedly. One study found no amyloid deposits in 16 cases using Congo red staining viewed under fluorescent and polarised light (Sherriff et al., 1995). This was the only study to include positive control tissue. In the studies that did find amyloid the number of positive fibres and the proportion of positive cases varied greatly. Amyloid was found in 50-100% of cases and the number of affected muscle fibres varied almost 10 fold.

These studies used different methods to detect amyloid, clinical details are absent and positive controls were not used. It is important to differentiate between true-fluorescence and auto-fluorescence when using fluorescent microscopy. Auto-fluorescence, unlike true-fluorescence, is due to the natural emission of light by a biological structure. It usually occurs over a wide excitation range and therefore can be observed under more than one fluorescent filter. The presence of auto-fluorescence in muscle is most often due to lipofuscin. Any fluorescent material must be visualised in two different channels to exclude auto-fluorescence. Many studies did not appear to exclude auto-fluorescence, making the findings difficult to interpret. Therefore, despite

fifteen studies, the sensitivity and specificity of amyloid staining in IBM and the best methodology for demonstrating it remain uncertain.

1.3.1.3 Rimmed vacuoles

Rimmed vacuoles were traditionally thought to be synonymous with IBM. They were initially noted on EM (Chou, 1967), then light microscopy (Yunis and Samaha, 1971) and are unique to IBM among IIM. Their importance in differentiating IBM from PM was highlighted in four cases of treatment resistant PM, three of whom were later noted to have rimmed vacuoles on their initial biopsy and the fourth on a second biopsy (Calabrese et al., 1987). Despite early recognition that rimmed vacuoles are not specific to IBM (Lotz et al., 1989)(de Visser et al., 1990)(Villanova et al., 1993)(Uyama et al., 1998)(Nishii et al., 2011)(Rajakulendran et al., 2011) and can be found in a number of other myopathies some of which are considered in the differential diagnosis of IBM (van der Meulen et al., 2001)(Olivé et al., 2004)(Olivé et al., 2005)(Greenberg et al., 2006) they were considered essential for diagnosis in earlier pathologically-based diagnostic criteria.

Although they were initially thought to be lysosomal in origin they lacked acid-phosphatase activity (Yunis and Samaha, 1971). Staining with IHC, many neurodegenerative proteins have been associated with rimmed vacuoles in IBM; APP (Villanova et al., 1993), Aβ (Askanas et al., 1992b), Aβ 1-42 (Vattemi et al., 2009), ubiquitin (Villanova et al., 1993), tau and hyperphosphorylated tau (Askanas et al., 1994a), apolipoprotein E (ApoE), presenilin-1 (Askanas et al., 1998), PrP (Askanas et al., 1993a), α-synuclein (Askanas et al., 2000), α 1-antichymotrypsin (Bilak et al., 1993), lysosomal proteins (Lotz et al., 1989)(Tsuruta et al., 2001)(Nishii et al., 2011) and nuclear proteins (Greenberg et al., 2006)(Nishii et al., 2011). The presence of an unknown DNA binding protein (Nalbantoglu et al., 1994) and nuclear membrane proteins in rimmed vacuoles suggest a link with myonuclei (Greenberg et al., 2006)(Nakano et al., 2008). Other reports have documented the presence of nuclear and lysosomal proteins in rimmed vacuoles (Nishii et al., 2011). These findings have led to the hypothesis that they are derived from

degenerating muscle nuclei though neither pathological finding is consistent (Villanova et al., 1993)(Temiz et al., 2009) and their aetiology remains unresolved. The presence of rimmed vacuoles in a number of acquired and genetic myopathies suggests that they are the result of a number of different pathologies and therefore non-specific and possibly indicative of a degenerating muscle fibre.

1.3.1.4 Inflammatory cell infiltrate and partial invasion

An endomysial lymphocytic inflammatory infiltrate with partial invasion is, along with rimmed vacuoles, a pre-requisite for a diagnosis of IBM. However, in some early case reports it is conspicuously absent. The first case series reported the mononuclear inflammatory infiltrate to be variably present in six cases (Carpenter et al., 1978); large endomysial lymphocytic foci were observed in two cases, small infiltrates in two, no infiltrates in two and partial invasion in three cases. Detailed analysis of the inflammatory cell types in IBM, other IIM and non-inflammatory myopathies (Arahata and Engel, 1984)(Engel and Arahata, 1984)(Arahata and Engel, 1986)(Arahata and Engel, 1988a)(Arahata and Engel, 1988b) revealed similarities and differences in the inflammatory infiltrate in IBM, PM and DM. In all there was found to be a positive gradient for T-cells [cluster of differentiation protein (CD) 8 positive and activated T-cells] and a negative gradient for B-cells and CD4 positive T-cells between the perivascular and endomysial areas. However, B-cells and endomysial CD4 positive T-cells were more common in DM and CD8 endomysial T-cells were more frequent in IBM and PM. More recent assessment of the inflammatory infiltrate in IBM found it to be absent in 16% cases (Dahlbom et al., 2002) confirming earlier findings that inflammation is not a consistent feature in IBM.

Arahata and Engel documented partial invasion, this being the invasion of morphologically normal fibres by mononuclear inflammatory cells, to be found in IBM, PM, DM and muscular dystrophies (Arahata and Engel, 1984). However, the number of partially invaded fibres was much greater in IBM and PM. Two-thirds of invading cells were found to be CD8 positive T-cells, the rest were

macrophages. The presence of partial invasion as a feature of PM has been disputed. The authors of a recent article questioned whether cases of PM with partial invasion were mis-diagnosed cases of IBM (Hengstman and van Engelen, 2004). The cause of partial invasion and why it would be specifically associated with IBM is unknown.

1.3.2 Protein aggregates and mitochondrial changes

Over the last two decades accumulations of many different proteins have been reported in IBM using IHC and immunofluorescent (IF) staining and immunoblotting (Table 1.1). These include proteins classically associated with neurodegenerative diseases, proteins involved in ribonucleic acid (RNA) transcription and translation, myofibrillar associated proteins, protein degradation and autophagy related proteins and markers of apoptosis. The former include APP, Aβ, α-synuclein, α 1-antichymotrypsin, PrP, DJ-1, ApoE, parkin, superoxide dismutase, tau and hyperphosphorylated tau. Transactivation response DNA binding protein 43 (TDP-43), fused in sarcoma protein (FUS) and valosin containing protein (VCP) are examples of proteins associated with RNA transcription and translation. Myofibrillar and myofibrillar associated proteins include α B-crystallin and desmin. Proteins related to autophagy and protein degradation that have been identified include ubiquitin, sequestosome 1 (p62) and Microtubule-associated protein 1A/1B-light chain 3 (LC3). The apoptosis-related proteins include B-cell lymphoma 2 (Bcl-2) and Bcl-2-associated X protein. Some of these protein accumulations are claimed to be specific and sensitive to IBM, though this is a topic of some debate. Several reports stated that controls cases did not contain "protein aggregates characteristic of IBM", leaving the reader in some doubt as to whether aggregates are present in disease controls or not and therefore, their specificity. The most widely described biomarkers in IBM, which are also believed to be important in the pathogenesis and diagnosis, are APP and Aβ, ubiquitin, tau and hyperphosphorylated tau, p62 and TDP-43.

1.3.2.1 APP and Aβ

Aβ is produced by sequential cleavage of the transmembrane protein APP by β- and γ-secretases

Table 1.1 Proteins reported in IBM

α 1-Antichymotrypsin	Interleukin 6
α B-crystallin	Latent membrane protein 2
α-Synuclein	Latent membrane protein 7
β-Amyloid	Microtubule-associated protein 1A/1B-light chain 3
γ-Secretase	Mutant ubiquitin
γ-Tubulin	Myostatin
Amyloid precursor protein	Neighbour of BRCA1 gene 1
Apolipoprotein E	Neprilysin
B-cell lymphoma 2	Neuronal nitrous oxide synthase
Bcl-2-associated X protein	Nicotinic acetylcholine receptor
β-secretase 1	Nitrotyrosine
Calnexin	Nogo-B receptor
Calreticulin	Nuclear factor kappa-light-chain-enhancer of activated B cells
Casein kinase 1α	Parkin
Cathepsin B	Platelet growth factor
Cathepsin C	Presenilin-1
Clusterin	Prion protein
Cyclin-dependent kinase 5	Proteasomal subunit 19s
Cystatin c	Proteasomal subunit 20s
Desmin	Proteasomal subunit β type-10
DJ-1	Proteasome subunit β type-8
Endoplasmic reticulum protein 72	Proteasome subunit β type-9
Extracellular signal-regulated kinase	Redox factor 1
Fibroblast growth factor receptor	RNA polymerase II
Fused in sarcoma protein	Semicabazide-sensitive amine oxidase
Glucose-regulated protein precursor 78	Sequestosome 1
Glucose-regulated protein precursor 94	Superoxide dismutase 1
Glycogen synthase kinase-3 β	Survival motor neuron protein 1
Hairy/enhancer-of-split related with YRPW motif protein 2	Synemin
Heat shock protein 27	Tau
Heat shock protein 40	Trans-activation DNA-binding protein-43
Heat shock protein 65	Transforming growth factor-β 1
Heat shock protein 70	Transglutaminase 1
Inducible nitrous oxide synthase	Transglutaminase 2
Insulin-like growth factor 1	Ubiquitin
Interleukin 1α	Vaccinia virus complement control protein
Interleukin 1β	Valosin containing protein

List adapted from article by Greenberg (Greenberg, 2010).

and is the main constituent of extracellular amyloid plaques in AD. It was first demonstrated in human muscle fibres using in-situ hybridisation (Zimmermann et al., 1988). It was described in vacuolated fibres in IBM by Askanas *et al.* (Askanas et al., 1992b) after the discovery of amyloid in IBM. Aβ and APP were observed to co-localise with ubiquitin but ultrastructurally APP and Aβ decorated 6-8 nm filaments whereas ubiquitin was localised to larger tubulofilaments typically associated with IBM (Askanas et al., 1992a)(Askanas et al., 1993c). In agreement with the IHC findings, APP and Aβ messenger RNA (mRNA) were found to be increased in vacuolated muscle fibres (Sarkozi et al., 1993). Enzymes participating in the processing of APP (β-secretases and protease inhibitors) and the more fibrillogenic form of Aβ, Aβ 1-42 have been demonstrated in IBM (Vattemi et al., 2001)(Vattemi et al., 2003)(Vattemi et al., 2009).

Aβ is thought to account for Congophilic amyloid deposits in IBM and rare fibres containing non-congophilic Aβ deposits are believed to precede amyloid formation and fibre vacuolisation and represent an earlier stage in the pathogenesis (Askanas et al., 1992a). However, several groups have failed to demonstrate APP or Aβ using IHC (Nalbantoglu et al., 1994)(Sherriff et al., 1995)(De Bleecker et al., 1996)(Salajegheh et al., 2009a)(Temiz et al., 2009) or increased expression of APP mRNA in IBM (Nalbantoglu et al., 1994). The presence of Aβ 1-42 in the absence of Aβ 1-40 surprised some authors as under normal conditions cleavage of APP produces ten times more Aβ 1-40 (Weihl and Pestronk, 2010). Despite concerns expressed over the Aβ hypothesis it has been widely accepted and cellular and animal models of IBM which over-express APP and Aβ have been developed (Sugarman et al., 2002)(Terracciano et al., 2010)(Kim et al., 2011)(Rebolledo et al., 2011).

1.3.2.2 Ubiquitin

Sarcoplasmic ubiquitin aggregates were first reported in IBM by Askanas *et al.* (Askanas et al., 1992b). They co-localised with Aβ and were observed in all cases of patients with IBM and were intranuclear, vacuolar and sarcoplasmic (Albrecht and Bilbao, 1993)(Villanova et al., 1993).

Ultrastructurally they localised to the 15-18 nm tubulofilaments. These findings were confirmed and ubiquitin aggregates were found to be highly sensitive and specific for IBM. However, further studies observed ubiquitin aggregates in less than half of cases tested (Sherriff et al., 1995)(Temiz et al., 2009). The percentage of positive fibres in cases was extremely variable 0.7%-21.8% (Banwell and Engel, 2000)(Muth et al., 2009). Aβ, tau and an aberrant form of ubiquitin, mutant ubiquitin (UBB^{+1}), have been found to co-localise with ubiquitin in IBM but not in other inflammatory myopathies. UBB^{+1} is thought to contribute to the pathogenesis of IBM through inhibition of the proteasome causing protein aggregation (Fratta et al., 2005); it has now been described in other vacuolated myopathies (Olivé et al., 2008).

1.3.2.3 Tau, hyperphosphorylated tau and SMI-31

Tau belongs to the microtubule associated protein family. Six different isoforms are present in adult brain, all derived from a single gene on chromosome 17. Hyperphosphorylated tau is the major cytoskeletal protein in the neurofibrillary tangles of AD. Several studies have reported its presence in IBM (Askanas et al., 1994a)(Mirabella et al., 1996)(Ferrer et al., 2004)(Maurage et al., 2004)(Kannanayakal et al., 2008)(Salajegheh et al., 2009a) and absence in other myopathies leading to claims that IBM is a tauopathy (Maurage et al., 2004). These authors claimed that tau, like Aβ, is both diagnostic and central to the pathogenesis of IBM. Casein kinase 1α, a phosphotransferase enzyme implicated in the hyperphosphorylation of tau in AD, was also observed in IBM (Kannanayakal et al., 2008).

Despite the initial claims to the sensitivity and specificity of tau aggregates in IBM, tau aggregates have not been consistently observed in IBM and immunoblotting failed to confirm increased levels of tau in IBM (Lübke et al., 1994)(Sherriff et al., 1995)(Gayathri et al., 2000). Subsequently, tau deposits have been described in a number of other myopathies and neuropathies including hIBM, DM, PM, OPMD, central core disease, Becker muscular dystrophy (BMD), denervation, acid maltase deficiency and myofibrillar myopathies (MFM) (Lübke et al., 1994)(Ferrer et al., 2004). In

these studies, tau was noted to localise with tubulin, vimentin and desmin suggesting that it is increased in regenerating fibres.

One possible explanation for the inconsistent findings of studies looking at tau deposition in IBM is that different antibodies have been used to identify tau. The most common of these is SMI-31; SMI-31 immunoreactivity in IBM has been used repeatedly to claim that hyperphosphorylated tau is present in IBM (Mirabella et al., 1996)(Banwell and Engel, 2000)(Gayathri et al., 2000)(van der Meulen et al., 2001)(Temiz et al., 2009). However, its primary target is in fact phosphorylated neurofilament H not tau and it has been reported to cross react with a number of other proteins (Salajegheh et al., 2009a). Despite the fact that tau is not the primary target of SMI-31, SMI-31 staining has become embedded in the literature as a marker for hyperphosphorylated tau and the two are used interchangeably. Although the epitope that SMI-31 is binding to in IBM is unknown, one study found SMI-31 staining was able to differentiate between IBM and PM (van der Meulen et al., 2001). However, rimmed vacuoles were present in 47% of the control PM cases indicating that the initial diagnosis may have been incorrect. Further studies have observed SMI-31 aggregates in PM (Temiz et al., 2009), DM (Spuler and Engel, 1997) and hIBM (Gayathri et al., 2000), questioning its diagnostic utility.

1.3.2.4 p62 and components of autophagy

p62 is a component of proteinaceous inclusions in several neurodegenerative diseases including AD, Parkinson's disease (PD) and motor neuron disease (MND). It is thought to play a number of roles in cellular homeostasis; its level increases in response to the expression of aggregation prone proteins, impairment of the ubiquitin-proteasome system and impairment of autophagy. It consists of three domains that enable it to bind poly-ubiquitinated proteins and organelles, self-aggregate sequestering potentially damaging ubiquitinated proteins into cellular aggregates, bind to the lipidated form of LC3 and deliver bound proteins and organelles for autophagic degradation. It has

been implicated in nuclear factor kappa-light-chain-enhancer of activated B cells (NF-κB) activation, gene expression and apoptosis.

p62 aggregates were first reported in MFM (Olivé et al., 2008); they were present in 100% (*n* =17; 12 myotilinopathies and 5 desminopathies) of cases tested. In IBM, p62 aggregates were observed in 80% of vacuolated and up to 25% of non-vacuolated fibres and co-localise with aggregates stained with antibodies to AT100, AT8 and SMI-31. p62 protein levels were increased but mRNA levels were not elevated suggesting the increase was due to a reduction in degradation (Nogalska et al., 2009). To date, the presence of p62 aggregates in IBM have only been replicated by a single group and the number of fibres affected between these two studies varied widely (D'Agostino et al., 2010)(Dubourg et al., 2011).

Other autophagy related proteins have been found accumulated in IBM, namely LC3 and neighbour of BRCA 1 gene 1 (NBR1) (Lünemann et al., 2007)(Temiz et al., 2009)(D'Agostino et al., 2011). LC3 was found to co-localise with APP suggesting that muscle fibres degraded APP through autophagy (Lünemann et al., 2007). One study evaluated LC3 staining in IBM and found that aggregates were present in 85% of cases of IBM and 17% of PM (Temiz et al., 2009). Further studies have found LC3 staining in other vacuolated myopathies (Lünemann et al., 2007).

1.3.2.5 TDP-43

TDP-43 is a heterogeneous nuclear ribonucleoprotein encoded by TARDBP gene on chromosome 1. It is involved in the regulation of RNA transcription, splicing, mRNA stabilisation and trafficking. It was identified as part of ubiquitinated cytoplasmic inclusions in neurons and glial cells in familial frontotemporal dementia with ubiquitin-positive, tau-negative inclusions [now known as frontotemporal lobar degeneration with TDP-43 positive inclusions (FTLD-TDP)] (Neumann et al., 2006). Mutations in TARDBP are now known to cause familial MND (Van Deerlin et al., 2008). TDP-43 is normally located in the nucleus and shuttles between the nucleus

and cytoplasm. In these disorders it is found accumulated in the cytoplasm and is hyperphosphorylated, ubiquitinated, or cleaved. Why the redistribution occurs and whether loss of nuclear TDP-43 is pathogenic is unknown.

Eight studies have demonstrated TDP-43 aggregates in IBM (Weihl et al., 2008)(Küsters et al., 2009)(Olivé et al., 2009)(Salajegheh et al., 2009b)(Temiz et al., 2009)(D'Agostino et al., 2010)(Dubourg et al., 2011)(Hernandez Lain et al., 2011). However, they also reported TDP-43 positive aggregates in IBMPFD (Weihl et al., 2008)(Olivé et al., 2009), PM (Weihl et al., 2008)(Temiz et al., 2009), MFM (Olivé et al., 2009)(Salajegheh et al., 2009b), OPMD and DMRV (Küsters et al., 2009). The numbers of affected fibres observed are very variable, ranging from 1.1% (D'Agostino et al., 2010) to 12% (Dubourg et al., 2011). Immunoblots in FTLD-TDP and MND revealed a 45 kDa band that reduced to 43 kDa on dephosphorylation and several truncated C-terminal bands between 23-27 kDa (Neumann et al., 2006). Weihl *et al*. found the expected 43 kDa band in IBM, but also a higher band at ~50 kDa (Weihl et al., 2008). Olivé *et al.* demonstrated the presence of the normal 43 kDa and lower molecular weight bands in IBM (Olivé et al., 2009). Both studies found altered bands were also present in disease controls. mRNA levels have been found to be normal or increased in IBM and increased in other inflammatory myopathies used as controls, even though TDP-43 aggregates are rarely observed in the latter (Olivé et al., 2009)(Salajegheh et al., 2009b).

1.3.2.6 Mitochondrial changes

Mitochondrial changes are common in IBM and observed to affect more fibres than any other pathological features (Chou, 1967)(Carpenter et al., 1978)(Dahlbom et al., 2002)(Needham and Mastaglia, 2007); cytochrome c oxidase (COX) deficient fibres can be present in up to 98% of cases (Dahlbom et al., 2002) and in as many as 10% of fibres (Temiz et al., 2009). Studies have found the median length of the COX-deficient section to be 330 μm and therefore, it is estimated that the majority of muscle fibres in IBM contain at least one COX-deficient segment (Oldfors et

al., 2006). These fibres are morphologically normal and do not contain other pathological features associated with IBM (Oldfors et al., 2006). In association with the pathological changes multiple different mitochondrial deoxyribonucleic acid (DNA) deletions, including large scale deletions, have been found in IBM and shown to be more frequent than in aged matched controls (Oldfors and Moslemi, 1995)(Santorelli and Sciacco, 1996)(Oldfors and Moslemi, 2006).

Despite their frequency, the diagnostic use of mitochondrial changes in IBM is uncertain as they are commonly found in a number of other conditions and increase with normal aging. However, although they may not be specific for IBM, there is evidence to suggest they may be sensitive (Chahin and Engel, 2008)(Temiz et al., 2009).

1.3.2.7 MHC Class I

MHC Class I expression on cells is necessary for T-lymphocyte mediated cytotoxicity. Increased MHC Class I and β_2 microglobulin (part of the MHC molecule) expression is found in muscle fibres in PM, IBM and DM (Karpati et al., 1988). In PM, in excess of 80% of fibres have been reported to show increased staining whereas in IBM increased staining was confined to fibres undergoing partial invasion and small clusters of fibres in the biopsy, some of which contained rimmed vacuoles. A further study demonstrated that increased MHC Class I expression was not confined to IIM, but was also present in muscular dystrophies (Emslie-Smith et al., 1989). However, a marked increase in MHC Class I staining is thought to be indicative of an inflammatory myopathy and although not specific to IBM it has been found to be a consistent feature (Dahlbom et al., 2002)(Temiz et al., 2009). Whether it is a primary phenomenon resulting in the inflammatory infiltrate or occurs as a secondary mechanism is unknown (Isenberg et al., 1986)(Emslie-Smith et al., 1989).

1.4 Biomarkers

A biomarker is a consistent biological observation that is indicative of a disease process and when objectively measured may give prognostic information. Their sensitivity and specificity allow them to be used as diagnostic tools alone or in combination with other factors. All of the pathological features discussed have been promoted as biomarkers for IBM and the pathogenesis of IBM has been inferred from their presence. However, many of the studies have lacked detailed clinical data and appropriate disease controls and therefore, these so-called biomarkers have often been subsequently observed in other myopathies important in the differential diagnosis of IBM. What's more, published findings have not been consistently replicated and validated by independent groups. To date no pathological features have been found to correlate with disease progression or severity in IBM. However, quantification of the findings is lacking or vague in most studies. The quantity of fibres containing immunoreactive protein deposits is sometimes reported as the percentage of vacuolated fibres e.g. 25% of vacuolated fibres contained tau positive deposits. However, the number of vacuolated fibres is extremely variable between cases and often the percentage of vacuolated fibres is not included in the report obscuring the number of affected fibres.

The specificity and sensitivity of pathological findings described in IBM remains unknown and therefore, recommendations on their use in diagnostic criteria are uncertain. To distinguish IBM from inflammatory and vacuolated myopathies, the development of a reliable biomarker(s) is crucial. Future biomarkers need to be easily identified, reliable, quantifiable and their sensitivity and specificity validated in IBM using appropriate disease controls. This may only be achieved through the combination of clinical and pathological features.

1.5 Pathogenesis

The varied pathological findings in IBM (inflammation, partial invasion, amyloid, rimmed vacuoles, protein aggregates and mitochondrial changes) have driven the various theories as to its

aetiology and pathogenesis. These have included viral infection, accumulation of toxic oligomers of Aβ causing fibre vacuolation and degeneration, autoimmune attack, myonuclear degeneration, endoplasmic reticulum (ER) stress, and impairment of the ubiquitin-proteasome system (UPS) or autophagy.

It may not be possible to infer the pathogenesis of IBM from individual proteins or pathological features, particularly as no one feature is consistently found in all cases of IBM. Described below are some of the current theories of the pathogenesis of IBM, which remains an enigma. Though they have been described separately, there is increasing evidence of a link between them (Ding et al., 2007).

1.5.1 Inflammation

Inflammatory infiltration is a secondary phenomenon in genetic muscular dystrophies. In IBM, partial invasion, widespread MHC Class I up-regulation and genetic factors support an immunopathogenic mechanism. Arahata and Engel found that the majority of invading CD8 positive T-cells were activated (Engel and Arahata, 1984). As T-cell mediated injury is antigen-driven they postulated that the T-cells had become sensitised to a muscle fibre antigen. Further work showed that T-cell receptors show clonal restriction in different muscles in IBM and these persist over time suggesting activation by a specific antigen (Lindberg et al., 1995)(Amemiya et al., 2000). Whether humoral immunity plays a role is uncertain. CD20 positive B-cells are rarely present in IBM (Arahata and Engel, 1984)(Temiz et al., 2009); however, some studies have demonstrated clonally expanded transcriptionally active CD138 positive B-cells to be present (Greenberg et al., 2005). However, although auto-immune diseases and non-organ specific auto-antibodies are associated with IBM (Lotz et al., 1989)(Dalakas, 2006)(Chahin and Engel, 2008)(Rojana-Udomsart et al., 2012)(Benjamin Larman et al., 2013)(Pluk et al., 2013) no muscle specific antibody has yet been identified.

Evidence of a genetic susceptibility to IBM provides the strongest evidence for immunological involvement. IBM is associated with 8.1 ancestral haplotype (AH) which is known as the auto-immune haplotype due to its association with a number of autoimmune diseases. All IBM patients have been found to carry at least some of the extended 8.1 AH (B8/C4A*Q0/C4B1/BfS/DR3/DR52) compared with 11% of the general population (Garlepp et al., 1994). These findings have been confirmed in several Caucasian populations (Lampe et al., 2003)(Koffman et al., 1998)(Badrising et al., 2004)(Price et al., 2004).

The link between the inflammatory changes observed in IBM and the degenerative features is unknown. Partial invasion was found to be ten times more frequent than amyloid in IBM (Pruitt et al., 1996), suggesting that inflammation plays a more central role than degeneration in the pathogenesis of IBM. It is postulated that an unknown, possibly infectious, trigger initiates the inflammatory response. Local production of inflammatory chemokines and cytokines is well documented in IBM (Lundberg et al., 1997)(Raju et al., 2003)(De Paepe et al., 2008) and may trigger increased MHC Class I expression causing ER stress and the accumulation of misfolded aggregation prone proteins and activation of NF-κB, leading to a self-sustaining inflammatory response (Dalakas, 2006). This theory is supported by two observations in animal models. Firstly, constitutive MHC Class I up-regulation in transgenic mice causes myositis and ER stress (Nagaraju et al., 2005) and secondly, chronic inflammation leads to protein accumulation in animal models (Kitazawa et al., 2008). However, immunosuppressive therapy has failed to alter the disease course in IBM (Benveniste et al., 2011) and the degenerative pathological features continue to increase over time despite a reduction of the inflammatory infiltrate (Barohn et al., 1995).

1.5.2 Myonuclear degeneration

Myonuclear abnormalities are commonly found in IBM (Carpenter et al., 1978)(Chou, 1986). The presence of nuclear and lysosomal proteins in rimmed vacuoles led to the hypotheses that rimmed vacuoles are derived from degenerating myonuclei (Nalbantoglu et al., 1994)(Greenberg et al.,

2006)(Nakano et al., 2008). However, these findings were not replicated (Temiz et al., 2009). Other indicators of myonuclear involvement in the pathogenesis of IBM are the loss of myonuclear TDP-43 (Olivé et al., 2009)(Salajegheh et al., 2009b) and myonuclear ubiquitin aggregates. Whether these changes indicate or cause myonuclear breakdown is uncertain. Sarcoplasmic TDP-43 inclusions are the most abundant protein reported in IBM, reported in 23% of fibres, suggesting that TDP-43 redistribution may play a significant role in the pathogenesis (Salajegheh et al., 2009b). Though whether TDP-43 is directly pathogenic (gain of function), or whether its redistribution leads to a loss of function effect is unknown. There is some evidence that TDP-43 loss from the myonuclei leads to abnormalities in the morphology of nuclei and apoptosis (Ayala et al., 2008). However, sarcoplasmic TDP-43 aggregates are not specific to IBM (Weihl et al., 2008)(Olivé et al., 2009)(Küsters et al., 2009) and other publications have not reported such impressive changes (Nogalska et al., 2009).

1.5.3 Autophagy

Autophagy is responsible for protein and organelle degradation and recycling (Needham and Mastaglia, 2007)(Temiz et al., 2009). Three different forms of autophagy are commonly described; macroautophagy, microautophagy and chaperone mediated autophagy. They all result in the delivery of cellular components to lysosomes for degradation. Initially it was thought to be an indiscriminate process; however, there is increasing evidence that it is selective e.g. mitophagy is the selective degradation of mitochondria (Kim et al., 2007). Impairment of autophagy leads to the accumulation of p62 (Bjørkøy et al., 2005)(Pankiv et al., 2007). In IBM, p62 has been found to co-localise with NBR1 protein and LC3, both components of the autophagic system. NBR1, like p62, is believed to shuttle ubiquitinated proteins for degradation and has been found to be co-localised with not only p62 but also ubiquitin and phosphorylated tau in IBM (Bjørkøy et al., 2005)(D'Agostino et al., 2011). LC3 has been found to be commonly aggregated in IBM, present in 85% of patients (Weihl et al., 2008). However, an increase in the quantity of autophagic proteins present in muscle may reflect increased autophagic turnover, not only impairment.

Autophagy may play a part in MHC Class I expression and inflammation. Treatment of cells with Rapamycin, which increases autophagy via inhibition of the mammalian target of rapamycin (Wullschleger et al., 2006), has been shown to reduce MHC Class I and inhibition of autophagy to cause increased cell surface expression of MHC Class I (Patterson and Mintern, 2012). Therefore, impairment in autophagy may explain the presence of inflammatory features such as increased MHC Class I expression and protein accumulation observed in IBM.

Mitochondria are the site of aerobic respiration and adenosine triphosphate (ATP) production; a by-product of this process is reactive oxygen species (ROS). ROS can cause mitochondrial damage and DNA mutations; the resulting defective mitochondria can cause necrosis or apoptotic cell death. Therefore, recycling of damaged and dysfunctional mitochondria is essential to cell survival. Autophagy is responsible for the destruction of cellular organelles such as mitochondria. It is impaired in Ullrich and Bethlem collagen VI muscular dystrophies resulting in mitochondrial dysfunction and structural changes (Grumati et al., 2010). Multiple different mitochondria mutations have been demonstrated in IBM muscle (Dahlbom et al., 2002). Different deletions are present in different segments of the same fibre implying that mitochondria harbouring mutations expand locally (Oldfors et al., 1995) and they are similar to those found in normal aging and mitochondrial disorders secondary to mutations in nuclear genes (Santorelli et al., 1996)(Moslemi et al., 1997). However, in IBM no mutations have been found in nuclear genes known to result in mitochondrial DNA mutations, namely mitochondrial DNA polymerase subunit gamma, twinkle and adenine nucleotide translocator 1 (Oldfors et al., 2006). If autophagy was impaired in IBM, this would result in reduced mitochondrial turnover and the accumulation of mitochondria harbouring DNA mutations that would proliferate leading to the pathological changes observed (Moraes et al., 1992). Therefore, inhibition of autophagy in IBM could explain the accumulation of mitochondria harbouring DNA mutations, protein accumulation and MHC Class I up-regulation observed. Exercise has been shown to reduce mitochondrial mutations and improve biogenesis in

animal models (Safdar et al., 2011), and this may, in part, explain the clinical observation that exercise is of benefit in patients with IBM.

Finally, in animal models, mice with a specific skeletal knock-out of a crucial autophagy gene, ATG 7, develop muscle atrophy, weakness and pathological changes similar to those observed in IBM (Masiero et al., 2009). Taken together these findings suggest that autophagy may play a role in the pathogenesis of IBM.

1.5.4 Endoplasmic reticulum stress

The ER is the site of protein synthesis, folding and processing of secreted proteins. Many perturbations in cellular function cause ER stress resulting in the accumulation of unfolded and mis-folded proteins. The increased expression of MHC Class I observed in IBM has been postulated to cause ER stress and protein misfolding leading to the production of aggregation prone proteins. However, the triggering factor leading to MHC Class I over-expression is unknown.

ER stress activates two pathways, the "unfolded protein response" (UPR) and the ER overload response (EOR). These work together to restore cellular homeostasis by i) increasing NF-κB transcription, ii) halting the cell cycle, iii) reducing protein synthesis, iv) inducing chaperone proteins and folding catalysts [78 kDa glucose-regulated protein (Grp78), 94 kDa glucose-regulated protein (Grp94), calnexin and calreticulin] and v) activation of ER associated protein degradation which occurs via the UPS. In IBM, IHC and immunoblotting studies have shown an increase in several ER-chaperone proteins namely calnexin, calreticulin, Grp78, Grp74 and NF-κB (Yang et al., 1998)(Vattemi et al., 2004). EOR triggers increased NF-κB expression which in turn increases expression of MHC Class I and other pro-inflammatory mediators. Therefore, increased MHC Class I staining observed in IBM may be secondary to ER stress and may play no causal role.

1.5.5 Ubiquitin-proteasome system

UPS, alongside autophagy, is another pathway for protein degradation (Hershko and Ciechanover, 1998). Misfolded or unfolded proteins are marked for destruction by ubiquitination. Inhibition of the UPS leads to the accumulation of ubiquitinated proteins. Several studies have shown ubiquitin accumulation in IBM (Askanas et al., 1992d)(Villanova et al., 1993)(Nalbantoglu et al., 1994)(Sherriff et al., 1995)(Prayson and Cohen, 1997)(Banwell and Engel, 2000) but only two have investigated the UPS in detail (Ferrer et al., 2004)(Fratta et al., 2005). Increased immunoreactivity to proteasomal subunits and its regulators in IBM was observed in both studies. Proteasomal subunits co-localised with phosphorylated tau, Aβ, ubiquitin, desmin and α B-crystallin. Despite similar IHC findings, one study found no impairment of the proteasomal function whilst the other found it to be impaired. In addition, IHC studies have demonstrated the presence of UBB^{+1} in IBM (Fratta et al., 2005), which if present in sufficient quantities may lead to inhibition of UPS function and therefore, the accumulation of protein aggregates. Thus, impaired UPS may play a role in the pathogenesis of IBM.

1.6 Diagnostic criteria

Once IBM was accepted as a separate disease entity from PM diagnostic criteria were developed to differentiate between the two conditions. To date, six diagnostic criteria have been proposed for IBM (Calabrese et al., 1987)(Lotz et al., 1989)(Griggs et al., 1995)(Vershuuren et al., 1997)(Needham and Mastaglia, 2007)(Benveniste and Hilton-Jones, 2010)(Hilton-Jones et al., 2010). Five are focussed on the pathological findings and require a combination of tubulofilaments, amyloid, rimmed vacuoles and endomysial inflammation with partial invasion for a definite diagnosis. The other includes a pathologically diagnosed group but also introduces a clinically diagnosed group (Benveniste and Hilton-Jones, 2010)(Hilton-Jones et al., 2010).

The first diagnostic criteria for IBM were suggested by Calabrese *et al.* (Calabrese et al., 1987). These required the presence of tubulofilaments and rimmed vacuoles for a diagnosis of definite

IBM, reflecting the belief that these pathological findings were sensitive and specific for IBM. Revised criteria were proposed by Lotz *et al.* after examining 40 patients with IBM (Lotz et al., 1989). They acknowledged that the individual pathological findings associated with IBM were not specific in isolation; however, they believed them to be highly sensitive and specific in combination. They found the clinical features associated with IBM to be variable and therefore these were not deemed essential for the diagnosis. These criteria were based only on the analysis of patients with rimmed vacuoles, falsely emphasising their diagnostic importance. The variability of the clinical picture may have been due to the inclusion of patients with other vacuolated myopathies.

The seminal Griggs criteria were published in 1995 (Griggs et al., 1995). These were heavily based upon the previous two criteria and therefore pathologically focused. A diagnosis of definite IBM could be made solely on the pathological findings. A diagnosis of possible IBM required an auto-aggressive inflammatory infiltrate and associated clinical and laboratory features. These criteria were based on expert opinion and no clinical data were included. Four articles are cited in support of the criteria (Dalakas, 1991)(Sayers et al., 1992)(Sekul and Dalakas, 1993)(Askanas et al., 1994b); however, only one of these provides any clinical data, the others being review articles, and the need to demonstrate all the pathological features is questioned (Sayers et al., 1992). The Griggs criteria were re-published in a separate review article in 2002 (Tawil and Griggs, 2002); however they were inadvertently altered leading some to believe they had been modified. Unfortunately this confusion still persists (personal communication with author) (Needham and Mastaglia, 2007).

The European Neuromuscular Centre (ENMC) consensus criteria were published in 1997 (Vershuuren et al., 1997). A significant change was the ability to make the diagnosis of IBM in the absence of rimmed vacuoles and tubulofilaments. However, these criteria are cumbersome and include 13 clinical and pathological elements, many of which lack precise definitions. They were shown to be more sensitive than the Griggs criteria (Badrising et al., 2000) though this was

somewhat inevitable as the authors did not apply the ENMC criteria in full. Needham and Mastaglia (2007) suggested the addition of mitochondrial changes [cytochrome c oxidase (COX) deficient fibres] and MHC Class I up-regulation to the Griggs criteria, though in essence the criteria remained unchanged (Needham and Mastaglia, 2007) and these suggestions were not widely adopted.

It is now recognised that the diagnosis of IBM is dependent upon pathological findings no longer considered to be specific or sensitive. Newer criteria have tried to address this issue by including alongside pathologically diagnosed IBM a category of clinically defined IBM (Benveniste and Hilton-Jones, 2010)(Hilton-Jones et al., 2010). These various diagnostic criteria arose because of the lack of a gold standard diagnostic test, inevitable given our lack of understanding of pathogenesis. Consequently, there must be uncertainty about their sensitivity and specificity. An additional problem is that the individual pathological criteria lack definition or quantification.

1.7 Patients with clinical features of IBM but non-diagnostic biopsies

Only a few cases have been reported of patients lacking the initial diagnostic pathological features associated with IBM but then being found to have them on repeat biopsy (Amato et al., 1996)(van der Meulen et al., 1998). However, clinical experience would suggest that these patients are not uncommon. Badrising *et al.* reported one or more of the necessary pathological features to be absent in 21 cases with clinically typical IBM (Badrising et al., 2000). Patients lacking the diagnostic pathological features at presentation may be misdiagnosed, typically as PM, and therefore treated inappropriately (Benveniste et al., 2011). Some authors have suggested performing a further muscle biopsy (Dahlbom et al., 2002)(Benveniste and Hilton-Jones, 2010) to identify the necessary features. However, even with a further biopsy the diagnosis may not be achieved for many years (Amato et al., 1996)(van der Meulen et al., 2001).

Because of the widespread acceptance of the pathological criteria as a pre-requisite for a diagnosis of IBM, little is known about patients with non-diagnostic biopsies. Indeed, authors have avoided

labelling such patients as IBM, considering them as a separate disorder, a half-way house been IBM and PM, similar to yet different from both (Temiz et al., 2009). Although a few reports have described patients with clinically typical IBM but lacking the diagnostic pathological features on biopsy (Calabrese et al., 1987)(Amato et al., 1996)(Blume et al., 1997)(van der Meulen et al., 1998)(Chahin and Engel, 2008)(Temiz et al., 2009)(Benveniste et al., 2011)(Dubourg et al., 2011) only one of these included detailed examination findings at presentation and only two provided detailed data on the pathological features. The findings of these studies that provided information on patients lacking the pathological features of IBM are summarised in Table 1.2. Therefore, detailed clinical, pathological and prognostic information is lacking to help one determine whether these patients should be diagnosed as IBM.

1.7.1 Clinical features

As mentioned in the previous section, eight publications report patients lacking at least one of the diagnostic pathological features (Calabrese et al., 1987)(Amato et al., 1996)(Blume et al., 1997)(van der Meulen et al., 1998)(Chahin and Engel, 2008)(Temiz et al., 2009)(Benveniste et al., 2011)(Dubourg et al., 2011). Amato *et al.* described the clinical features of seven steroid resistant cases of PM in detail; all had finger flexor and knee extensor weakness. Further biopsies were performed in two patients and revealed the diagnostic pathological features associated with IBM, confirming that these patients indeed had IBM. Chahin *et al.* performed a similar study noting that in addition to typical IBM and PM cases a third group of patients existed which they called PM/IBM. These patients had the clinical features of IBM (knee extension and finger flexion weakness) without the pathological findings on biopsy and, similar to patients with pathologically-definite IBM, they did not respond to immunosuppressive treatment. Using the clinical criteria suggested by Hilton-Jones *et al.*(Hilton-Jones et al., 2010), Benveniste *et al.* showed that patients with clinically defined IBM were clinically similar to pathologically diagnosed cases (Benveniste et al., 2011). Although some of these studies alluded to the sensitivity and specificity of the clinical examination in the absence of the pathological features others found the clinical presentation to be

Table 1.2 Summary of studies characterising patients with clinical features suggestive of IBM but who lack diagnostic pathological features of IBM

Study	No. of patients	Gender, M : F	Age at onset, years	Pattern of weakness	Improvement with immunosuppression	Disease progression
Calabrese *et al.*,1987	1	0:1	23	Neck and proximal arms and legs weakness.	No	Unknown
Amato *et al.*, 1996	7	4:3	58 (±10)	Finger flexor and knee extensor weakness in all.	No	Unknown
Van der Meulen *et al.*, 1997	2	0:2	50 and 42	1. Facial, finger flexor and hip flexor weakness. 2. Facial, neck flexor and limb-girdle weakness with sparing of the quadriceps muscles.	No	Unknown
Blume *et al.*, 1997*	10	4:6	61 (±3)	Proximal weakness in all patients, facial weakness in five and distal weakness in four.	No	Three cases showed a loss of strength of 4% per year over four years.
Chahin *et al.*, 2008	16	5:11	69 (±11)	Resembled that seen in IBM at presentation in 88% and 100% within two years after biopsy.	No (*n*=14)	Unknown
Temiz *et al.*, 2008*	26	10:16	60 (±11)	62% had selective severe weakness of finger flexors or knee extensors.	No (*n*=20)	Unknown
Beveniste *et al.*, 2011**	51	28:23	59 (55-68)	100% had finger flexor weakness greater than shoulder abductor and knee extensor weakness greater than hip flexor.	No	Similar to pathological IBM at last follow-up.

*Follow-on studies. **Cumulative clinical features exhibited during the course of the illness.

varied (van der Meulen et al., 1998)(Temiz et al., 2009). Therefore the specificity and sensitivity of the clinical features in the absence of all the diagnostic pathological features remains uncertain.

1.7.2 Disease progression

Two studies have examined the disease progression in patients with characteristic clinical features who lack the diagnostic pathological findings. Benveniste *et al.* found the functional disability at last follow-up (requirement of a walking aid or wheelchair) to be similar in pathologically diagnosed IBM and clinically diagnosed patients. However, using a hand-held dynamometer, Temiz et al. found a more rapid loss of strength in pathologically typical IBM compared to pathologically typical PM cases with greater than one per cent COX negative fibres (referred to in the study as PM.Mito) (Temiz et al., 2009). Thus these studies raise questions about whether IBM lacking the pathological features is a separate disorder with a better outcome than IBM.

1.7.3 Pathological features

The absence of one or more of the diagnostic pathological features was detailed in each of the studies mentioned in section 1.7.1. Reasons for their absence may have been the examination of paraffin embedded tissue in one study, making rimmed vacuoles difficult to identify (Calabrese et al., 1987)(van der Meulen et al., 1998). Van der Meulen *et al.* described two patients who initially lacked typical findings on assessment of frozen biopsy material (van der Meulen et al., 1998). Only repeat biopsies 12 and 18 years later confirmed the diagnosis, indicating that the pathological features may increase with time and may therefore only be present in advanced disease. Alternatively, the pathological features may be multifocal and thus easily missed on a single biopsy (Amato et al., 1996).

A greater number of mitochondrial changes (COX deficient fibres) have been found in these cases with clinical features suggestive of IBM but non-diagnostic biopsies (PM.Mito) compared to PM (Temiz et al., 2009) and pathologically typical IBM. However, PM.Mito patients had to have

mitochondrial changes present on biopsy unlike PM and IBM. Therefore these findings were most likely a reflection of the inclusion criteria used in the study. Otherwise the pathological abnormalities in cases of clinically typical IBM lacking the diagnostic pathological features are reportedly fewer than in pathologically typical IBM (Chahin and Engel, 2008)(Temiz et al., 2009)(Dubourg et al., 2011). Greater numbers of partially invaded fibres and SMI-31, TDP-43, Congophilic deposits and p62 and ubiquitin accumulations have been observed in pathologically typical IBM. This has led some researchers to conclude that they may be separate disorders. However, against this theory is the fact that no differences were found in MHC Class I up-regulation, LC3 or α B-crystallin deposits (Chahin and Engel, 2008)(Temiz et al., 2009). However, one of these studies did not quantify the pathological findings described and another was methodologically flawed including patients without rimmed vacuoles as pathologically definite IBM and patients with few rimmed vacuoles on biopsy as non-diagnostic.

1.8 Concluding remarks

Despite almost four decades of research into IBM, our knowledge of its aetiopathogenesis has progressed little. Indeed, in a review in 1988, Sawchak and Kula commented on issues that remain unresolved to this day, notably the absence of a pathognomonic sign or test for IBM (Sawchak and Kula, 1988) and therefore the possibility that IBM may be a collection of several muscle diseases of diverse causes rather than a single disease. Investigation has been hampered by a belief in the sensitivity and specificity of the pathological features which may have led to the inclusion of patients that do not have IBM and the exclusion of many that do. Indeed, the very first patient described as having IBM most likely did not (Yunis and Samaha, 1971). The absence of patients lacking the classical pathological features from natural history, pathological and treatment studies may have biased much of the published data for IBM. Due to the similarity in names between IBM and the genetic inclusion body myopathies confusion has often arisen with authors extrapolating study findings from each to encompass the other.

IHC studies of IBM have predominated in the investigation of biomarkers for the disease. However, the diagnostic and pathogenic significance of many of the proposed markers has not been well established and in some cases is controversial. The theories of IBM pathogenesis have revolved around muscle biomarkers; however, many of the proteins selected for study were based upon their presence in neurodegenerative disease and therefore, drove the association between IBM and these conditions. Studies have only included pathologically diagnosed cases of IBM. None of these features are specific to IBM. Their presence in a variety of genetic and inflammatory myopathies suggests that they are not causative. Rather they may reflect the down-stream consequences of several primary pathologies and advanced disease. Studies have often lacked controls known to contain the epitope of interest. Suitable disease controls are often absent and therefore, data on the sensitivity and specificity of findings in IBM are missing. Possible issues with analysis of the abnormalities on muscle biopsy have been raised by some commentators (Greenberg, 2010). Differences in staining methodology and a lack of quantitative data have made studies difficult to compare. Many of the pathological findings have not been corroborated by independent groups (Greenberg, 2009). Despite the controversy surrounding many of the purported pathological findings in IBM the premise that it is similar to neurodegenerative conditions such as AD has been widely accepted and led to the development of cellular and animal models of IBM based on the over-expression APP, Aβ and tau.

Determining the clinicopathological spectrum associated with IBM is of paramount importance. It will enable the development of clinical and pathological biomarkers and diagnostic criteria for IBM, which to-date has depended on pathological features no longer considered to be specific or sensitive. Finding biomarkers that differentiate IBM from other IIM and vacuolated myopathies will facilitate the identification of a homogenous group of patients and ultimately advance our understanding of the pathogenic mechanisms central to IBM.

1.9 Hypotheses

1. IBM has a characteristic clinical presentation that is both specific and sensitive and independent of the current diagnostic pathological features.

2. Protein aggregates are early pathological markers of IBM aiding earlier diagnosis and giving insight into the pathogenesis of IBM.

1.10 Aims

Many uncertainties remain concerning the clinical and pathological features of IBM. Recently, patients with clinical characteristics similar to those observed in IBM, but lacking the diagnostic pathological features, have been described. However, authors have avoided calling these patients IBM preferring to highlight their similarities to both IBM and PM; others have emphasised their differences suggesting they are possibly a separate condition. Detailed clinical and pathological descriptions and long term natural history data confirming these patients to have IBM are absent. Thus, the aims of this thesis are:

1. To compare the demographic, clinical and para-clinical features of patients with clinical features suggestive of IBM that i) have the characteristic pathological findings and ii) lack these findings, to establish whether these patients represent a homogeneous group (Chapter 3).

2. To systematically determine which pathological features are consistently present in IBM and may be of use as disease biomarkers (Chapter 4).

3. To determine the sensitivity and specificity of the potential biomarkers identified in differentiating IBM from myopathies important in the differential diagnosis (Chapter 5).

4. To investigate potential pathogenic mechanisms in IBM (Chapter 6).

Chapter 2

MATERIALS AND METHODS

2.1 General points

Studies were approved by the Departments of Research and Development at Oxford University NHS Trust, Oxford and University College London Hospitals NHS Foundation Trust, London.

Patients included had been assessed, diagnosed and managed by the muscle services at the Radcliffe Infirmary/John Radcliffe Hospital, Oxford, United Kingdom (UK) or the National Hospital for Neurology and Neurosurgery, London, UK. None of the patients were used in more than one of Chapters 4, 5 and 6.

Muscle biopsies were taken for diagnostic purposes and prior to any treatment.

Statistical analyses were performed using GraphPad Prism version 5. Statistical significance was set at $p < 0.05$.

2.2 Clinical characteristics of patients

2.2.1 IBM Cases

2.2.1.1 Clinical characteristics and patients selection

IBM patients used for this part of the work had a clinical diagnosis of IBM or fulfilled Griggs' pathologically-definite criteria for IBM and had to have been seen and managed in the Muscle Clinic at the John Radcliffe Infirmary or the John Radcliffe Hospital, Oxford. Patients were identified from three sources, i) patients currently attending the Muscle Clinic, ii) a database compiled for a previous study and iii) a keyword search of the Department of Neuropathology results system. Pathology reports were searched for the following terms – inflammatory myopathy, myositis, rimmed vacuoles, inclusion body myositis and IBM. A clinical diagnosis of IBM

required patients to have (either at presentation or during follow-up) prominent finger flexor and/or knee extensor weakness with compatible laboratory features (normal-moderately elevated CK) and a supportive muscle biopsy i.e. not incompatible with a diagnosis of IBM. Only patients whose muscle biopsy and clinical data were available from their first presentation were included. Additionally, to ensure uniformity in the clinical examination at first presentation, only patients seen in the Muscle Clinic within 12 months of their initial outpatient appointment with another physician for neuromuscular symptoms attributable to IBM were included. The following data were collected prospectively at hospital appointments and collated retrospectively: date of birth, gender, ethnicity, past medical history, nature and onset of the disease, date of first symptoms, date IBM diagnosed, alternative initial diagnoses, physical examination at presentation and last follow-up, laboratory investigations at presentation, details of immunosuppressive treatment given for their presenting muscle problem, date requiring walking aid (walking stick or frame) and wheelchair. Disease onset was approximated to the year the patient recalled their first symptoms. The delay to diagnosis was taken as the time from symptom onset until the diagnosis of IBM was confirmed either by muscle biopsy or specialist clinical opinion.

2.2.1.2 Muscle biopsies

Muscle biopsies were reviewed blinded to the clinical details. Mitochondrial changes were assessed on combined cytochrome c oxidase and succinate dehydrogenase (COX/SDH) staining which was available for 56 cases. MHC Class I stained sections were available for review in 50 cases. Definitions of pathological features are summarised in Table 2.1.

2.2.1.3 Diagnostic criteria

Patients were classified according to the pathological Griggs criteria (Griggs et al., 1995), the 1997 ENMC criteria (Vershuuren et al., 1997) and the clinical 2011 ENMC criteria (Chapter 3; Table 3.1). To enable comparisons between the pathologically and clinically diagnosed groups, Griggs

definite and Griggs possible IBM were combined into a single group, as were 2011 ENMC clinically defined and probable IBM.

2.2.2 Control cases

Control cases were patients with adult-onset steroid-responsive inflammatory myopathy (PM&DM) and protein accumulation myopathies (PAM) who were diagnosed and managed in the Muscle Clinic at the John Radcliffe Hospital, Oxford. Patients were identified from the Muscle Clinic clinical database. Criteria for PM&DM were i) subacute onset limb girdle weakness; ii) raised CK; iii) muscle biopsy revealing an inflammatory myopathy without features inconsistent with the diagnosis; and iv) sustained unequivocal clinical and biochemical response to steroid immunosuppression. PAM cases were genetically confirmed diagnosis of MFM or hIBM. To ensure uniformity in the clinical examination at first presentation, only PM&DM patients whose first referral was to the Muscle Clinic and PAM patients who were seen in the Muscle Clinic within 12 months of their first outpatient appointment with another physician for neuromuscular symptoms were included.

2.2.3 Statistical analysis

Continuous variables are presented as medians (interquartile range). Groups were compared using the Mann Whitney *U*-test. Categorical variables were analysed using a Fisher's exact or chi squared test. Kaplan-Meier survival curves were used to estimate time to disability end-points. Survival curves were compared using Cox proportional hazards model. Patients who had received immunosuppressive treatment for conditions other than IBM were excluded from comparisons between treated and untreated patients. Statistical significance was set at $p < 0.05$.

Table 2.1 Pathological definitions

Feature	Definition
Rimmed vacuole	Irregular vacuole with a granular basophilic rim, or containing granular basophilic material visualised when stained with H&E or stained red in the GT. Both H&E and GT stains were reviewed before concluding the absence of rimmed vacuoles.
Inflammation and partial invasion	Assessed on H&E stained sections and sections stained using immunohistochemistry for inflammatory cell markers if available. Partial invasion was defined as unequivocal invasion of an otherwise structurally normal muscle fibre by one or more mononuclear cell(s). Unequivocal invasion = the presence of a mononuclear cell(s) within a muscle fibre so that a line drawn along the edge of fibre would completely enclose the mononuclear cell within a fibre.
COX-/SDH+ muscle fibres	Complete absence of COX reaction product (brown) with retained SDH reactivity (blue).
MHC Class I	Normal = capillary staining only; increased = widespread sarcolemmal staining ± scattered or diffuse sarcoplasmic staining.

H&E = Haematoxylin and eosin, GT = Gomori trichrome, COX-/SDH+ = Cytochrome c oxidase negative/succinate dehydrogenase positive; COX = Cytochrome c oxidase; SDH = succinate dehydrogenase; MHC Class I = Major histocompatibility complex class I.

2.3 Pathological description of IBM

2.3.1 Cases

Six Griggs pathologically definite and clinically typical cases of IBM were identified; all IBM cases had an endomysial inflammatory infiltrate with partial invasion, rimmed vacuoles and 15-18 nm tubulofilaments on EM. Six cases with no clinical or pathological evidence of neuromuscular disease were used as controls; all controls had been investigated for cramps and had a normal examination performed by a muscle specialist, normal CK, normal neurophysiological examination and normal muscle biopsy. Tonsillar tissue and tissue from brains donated to the Queen Square Brain Bank for Neurological Disorders (QSBB), UCL Institute of Neurology, London, UK were used as positive controls; donations to the QSBB were made according to ethically approved protocols and tissue is stored under a Human Tissue Authority licence: No. 12198.

For each IBM patient, medical notes were reviewed for baseline clinical characteristics and the following data were collected: date of birth, nature and onset of the disease, date of first symptoms, date IBM diagnosed, date of muscle biopsy, alternative initial diagnoses, physical examination at initial presentation and follow-up and CK level at initial presentation. The disease duration was calculated as the time between first symptoms and muscle biopsy.

2.3.2 Tissue preparation and staining

Muscle samples were frozen at the time of biopsy in isopentane cooled liquid nitrogen. Prior to sectioning, muscle tissue and control brain tissue were stored at -80^{o}C. Tissue sections were cut to a thickness of 8µm using a Bright cryostat, allowed to air dry and stored at -80^{o}C until stained.

2.3.2.1 IHC staining

Details of commercial antibodies are provided in Table 2.2. To determine the optimal staining conditions different methods of fixation, different primary and secondary antibodies for different

Antibody	Epitope	Host	Source	Clone	Catalogue number
p62	Human p62 ligand amino acid - 257-437	Mouse monoclonal	BD Transduction	3/P62 LCK	610832
TDP-43	N-terminal-260 amino acids	Rabbit polyclonal	Proteintech	NA	10782-2-AP
TDP-43	C-terminal-154 amino acids	Rabbit polyclonal	Proteintech	NA	12892-1-AP
TDP-43	Full length TDP-43	Rabbit polyclonal	ABNOVA	2E2-D3	H00023435-M01
TDP-43	CMDSKS(p)S(p)GWGM, S(p):phosphoserine 409/410.	Rabbit polyclonal	Cosmo Biologicals	pS409/410-1	CAC-TIP-PTD-M01
Tau	Amino acids 243-441	Rabbit polyclonal	Dako	NA	A002401-2
AT8	Amino acids around phosphorylated serine 202	Mouse monoclonal	Autogen Bioclear	AT8	90206
SMI 31	Phosphorylated epitope in neurofilament H and M	Mouse monoclonal	Covance	SMI-31	SMI-31P
Ubiquitin	Bovine ubiquitin	Rabbit polyclonal	Dako	NA	Z045801-2
Ubiquitin	NA	Rabbit polyclonal	Novocastra	NA	NCL-UBIQ
Ubiquitin	NA	Mouse monoclonal	Novocastra	Ubi-1	NCL-Ubi-1
Ubiquitin	Bovine ubiquitin	Mouse monoclonal	Chemicon	NA	MAB1510
$A\beta_{1-40}$	Residues 8-17 including C-terminal cysteine	Mouse monoclonal	Dako	6F/3D	M087201-2
$A\beta_{1-42}$	C-terminal	Mouse monoclonal	Autogen Bioclear	6G12	ABT112
α-Synuclein	Recombinant human alpha synuclein	Mouse monoclonal	Abcam	4D6	ab1903
α-Synuclein	Human alpha-synuclein residue 111-131 coupled to KLH	Rabbit polyclonal	Chemicon	NA	AB5038
FUS	Residues 500 and the C-terminus (residue 526)	Rabbit polyclonal	Novus Biologicals	NA	NB100-562
FUS	Residues 1 and 50 of human protein	Rabbit polyclonal	Novus Biologicals	NA	NB100-565
FUS	Synthetic peptide corresponding to a region of human FUS	Rabbit polyclonal	Sigma-Aldrich	NA	AV40278
Desmin	Human desmin	Mouse monoclonal	Dako	D33	M076001-2
Myotilin	C-terminal region of 266 amino acids	Mouse monoclonal	Novocastra	RSO34	NCL-Myotilin
α B-crystallin	Amino acids 1 to 10	Mouse monoclonal	Novocastra	G2JF	NCL-ABCRYS-512
VCP	Synthetic peptide corresponding to amino acids 792-806 of human VCP	Mouse monoclonal	Abcam	5	ab11433
Lamin A/C	NA	Mouse monoclonal	Novocastra	636	NCL-LAM-A/C
Emerin	222 amino acids near the N-terminus	Mouse monoclonal	Novocastra	4G5	NCL-Emerin
MHC Class I	NA	Mouse monoclonal	Novocastra	W6/32	NA
MHC Class I	45 kDa polypeptide products of the HLA-A, B and C loci.	Mouse monoclonal	Dako	W6/32	M073601-2
T-cell (CD3)	22/26/30 kD LSM and T cell ARC	Mouse monoclonal	Novocastra	UCHT1	NCL-CD3
Helper T-cell (CD4)	External domain of the human CD4 molecule	Mouse monoclonal	Novocastra	4B12	NCL-CD4-368
Cytotoxic T-cell (CD8)	Alpha chain cytoplasmic portion of human CD8	Mouse monoclonal	Novocastra	1A5	NCL-CD8-295
B-cell (CD20)	33 and 30 kDa intracytoplasmic epitope to human CD20	Mouse monoclonal	Novocastra	L26	NCL-CD20
Macrophage (CD68)	Lysosomal granules	Mouse monoclonal	Novocastra	KP1	NCL-CD68-KP1

Table 2.2 Commercial antibodies tested

p62 = Sequestosome 1; TDP-43 = Transactivation response DNA binding protein 43; Aβ = β – Amyloid; FUS = Fused in sarcoma protein; VCP = Valosin containing protein; MHC Class I = Major histocompatibility complex class I; HLA = Human leucocyte antigen; NA = Not available; LSM = Lymphocyte surface marker; ARC = Antigen receptor complex.

incubation times and at various dilutions were tested in control tissue known to contain the epitope of interest.

2.3.2.1.1 Fixation and post-fixation treatment

Frozen sections were warmed to room temperature and allowed to dry; brain tissue sections were left for ten minutes prior to fixation and muscle tissue sections one hour. Different methods of fixation were tried alone and in combination. Methods of fixation trialled prior to staining included acetone and 4% paraformaldehyde (PFA). Incubation times between five and 30 minutes were trialled. Post-fixation formic acid was trialled at different concentrations to enhance staining for Aβ. Tissue sections were then washed in running water for five minutes and incubated in 0.5% hydrogen peroxide for 20 minutes to eliminate any endogenous peroxidase activity. After a further wash in running water for five minutes sections were incubated in 5% normal goat serum (Vector Laboratories, Burlingame, California) for 30 minutes at room temperature (RT).

2.3.2.1.2 Primary antibodies

After fixation, tissue sections were stained using IHC for a number of proteins (Table 2.2). The optimum titration was determined by trialling serial dilutions for different incubation times and at different ambient temperatures in control tissue. Positive and negative controls were included on each occasion. Negative controls were a positive control tissue section treated in the same manner except the tissue sections were incubated with phosphate buffered saline (PBS) instead of the primary antibody.

2.3.2.1.3 Visualisation of antigen antibody binding

A number of different protocols were trialled to achieve the best visualisation of the antigen-antibody complex:

i) Dako REAL™ EnVision™ Detection System (Dako, Cambridgeshire)

Following incubation with the relevant primary antibody, tissue sections were incubated in a horseradish-peroxidase (HRP) rabbit/mouse reagent for 30 minutes at 25°C. They were then washed three times for three minutes with PBS and incubated in a 1:50 solution of 3,3'-diaminobenzidine (DAB) for three to five minutes.

ii) Vector stain Elite ABC kit (Vector Laboratories, Burlingame, California)

Following incubation with the relevant primary antibody, tissue sections were incubated with a biotinylated anti-immunoglobulin at a dilution of 1:200 for 30 minutes at 25°C then washed again three times for three minutes with PBS. After washing, the tissue sections were incubated in vectastain® Elite ABC Reagent (avidin DH-biotinylated HRP H) 1:25 complex solution for 30 minutes at 25°C. The sections were washed three times for three minutes with PBS and incubated in a peroxidase solution containing 5% DAB solution (Sigma, D5637) activated with hydrogen peroxide (32 µl per 100 ml of solution) for five to 10 minutes until the desired stain intensity developed.

iii) Glucose oxidase nickel method

Tissue sections were incubated with a biotinylated anti-rabbit or anti-mouse IgG antibody at a dilution of 1:200 for 30 minutes at 25°C. Tissue sections were washed three times for three minutes with PBS and then incubated with an avidin-biotin complex at RT for 30 minutes. After a further three washes with PBS they were incubated in 100 ml of reaction solution [reaction solution: 2000 ml 0.1% acetate buffer (200 ml 0.1% glacial acetic acid and 3800 ml of 1 M sodium acetate), 50 g nickel ammonium sulphate and 0.8g ammonium chloride] to which 120mg of beta-D-glucose, 50 mg DAB and 10 µl glucose oxidase were added for approximately nine minutes. The tissue sections were washed in cold running tap water for five minutes. The staining of control sections were checked using a light-microscope. If required, sections were replaced back in the chromogen solution to intensify the staining observed.

2.3.2.1.4 Counterstain and mounting

Tissue sections were counterstained with Mayer's haematoxylin for 20 seconds and washed in warm running tap water for ten minutes. Tissue sections were dehydrated in graded alcohol solutions (70%, 90% and 100%), cleared in three changes of xylene and mounted with DPX (VWR BDH Prolabo), a synthetic mounting media made of distyrene, a plasticizer, and xylene.

2.3.2.1.5 Tinctoral staining

Samples were stained with H&E and for amyloid using Congo red, alkalinised Congo red, crystal violet and thioflavin S. These staining techniques were optimised in AD brain tissue by varying concentration of dye solutions and the duration of incubations and washes. Tissue sections were warmed to room temperature and allowed to dry prior to staining.

2.3.2.1.6 H&E staining

Muscle sections were allowed to equilibrate to RT then stained and mounted using an automated system comprising a Leica ST 5020 automated staining machine (Leica Microsystems, Wetzlar, Germany) and Leica CV 5030 glass cover slipping machine (Leica Microsystems, Wetzlar, Germany).

2.3.2.1.7 Alkalinised Congo red staining

The method was adapted from the 'Manual of histological techniques and their diagnostic application' (Bancroft et al., 1994).

Tissue sections were placed in Mayer's haematoxylin for five minutes and then rinsed in three changes of distilled water. They were then transferred to a solution containing 80% ethanol saturated with sodium chloride. The pH of this solution had been adjusted to between 10.5 and 11.0 with concentrated sodium hydroxide. Tissue sections were then placed in filtered alkalinised Congo red dye (0.2 g of Congo red dye; 100 ml of 80% ethanol saturated with sodium chloride; pH

adjusted to 10.5-11.0 with concentrated sodium hydroxide). The tissue sections were then dehydrated in 95% ethanol cleared in xylene and mounted with DPX (VWR BDH Prolabo).

2.3.2.1.8 Crystal violet staining

Method kindly provided by W. King Engel and Valerie Askanas MD, PhD Laboratories, USC Neuromuscular Center, Los Angeles, California, USA.

Tissue sections were fixed in formal-saline (450 ml distilled water; 50 ml formaldehyde; 4.25 g sodium chloride) for 15 minutes and then placed in a bath of crystal violet solution [equal volumes of crystal violet stock (14 g crystal violet powder; 100 ml of 95% ethanol) and 95% ethanol] for ten minutes. Tissue sections were then washed in cold running water for ten minutes and mounted using VECTASHIELD® aqueous mounting media - not Apathy's gum syrup as described in the original method, sealed with nail-varnish and stored at 4^{o}C.

Incubation times, washing times and concentration of crystal violet stock were altered to achieve the optimum staining results.

2.3.2.1.9 Thioflavin S staining

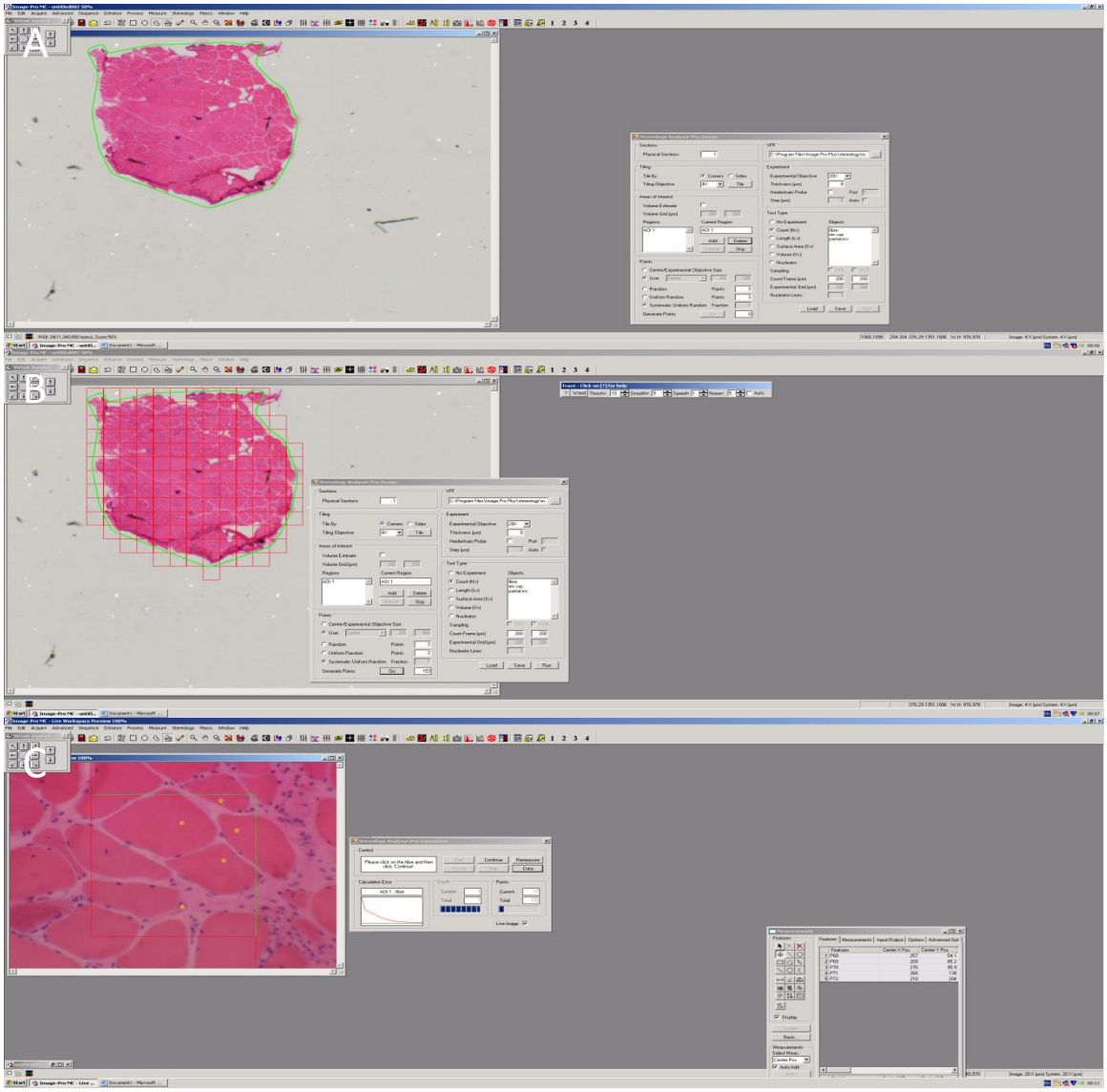
Tissue sections were fixed in acetone for ten minutes then washed in cold running tap water for ten minutes. They were then placed in thioflavin S solution for seven minutes and differentiated in 70% alcohol until the white matter of the positive control turned a pale yellow colour. Tissue sections were then left in a light-tight jar of PBS overnight and mounted the following day using VECTASHIELD® aqueous mounting media, sealed with nail-varnish and stored in a light-tight package in the refrigerator at 4^{o}C.

2.3.3 Definitions and quantification

Slides were assessed in a random order and blind to the clinical details. Slides stained with H&E and for p62, TDP-43, desmin, α B-crystallin, myotilin, ubiquitin, FUS, VCP, AT8, tau, Aβ, α-synuclein, lamin A/C and emerin were analysed using a light microscope fitted with an automated XY stage controlled by image analysis software ImagePro version 6.2 (Media Cybernetics, Rockville, MD, USA) to ensure that the whole biopsy was systematically analysed. Using ImagePro 6.2 the whole tissue section was selected at an objective magnification of x4 and then divided into consecutive 100 x 100μm boxes (Figure 2.1). The microscope is then sequentially guided at an objective magnification of x40 through the tissue section in 100 x 100 μm boxes, allowing the whole biopsy to be assessed without repetition. The numbers of abnormal muscle fibres in the biopsies were quantified (Table 2.3). Muscle fibres were counted if they were within the confines of the box or crossed the upper or right-hand border and excluded if they crossed the lower or left-hand border. The total number of muscle fibres and number of muscle fibres containing rimmed vacuoles or undergoing partial invasion in each case were quantified using H&E stained sections. Following specific staining, the number of muscle fibres containing protein aggregates was quantified and expressed as a percentage of the total number of muscle fibres in the biopsy. Only transversely orientated fibres were quantified; abnormalities in longitudinally orientated and necrotic muscle fibres were excluded from the analysis.

Tissue sections stained with Congo red were visualised with a fluorescence microscope using a x40 objective lens and a polarising microscope using a x100 oil-immersion objective lens. Areas of fluorescence were examined using both the rhodamine red (excitation 512-546 and emission 600-640) and fluorescein isothiocyanate (FITC) (excitation 440-480 and emission 527-530) filters to exclude auto-fluorescence. The sections were analysed systematically in the following manner: starting at the top left hand corner, the tissue section was scanned horizontally from left to right until the edge was reached. Once the edge of the tissue was reached the counting frame was moved

Figure 2.1 Depiction of stereological assessment of tissue sections using ImagePro 6.2



With ImagePro 6.2 software the area to be quantified was selected at an objective magnification of x4 (A). The area selected was converted into 100 x100 µm grid (B). The microscope is guided around the grid box by box at an objective magnification of x40. Muscle fibres, rimmed vacuoles or protein aggregates within each box are then counted if they are within the confines of the box or cross the upper or right-hand border (green lines) and excluded if they crossed the lower or left-hand border (red lines).

Table 2.3 Definitions of pathological features

Stain/feature	Criteria
Haematoxylin and eosin	
Rimmed vacuole	As per Table 2.1
Partial invasion	As per Table 2.1
Immunohistochemistry	
Protein aggregates	Area of definite staining within the same plane as the muscle tissue, residing within the sarcolemma in either a structurally normal or vacuolated muscle fibre. Diffuse staining affecting the whole of a fibre was not counted as an aggregate nor were protein aggregates in necrotic fibres or regenerating fibres. Intra-nuclear staining was noted but not quantified.
Inflammatory cell	A nucleus fully circumscribed by a ring of positive staining. Cells had to be of lymphoid shape, this was to specifically avoid inclusion of CD4 positive dendritic cells.
Cytotoxic T-cell partial invasion	Assessed on sections stained with an antibody to CD8. As per Table 2.1
MHC Class I	As per Table 2.1
Amyloid staining	
Alkalinised Congo red	Polarising microscope: positive staining had to have apple-green birefringence and reside within the sarcolemma. Fluorescence microscope: fluorescent areas must be within the sarcolemma and fluorescent in only the rhodamine red (Texas red) channel. Areas of auto-fluorescence were excluded by examining slides with two channels.
Crystal violet	Amyloid aggregates were defined as bright pink to red in colour on a blue-purple background of the tissue and within the sarcolemma.
Thioflavin S	Fluorescence microscope: fluorescent areas must be within the sarcolemma and fluorescent in a single channel. Areas of auto-fluorescence were excluded by examining slides with two channels.

MHC Class I = Major histocompatibility complex class I; CD = Cluster of differentiation protein.

down by one frame and then across the section from right to left. This was repeated until the whole tissue section had been covered (Figure 2.2).

Inflammatory cells present in the biopsy were quantified by two methods. Firstly, all positive cells in five adjacent fields were counted using a x20 objective lens in the following manner: the first field selected was the top left corner of the tissue section. Secondly, the quantity of inflammatory cells in the entirety of the biopsy was assessed using a modified version of the juvenile dermatomyositis score tool (Figure 2.3) (Wedderburn et al., 2007). The score tool was altered to concentrate on inflammatory features, other domains in the score tool: vascular domain, muscle fibre domain, connective tissue domain and visual analogue scale were excluded.

Ten per cent of tissue sections were recounted a minimum of two weeks after the initial count to ensure the reliability of the quantification.

2.3.4 Statistical analyses

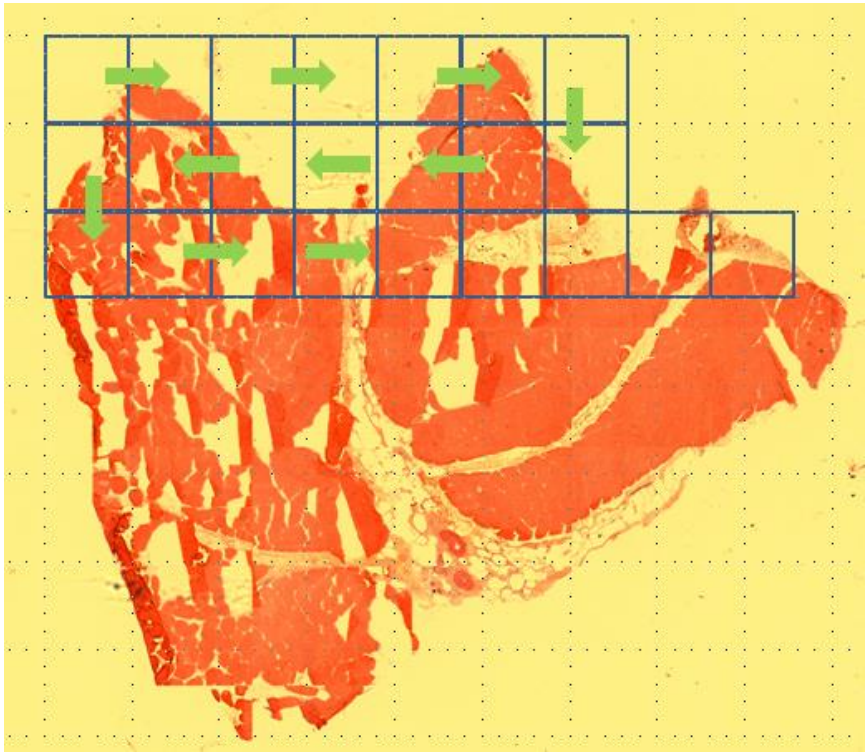
Intra-observer variability was calculated using a Bland-Altman plot. Groups were compared using the Mann Whitney *U*-test. Spearman's rank order correlation was used to determine strength and direction of associations between pathological findings. Linear regression was used to determine relationships between clinical features and pathological findings.

2.4 Assessment of pathological biomarkers in IBM and disease controls.

2.4.1 Cases

Forty-eight patients were categorised, depending on clinical features and pathological findings, into five groups: IBM with rimmed vacuoles on muscle biopsy (IBM+RV), IBM without rimmed vacuoles on muscle biopsy (IBM-RV), steroid-responsive inflammatory myopathies (PM&DM), protein accumulation myopathies with rimmed vacuoles on muscle biopsy (PAM+RV) and normal muscle. Inclusion criteria are detailed in Table 2.4.

Figure 2.2 Stereological assessment of a tissue section



Tissue sections stained for amyloid and inflammatory cells were analysed systematically in the following manner: starting at the top left hand corner the tissue section was scanned horizontally from left to right until the tissue edge was reached. The counting frame was then moved down by one frame and the tissue section was scanned from right to left. This process was repeated until the whole tissue section was covered.

Figure 2.3 Modified inflammatory score tool

IBM Inflammatory Score Tool

Case Number:_____ Date:_____

	Score	Description
CD3+ endomysial infiltration	0, 1, 2	For each inflammatory cell type in the endomysial, perimysial and perivascular locations score positive infiltrating cells as follows: if none or <4 cells in a x20 field- score 0; if >4 cells in a x20 field and/or 1 cluster (where a cluster is ≥10 cells) - score 1; if >2 clusters in the entire biopsy, and/or diffusely infiltrating cells (i.e.> 20 cells in a x20 field) - score 2.
CD3+ perimysial infiltration	0, 1, 2	
CD3+ perivascular infiltration	0, 1, 2	
CD4+ endomysial infiltration	0, 1, 2	
CD4+ perimysial infiltration	0, 1, 2	
CD4+ perivascular infiltration	0, 1, 2	
CD8+ endomysial infiltration	0, 1, 2	
CD8+ perimysial infiltration	0, 1, 2	
CD8+ perivascular infiltration	0, 1, 2	
CD20+ endomysial infiltration	0, 1, 2	
CD20+ perimysial infiltration	0, 1, 2	
CD20+ perivascular infiltration	0, 1, 2	
CD68+ endomysial infiltration	0, 1, 2	
CD68+ perimysial infiltration	0, 1, 2	
CD68+ perivascular infiltration	0, 1, 2	
MHC Class I	0, 1, 2	For the whole biopsy score as follows: normal (capillary staining only) - score 0; if increased: i) mildly (weak diffuse sarcolemmal staining or scattered positive muscle fibres) - score 1; ii) strongly increased (diffuse definite sarcoplasmic and sarcolemmal increase in staining) score 2.

*Adapted from the published juvenile dermatomyositis score tool (Wedderburn et al., 2007).
MHC Class I = Major histocompatibility complex class I; CD = Cluster of differentiation protein.

Table 2.4 Clinical and pathological inclusion criteria

Diagnosis	Clinical features
IBM+RV	Age at symptom onset >35 years; symptoms present for >12 months; typical distribution of weakness including finger flexion strength less than shoulder abduction and knee extension weakness greater than hip flexion; CK <15 times the upper limit of normal; and rimmed vacuoles present on H&E or GT stained sections without atypical features present with standard diagnostic histological assessment.
IBM-RV	Age at symptom onset >35 years; symptoms present for >12 months; typical distribution of weakness including finger flexion strength less than shoulder abduction strength and knee extension weakness greater than hip flexion weakness; CK <15 times the upper limit of normal; and without atypical features present with standard diagnostic histological assessment nor rimmed vacuoles on H&E and GT stained sections.
PM&DM	PM - subacute onset of limb girdle weakness without distal weakness; significantly raised CK; an inflammatory cell infiltrate without the presence of pathological features inconsistent with the diagnosis of a steroid-responsive inflammatory myopathy; and a sustained unequivocal clinical and biochemical response to steroid immunosuppression. DM – as for PM with cutaneous manifestations consistent with a diagnosis of DM.
PAM+RV	Genetically or clinically and pathological confirmed cases of protein accumulation myopathy with typical rimmed vacuoles present on muscle biopsy.
Normal muscle	Investigated for cramps and/or fatigue; normal clinical examination performed by a muscle specialist; normal CK; normal neurophysiological assessment; and normal muscle biopsy.

CK = Creatine kinase; H&E = Haematoxylin and eosin; GT = Gomori trichrome; IBM+RV = IBM with rimmed vacuoles on muscle biopsy; IBM-RV = IBM without rimmed vacuoles on muscle biopsy; PM&DM = Steroid-responsive inflammatory myopathies; DM = Dermatomyositis; PAM+RV = Protein accumulation myopathies with rimmed vacuoles on muscle biopsy.

2.4.2 Tissue staining

2.4.2.1 IHC and Congo red staining

Details of the H&E and alkalinised Congo red staining are documented above in sections 2.3.2.2.1 and 2.3.2.2.2 respectively. Details of the antibodies used and their optimum conditions are provided in Chapter 4, Table 4.2. Eight µm thick frozen sections were stained with tinctoral stains H&E and alkalinised Congo red and histochemically (HC) with combined COX/SDH. Tissue sections were stained using IHC with antibodies to p62, TDP-43, myotilin, ubiquitin, MHC Class I, T-cells (CD3), helper T-cells (CD4), cytotoxic T-cells (CD8), macrophages (CD68) and B-cells (CD20). Positive and negative controls were included on each occasion. Tonsillar tissue and tissue from brains donated to the QSBB, UCL Institute of Neurology, London were used as positive controls for IHC and alkalinised Congo red staining.

2.4.2.2 COX/SDH HC staining

Tissue sections were thawed and warmed to RT and then incubated with COX solution (Appendix 1) for 60 minutes at 37^{o}C. They were then washed with distilled water and incubated with SDH solution (Appendix 2) for 45 minutes at 37^{o}C. Sections were drained and placed in a bath of 10% formalin in tap water for 15 minutes then washed well in running tap water, dehydrated in 95% ethanol and mounted using DPX (VWR BDH Prolabo).

2.4.3 Definitions and quantification

Definitions of pathological features are summarised in Tables 2.1 and 2.3.

The quantification was performed in the same manner as that documented in section 2.3.3. However, instead of using a light microscope tissue sections were digitally scanned at an objective magnification of x40 using a Leica SCN400 slide scanner (Leica Microsystems, Wetzlar, Germany) and visualised using SlidePath digital image hub (Leica Microsystems, Wetzlar, Germany). The whole biopsy was assessed starting from the top left hand corner. Each tissue

section was scanned horizontally from left to right until the edge of the tissue was reached. Once the edge was reached the counting frame was moved down by one frame and then across the section from right to left. This was repeated until the whole tissue section had been systematically covered (Figure 2.2). As previously, to avoid counting histological features more than once they were only counted if the fibre they were in resided within the confines of the counting frame or crossed the upper or right-hand border and were excluded if they crossed the lower or left-hand border. Congo red stained slides were analysed on fluorescent and polarising microscopes with a x40 and a x100 magnification objective lens in the same manner as described above in section 2.3.3. Inflammatory changes were assessed as described in section 2.3.3.

Ten per cent of tissue sections were recounted a minimum of two weeks after the initial count to ensure the reliability of the quantification. The presence of pathological features in sections stained with H&E, alkalinised Congo red and IHC for protein aggregates was independently assessed by two observers.

2.4.4 Statistical analysis

Continuous and categorical variables were compared using Mann Whitney *U*-test and chi-squared or Fisher's exact test respectively. The median and mean values are accompanied by the interquartile range and standard deviation respectively. Sensitivity and specificity were calculated using 2x2 contingency tables. The diagnostic performance of different cut-offs was assessed using Receiver Operating Characteristic (ROC) curves. Intra-observer and inter-observer agreement were calculated using Bland-Altman plots and Cohen kappa (κ) statistic respectively. Statistical significance was set at $p < 0.05$.

2.5 Proteomic analysis of IBM muscle

2.5.1 Cases

Five clinically typical and pathologically definite cases of IBM were identified from the archives at the National Hospital for Neurology and Neurosurgery, Queen Square, London. All five cases satisfied the 2011 ENMC criteria for clinically-defined IBM and the Griggs criteria for possible IBM. One further case was identified from the Berufsgenossenschaftliches Universitätsklinikum Bergmannsheil and included in the study.

2.5.2 Detection of rimmed vacuoles and immunofluorescent aggregates

Consecutive ten μm thick frozen sections were cut and placed on glass slides or polyethylene terephthalate (PET) membrane slides (Leica Microsystems, Wetzlar, Germany) to air-dry prior to being stained. Tissue sections were stained with H&E and immunofluorescence (IF) techniques to identify rimmed vacuoles and immunofluorescent protein aggregates respectively.

2.5.3 IF staining

IF staining was performed with antibodies directed against p62, LC3 and myotilin. Tissue sections were incubated with two per cent bovine serum albumin (BSA) for 30 minutes. Tissue sections were then incubated with one of the three primary antibodies at 4^{o}C overnight. The tissue sections were washed three times with PBS and then incubated in the dark with an appropriate secondary antibody conjugated to fluorescent marker - DyLight 488 (Dianova, Hamburg, Germany). The conditions for each antibody are detailed in Table 2.5. Tissue sections were washed a further three times with PBS. PET membrane slides were then air dried and stored at 4^{o}C. Tissue sections on glass slides were mounted and cover-slipped using glycerol gelatine mounting media.

2.5.4 Laser capture microscopy

For each case, areas identified for laser capture microscopy (LCM) were individually dissected and collected using a Leica laser dissecting microscope (LMD 6500, Leica Microsystems, Wetzlar,

Table 2.5 Primary antibodies and conditions for IF staining

	Antibody	Source	Clone	Dilution	Primary incubation conditions	Blocking	Secondary	Secondary incubation conditions
1	p62	BD Transduction	3/P62 LCK	1:400	24 hours, 4^0C	2% BSA	Anti-mouse conjugated with Dylight 488	45 minutes, RT
2	LC3 A/B	Cell Signaling	NA	1:50	24 hours, 4^0C	2% BSA	Anti-rabbit conjugated with Dylight 488	45 minutes, RT
3	Myotilin	Novocastra	RS034	1:20	24 hours, 4^0C	2% BSA	Anti-mouse conjugated with Dylight 488	45 minutes, RT

p62 = Sequestosome 1; LC3 A/B = Microtubule-associated protein 1A/1B-light chain 3; BSA = Bovine serum albumin; RT = Room temperature; NA = Not available.

Germany). Two hundred and fifty thousand μm^2 of muscle per sample was collected in individual 1.5 ml Eppendorff tubes. Forty µl of 98-100% formic acid (FA) was added to each sample. Samples were left to stand for 30 minutes at RT. They were then vortexed briefly and sonicated (RK31, BANDELIN electronic, Berlin, Germany) for five minutes. Finally, samples were centrifuged for five minutes at 10,000 rpm before being stored at -80^{o}C.

2.5.5 Protein digestion

Once all samples had been collected, they were removed from the freezer and warmed to RT. FA was removed by vaporisation in a rotational vacuum (RVC2-25CD plus, Martin Christ GmBH, Osterode am Harz, Germany). The samples were made up to a volume of 74.25 µl with 50 mM ammonium bicarbonate (pH 7.8) and reduced by adding 0.25 µl of dithiothreitol. Following this, the samples were incubated at 56^{o}C for 20 minutes before 0.55 M iodoacetamide was added. They were then left to rest for 15 minutes at RT. The sample pH was then adjusted to 7.4 and 1 µl of 1% Trypsin Enhancer ProteaseMAX Surfactant (Promega, Mannheim, Germany) and 1.8 µl of trypsin (Serva Electrophoresis GmBH, Heidelberg, Germany) were added to them. The samples were then incubated overnight at RT. Samples were individually filtered with OMIX C_{18} pipette tips (Varian, Agilent Technologies, Böblingen, Germany) and concentrated in a rotational vacuum. They were then made up to a volume of 63 µl with 1% trifluoroacetic acid.

2.5.6 High-performance liquid chromatography and tandem mass spectrometry

Fifteen µl from each sample was used for analysis. Chromatographic separation was performed by high performance liquid chromatography (HPLC) using an Ultimate 3000 RSLCnano LC system (Dionex, Idstein, Germany) which was attached to a nanoelectrospray ionisation source (Thermo Fisher Scientific, Schwerte, Germany). Samples were loaded onto the HPLC and separated at a flow rate of 400nl per minute. Tandem mass spectrometry (MS/MS) was performed on an LTQ Orbitrap Velos (Thermo Fisher Scientific, Schwerte, Germany). Mass spectrometry (MS) spectra were acquired for a mass range between 300 and 2000 m/z. The twenty most intensely charged

ions were isolated for fragmentation in the ion trap with collision energy of 35%. The acquisition time was set at 50 ms.

2.5.7 Data processing

The raw files generated were analysed using Mascot (Matrixscience, London, UK). Peptides were identified against a database created by DecoyDatabaseBuilder containing the Uniprot/Swissprot database. Mass tolerance was set at 10 parts per million for peptides. Fragment mass tolerance was set at 0.5 Da. One missed cleavage site was allowed and carbidomethylation, oxidation and phosphorylation were defined as variable modifications. After peptide identification, a false discovery rate (FDR) was calculated for each protein group. FDR was set at 5%.

2.5.8 Data analysis

Data produced were analysed using Microsoft Excel pivot tables. Peptides whose sequence could be attributed to more than one protein were excluded. Only unique peptides were entered into the database and used to identify proteins. Quantification was based upon spectral index (SI) calculation. The spectral counts were summed to produce SI. Protein lists were then interrogated to identify differentially expressed proteins between samples. For a protein to be classed as differentially expressed the ratio between mean SI of samples being compared was set at greater than 1.8 or less than 0.55 and $p < 0.05$. Bioinformatic analyses were performed using Cytoscape 2.8.3 [National Institute of General Medical Sciences (NIGMS), America] with a Biological Networks Gene Ontology (BiNGO) plugin. *P* values were adjusted for multiple-testing using Benjamini-Hochberg FDR correction.

Chapter 3

CLINICAL CHARACTERISATION OF PATIENTS WITH IBM

3.1 Introduction

Historically, IBM has been classified as an IIM, along with DM and PM. However, clinically there are rather more differences than similarities with early involvement of finger flexor and knee extensor muscles, often asymmetric weakness, and lack of a significant response to immunosuppression in IBM (Amato et al., 1996). Weakness of the knee extensors often causes patients to present with falls and finger flexion weakness leads to profound problems with many activities of daily living. The clinical course is invariably slowly progressive with most patients eventually requiring mobility aids and many becoming severely incapacitated by the disease, although given the generally late onset it only infrequently shortens life-expectancy (Benveniste et al., 2011).

Whether IBM is primarily an inflammatory or degenerative disease is debated, with a consistently poor response to immunosuppressive medication taken as an argument in favour of the latter (Amato et al., 1996)(Benveniste et al., 2011). Largely because of our lack of knowledge as to the cause of IBM, there is currently no single gold-standard diagnostic test and consequently a number of diagnostic criteria have been proposed, most of which have emphasised the pathological features. The most extensively used and quoted diagnostic criteria are the Griggs criteria (Griggs et al., 1995); these require the presence of an inflammatory infiltrate, inflammatory cell invasion of intact fibres (partial invasion), rimmed vacuoles and either amyloid using an appropriate histological method or 15-18 nm tubulofilaments on EM for a diagnosis of definite IBM. A diagnosis of possible IBM can be made if the first three light microscopic pathological features are present in addition to certain clinical features.

The pathological features in combination are thought to be highly specific; however their sensitivity is increasingly being questioned (Chahin and Engel, 2008). Since the delineation of IBM as a separate entity to PM in the early 1970s, it has been realised that many patients have a characteristic clinical picture in terms of their presentation, pattern of muscle weakness and progression over time. However, patients with the characteristic clinical features may lack the diagnostic pathological findings, even despite repeated muscle biopsy (Amato et al., 1996)(van der Meulen et al., 1998)(Chahin and Engel, 2008)(Benveniste et al., 2011). Few studies have assessed in detail patients lacking the pathological features on biopsy. Newer criteria have been suggested to allow a diagnosis of IBM to be made with a supportive, if not diagnostic, muscle biopsy (Benveniste and Hilton-Jones, 2010)(Hilton-Jones et al., 2010). However, little data is available on the sensitivity and specificity of the individual clinical findings or the disease outcomes in patients lacking the currently necessary diagnostic pathological features to categorically label them as having IBM.

3.2 Hypothesis

IBM has a characteristic clinical presentation that is both specific and sensitive and independent of the current diagnostic pathological features.

3.3 Aims

To address the current uncertainties discussed above by studying and comparing the clinical presentation, pathological findings and disease progression in patient with clinically typical IBM that lack the current diagnostic pathological features and patients with pathologically typical IBM.

3.4 Methods

Clinical data on disease presentation and progression for all patients with a final diagnosis of IBM who were seen within the muscle service at the Radcliffe Infirmary/John Radcliffe Hospital, Oxford, UK between 1982 and 2011 and whose muscle biopsy and clinical data were available

from their first presentation were collected. All muscle biopsies were reviewed blinded to the clinical details. The clinical presentation and outcomes between patients of different genders, different ages at presentation and those that were or were not treated with immunosuppressive therapy were compared. Patients were classified as either pathologically diagnosed (Griggs definite and possible IBM) or clinically diagnosed [revised ENMC criteria (Table 3.1)] IBM and comparisons between these two groups were made. Additionally, the clinical features of IBM patients were compared with patients with other diseases considered in the differential diagnosis of IBM; these included 15 cases of steroid-responsive inflammatory myopathy (PM&DM) and 12 cases of adult onset protein accumulation myopathy (PAM) (11 MFM and 1 hIBM). Further, because rimmed vacuoles are traditionally considered a hallmark of IBM, patients were divided into two groups depending on the presence or absence of rimmed vacuoles, and features between these two groups were compared.

3.5 Results

3.5.1 Demographics

The demographic characteristics of patients with IBM are summarised in Table 3.2.

A total of 67 patients were included; 66 (99%), patients were Caucasian and one was Asian. There were twice as many male than female patients, 46 (69%) *v.* 21 (31%). The median disease duration at last follow-up was 9 years (6-14). The median age of disease onset was 62 years (55-70) and no patients were aged less than 30 years at disease onset. The median age at muscle biopsy was 67 years (61-75). The median delay to diagnosis from disease onset was 62 months (34-75) and twenty five patients (37%) received at least one alternative diagnosis before being diagnosed with IBM; most commonly PM. Other diagnoses included neuropathies, drug induced myopathies and auto-immune diseases. Eight (14%) patients received immunosuppressive therapy for IBM. The immunosuppressive treatments received were a combination of prednisolone with either azathioprine or methotrexate.

Table 3.1 Revised 2011 ENMC diagnostic criteria for IBM

Clinical features	Classification	Histopathological features
Duration of weakness >12 months Creatine kinase ≤15x ULN Age at onset >45 years Finger flexion weakness > shoulder abduction weakness ***AND/OR*** Knee extension weakness ≥ hip flexor weakness	Clinicopathologically defined IBM	*All of the following:* Endomysial inflammatory infiltrate Rimmed vacuoles Protein accumulation* or 15-18 nm filaments
Duration of weakness >12 months Creatine kinase ≤15x ULN Age at onset >45 years Finger flexion weakness > shoulder abduction weakness ***AND*** Knee extension weakness ≥ hip flexor weakness	Clinically defined IBM	*One or more, but not all, of:* Endomysial inflammatory infiltrate Up-regulation of MHC Class I Rimmed vacuoles Protein accumulation* or 15-18 nm filaments
Duration of weakness >12 months Creatine kinase ≤15x ULN Age at onset >45 years Finger flexion weakness > shoulder abduction weakness ***OR*** Knee extension weakness ≥ hip flexor weakness	Probable IBM	*One or more, but not all, of:* Endomysial inflammatory infiltrate Up-regulation of MHC Class I Rimmed vacuoles Protein accumulation* or 15-18 nm filaments

ULN = Upper limit of normal; MHC Class I = Major histocompatibility complex class I.
*Demonstration of amyloid or other protein accumulation by established methods (e.g. for amyloid Congo red, crystal violet, thioflavin T/S, for other proteins p62, SMI-31, TDP-43). Current evidence favours p62 in terms of sensitivity and specificity but the literature is limited and further work required.

Table 3.2 Demographic characteristics of the groups analysed

Characteristic	IBM	IBM+RV	IBM-RV	IBM+RV *v.* IBM-RV *p* value	IBM-C	IBM-P	IBM-P *v.* IBM-C *p* value	Male	Female	Male *v.* female *p* value	IBM+IS	IBM-IS	IBM+IS *v.* IBM-IS *p* value
No. of patients	67	29	38	-	43	18	-	46	21	-	8	57	-
Gender, M:F	46:21	20:9	26:12	0.96	30:13	15:3	0.35	-	-	-	3:5	42:15	0.09
Age at onset (IQR), years	62 (55-70)	63 (57-72)	61 (52-68)	0.19	62 (57-70)	63 (56-72)	0.73	62 (55-71)	61 (51-70)	0.39	52 (39-63)	63 (51-70)	0.02*
Age at biopsy (IQR), years	67 (61-75)	73 (64-76)	66 (59-74)	0.04*	67 (63-75)	74 (61-77)	0.33	67 (61-75)	71 (61-77)	0.69	56 (45-67)	71 (61-77)	0.01*
Delay to diagnosis (IQR), months	62 (34-90)	58 (33-106)	63 (35-89)	0.44	52 (32-90)	65 (36-115)	0.43	50 (30-75)	80 (43-146)	0.005*	57(10-88)	62 (38-99)	0.42
Onset, *n* (%)													
Lower limbs	55 (82)	24 (83)	31 (82)	0.90	34 (79)	15 (3)	1.00	40 (87)	15 (79)	0.12	6 (75)	47 (82)	0.63
Upper limbs	5 (8)	1 (3)	4 (12)	0.38	5 (12)	0 (0)	0.31	2 (4.3)	3 (14.3)	0.32	0 (0)	5 (9)	1.00
Bulbar weakness	1 (1)	1 (3)	0 (0)	0.43	1 (2)	0 (0)	1.00	0 (0)	1 (5)	0.31	1 (13)	0 (0)	0.12
Lower and upper limbs	4 (6)	1 (3)	3 (8)	0.63	3 (7)	1 (6)	1.00	3 (7)	1 (5)	0.53	1 (13)	3 (5)	0.42
Bulbar and lower limbs	2 (3)	2 (7)	0 (0)	0.18	0 (0)	2 (11)	0.10	1 (2)	1 (5)	0.53	0 (0)	2 (4)	1.00
Alternative diagnosis	26 (39)	8 (28)	18 (47)	0.10	16 (37)	6 (33)	0.77	15 (32)	11 (52)	0.12	5 (63)	19 (33)	0.14
Associations, *n* (%)													
Neoplastic disease	6 (9)	2 (7)	4 (11)	0.69	3 (7)	2 (11)	0.63	4 (9)	2 (10)	1.00	0 (0)	6 (11)	1.00
Auto-immune disease	8 (12)	6 (21)	2 (6)	0.07	5 (12)	3 (11)	1.00	5 (11)	3 (14)	0.70	1 (13)	7 (12)	1.00

IQR = Interquartile range; IBM+RV = IBM with rimmed vacuoles on muscle biopsy; IBM–RV = IBM without rimmed vacuoles on muscle biopsy; IBM–C = Clinically diagnosed IBM (ENMC clinically defined and ENMC probable); IBM-P = Pathologically diagnosed IBM using the Griggs criteria (Griggs definite and Griggs possible); IBM+IS = IBM patients treated with immunosuppressive medication; IBM–IS = IBM patients not treated with immunosuppressive medication; CK = Creatine kinase. *Statistically significant results (p <0.05).

Age at biopsy was younger in patients lacking rimmed vacuoles on muscle biopsy compared to those in whom rimmed vacuoles were present (66 *v*. 74 years; p=0.04); delay to diagnosis was longer in female patients compared to male patients (80 *v*. 50 months; p=0.005); and age at disease onset and biopsy were younger in patients treated with immunosuppressive medication compared to those who were not (52 *v*. 63 years; p=0.02; and 56 *v*. 71 years; p=0.01 respectively).

3.5.2 Presentation and associated conditions

The clinical findings at presentation are summarised Table 3.2.

The initial symptoms in all patients were falls and/or weakness. Fifty-five (82%) reported, predominantly proximal, lower limb weakness as their initial symptom, five (8%) presented with weakness of grip and one (2%) with dysphagia. The remaining six patients' initial symptoms were a combination of upper and lower limb weakness (6%) or dysphagia and lower limb weakness (3%). There were no differences in clinical features at presentation in the subgroups analysed.

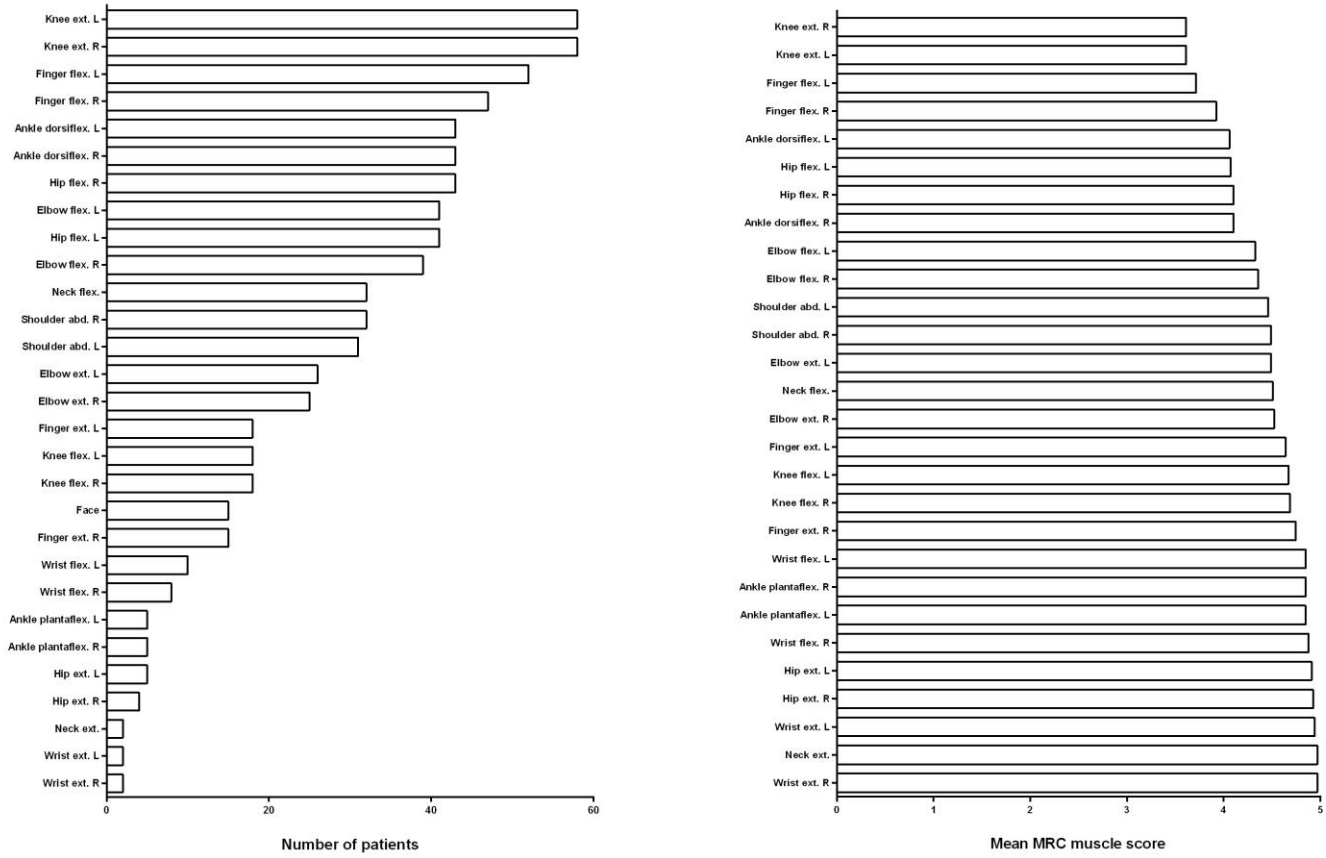
Six (9%) patients had a prior history of neoplastic disease at presentation. The commonest neoplasia was leukaemia, diagnosed in three patients. There was no obvious temporal association between the diagnosis of IBM and the diagnosis of neoplastic disease. Auto-immune diseases were present in eight (12%) patients. These included coeliac disease (n=2), rheumatoid arthritis (n=2), vitiligo (n=2), pemphigoid (n=1) and one patient with ulcerative colitis and sarcoidosis.

3.5.3 Pattern and distribution of weakness in IBM

The clinical examination findings at presentation are summarised in Figures 3.1 and Table 3.3.
The five most frequently affected muscle groups at presentation were the knee extensors 58 (87%), finger flexors 53 (79%), ankle dorsiflexors 44 (66%), hip flexors 43 (64%) and elbow flexors 42 (63%) (Figure 3.1 A).

Figure 3.1 Distribution and severity of weakness at presentation

A. **B.**



Bar charts showing the frequency different muscle groups are affected at presentation (A) and the severity of weakness in different muscle groups as measured by the Medical Research Council muscle score (B). The most frequently affected muscles were also the most significantly affected muscles. These were the knee extensors, finger flexors and ankle dorsiflexors.
Ext. = extension; Flex. = flexion; L = Left; R = Right.

Table 3.3 Patterns of weakness included in current diagnostic criteria assessed at first presentation

Characteristic	IBM	IBM+RV	IBM-RV	IBM+RV *v.* IBM-RV *p* value	Male	Female	Male vs. female *p* value	IBM+IS	IBM-IS	IBM+IS *v.* IBM-IS *p* value
No. of patients, *n*	67	29	38	-	46	21	-	8	57	-
Examination, *n* (%)										
Finger flexion weakness	53 (79)	20 (69)	33 (87)	0.13	38 (83)	15 (71)	0.30	4 (50)	38 (67)	0.44
Wrist flexion weakness	10 (15)	3 (10)	7 (18)	0.50	7 (15)	3 (14)	1.00	1 (13)	9 (16)	1.00
Knee extension weakness	58 (87)	27 (93)	31 (82)	0.28	40 (87)	18 (86)	1.00	6 (75)	50 (88)	0.31
Pattern of weakness, *n* (%)										
Finger flexion weakness > shoulder abduction	43 (64)	16 (55)	27 (71)	0.18	33 (72)	10 (48)	0.06	4 (50)	38 (67)	0.44
Wrist flexion weakness > wrist extension	9 (13)	6 (21)	3 (8)	0.16	7 (15)	2 (10)	0.71	0 (0)	9 (16)	0.59
Knee extension weakness > hip flexion	32 (48)	16 (55)	16 (42)	0.33	25 (54)	7 (33)	0.12	5 (63)	27 (47)	0.48
Knee extension weakness ≥ hip flexion	55 (82)	25 (86)	30 (79)	0.53	39 (85)	16 (76)	0.40	6 (75)	49 (86)	0.60

IBM+RV = IBM with rimmed vacuoles on muscle biopsy; IBM–RV = IBM without rimmed vacuoles on muscle biopsy; IBM+IS = IBM patients treated with immunosuppressive medication; IBM–IS = IBM patients not treated with immunosuppressive medication. *Statistically significant results (p <0.05).

The median Medical Research Council (MRC) muscle scores revealed that the five most severely affected muscle groups at presentation were also knee extensors (3.61), finger flexors (3.77), ankle dorsiflexors (4.01), hip flexors (4.10) and elbow flexors (4.23) (Figure 3.1 B). The sensitivities of different patterns of weakness associated with IBM were calculated (Table 3.3). The most sensitive pattern was found to be knee extensor greater than or equal to hip flexor weakness; this pattern of weakness was present in 82% of patients at initial presentation.

3.5.4 Investigations

3.5.4.1 Serum CK and muscle biopsy

Serum CK and muscle biopsy findings in the cohort and individual subgroups are summarised in Table 3.4.

The median CK at the time of diagnosis was 587 IU/L (IQR 286-1036; normal range 0-250IU/L). The CK was less than 15 times the maximum normal serum level in all patients. Nine patients had a normal CK at presentation. The maximum CK was 3673 IU/L; in only two cases was it greater than 3000 IU/L.

Endomysial inflammation was the most frequent pathological feature, present in 62 (93%) muscle biopsies. Partial invasion was seen in 56 (84%) biopsies and rimmed vacuoles in 29 (43%). All three pathological features were found in only 26 (39%) muscle biopsies. EM is not routinely performed in our centre; in the 22 cases in which it was performed, 14 (64%) were positive for 15-18 nm tubulofilaments. In 13 of the 14 cases with tubulofilaments rimmed vacuoles were present. MHC Class I stained tissue sections were available for review in 50 cases and sarcolemmal MHC Class I was diffusely increased in 46 (92%). Mitochondrial changes [cytochrome c oxidase negative/ succinate dehydrogenase positive (COX-/SDH+) fibres] were observed in 41 (73%) cases. There were no differences in the presence of endomysial inflammation, partial invasion, MHC Class I up-regulation or mitochondrial changes between cases with and without rimmed vacuoles.

Table 3.4 Serum CK and muscle biopsy findings

Characteristic	IBM	IBM+RV	IBM-RV	IBM+RV vs. IBM-RV	IBM-C	IBM-P	IBM-P vs. IBM-C	Male	Female	Male vs. female
				p value			*p* value			*p* value
No. of patients	67	29	38	-	43	18	-	46	21	-
Investigations, median (IQR)										
CK, IU/L	587 (286-1036)	521 (201-1025)	608 (328-1048)	0.40	396 (164-919)	591 (335-1050)	0.19	608 (319-1048)	573 (164-1058)	0.39
Muscle biopsy, n (%)										
i) Endomysial inflammation	62 (93)	29 (100)	33 (87)	0.06	39 (91)	18 (100)	0.31	44 (96)	18 (86)	0.32
ii) Partial invasion	56 (84)	26 (90)	30 (77)	0.33	35 (81)	18 (100)	0.09	42 (91)	14 (67)	0.03*
iii) Rimmed vacuoles	29 (43)	29 (100)	0 (0)	-	9 (21)	18 (100)	-	20 (44)	9 (43)	0.96
All of i-iii	26 (39)	26 (90)	0 (0)	-	7 (16)	18 (100)	-	19 (41)	7 (33)	0.39
Mitochondrial**	41 (73)	15 (65)	26 (79)	0.36	32 (76)	8 (57)	0.19	24 (67)	17 (85)	0.21
MHC Class I ‡	46 (92)	17 (89)	29 (94)	0.63	35 (95)	9 (90)	0.52	31 (97)	15 (83)	0.13

CK = Creatine kinase; IBM+RV = IBM with rimmed vacuoles on muscle biopsy; IBM–RV = IBM without rimmed vacuoles on muscle biopsy; IBM–C = Clinically diagnosed IBM (ENMC clinically defined and ENMC probable); IBM-P = Pathologically diagnosed IBM (Griggs definite and Griggs possible); IQR = Interquartile range; MHC Class I = Major histocompatibility complex class I. **IBM (*n*=56); IBM + RV (*n*=23); IBM–RV (*n*=33); IBM–C (*n*=42); IBM-P (*n*=14); Male (*n*=20); Female (*n*=36).‡ IBM (*n*=50); IBM+RV (*n*=19); IBM–RV (*n*=31); IBM –C (*n*=37); IBM-P (*n*=10); Male (*n*=32); Female (*n*=18). *Statistically significant results ($p < 0.05$).

Male and female patients had similar findings on muscle biopsy, the only difference was that male patients were significantly more likely to have partial invasion present. The site and strength of the muscle biopsied did not affect the likelihood of identifying all three light microscopic pathological features necessary for the Griggs criteria (p=0.23 and 0.13 respectively) (Table 3.5).

3.5.4.2 Repeat muscle biopsy

Nine patients who lacked the three light microscopic features necessary for the Griggs criteria (rimmed vacuoles, inflammatory infiltrate and partial invasion) on their initial muscle biopsy went on to have a second biopsy performed; this revealed all three diagnostic light microscopic pathological features in four cases. The median time between first and repeat biopsies was 23 months (4-58). Ten biopsies which lacked rimmed vacuoles had an additional 20 sections cut and stained. However, rimmed vacuoles were discovered in only one case.

3.5.5 Immunosuppression

Eleven (16%) patients received immunosuppressive treatment. In three of these immunosuppression was given for other diseases and these were excluded from further analyses. The remaining eight patients (12%) received a combination of prednisolone and azathioprine or methotrexate. The median duration of treatment was 60 months (9-120). Five patients reported an initial benefit; though slight objective improvement was observed in two cases it was of short duration. Immunosuppression was withdrawn in seven cases due to lack of efficacy and in one because of side-effects. Patients who received immunosuppressive treatment were younger at the time of disease onset (p=0.02) and biopsy (p=0.01) than those who did not. However, there were no differences in the symptoms at presentation, clinical examination and findings on muscle biopsy between the two groups.

3.5.6 Disability

Forty-two (63%) patients required a walking aid by last follow-up and 19 (28%) required a

Table 3.5 Pathological features dependant on the site and strength of the muscle biopsied

	MRC grade strength of biopsied muscle				Site of biopsy		
	5	4	3	*p* value	Quadriceps	Deltoid	*p* value
No. of patients	20	30	9		31	28	
Pathological features							
i) Inflammation, *n* (%)	19 (95)	28 (93)	8 (89)	0.73	29 (94)	26 (93)	1.00
ii) Partial invasion, *n* (%)	18 (90)	25 (83)	6 (66)	0.80	24 (77)	24 (86)	0.67
iii) Rimmed vacuoles, *n* (%)	6 (30)	16 (53)	3 (33)	0.27	10 (32)	15 (54)	0.12
i), ii) and iii) , *n* (%)	6 (30)	15 (50)	2 (22)	0.13	9 (29)	13 (46)	0.23

MRC = Medical Research Council. *Statistically significant results (p <0.05).

wheelchair. The median disease duration from disease onset to requiring a walking aid or wheelchair was 96 and 228 months respectively. Age at disease onset and gender appeared to influence disability (Figures 3.2 and 3.3 and Table 3.6). When patients were grouped according to age at disease onset patients with symptoms starting at an older age required a walking aid sooner than younger patients (p=0.01). Time to requiring a wheelchair was influenced by gender; male patients required a wheelchair sooner than female patients (p=0.01). However multivariate analysis in which age was assessed as a continuous variable revealed that only age at disease onset influenced disability; time to requiring walking aid (p=0.001; hazard ratio 1.07; 95% confidence interval 1.03-1.11). No other clinical or pathological features influenced the time to disability including immunosuppressive therapy, presence of rimmed vacuoles and clinical or pathological diagnosis (Table 3.6).

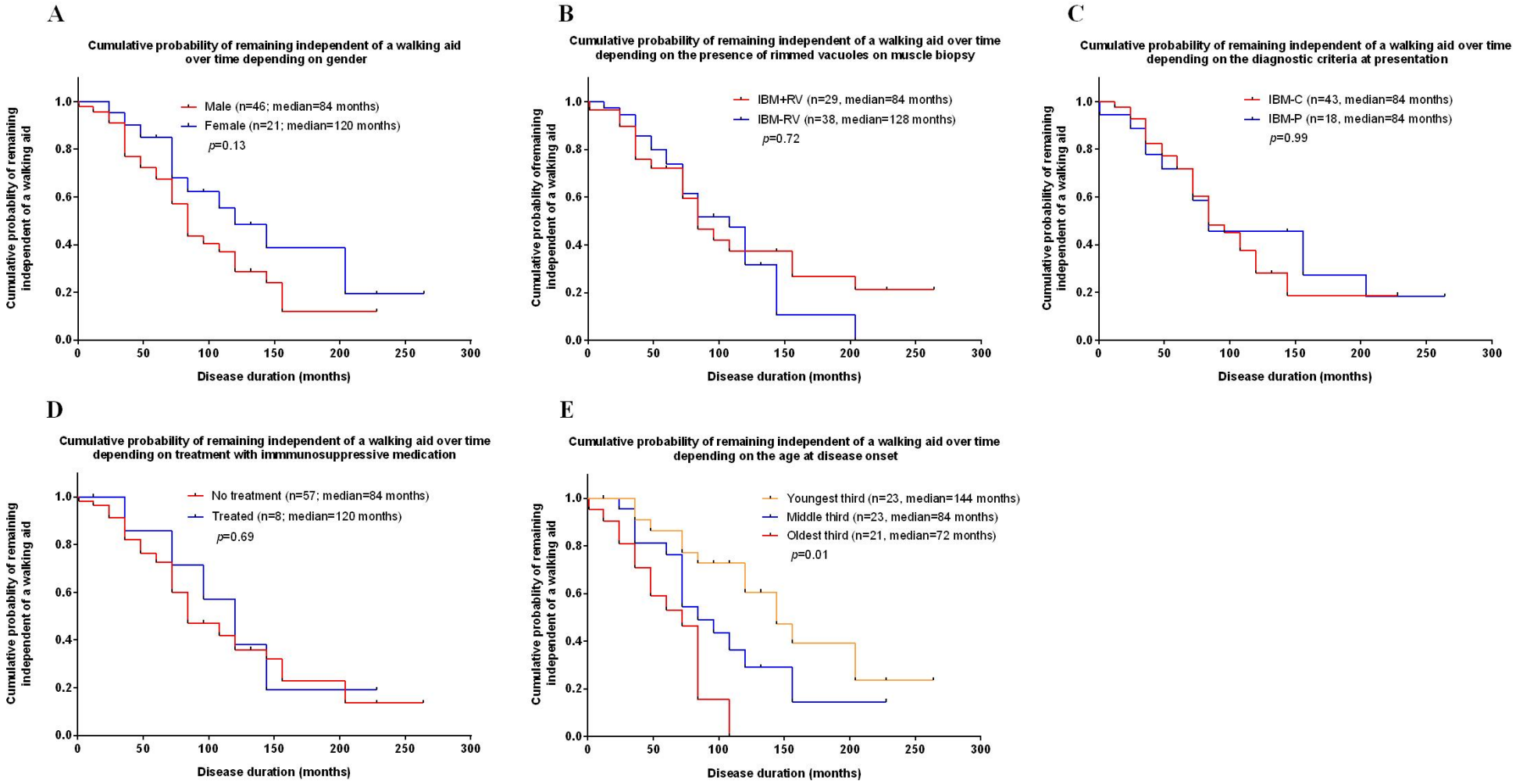
3.5.7 Comparison of the pattern of weakness observed in IBM and disease controls

Clinical characteristics of PM&DM and PAM and IBM cases are summarised in Table 3.7.

IBM patients were significantly older than patients with PM&DM and PAM ($p \leq 0.007$). The lower limbs were affected at onset more commonly in IBM than in PM&DM at disease onset ($p < 0.0001$). There was no difference in the frequency of lower limb involvement at disease onset between IBM and PAM. There were no differences in the frequency of upper limb or bulbar involvement at disease onset between IBM and PM&DM or IBM and PAM. Pain at onset was a feature of PM&DM, but not IBM or PAM. Serum CK at presentation was significantly higher in PM&DM than in IBM ($p < 0.0001$). There was no difference in the level of serum CK between IBM and PAM.

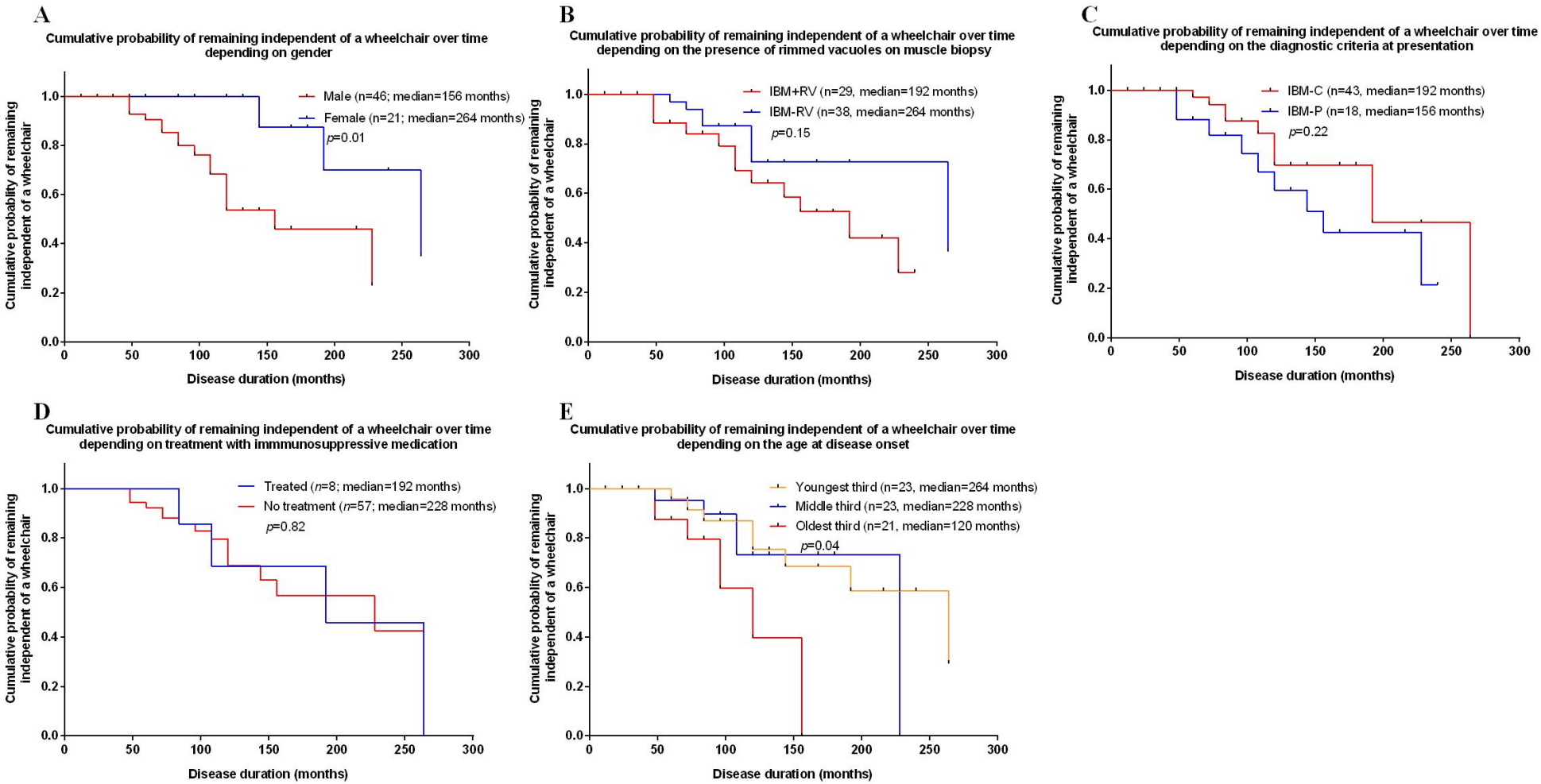
Weakness of elbow flexion, finger flexion and knee extension was more common in IBM than PM&DM and PAM ($p \leq 0.04$) (Table 3.8). Comparing the median MRC muscle strength scores for

Figure 3.2 Probability of remaining independent of a walking aid over time



Kaplan-Meier curves showing the cumulative probability over time of requiring a walking aid depending on gender (A), the presence of rimmed vacuoles on muscle biopsy (B), whether they were diagnosed using by pathological or clinical criteria (C), immunosuppressive treatment (D) and age at disease onset (E). Time to requiring a walking aid was influenced by age at disease onset. Older patients required a walking aid earlier than younger patients (p=0.01).
IBM+RV = IBM with rimmed vacuoles on muscle biopsy; IBM–RV = IBM without rimmed vacuoles on muscle biopsy; IBM–C = Clinically diagnosed IBM (ENMC clinically defined and ENMC probable); IBM-P = Pathologically diagnosed IBM (Griggs definite and Griggs possible).

Figure 3.3 Probability of remaining independent of a wheelchair over time



Kaplan-Meier curves showing the cumulative probability over time of requiring a wheelchair depending on gender (A), the presence of rimmed vacuoles on muscle biopsy (B), pathological or clinical criteria (C), immunosuppressive treatment (D) and age at disease onset (E). Time to requiring a wheelchair was influenced by gender. Male patients were significantly more likely to require a wheelchair over time than female patients (p=0.01).
IBM+RV = IBM with rimmed vacuoles on muscle biopsy; IBM–RV = IBM without rimmed vacuoles on muscle biopsy; IBM–C = Clinically diagnosed IBM (ENMC clinically defined and ENMC probable); IBM-P = Pathologically diagnosed IBM (Griggs definite and Griggs possible).

Table 3.6 Multivariate analysis of the influence of clinical and pathological features on disability outcomes

Variable	*p* value	Hazard ratio	95% confidence intervals
Time to walking aid			
Male gender	0.17		
Presence of rimmed vacuoles	0.66		
Diagnostic criteria	0.71		
Immunosuppressive treatment	0.70		
Age	0.001*	1.07	1.03-1.11
Time to wheelchair			
Male gender	0.28		
Presence of rimmed vacuoles	0.16		
Diagnostic criteria	0.12		
Immunosuppressive treatment	0.82		
Age	0.27		

Analysis showing the likelihood of requiring a walking aid was associated with the age at disease onset, with age as a continuous variable. Older patients more likely to require a walking aid sooner (hazard ratio of 1.07 for each year of increasing age at disease onset). *Statistically significant results (p <0.05).

Table 3.7 Clinical characteristics in IBM and control patients

Characteristic	IBM	PM&DM	IBM *v*. PM&DM *p* value	PAM	IBM *v*. PAM *p* value
No. of patients	67	15		12	
Gender, M:F	46:21	7:8	0.11	7:5	0.48
Age at onset (IQR), years	62 (55-70)	52 (43-62)	0.007*	51 (36-54)	0.0005*
Age at biopsy (IQR), years	67 (61-75)	56 (45-63)	0.0002*	52 (38-61)	0.0004*
Delay to diagnosis (IQR), months	62 (34-90)	15 (6-31)	<0.0001*	43 (36-96)	0.68
Onset, *n* (%)					
Lower limbs	55 (82)	3 (20)	<0.0001*	9 (75)	0.69
Upper limbs	5 (8)	1 (7)	1.00	2 (17)	0.29
Bulbar weakness	1 (1)	0 (0)	1.00	0 (0)	1.00
Lower and upper limbs	4 (6)	10 (67)	<0.0001*	1 (8)	0.57
Pain	0 (0)	3 (20)	0.005*	0 (0)	1.00
Bulbar and lower limbs	2 (3)	1 (7)	0.46	0 (0)	1.00
Associations, *n* (%)					
Neoplastic disease	6 (9)	2 (13)	0.63	0 (0)	0.58
Auto-immune disease	8 (12)	3 (20)	0.41	0 (0)	0.35
Investigations					
CK, IU/L	587 (286-1036)	2000 (1650-3250)	<0.0001*	404 (310-790)	0.49

IQR = Interquartile range; CK = Creatine kinase; PM&DM = Steroid-responsive inflammatory myopathies; PAM = Protein accumulation myopathies. *Statistically significant results (p <0.05).

Table 3.8 Pattern of weakness observed in IBM and control patients at first presentation

Characteristic	IBM	PM&DM	IBM *v*. PM&DM	PAM	IBM *v*. PAM	IBM *v*. PM&DM and PAM		
			p value		*p* value	*p* value	Sensitivity (%)	Specificity (%)
No. of patients, *n*	67	15		12				
Examination, median MRC grade (range)†								
Shoulder abduction weakness	10 (6-10)	8 (4-10)	<0.0001*	10 (4-10)	0.90			
Elbow flexion	8 (6-10)	10 (6-10)	0.42	10 (8-10)	0.01*			
Finger flexion weakness	8 (4-10)	10 (8-10)	<0.0001*	10 (4-10)	<0.0001*			
Knee extension weakness	8 (4-10)	10 (8-10)	<0.0001*	10 (8-10)	<0.0001*			
Ankle dorsiflexion weakness	8 (4-10)	10 (8-10)	<0.0003*	8 (4-10)	0.02			
Examination, *n* (%)								
Shoulder abduction weakness	32 (48)	14 (93)	0.001*	5 (42)	0.76	0.01*	48	22
Elbow flexion weakness	47 (70)	6 (40)	0.04*	2 (17)	0.007*	0.0001*	70	70
a) Finger flexion weakness	53 (79)	1 (7)	<0.0001*	1 (8)	<0.0001*	<0.0001*	79	93
b) Knee extension weakness	58 (87)	2 (13)	<0.0001*	5 (42)	0.002*	<0.0001*	87	74
Ankle dorsiflexion weakness	44 (66)	2 (13)	0.0003*	11 (92)	0.09	0.16	66	52
Pattern of weakness, *n* (%)								
i) Finger flexion weakness > shoulder abduction	43 (64)	0 (0)	<0.0001*	1 (8)	0.0004	<0.0001*	64	96
ii) Knee extension weakness > hip flexion	32 (48)	0 (0)	0.0003*	0 (0)	0.001*	<0.0001*	48	100
iii) Knee extension weakness ≥ hip flexion	55 (82)	2 (13)	<0.0001*	4 (67)	0.001*	<0.0001*	83	90
i) and ii)	24 (43)	0 (0)	0.004*	0 (0)	0.0002*	0.0001*	36	100
i) and iii)	34 (51)	0 (0)	0.0002*	0 (0)	0.0008*	<0.0001*	51	100
a) and b)	45 (67)	0 (0)	<0.0001*	0(0)	<0.0001*	<0.0001*	67	100

IQR = Interquartile range; CK = Creatine kinase; PM&DM = Steroid-responsive inflammatory myopathies; PAM = Protein accumulation myopathies. *Statistically significant results (p <0.05). Only results that were statistically significant in at least one comparison are shown.

individual muscle groups revealed that finger flexion, knee extension and ankle dorsiflexion strength were weaker in IBM than PAM and PM&DM ($p \leq 0.02$). Knee flexion and finger flexion weakness individually had a sensitivity and specificity greater than 70% for IBM compared to controls.

Patterns of weakness in the upper and lower limbs were compared (Table 3.8). The pattern with the greatest sensitivity and 100% specificity for IBM was the presence of finger flexion and knee extension weakness (sensitivity 67% and specificity 100%).

3.5.8 Diagnostic criteria

The diagnostic utility of three current diagnostic criteria (pathologically focused Griggs criteria, 1997 ENMC and the clinically based revised 2011 ENMC criteria) were compared. The 2011 ENMC criteria are split into three categories: clinicopathologically defined IBM, clinically defined IBM and probable IBM.

Fifty-nine (88%) patients fulfilled the 2011 ENMC criteria at presentation [11 (16%) clinicopathologically defined IBM, 26 (39%) clinically defined IBM and 22 (33%) probable IBM], whilst 18 (27%) fulfilled the pathological Griggs criteria [11 (16%) definite IBM and seven (10%) possible IBM] and 51 (76%) of patients satisfied the 1997 ENMC criteria [definite IBM 23 (34%), probable IBM 27 (40%) and possible IBM one (1%)]. Failure to satisfy the Griggs criteria was due to incompletely fulfilling the biopsy criteria in 15 (22%) cases, the clinical criteria in eight (12%) and both in 26 (39%) cases. Sixteen (89%) patients who fulfilled the Griggs criteria also fulfilled the 2011 ENMC criteria. Eight patients did not fulfil 2011 ENMC criteria, this was due to age at onset being <45 years in five (7%) and failure to fulfil the examination criteria in two (3%) and the biopsy criteria in one (1%).

Clinicopathologically defined IBM (2011 ENMC criteria) is essentially the same as Griggs' definite IBM and was excluded from the 2011ENMC group reviewed here to enable comparisons between clinically and pathologically diagnosed patients to be made. There were no differences in the age at presentation, gender, presenting symptoms, clinical examination findings, number of concomitant diseases, mean CK, biopsy site or pathological findings (excluding rimmed vacuoles and tubulofilamentous inclusions) nor immunosuppressive therapy received between clinically diagnosed and pathologically diagnosed patients.

3.6 Discussion

Comprehensive and systematic comparisons of patients with pathologically diagnosed IBM and clinically typical IBM are lacking. Here the clinical and pathological features at presentation and follow-up of 67 patients with IBM and 27 disease controls with conditions that are in the clinical and pathological differential diagnosis for IBM have been reviewed. The most important findings were that patients with IBM have a very characteristic clinical presentation, featuring painless weakness of the knee extensors often leading to frequent falls initially and weakness of the finger flexors. Patients with this characteristic pattern of weakness behave similarly in terms of disease progression regardless of whether or not they possess previously proposed specific diagnostic pathological features at presentation. Of note, patients lacking rimmed vacuoles on muscle biopsy were younger at the time of biopsy than patients with rimmed vacuoles on muscle biopsy suggesting that their presence may be indicative of more advanced disease. Finally, clinical examination at presentation that reveals the characteristic pattern of weakness is sensitive and specific for the diagnosis of IBM.

3.6.1 Previous studies

The majority of clinical IBM studies have used pathologically focussed diagnostic criteria to define patient cohorts and therefore, by definition, excluded patients lacking such features. It is now recognised that a proportion of patients with clinically typical IBM lack one or more of the

pathological features that are currently demanded by the Griggs criteria and that the individual pathological features are not specific for IBM and may be seen in other conditions, including those that mimic IBM. However, when present together they are essentially diagnostic of IBM. Clinical experience has supported the early observations that IBM is associated with a characteristic pattern of weakness with involvement of the finger flexor and knee extensor muscles, and occasionally the muscles associated with swallowing. In clinical practice, patients with this clinical presentation, that do not fulfil the pathologically focussed diagnostic criteria, are not uncommon.

Only a few previous studies have described the clinical or pathological findings in patients lacking the diagnostic pathological findings. Amato *et al.* performed a detailed clinical study of seven patients with 'steroid-unresponsive PM' and were the first to propose that patients with clinical features of IBM, but who lacked typical pathological features, may nonetheless have IBM (Amato et al., 1996). Benveniste *et al.* found that patients with the characteristic pattern of weakness (fulfilling the Hilton-Jones clinically-defined criteria) had similar disability at last follow-up to patients fulfilling the Griggs criteria (Benveniste et al., 2011). Interestingly, in one study, muscle strength was quantitatively measured and disease progression (loss of strength) was slower in patients lacking the diagnostic pathological features; however, the duration of follow-up in this study is unknown and clinical data is lacking (Temiz et al., 2009). Widespread acceptance of the Griggs pathological criteria and a general anxiety about deviating from them has resulted in a situation whereby clinicians are reluctant to acknowledge or accept that patients with the clinical features of IBM but lacking histological confirmation have IBM. Some authors preferring to refer to these patients using alternative diagnostic tags emphasising their similarities to both PM and IBM (Chahin and Engel, 2008)(Temiz et al., 2009). We found that patients without the diagnostic pathological findings at presentation are identical, except for age at biopsy, in terms of demographics, disease presentation and disease course when compared to patients with the 'full-house' of diagnostic pathological features on biopsy. Thus we have been able to show that

independently of whether patients are clinically diagnosed or pathologically diagnosed we are dealing with a homogeneous disorder.

3.6.2 The clinical picture is sensitive and specific independently of the pathological features

We have shown that presenting symptoms and physical examination are similar in IBM patients independent of whether the diagnostic pathological features are present on biopsy. Finger flexors and knee extensors were the most commonly affected muscles in IBM, either were affected in 96% of patients and both were affected in 39% of patients at first assessment and in 82% with follow-up. Although, in our experience finger flexion or knee extension weakness are not common in conditions to be considered in the differential diagnosis of IBM such as steroid-responsive inflammatory myopathy, hIBM or MFM we found that they can be seen infrequently (Table 3.8). However, the presence of both finger flexion and knee extension weakness was sensitive and specific to IBM (Table 3.8).

3.6.3 Pathological features are associated with disease duration

It has been suggested that the absence of classical pathological features associated with IBM on muscle biopsy may be because they are late features of the disease (Benveniste and Hilton-Jones, 2010), or because they are patchy and therefore may be missed by a single biopsy (Amato et al., 1996). The insidious nature of IBM makes it is difficult to accurately identify the disease onset and therefore the disease duration prior to muscle biopsy. In agreement with other studies, we found age at disease onset did not influence the pathological findings (Amato et al., 1996)(Temiz et al., 2009)(Benveniste and Hilton-Jones, 2010). Despite this, and in contrast to previous studies (Chahin and Engel, 2008), we observed that patients without rimmed vacuoles on muscle biopsy were younger at the time of muscle biopsy than patients with rimmed vacuoles. This observation lends support to the notion that rimmed vacuoles are a feature of long-standing disease and are therefore of limited diagnostic potential at the time of initial presentation. The reason that age of disease onset did not affect the pathological findings is most likely due to the difficulty in

accurately dating this time point given the slowly progressive nature of the disease. In our cohort, there were no differences in the proportion of patients with muscle fibres undergoing partial invasion, containing mitochondrial abnormalities or with increased MHC Class I staining depending on the presence of rimmed vacuoles. Differences in the frequency of partial invasion and mitochondrial changes have previously been described between cases with and without rimmed vacuoles (Chahin and Engel, 2008)(Temiz et al., 2009). These different observations may be due to differences in staining techniques and method of assessment of the biopsies; unlike these studies we did not quantify the number of affected fibres within the biopsies. In agreement with Chahin and Engel, we found the absence of both partial invasion and mitochondrial abnormalities to be strong evidence against the diagnosis of IBM (Chahin and Engel, 2008).

3.6.4 Disease progression is independent of pathological features

There was no difference in the speed of disease progression (time from disease onset to walking aid and/or wheelchair) between clinically and pathologically diagnosed patients or patients with and without rimmed vacuoles on biopsy. In concordance with previous studies, we found that age at disease onset predicted disease progression (Peng et al., 2000b)(Benveniste et al., 2011). Older-onset patients had a more rapid decline and required walking aids earlier. Suggested reasons for this have included age-related sarcopenia and the higher frequency of co-morbidities that may contribute to mobility problems in older patients. Although it appeared that male patients may reach certain disability end-points more rapidly than female patients this was an effect of age. Measuring strength quantitatively, Temiz *et al.* found that IBM patients lacking rimmed vacuoles had a slower disease progression than pathologically typical IBM (Temiz et al., 2009). This may be explained by our findings that rimmed vacuoles are present in older patients, who have been found to have more rapidly progressive disease.

3.6.5 Inclusion of the clinical examination in future diagnostic criteria

Historically, diagnostic criteria for IBM have focussed on the pathological features present on biopsy. Although they have been instrumental in helping to identify the clinical characteristics particular to IBM, these criteria were based largely on expert opinion. We have shown that there were no differences in the demographic characteristics, clinical features nor disability outcomes between IBM patients diagnosed clinically and pathologically. Thus, we have confirmed that these patients have the same disease. As such, adherence to pathologically predominant criteria will exclude a substantial proportion of IBM patients from studies, potentially leading to erroneous conclusions being drawn about the pathogenesis and treatment outcomes in IBM. Finger flexors and knee extensors were the most commonly and frequently affected muscles in IBM. Individually these signs were present in disease controls. At the cost of the sensitivity, combining these features made them highly specific for IBM. Thus, these findings could be incorporated into future diagnostic criteria.

3.6.6 Study limitations

Patients in our region with neuromuscular disease receive early referral to specialist neuromuscular services which may not be available in every area. Therefore, the majority of patients were assessed and managed by a single individual possibly affecting the speed of diagnosis and the management of patients. However, this meant that there was access to consistent high quality clinical data. The study was retrospective which could introduce patient recall bias, particularly with regard to timings in a slowly progressive disease such as IBM, though because many patients were still under follow-up this allowed the collection of the complete data set for nearly every patient and the inclusion of all patients who went on to be diagnosed as having IBM not only those considered to have typical IBM at presentation. Inevitably categorising weakness using the MRC scoring system leads to a loss of detail. The weakness was not quantified using an objective measure, such as a dynamometer; however disability outcomes such as when patients require a mobility aid are arguably better. They represent clinically meaningful points in the disease

progression which have a significant and understandable impact on a patient's life whereas a change in strength measured with a dynamometer does not. As the majority of patients did not receive immunosuppressive therapy the results from this study are an accurate representation of the natural history of IBM.

3.6.7 Final comments

Diagnostic criteria are useful in defining homogeneous cohorts for research purposes, but are often impractical for everyday clinical use. The characteristic pattern of weakness associated with IBM is found in the majority patients at first presentation independent of the pathological features and is highly specific for IBM. Patients with and without the diagnostic pathological features were clinically identical except for the age at biopsy; in particular, there was no difference in the pattern of weakness or disease progression. These findings support the diagnostic utility of the clinical examination, in the absence of the diagnostic pathological findings, in the out-patients clinic and the addition of a clinically defined group to the diagnostic criteria. Despite the sensitivity and specificity of the clinical presentation, muscle biopsy remains important tool in the assessment of patients with suspected IBM to exclude alternative diagnoses particularly as some IBM patients lack the characteristic clinical features at presentation.

Chapter 4

PATHOLOGICAL DESCRIPTION OF IBM

4.1 Introduction

Currently for a diagnosis of definite IBM to be made, several pathological findings must be present on biopsy, namely rimmed vacuoles and endomysial inflammation with invasion of non-necrotic fibres by mononuclear inflammatory cells (partial invasion), together with amyloid deposits or 15-18 nm tubulofilaments identified by EM. Although these features in combination are considered highly specific for the diagnosis, as discussed in Chapter 3, they lack sensitivity and require relatively specialist techniques to identify them, which may not be available in some centres.

IBM is typically associated with both inflammatory and myopathic features on biopsy. However, the significance of the individual pathological findings and their role in the disease pathogenesis is uncertain. Identification of 15-18 nm tubulofilaments in IBM but not PM (Chou, 1967) led to the appreciation that IBM is a distinct disease separate from PM. Because the tubulofilaments observed in IBM shared ultrastructural similarities with amyloid filaments, amyloid staining was then performed and the presence of amyloid in IBM was demonstrated, initially using Congo red staining visualised under polarised light. This led to a search, using IHC, for proteins known to aggregate in a beta-pleated sheet formation, such as Aβ and associated proteins such as APP, in IBM muscle. Subsequently, many proteins associated with neurodegenerative disease, particularly AD have been observed to aggregate in IBM using IHC staining techniques. This led IBM to be likened to neurodegenerative disease and parallels have been drawn between both with respect to the pathogenesis and possible treatment strategies. Additionally a number of cellular and animal disease models for IBM based on the over-expression of APP, Aβ and tau have been developed.

Currently around 80 different proteins have been reported in IBM muscle using IHC and IF techniques leading some to describe it as a "promiscuous proteinopathy" (Weihl and Pestronk, 2010). These include proteins classically associated with neurodegenerative diseases such as Aβ 1-40 and Aβ 1-42, α-synuclein, PrP, phosphorylated tau, ubiquitin and, more recently described, p62 and TDP-43, together with proteins which are found to accumulate in the genetic MFM such as α B-crystallin and desmin, and autophagy related proteins LC3 and NBR1. A number of protein accumulations are thought to be unique to IBM. However, these pathological features have not translated into greater understanding of either the pathogenesis of IBM or led to improved diagnosis. This is most likely because many of the observations in IBM have not been consistently and independently reproduced and therefore, their association with IBM is controversial. Studies have often lacked robust inclusion criteria and patients with pathologically similar myopathies may inadvertently have been included as cases of IBM and patients with IBM but lacking the classical diagnostic pathological features, may have been included as controls as inflammatory myopathies. Quantitative assessment of the pathological findings is frequently absent from studies and different staining techniques are used making individual studies difficult to compare. Therefore, the significance of much of the current IHC data is unknown and recommendations of how to incorporate it into any new diagnostic criteria have not been established.

4.2 Hypothesis

Aggregated proteins are more sensitive than the current pathological features typically associated with IBM and included in the current pathologically focussed diagnostic criteria.

4.3 Aims

To determine in a systematic quantitative manner which pathological features can be reliably detected in IBM using techniques readily available to any UK diagnostic pathology laboratory and taking into account recently published findings.

4.4 Methods

Six clinically typical and pathologically definite cases of IBM and six cases of normal muscle were identified (Table 4.1), none had received immunosuppressive medication prior to muscle biopsy. Brain tissue from pathologically proven cases of AD, multiple system atrophy, corticobasal degeneration (CBD), FUS and TDP-43 variants of frontotemporal lobar degeneration (FTD-FUS and FTD-TDP) and normal muscle and normal tonsil were used as positive controls.

Consecutive eight μm thick frozen sections were stained for: tau and hyperphosphorylated tau, ubiquitin, Aβ, α-synuclein, p62, TDP-43, FUS, VCP, lamin A/C, emerin, desmin, myotilin and α B-crystallin, T-cells (CD3), helper T-cells (CD4), cytotoxic T-cells (CD8), B-cells (CD20), macrophages (CD68) and MHC Class I using IHC. Samples were also stained for amyloid using alkalinised Congo red, crystal violet and thioflavin S. Quantification was blind to the diagnosis. The total number of fibres in each biopsy and the number containing rimmed vacuoles, protein aggregates identified using each protein marker or undergoing partial invasion were quantified. The findings are expressed as a percentage of the total number of fibres in the biopsy.

4.5 Results

4.5.1 Clinical characteristics of IBM and control patients

Demographic and clinical characteristics of the individual IBM and normal control cases are shown in Table 4.1.

Of the six IBM patients included five (83%) patients were Caucasian and one was Asian. Five patients (83%) were male. The median age at disease onset was 66 years (64-70) and median age at muscle biopsy was 74 years (67-79). The median delay to diagnosis was 66 months (21-126) and two (33%) received one alternative diagnosis before being diagnosed with IBM. The mean

Table 4.1 Clinical characteristics of IBM patients and control cases

Group	Gender	Ethnicity	Age at onset, years	Age at biopsy, years	Delay to diagnosis, months	Initial symptom	Initial diagnosis	CK (0-250 IU/L)	EMG	NCS	Weakness*
IBM	Female	Caucasian	70	77	84	PLL	IBM	110	Myopathic	Normal	KE
IBM	Male	Caucasian	66	61	48	PLL	IBM	450	Myopathic	Normal	KE
IBM	Male	Asian	76	70	12	PLL	MND	267	Myopathic	Normal	FF
IBM	Male	Caucasian	70	82	144	PLL	PM	412	Myopathic	Denervation	KE
IBM	Male	Caucasian	58	77	36	S	IBM	289	Myopathic	Normal	FF and KE
IBM	Male	Caucasian	67	77	120	PLL	IBM	735	Myopathic	Normal	FF and KE
Control	Female	Caucasian	-	26	-	-	-	Normal	Normal	Normal	None
Control	Female	Caucasian	-	44	-	-	-	Normal	Normal	Normal	None
Control	Female	Asian	-	48	-	-	-	Normal	Normal	Normal	None
Control	Male	Caucasian	-	59	-	-	-	Normal	Normal	Normal	None
Control	Female	Asian	-	38	-	-	-	Normal	Normal	Normal	None
Control	Female	Caucasian	-	57	-	-	-	Normal	Normal	Normal	None

CK = Creatine kinase; EMG = Electromyography; NCS = Nerve conduction studies; PLL = Proximal lower limb weakness; S = Dysphagia; MND = Motor neuron disease; PM = Polymyositis; KE = Knee extensors; FF = Finger flexors. *At initial presentation.

serum CK at presentation was 377 IU/L (±213). Nerve conduction studies in one patient were abnormal showing denervation. This patient had pre-existing diabetes mellitus type II which was believed to account for this finding. There was a difference in median age at time of muscle biopsy between the control and IBM groups (46 *v*. 74 years; p=0.002).

4.5.2 Optimisation of primary antibodies and conditions

Antibodies were titrated in frozen control tissue known to contain the epitope of interest. Subsequently these were used as positive and negative controls. Twenty three commercial antibodies were selected for protein detection after titration (Table 4.2). FA pre-treatment improved Aβ staining in frozen brain tissue sections of AD. Previously, this method has been shown to improve the Aβ staining in cerebral and systemic amyloid deposits (Kitamoto et al., 1987). However, this was in formalin fixed paraffin embedded tissue sections. Four different detection systems were trialled for visualising the antigen-primary antibody complex. From these the Dako REAL™ EnVision™ Detection System was found to be the most sensitive.

4.5.3 Alkalinised Congo red staining and thioflavin S staining are more sensitive than crystal violet for identifying amyloid in AD

Amyloid staining was performed on AD tissue sections with alkalinised Congo red, crystal violet and thioflavin S. Amyloid deposits were easily visualised in tissue sections stained with alkalinised Congo red staining and visualised with polarised and fluorescent light and thioflavin S visualised with fluorescent light. No amyloid deposits were detected using the published method of Crystal violet staining (Section 2.3.2.1.8). Modifications to the method were tried without success.

4.5.4 Intra-observer reliability was good

To determine the reliability of the results tissue sections stained for p62 and TDP-43 were quantified on two separate occasions at four weeks apart. p62 and TDP-43 were chosen as they

Table 4.2 Antibodies and optimum conditions

	Antibody	Source	Clone	Control tissue	Fixative	Dilution	Primary incubation conditions	Secondary	Secondary incubation time
1	p62	BD Transduction	3/P62 LCK	AD brain	A	1:400	1 hour, RT	Dako Envision	5 minutes
2	TDP-43	Proteintech	NA	FTLD-TDP brain	PFA	1:800	24 hours, 4°C	Dako Envision	5 minutes
5	Tau	Dako	NA	AD brain	A	1:1600	1 hour, RT	Dako Envision	5 minutes
6	P-tau	Autogen Bioclear	AT8	AD brain	A	1:1600	1 hour, RT	Dako Envision	5 minutes
7	SMI 31	Covance	SMI-31	AD brain	A	1:100	1 hour, RT	Dako Envision	5 minutes
8	Ubiquitin	Dako	NA	AD brain	A	1:100	1 hour, RT	Dako Envision	5 minutes
9	β amyloid	Dako	6F/3D	AD brain	PFA and FA	1:100	1 hour, RT	Dako Envision	5 minutes
10	α-synuclein	Abcam	4D6	MSA brain	PBS	1:800	1 hour, RT	Dako Envision	5 minutes
11	FUS	Novus Biologicals	NA	FTLD-FUS brain	A	1:2000	1 hour, RT	Dako Envision	5 minutes
12	Desmin	Dako	D33	Normal muscle	A	1:50	24 hours, 4°C	Dako Envision	5 minutes
13	Myotilin	Novocastra	RSO34	Normal muscle	A	1:500	24 hours, 4°C	Dako Envision	5 minutes
14	α B-crystallin	Novocastra	G2JF	CBD brain	A	1:300	1 hour, RT	Dako Envision	5 minutes
15	VCP	Abcam	5	Normal muscle	A and PFA	1:100	1 hour, RT	Dako Envision	5 minutes
16	Lamin A/C	Novocastra	636	Normal muscle	A	1:50	1 hour, RT	Dako Envision	5 minutes
17	Emerin	Novocastra	4G5	Normal muscle	A	1:400	1 hour, RT	Dako Envision	5 minutes
18	MHC Class 1	Novocastra	W6/32	Normal muscle	A	1:25	24 hours, 4°C	Dako Envision	5 minutes
19	CD3	Novocastra	UCHT1	Tonsil	A	1:100	1 hour, RT	Dako Envision	5 minutes
20	CD4	Novocastra	4B12	Tonsil	A	1:400	1 hour, RT	Dako Envision	5 minutes
21	CD8	Novocastra	1A5	Tonsil	A	1:50	1 hour, RT	Dako Envision	5 minutes
22	CD20	Novocastra	L26	Tonsil	A	1:400	1 hour, RT	Dako Envision	5 minutes
23	CD68	Novocastra	KP1	Tonsil	A	1:1600	1 hour, RT	Dako Envision	5 minutes

NA = Not applicable; p62 = Sequestosome 1; AD = Alzheimer's disease; TDP-43 = Transactivation response DNA binding protein 43; FTLD-TDP = Frontotemporal lobar degeneration with TDP-43 positive inclusions; P-tau = Hyperphosphorylated tau; MSA = Multiple systems atrophy; FUS = Fused in sarcoma protein; FTLD-FUS = Frontotemporal lobar degeneration with FUS positive inclusions; CBD = Cortico-basal degeneration; MHC Class 1 = Major histocompatibility complex class 1; CD3-68 = Cluster of differentiation protein 3-68; VCP = Valosin containing protein; A = Acetone; PFA = Paraformaldehyde; PBS = Phosphate buffered saline; FA = Formic acid; RT = Room temperature (25 ^{o}C).

were subjectively the easiest and most difficult to count respectively. The correlation between first and second counts for p62 and TDP-43 were high [0.99; 95% CI (0.89-1.00) and 0.98; (0.83-1.00) respectively] (Figure 4.1A). Bland-Altman plots were used to calculate intra-observer reliability. These revealed the difference between counts were small indicating good intra-observer reliability (Figure 4.1B and C). As expected, the greater the number of pathological findings the greater the variability; this was more marked for TDP-43 than p62.

4.5.5 Histological and pathological findings in IBM and normal control muscle

There was no difference in the median number of fibres in muscle biopsies between IBM and normal control muscle [1469 (888-4161) *v*. 2640 (1759-4287) respectively; p=0.24].

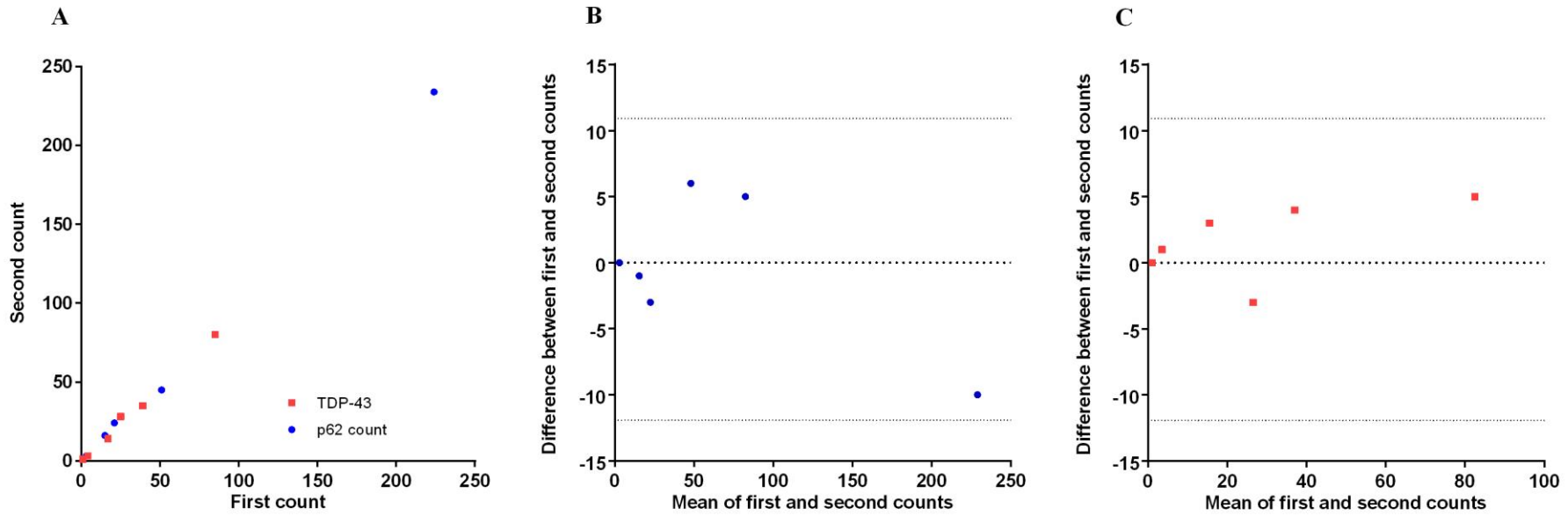
4.5.5.1 No histological abnormalities were observed in normal control muscle biopsies

No pathological features associated with the Griggs criteria nor protein aggregates were observed in any of the control muscle biopsies. No immunoreactivity was observed with antibodies to Aβ, α-synuclein, tau, p62, ubiquitin, α B-crystallin and hyperphosphorylated tau in normal muscle. Desmin and myotilin immunoreactivity was observed in the sarcoplasm of control tissue with a mild increase at the sarcolemma. The majority of nuclei were immunoreactive for lamin A/C, emerin, FUS and TDP-43. Immunoreactivity to VCP was present in the sarcoplasm, sarcolemma, connective tissue and endothelium. The results of the staining using IHC observed in IBM and normal control muscle are summarised in Table 4.3.

4.5.5.2 Griggs' diagnostic pathological features were present in IBM

Each IBM biopsy contained the essential pathological features described in the Griggs criteria. These were accompanied by variation in fibre size, fibre necrosis and regeneration, rounded and angular atrophic fibres and increased endomysial connective tissue. There were no pathological features observed in normal control muscle biopsies.

Figure 4.1 Intra-observer agreement



Scatter plot (A) and Bland-Altman plots (B and C) showing the correlation and agreement between the first and second counts for p62 [A (blue spots) and B] and TDP-43 [A (red squares) and C]. The correlation between counts was high for p62 and TDP-43 (>98%; p <0.003). The differences between first and second counts were small and fell within the 95% limits of agreement (B and C; upper and lower dotted lines). The bias for p62 and TDP-43 were -0.5 (SD 5.82) and 1.67 (2.94) respectively.
p62 = Sequestosome 1; TDP-43 = Transactivation response DNA binding protein 43; SD = Standard deviation.

Table 4.3 Pattern of immunoreactivity in normal muscle and the cellular location of protein aggregates in IBM

		Cellular distribution of protein aggregates							
						Rimmed vacuoles			
Stain	Location of immunoreactivity in normal muscle	Nuclear	Perinuclear	Sarcoplasmic	Subsarcolemmal	Periphery	Contents	Partial invasion	Clustering of positive fibres
p62	-	+	+	+	+	+	+	-	+
Ubiquitin	-	+	+	+	+	+	+	+	+
TDP-43	Nuclear	-	+	+	+	+	+	-	+
Myotilin	Sarcoplasmic	-	-	+	+	+	-	+	+
α B-crystallin	-	-	-	+	+	+	+	+	+
Congo red	-	-	-	+	+	+	+	+	+
Tau	-								
Phosphorylated tau	-								
SMI 31	-								
β Amyloid	-								
α-synuclein	-								
FUS	Nuclear								
Desmin	Sarcoplasmic								
VCP	Nuclear and sarcoplasmic								
Lamin A/C	Nuclear								
Emerin	Nuclear								

- = Absent; + = Present; p62 = Sequestosome 1; TDP-43 = Transactivation response DNA binding protein 43; FUS = Fused in sarcoma protein; VCP = Valosin containing protein.

4.5.5.3 Proteins classically associated with neurodegenerative disease were not present in IBM

The results of the staining using IHC observed in IBM and normal control muscle are summarised in Table 4.3.

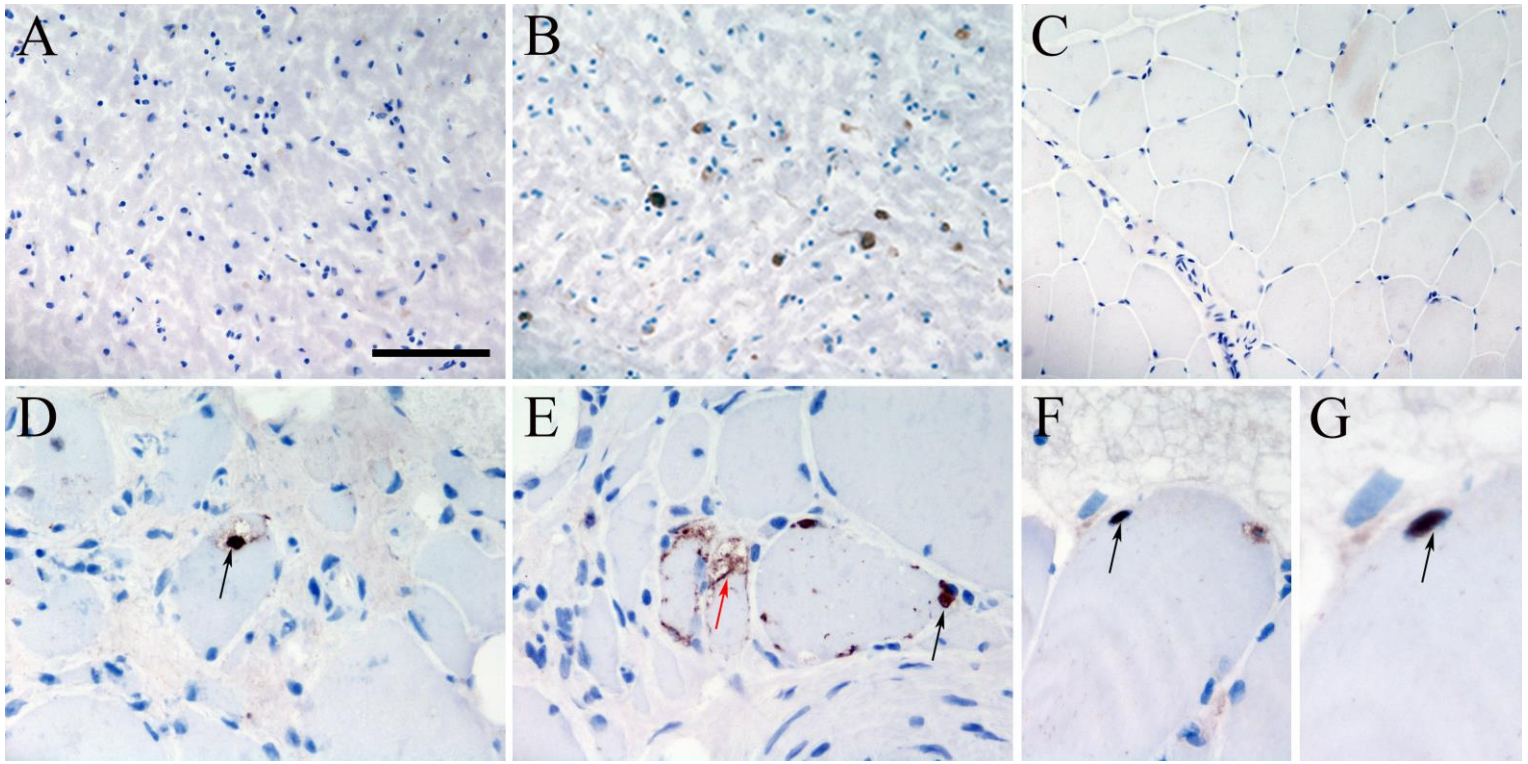
4.5.5.4 Protein aggregates were observed in morphologically normal and abnormal fibres in IBM

In IBM, protein aggregates were observed in both morphologically normal fibres and fibres exhibiting the Griggs diagnostic pathological features. They were immunoreactive for p62 (Figure 4.2), TDP-43 (Figure 4.3), α B-crystallin (Figure 4.4), myotilin (Figure 4.5) and ubiquitin (Figure 4.6). There were common characteristics in the morphology, size and location of protein aggregates between cases (Table 4.3). Fibres containing protein aggregates were often clustered together. Serial sections demonstrated that, occasionally, protein aggregates were stained by more than one antibody. In normal muscle, almost all myonuclei were TDP-43 positive. In comparison in IBM, fibres were not infrequently noted to have TDP-43 negative myonuclei. Though this was not formally quantified, this observation was most evident in muscle fibres containing sarcoplasmic TDP-43 positive aggregates (Figure 4.3E). No sarcoplasmic aggregates were observed with antibodies to tau and phosphorylated tau, Aβ, α-synuclein, desmin, FUS or VCP in IBM. The pattern of staining with antibodies to VCP and FUS in IBM was similar to that observed in normal muscle. Necrotic and regenerating fibres and fibres undergoing partial invasion frequently exhibited a diffuse non-specific sarcoplasmic immunoreactivity with desmin, FUS, p62, ubiquitin and VCP staining.

4.5.5.5 Protein aggregates were observed in a higher percentage of fibres than the current diagnostic pathological features

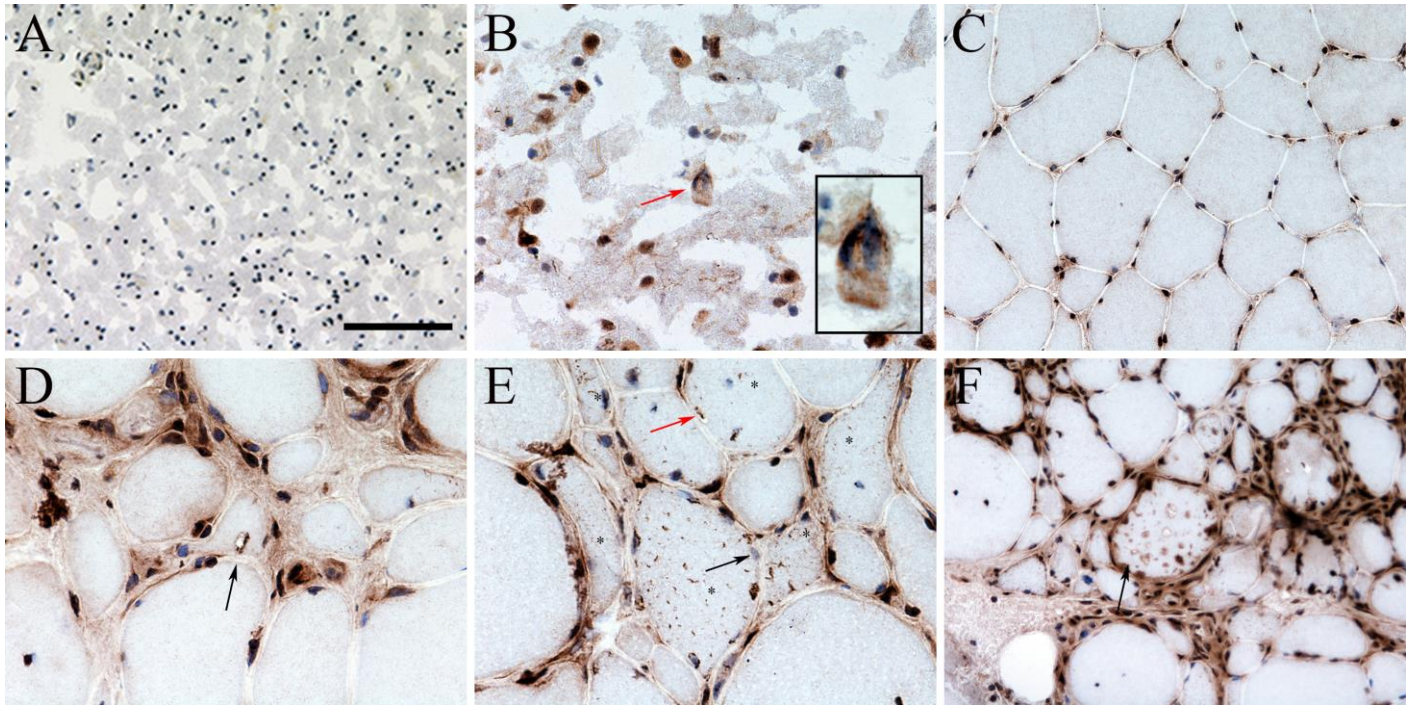
The percentage of fibres containing sarcoplasmic protein aggregates and the percentage of fibres containing pathological features used in the Griggs diagnostic criteria is summarised in Figure 4.7.

Figure 4.2 p62 immunoreactivity



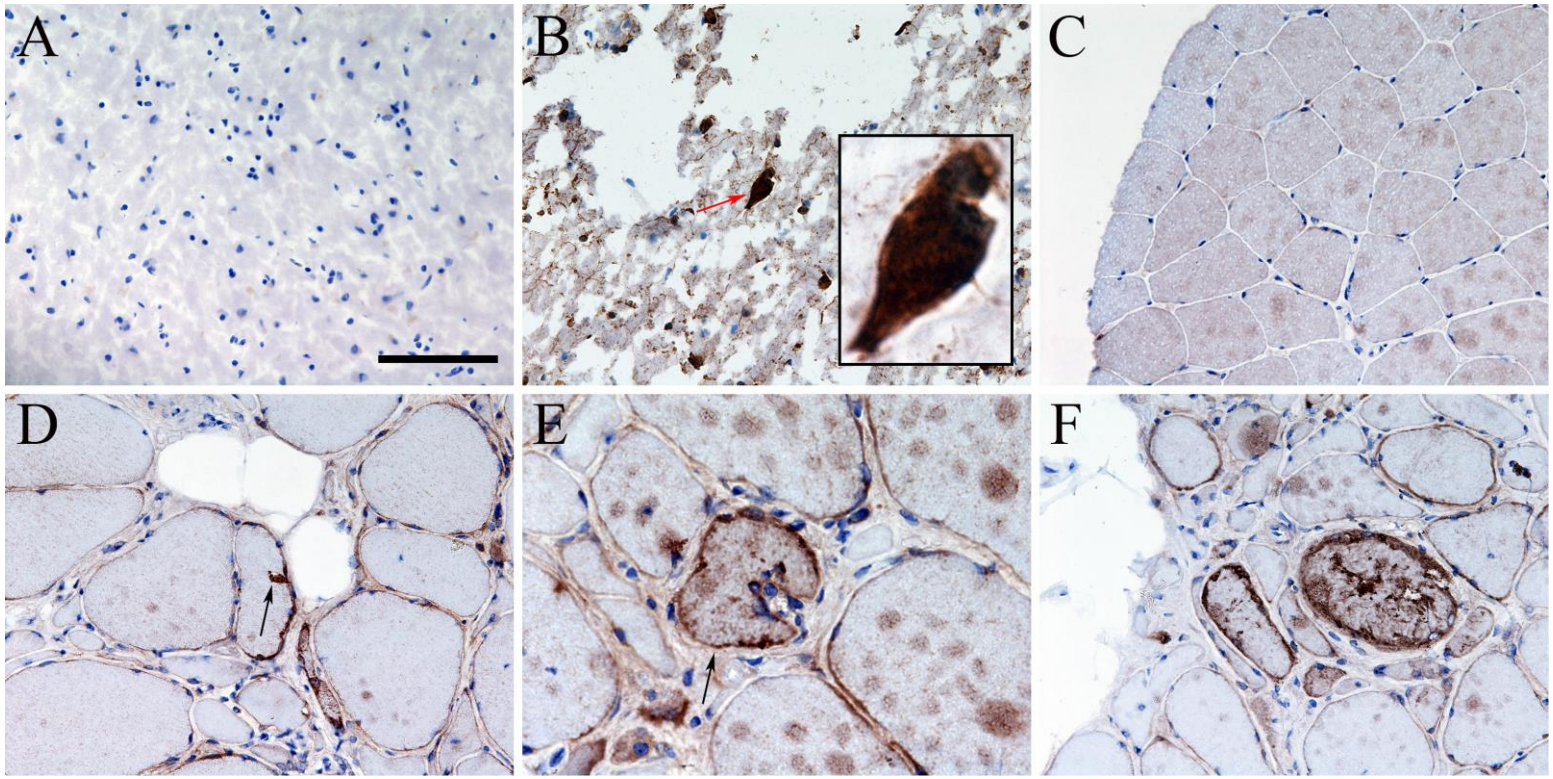
Eight µm thick cryostat sections stained for p62 using immunohistochemistry. Negative (A) and positive (B) control sections of AD brain, normal muscle (C) and IBM (D-G). No p62 immunoreactivity was observed in the negative control (A) and normal muscle (C). p62 immunoreactive aggregates were of varied size and staining intensity. They were observed within (D; arrow) and around (E; red arrow) rimmed vacuoles and in perinuclear (E, black arrow), sarcoplasmic (E), subsarcolemmal (E) and intranuclear (F and G; arrows) locations. Fibres contained single and multiple p62 deposits and were frequently found in clusters (E). Scale bar represents 100 µm in A-E, 50 µm in F and 25 µm in G.
p62 = Sequestosome 1; AD = Alzheimer's disease.

Figure 4.3 TDP-43 immunoreactivity



Eight µm thick cryostat sections stained for TDP-43 using immunohistochemistry. Negative (A) and positive (B) control sections of FTLD-TDP brain, normal muscle (C) and IBM (D-F). Positive control shows a neuron with absent nuclear TDP-43 and a cytoplasmic TDP-43 inclusion (B, red arrow and x100 insert). Sarcoplasmic aggregates were not observed in normal muscle (C). TDP-43 immunoreactivity was observed around some rimmed vacuoles (D; arrow) and within them (E; red arrow)(F; arrow). Nuclear immunoreactivity was present in both normal muscle (C) and IBM muscle fibres (D-F). Rarely myonuclei lacked TDP-43 in normal muscle; however, this was a common finding in IBM particularly in fibres containing sarcoplasmic aggregates (E; black arrow). TDP-43 sarcoplasmic aggregates were typically small and granular. Fibres containing aggregates were frequently clustered together (E). Scale bar represents 100 µm in A and C and F, 50 µm in B, D and E.
TDP-43 = Transactivation response DNA binding protein 43; FTLD-TDP = Frontotemporal lobar degeneration with TDP-43 positive inclusions.

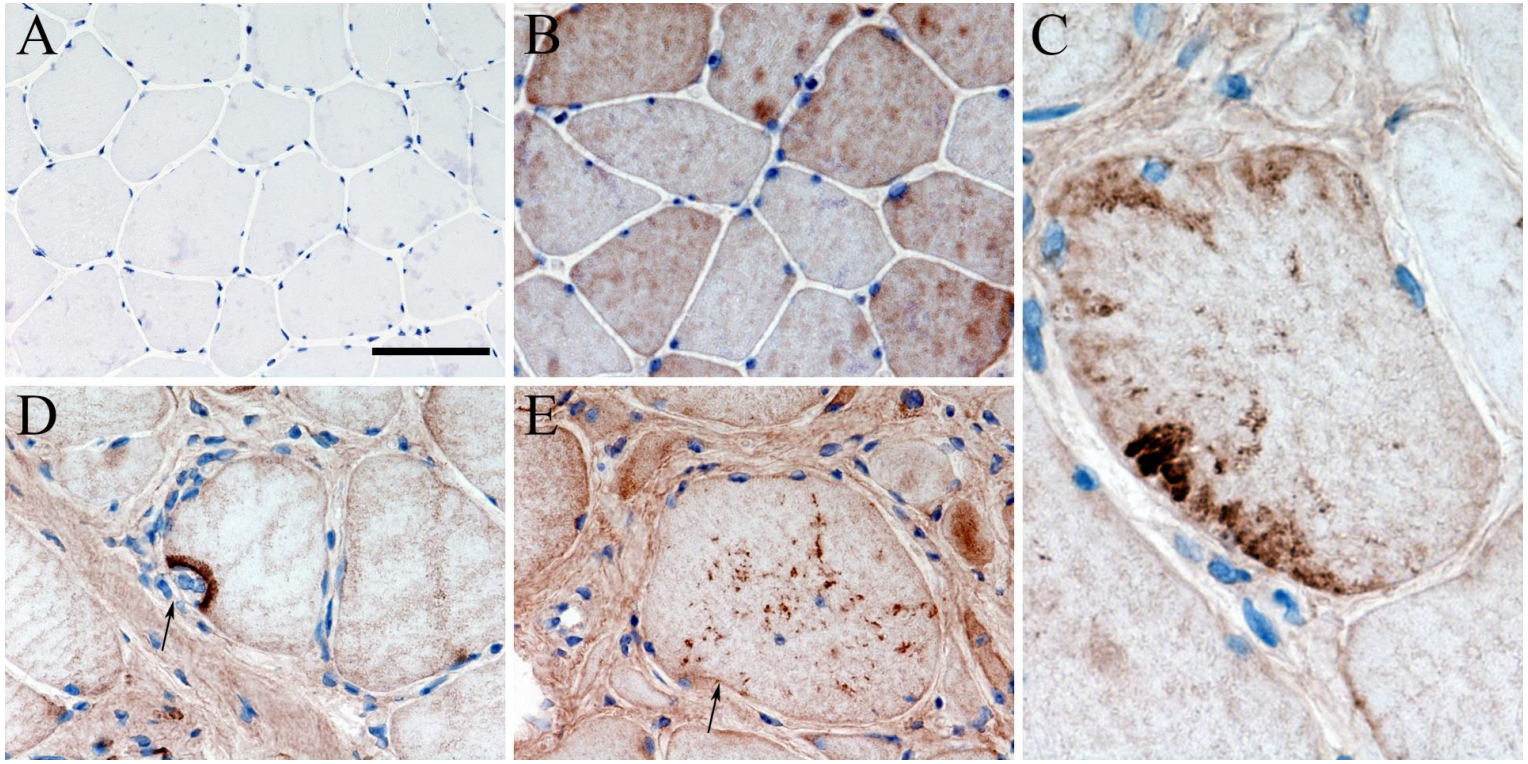
Figure 4.4 α B-crystallin immunoreactivity



Eight µm thick cryostat sections stained for α B-crystallin using immunohistochemistry. Negative (A) and positive (B) control sections of CBD brain, normal muscle (C) and IBM (D-F). Positive control shows an α B-crystallin positive balloon neuron (B; red arrow and x100 insert). No α B-crystallin immunoreactivity was observed in normal muscle (C). α B-crystallin immunoreactive deposits were observed in rimmed vacuoles (D; arrow) and around areas of partial invasion (E). Diffuse sarcoplasmic staining was present in atrophic fibres and fibres containing the Griggs pathological abnormalities (E; arrow and F). Clusters of fibres containing accumulations α B-crystallin were frequently observed (F). Scale bar represents 100 µm in A-D and F and 50 µm in E.

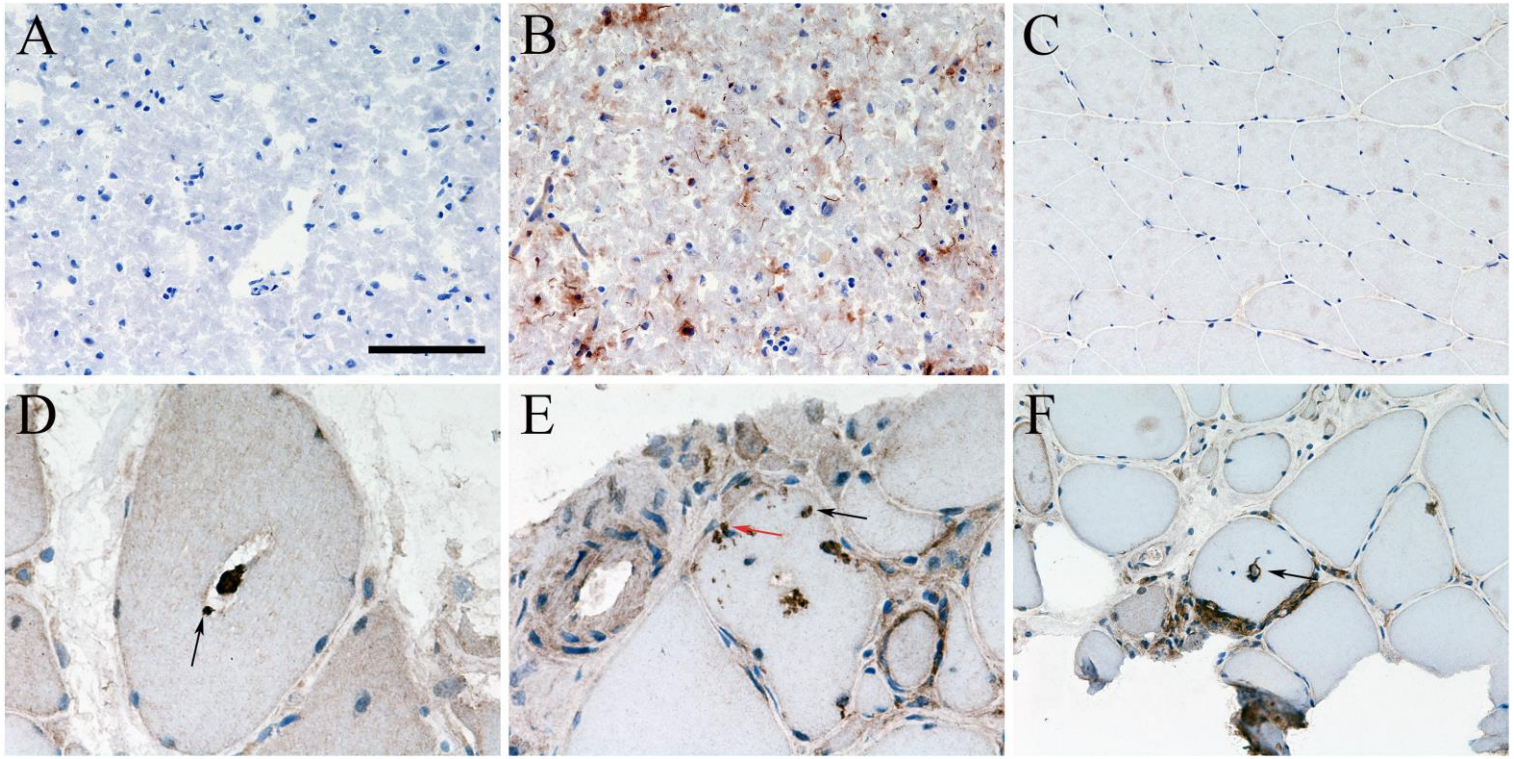
CBD = Corticobasal degeneration.

Figure 4.5 Myotilin immunoreactivity



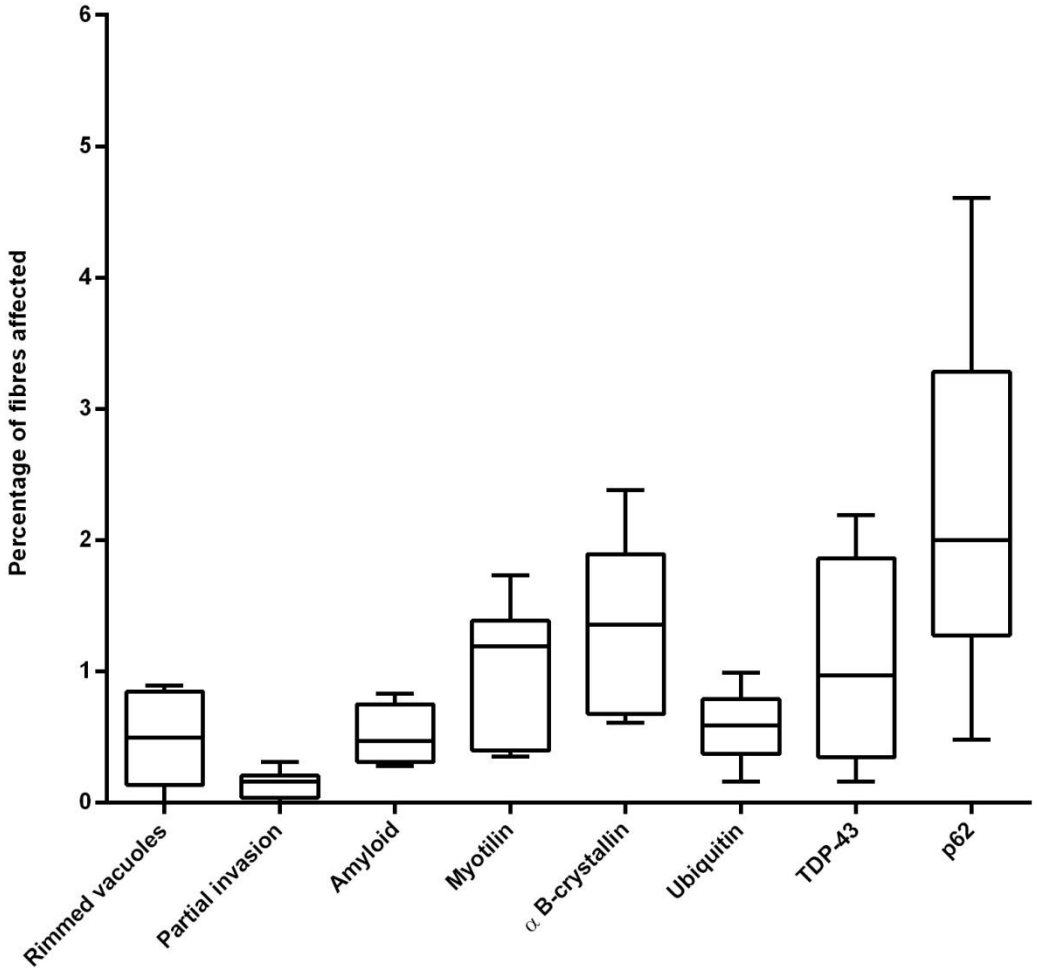
Eight µm thick cryostat sections stained for myotilin using immunohistochemistry. Negative (A) and positive (B) control muscle and IBM (C-E). Mild sarcoplasmic staining was observed in normal muscle (B). Myotilin aggregates in IBM were of varied size and shape and were most commonly subsarcolemmal (C). They were also found perinuclear, around rimmed vacuoles and in areas undergoing partial invasion (D; arrow). Small and medium sized central myotilin immunoreactive aggregates were not uncommon (E; arrow). Scale bar represents 100 µm in A, 50 µm in B, D and E and 25 µm in C.

Figure 4.6 Ubiquitin immunoreactivity



Eight µm thick cryostat sections stained for ubiquitin using immunohistochemistry. Negative (A) and positive (B) control AD brain, normal muscle (C) and IBM (D-F). No aggregates were observed in normal muscle (C). Ubiquitin immunoreactivity in IBM (D-F) was around and within rimmed vacuoles (D; arrow), nuclear (E; black arrow) and perinuclear (E; red arrow), sarcoplasmic and subsarcolemmal (E) and surrounding areas of partial invasion (F; arrow). Scale bar represents 100 µm in A-C and F, 50 µm in E and 25 µm in D.

Figure 4.7 Percentage of fibres containing protein aggregates and the Griggs diagnostic pathological features in IBM



Box and whisker plot illustrating the percentage of fibres containing pathological features in IBM [rimmed vacuoles 0.50 (0.14-0.85); partial invasion 0.16 (0.04-0.21); amyloid 0.47 (0.31-0.75); myotilin; 1.19 (0.40-1.39); α B-crystallin 1.36 (0.68-1.89); ubiquitin; 0.59 (0.37-0.79); TDP-43; 0.97 (0.35-1.86); and p62 2.00 (1.28-3.28)]. Fibres containing aggregates immunoreactive for p62 and α B-crystallin were more frequent than the diagnostic Griggs pathological features (p <0.05). p62, TDP-43, myotilin, α B-crystallin and myotilin immunoreactive deposits were observed in a higher percentage of fibres than partial invasion (p <0.02).
p62 = Sequestosome 1; TDP-43 = Transactivation response DNA binding protein 43.

Protein aggregates present were observed in a greater percentage of fibres than partial invasion; (p <0.02). p62 and α B-crystallin aggregates were present in a higher percentage of fibres than any of the Griggs pathological features: rimmed vacuoles, partial invasion and amyloid deposits (p <0.05). There was a trend towards all protein aggregates being present in a higher percentage of fibres than Griggs' diagnostic pathological features.

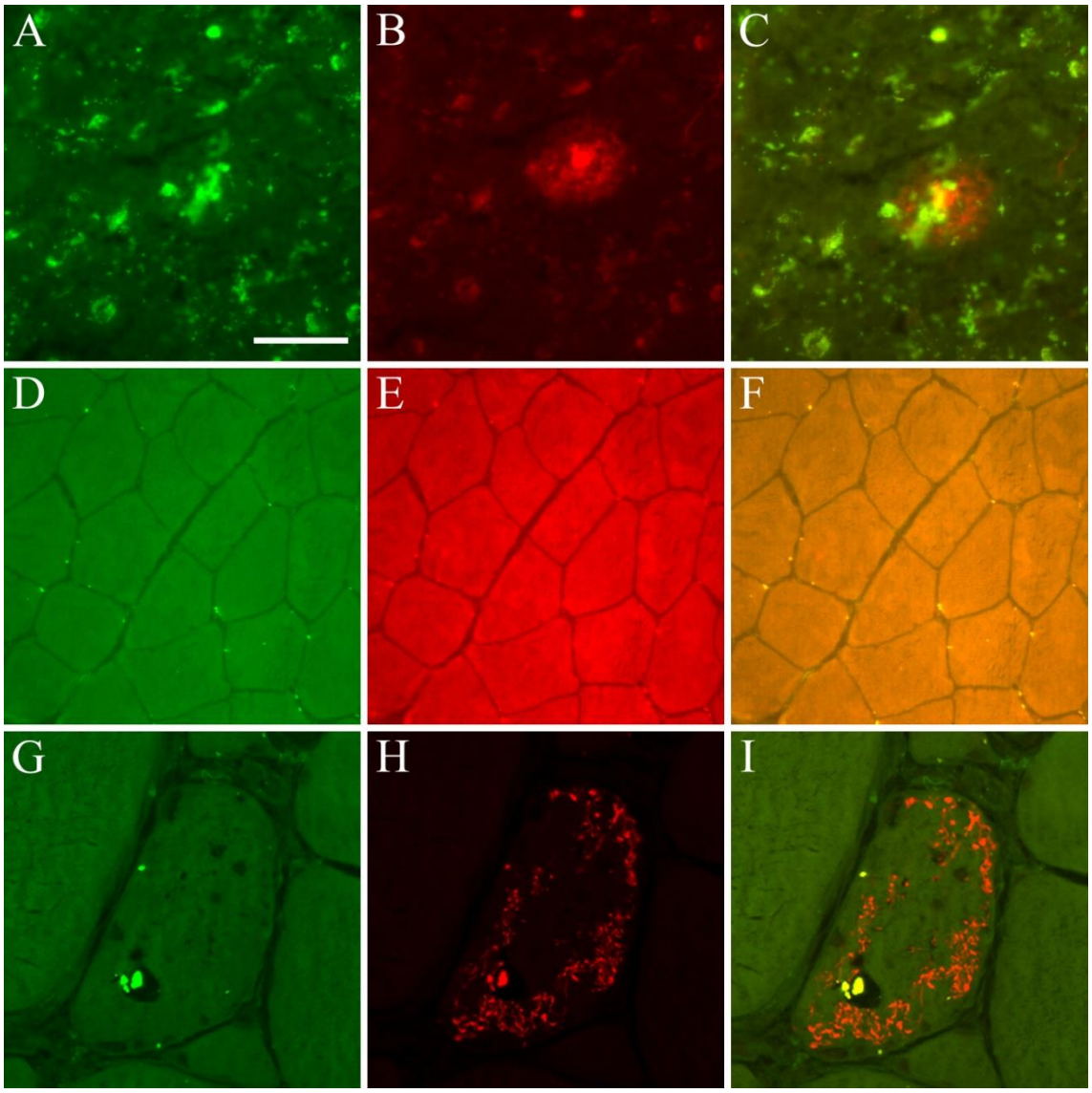
4.5.5.6 Congo red deposits were visible in IBM using fluorescent light but not polarised light

Alkalinised Congo red staining visualised under a rhodamine red filter (excitation 512-546 nm and emission 600-640 nm) was the most consistent method for staining and observing amyloid compared with crystal violet and thioflavin S staining. Fluorescent Congophilic aggregates were almost exclusively observed in vacuolated fibres. They were present throughout the sarcoplasm, around and within vacuoles. The deposits were typically filamentous or granular (Figure 4.8). No apple-green birefringence under polarised light was seen in IBM tissue sections stained with alkalinised Congo red, even when visualised using a x100 oil immersion objective lens. No amyloid was observed in normal muscle.

4.5.5.7 Nuclear membrane proteins were absent from rimmed vacuoles

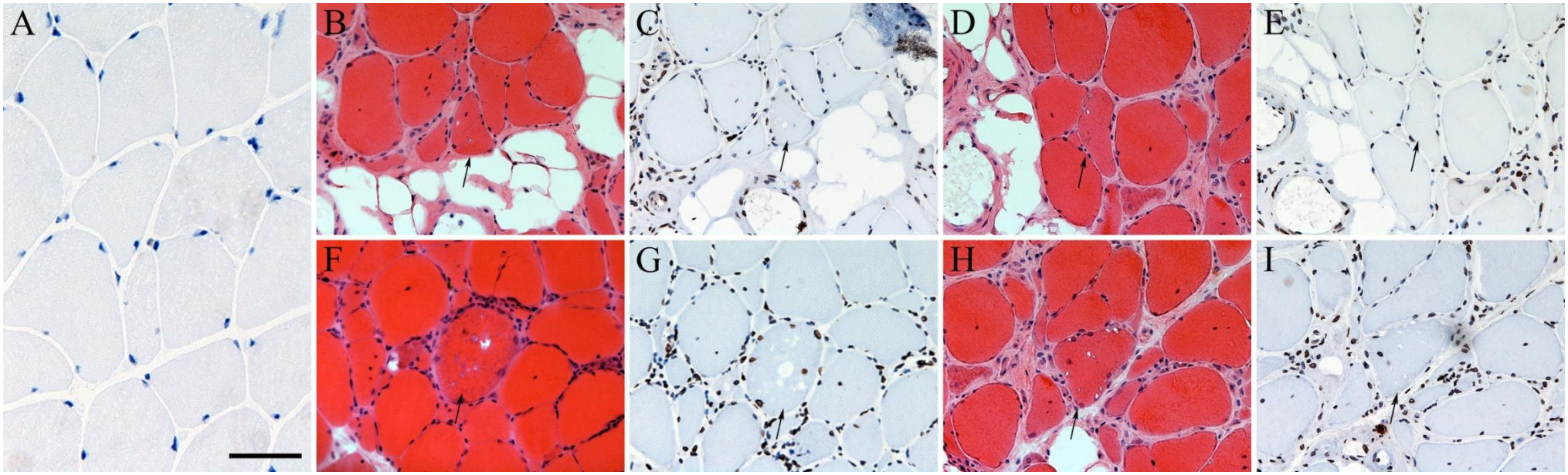
Rimmed vacuoles differed in size and morphology within and between cases. Some were empty but surrounded by a granular basophilic rim. Others contained basophilic granular material. They were located subsarcolemmal, centrally and not infrequently next to myonuclei. The majority of myonuclei were immunoreactive for emerin and lamin A/C. This was observed in normal muscle and IBM. Rimmed vacuoles and protein aggregates were not immunoreactive for emerin or lamin A/C (Figure 4.9). The occasional rimmed vacuole appeared to be positive for emerin and lamin A/C. However, when compared to the corresponding H&E stained section it was evident that the immunoreactivity corresponded to a myonucleus adjacent to the rimmed vacuole. p62, TDP-43, ubiquitin, and α B-crystallin staining were frequently found around and within rimmed vacuoles.

Figure 4.8 Alkalinised Congo red staining visualised under fluorescent light



Eight µm thick cryostat sections of AD brain (A-C) showing an amyloid plaque. Normal muscle (D-F) contained no amyloid deposits. Amyloid deposits were observed in IBM in vacuolated fibres (G-I) stained with alkalinised Congo red and visualised with fluorescent light. Tissue sections were examined using both the fluorescein isothiocyanate (excitation 440-480 nm and emission 527-530 nm) (A, D and G) and rhodamine red (excitation 512-546 nm and emission 600-640 nm) (B, E and H) filters to exclude areas of auto-fluorescence. Combined image are shown (C, F and I). Scale bar represents 50 µm in A-F and 25 µm in G-I.
AD = Alzheimer's disease.

Figure 4.9 Emerin and lamin A/C immunoreactivity



Eight µm thick cryostat tissue sections stained with H&E and immunohistochemistry for lamin A/C and emerin. Negative control (A) and consecutive sections from an IBM biopsy stained with H&E and emerin (B and C; D and E) and H&E and lamin A/C (F and G; H and I). Typical rimmed vacuoles on H&E stained sections did not display immunoreactivity for emerin and lamin A/C. Arrows denote the same vacuolated fibres in paired sections. Scale bar represents 33 µm in (A) and 100 µm in (B-I).
H&E = Haematoxylin and eosin.

4.5.5.8 MHC Class I was strongly up-regulated in IBM

MHC Class I staining was diffusely increased in IBM compared to normal muscle. In normal muscle there was no MHC Class I staining of fibres, but in IBM, MHC Class I was increased at the sarcolemma and throughout the sarcoplasm (Figure 4.10).

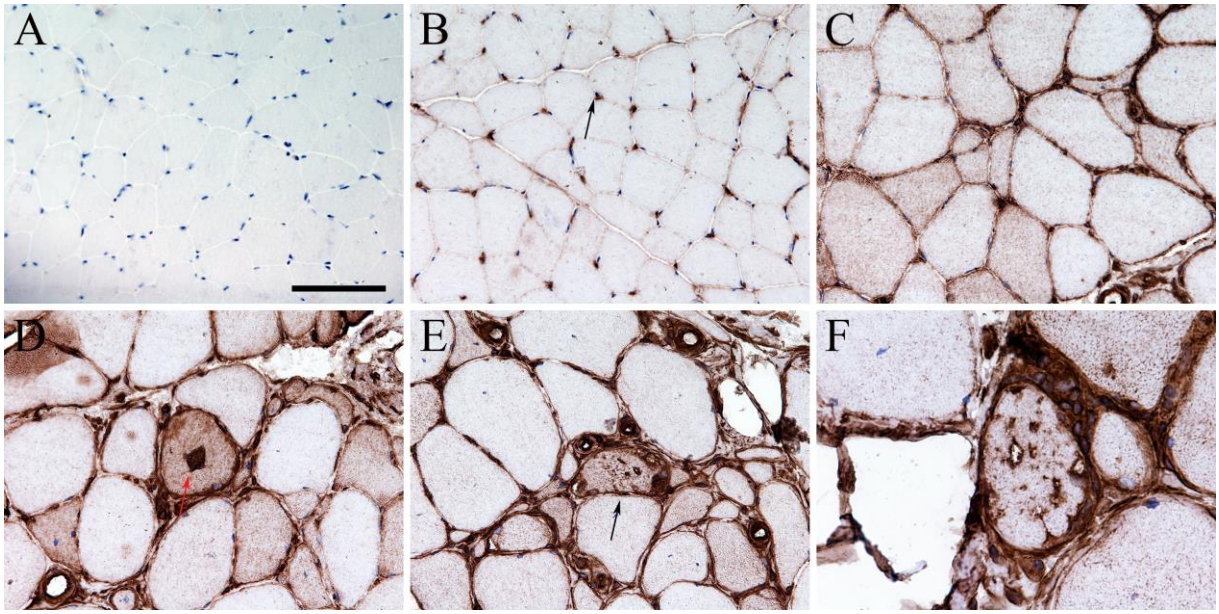
4.5.5.9 The inflammatory infiltrate was endomysial and predominantly composed of T-cells and macrophages

Few inflammatory cells were present in normal muscle. Macrophages were the most frequent inflammatory cell present and were predominantly found in the perimysium. All inflammatory cell types investigated (CD3 positive T-cells, cytotoxic T-cells, helper T-cells, macrophages and B-cells) were observed in greater numbers in IBM than in normal muscle (Figure 4.11). CD3 positive T-cells and macrophages were the commonest inflammatory cells present in IBM. There was no difference between the number of T-cells and macrophages (p=0.31). Cytotoxic T-cells were 1.5 times more common than helper T-cells (p=0.03). Very few B-cells were present in IBM.

So that the density and distribution of the inflammatory infiltrate in the entire tissue section could be assessed, a semi-quantitative inflammatory score-tool (Figure 2.3) was developed based on the juvenile dermatomyositis score tool (Wedderburn et al., 2007). The semi-quantitative score for each biopsy correlated well with the median number of cells quantified in five random x20 fields of magnification (r=0.71; p <0.0001). The score-tool analysis demonstrated that, all inflammatory cell types were predominantly present in the endomysium in IBM, with relatively fewer cells in the perimysium and perivascular area.

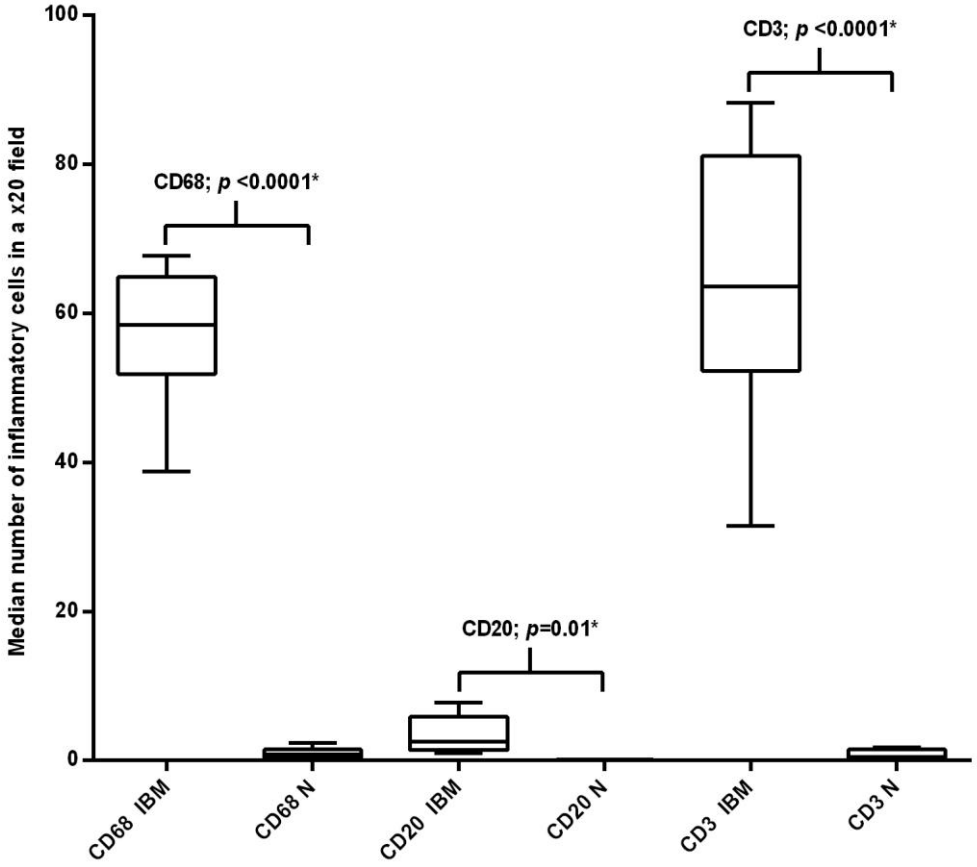
Partial invasion was present in all IBM cases on H&E stained sections. With IHC staining it was shown that partially invading cells were most often cytotoxic T-cells and macrophages. These were occasionally accompanied by helper T-cells and B-cells. Further sections revealed that partially invaded fibres were split (Figure 4.12).

Figure 4.10 MHC Class I staining in normal muscle and IBM



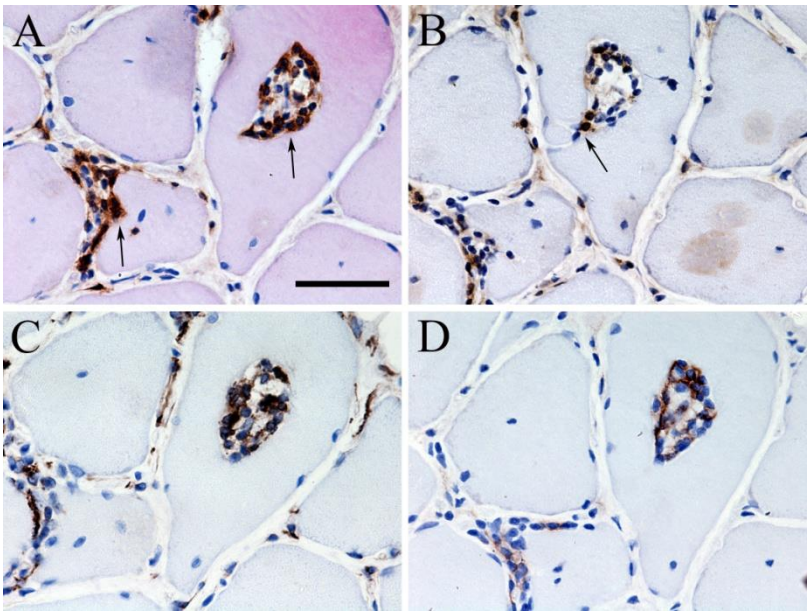
Eight µm thick cryostat sections stained for MHC Class I using immunohistochemistry. Negative control (A), normal muscle (B) and IBM (C-F). In normal muscle, capillaries show MHC Class I immunoreactivity (B; black arrow) but there is no sarcolemmal or sarcoplasmic staining. In IBM there is increased sarcolemma and sarcoplasmic immunoreactivity affecting all fibres (C). MHC Class I immunoreactivity was increased at sites of partial invasion (D; red arrow) and around rimmed vacuoles (E; black arrow) and (F). Scale bar represents 100 µm in A and B, 50 µm in C-E and 25µm in F.
MHC Class I = Major histocompatibility complex class I.

Figure 4.11 Median number of inflammatory cells in IBM and normal muscle



Box and whisker plot illustrating the median number of inflammatory cells present in IBM and normal muscle. All inflammatory cell types were present in significantly greater numbers in IBM than in normal muscle.
CD68 = Macrophages; N = Normal muscle; CD3 = T-cells; CD20 = B-cells. *Statistically significant results shown (p <0.05).

Figure 4.12 Partial invasion in IBM



Eight µm thick consecutive cryostat sections of IBM muscle stained using immunohistochemistry for CD8 (cytotoxic T-cells) (A), CD4 (helper T-cells) (B), CD68 (macrophages) (C) and CD20 (B-cells) (D). CD8 staining shows partial invasion of two fibres by cytotoxic T-cells (arrows) (A). The upper fibre is also invaded by helper T-cells (B), macrophages (C) and few B-cells (D) whereas the invading cells in lower fibre are only cytotoxic T-cells. Serial sections reveal a split in the upper partially invaded fibre (arrow) (B). Scale bar represents 50 µm in A-D.

4.5.5.10 There were no relationships between pathological findings or clinical features and pathological findings

There were no correlations between the number of fibres in a biopsy containing the following pathological features: rimmed vacuoles, partial invasion, fluorescent Congo red deposits and aggregates immunoreactive for p62, myotilin, TDP-43, ubiquitin and α B-crystallin immunoreactive deposits i.e. although the same protein aggregates were often identified with different antibodies, the number of fibres containing aggregates labelled with different antibodies did not correlate within each biopsy. There were no correlations between the inflammatory infiltrate and the previously listed pathological features. There were no identifiable relationships between the pathological findings and the age at disease onset, age at muscle biopsy, disease duration or serum CK level.

4.6 Discussion

Using IHC and IF staining, many abnormally aggregated proteins have been described in IBM. However, published results are conflicting and not always substantiated between laboratories. Therefore, the role that protein aggregates play in the pathogenesis of IBM and their diagnostic utility is uncertain. To answer the question of which proteins are present in IBM and warrant further investigation as potential markers to complement or replace currently recommended pathological diagnostic features, a systematic study of the pathological features present in a well-defined IBM cohort was performed. p62, TDP-43, myotilin, ubiquitin and α B-crystallin immunoreactive aggregates in addition to inflammatory changes typical of PM, namely MHC Class I up-regulation and endomysial inflammatory infiltrate, were found in all six IBM cases studied. Neurodegenerative proteins including Aβ, α-synuclein, tau and hyperphosphorylated tau were not identified, refuting the theory that Aβ and tau protein aggregates damage muscle fibres in IBM and the long-held belief in the pathogenic similarities between IBM and AD.

4.6.1 Previous studies

The purposes of the pathological studies in IBM have been two-fold. Firstly, to help elucidate the pathogenesis of IBM and therefore direct future therapeutic studies. Secondly, to identify biomarkers that differentiate IBM from other pathologically and clinically similar inflammatory and vacuolated myopathies such as PM, DM and MFM. The similarity between the tubulofilaments observed on EM and amyloid fibrils led to the search for proteins known to aggregate in a beta-pleated formation. However, as described in Chapter 1, the results from studies have not been consistent and therefore, our understanding of the pathogenesis of IBM has not progressed and no new biomarkers can currently be recommended for clinical use. The reasons for the variable results published in IBM are probably multiple. Criticisms of studies to date have included poor study methodology, lack of appropriate disease controls and an absence of quantitative data (Greenberg, 2010). Often, positive control tissues known to harbour the epitope of interest are absent, as are definitions of the pathological features assessed. Some authors state that "no abnormalities characteristic for IBM were observed in controls" (Askanas et al., 1992b)(Askanas et al., 1994a), it is therefore unclear whether other abnormalities were present. Published images have been criticised for showing abnormalities in structurally abnormal fibres or fibres undergoing necrosis or regeneration which are often observed to stain non-specifically. The incorrect interpretation of artefact especially on IF staining may be the cause of false-positive reporting in some studies. There is no standardised method of quantifying abnormalities observed on biopsy and a number of different methods are used. These include the proportion of biopsies containing an abnormality (Temiz et al., 2009), the number of abnormalities per mm^2 (Chahin and Engel, 2008), the number of affected fibres in a random field (Dubourg et al., 2011) and, peculiar to IBM, the percentage of vacuolated fibres affected (Askanas et al., 1994a). Although these various methods have virtues they can obscure the findings and limit comparisons between studies. To avoid these problems in the current study; i) all antibodies were initially titrated in control tissue known to contain the protein/epitope of interest and positive and negative controls were included, ii) IHC was used

rather than IF so that the structure and nature of affected fibres could be assessed, and iii) the entire biopsy was assessed enabling the findings to be expressed as a percentage of the total number of fibres affected in the biopsy.

4.6.2 Protein aggregates identified with IHC are more sensitive than the current diagnostic pathological features in IBM

p62, TDP-43, ubiquitin, myotilin and α B-crystallin positive accumulations were observed in all cases of IBM studied, confirming previous reports (Albrecht and Bilbao, 1993)(Banwell and Engel, 2000)(Olivé et al., 2008)(D'Agostino et al., 2010). They were all present in a higher number of fibres than partial invasion. In addition, p62 and α B-crystallin were observed in a higher percentage of fibres than the current Griggs diagnostic light microscopic features. Although TDP-43, ubiquitin and myotilin were present in a higher percentage of fibres than rimmed vacuoles and amyloid, the differences were not statistically significant. The greater percentage of fibres containing protein aggregates suggests that immunoreactive deposits may be better biomarkers than the current diagnostic features for IBM though further work needs to be done to assess their specificity in IBM. Earlier studies suggested that the presence of protein aggregates in fibres lacking the diagnostic pathological features to be an early feature of the disease and therefore more closely linked to the pathogenesis. Although this interpretation is likely to be an over-simplification, the more frequent a pathological feature the more attractive it is as a biomarker. This being said the presence of these protein aggregates may provide interesting insight into the potential pathogenesis of IBM, which is discussed below (Section 4.6.5).

There was no IHC evidence of Aβ, α-synuclein, hyperphosphorylated tau or tau in IBM and therefore no support for the hypothesis that these proteins are intimately involved in or responsible for the pathogenesis and fibre damage observed in IBM. It is likely that the presence of neurodegenerative proteins in IBM has been over-emphasised. Our findings are supported by

immunoblotting results reported in the literature and detailed in Chapter 1 and the IHC findings of Sheriff *et al.*(1995) who were unable to show Aβ, APP and hyperphosphorylated tau staining in sixteen IBM cases (Sherriff et al., 1995). Further studies also failed to show any or significant labelling with antibodies to these proteins in IBM (Nalbantoglu et al., 1994)(Salajegheh et al., 2009b)(Temiz et al., 2009)(Dubourg et al., 2011). Suggested explanations for these discrepancies are discussed above. In addition, misconceptions have crept into the IBM literature. For example, the SMI-31 antibody has been reported in IBM as a marker of tau, but it is marketed as recognising a phosphorylated epitope of neurofilaments H and M and has been reported to cross-react with a number of other proteins including phosphorylated tau. SMI-31 immunoreactivity has therefore been mistakenly used to strengthen the claim that tau is widely present in IBM (Salajegheh et al, 2009a).

4.6.3 Congophilic deposits as opposed to amyloid are present in IBM

Using alkalinised Congo red staining visualised under fluorescent light, Congophilic deposits were identified in all six IBM cases. Amyloid is classically identified by staining with Congo red and visualised using apple-green birefringence under polarised light. However, we did not observe apple-green birefringence under polarised light even at high magnification. Previously it was hypothesised that the small size of aggregates accounted for negative Congo red staining visualised through polarising filters in IBM (Benveniste and Hilton-Jones, 2010). However, fluorescent Congophilic inclusions in MFM, which may be large, have also been reported to lack apple-green birefringence (Selcen, 2011). The reason for the absence of the classical apple-green birefringence under polarised light in IBM and MFM is unknown. However, in its absence it may be more accurate to describe these inclusions as Congophilic as opposed to amyloid.

4.6.4 The inflammatory changes in IBM resemble those reported in PM

In agreement with earlier studies the inflammatory changes observed in our IBM cases were very similar to those associated with PM – endomysial inflammatory infiltrate predominantly comprising T-cells and macrophages and sarcolemmal MHC Class I up-regulation on every fibre. B-cells identified using a CD20 marker were relatively sparse compared to T-cells and macrophages. Others have shown B-cells to be frequent in IBM using CD138 marker (Greenberg et al., 2005). CD138 identifies mature antibody secreting B-cells. The presence of CD138 positive B-cells has led these authors to suggest that humoral immunity has a role in the pathogenesis of IBM. However, as yet no muscle surface auto-antibodies have been detected to suggest that humoral immunity plays a significant role in IBM. Assessing the degree and distribution of inflammatory infiltrate in a biopsy is problematic. We have shown that a semi-quantitative inflammatory score-tool can be used and correlates well with quantitative results. Partial invasion of fibres was observed with H&E and IHC. IHC revealed that invading cells were most commonly cytotoxic T-cells and macrophages. However, what results in inflammatory cells attacking individual fibres could not be discerned. There was no difference in the immunoreactivity between the fibres undergoing partial invasion and those not undergoing partial invasion in terms of protein aggregates or MHC Class I up-regulation. Although partial invasion is an essential feature of the current diagnostic criteria its rarity compared to other pathological features questions its continued use as a diagnostic criterion.

4.6.5 Possible disease mechanisms inferred from IHC findings

The proteins we observed to aggregate in IBM have varied cellular functions. p62 and ubiquitin are integral parts of autophagy (Bjørkøy et al., 2005) and UPS respectively, which have been shown to interact with each other (Ding et al., 2007). The precise role of TDP-43 is unknown. However, it is believed to be important in the regulation of gene transcription and mRNA expression primarily from its presence in aggregates and genetic mutations in frontotemporal lobar degeneration and MND. Mutations in the genes encoding myotilin, desmin and α B-

crystallin are responsible for some of the MFM which are pathological similar to IBM with protein aggregates and rimmed vacuoles present on biopsy (Wanschit et al., 2002)(Selcen and Engel, 2003)(Selcen and Engel, 2004). Myotilin and desmin are Z-disk associated proteins. α B-crystallin is a member of the small heat shock protein (HSP) family. Like other HSP its expression is increased by stress, but in contrast them it is not ubiquitously expressed and is only present in high levels in cardiac and skeletal muscle and the lens of the eye. In muscle, α B-crystallin is associated with the Z-disk. The presence of myotilin and α B-crystallin positive aggregates may be secondary to myofibrillar disruption. α B-crystallin has also been suggested as an auto-antigen in IBM (Banwell and Engel, 2000). It is hypothesised that because α B-crystallin is absent from the majority of other tissues in the body T-cells have not become tolerant of it. Therefore, when it is over-expressed in skeletal muscle it is processed and expressed on MHC Class II molecules instigating an auto-aggressive inflammatory response. However, fibres expressing α B-crystallin were not preferentially surrounded or invaded by inflammatory cells.

Mitochondrial abnormalities such as ragged red fibres, COX deficient fibres and mitochondrial DNA mutations are frequent in IBM (Moslemi et al., 1997)(Chahin and Engel, 2008). Alterations in two cellular pathways, autophagy and ER, may link the inflammatory infiltrate, protein aggregates and mitochondrial changes observed in IBM. Impairment of autophagy and therefore the degrading and recycling of cellular proteins and organelles could lead to the accumulation of dysfunctional mitochondria and aggregation-prone proteins. In addition, impaired autophagy has been shown to increase of MHC Class I (Li et al., 2010). Alternatively, MHC Class I up-regulation may be a consequence of the EOR. ER is the site of synthesis, folding and processing of secreted proteins. Perturbations in many cellular functions cause ER stress, activating the UPR and EOR, which work to restore cellular homeostasis. EOR increases NF-κB DNA binding in cultured human muscle (Nogalska et al., 2007), which in turn may result in increased MHC Class I transcription. Alternatively, it has been shown that MHC Class

I over-expression may precede ER stress in mice that constitutively overexpress MHC Class I (Nagaraju et al., 2005). From our findings, it is not possible to determine whether protein degradation via autophagy or the UPS are inhibited in IBM. The presence of protein aggregates may reflect increased synthesis of abnormal aggregation prone proteins exceeding the capacity of the UPS and autophagic machinery.

p62 and ubiquitin aggregates were observed within and around myonuclei. Together with the loss of normal myonuclear TDP-43 staining these findings implicate myonuclear degeneration in the pathogenesis of IBM. Rimmed vacuoles are often adjacent to myonuclei and it has been hypothesised that they may be derived from degenerating myonuclei. However, we found no evidence of emerin or lamin A/C immunoreactivity associated with rimmed vacuoles. The presence of protein aggregates in both morphologically normal and vacuolated muscle fibres and in a higher percentage of fibres compared to rimmed vacuoles suggests that protein aggregation may precede the development of rimmed vacuoles. However, this hypothesis needs to be confirmed in clinically typical patients lacking rimmed vacuoles on biopsy.

4.6.6 Study limitations

The small number of cases included could be said to introduce bias as the absence of a pathological finding in six cases may be due to chance. However, the aims of this study were to identify proteins central to the pathogenesis of IBM and robust biomarkers for further validation. Therefore the absence of a protein in six cases would suggest that it is not intimately involved in the pathogenesis or a reliable biomarker for IBM and exclude it from further evaluation. All the markers identified in this study require further validation in clinically typical IBM lacking the diagnostic pathological features to determine their sensitivity, and in inflammatory and vacuolated disease controls to determine their specificity (Chapter 5). As was shown in Chapter 3, patients with clinically typical IBM lacking the diagnostic pathological features are likely to be at an earlier stage in the disease course than cases in which all of the

diagnostic pathological features are present. Therefore the diagnostic pathological features may represent secondary late-stage changes in the muscle and the pathological findings in cases lacking these features may be more informative as to the underlying pathological processes in IBM. It is important to note that although no pathological abnormalities were observed in the control cases there was a difference in age between these cases and the IBM cases. The control cases were younger at the time of muscle biopsy. It cannot be ruled-out that the difference in age may have affected the results as alterations in protein metabolism have been shown to occur with aging in animal studies (Vittorini et al., 1999)(Cui et al., 2012).

4.6.7 Final comments

In conclusion, p62, α B-crystallin, TDP-43, ubiquitin and myotilin protein aggregates were present in IBM and may be more abundant than the current diagnostic pathological features. Therefore, the use of IHC for protein aggregates may aid in the diagnosis of IBM. However these findings need to be validated in clinically typical IBM lacking the diagnostic pathological features and disease controls need to be included to determine their specificity. The presence of protein aggregates in morphologically normal fibres suggests that they may be indicative of an earlier stage in the disease process, thus facilitating earlier diagnosis. This finding needs to be validated in cases of IBM that do not contain rimmed vacuoles. We found no evidence to support the notion that IBM is pathologically similar to AD or other neurodegenerative diseases or that the animal models, which over-express APP, Aβ and tau, currently used to mimic IBM represent adequate disease models.

Chapter 5

ASSESSMENT OF PATHOLOGICAL BIOMARKERS IN IBM AND DISEASE CONTROLS

5.1 Introduction

Since its first recognition, a variety of pathological features have been described in IBM including endomysial inflammatory infiltrate, invasion of morphologically normal fibres by inflammatory cells (partial invasion), rimmed vacuoles, eosinophilic inclusions, amyloid, protein aggregates and tubulofilamentous inclusions identified using EM (Chou, 1967)(Yunis and Samaha, 1971)(Carpenter et al., 1978)(Arahata and Engel, 1984)(Lotz et al., 1989)(Mendell et al., 1991)(Askanas et al., 1993b). Despite being described in other myopathies, a number of these features were thought to differentiate IBM from steroid-responsive inflammatory myopathies such as PM and genetic myopathies with rimmed vacuoles such as MFM and hIBM. Thus, in various combinations the pathological features have formed the basis of successive diagnostic criteria for IBM (Lotz et al., 1989)(Griggs et al., 1995)(Vershuuren et al., 1997). However, the need to demonstrate all the pathological features required by the diagnostic criteria has been questioned (Sayers et al., 1992). In addition, a small number of studies have indicated that the current diagnostic pathological features may be absent in patients with clinically typical IBM and may remain so for many years despite repeated biopsy (Amato et al., 1996)(Chahin and Engel, 2008)(Benveniste et al., 2011).

Since publication of the two most widely used sets of diagnostic criteria for IBM (Griggs et al., 1995)(Vershuuren et al., 1997), there have been many publications documenting different proteins observed to be accumulated in pathologically typical IBM. The most frequently reported are described in Chapter 1. It has been suggested, firstly, that staining for particular protein aggregates may improve the diagnosis of IBM, differentiating it from pathologically and clinically similar

myopathies. Secondly, that the aggregated proteins identified in IBM may provide insight into the underlying pathogenesis (Albrecht and Bilbao, 1993)(van der Meulen et al., 2001)(Askanas and Engel, 2008). However, very few studies have systematically evaluated the pathological findings in IBM and therefore claims of their use in discriminating between IBM and myopathies considered in the differential diagnosis of IBM are unsubstantiated (van der Meulen et al., 2001)(Temiz et al., 2009)(Dubourg et al., 2011). Furthermore, many of these studies i) assess pathological findings on their ability to differentiate between pathological typical IBM with PM, which is easily and simply done by identifying rimmed vacuoles on H&E stained sections, but not their ability to differentiate pathologically atypical IBM, e.g. IBM lacking rimmed vacuoles, and PM (van der Meulen et al., 2001), ii) lack quantitative data (Temiz et al., 2009), or iii) use disease controls that are neither clinically nor pathologically similar to IBM (Dubourg et al., 2011).

Previously in Chapter 3, we confirmed that patients with pathologically atypical IBM but the characteristic clinical pattern of weakness associated with IBM are clinically indistinguishable from patients with pathologically definite IBM and established that the clinical assessment with a supportive biopsy should be considered the 'gold-standard' for diagnosing IBM. However, not all patients will fulfil the clinical criteria at presentation. In Chapter 4, we found p62, TDP-43, myotilin and ubiquitin immunoreactive aggregates to be present in clinically and pathologically definite IBM. Therefore, these may be of diagnostic use. Having established the pathological findings present in pathologically definite IBM, the aim of this chapter was to assess the diagnostic value of pathological features identified in Chapter 4 by comparing clinically and pathologically typical IBM and clinically typical IBM lacking the diagnostic pathological findings with steroid-responsive inflammatory myopathies and myopathies containing rimmed vacuoles as controls.

5.2 Hypothesis

Protein aggregates identified using IHC are sensitive and specific for IBM and enable its differentiation from pathologically similar diseases such as MFM, PM and DM.

5.3 Aims

To determine in a systematic quantitative manner which pathological features can reliably differentiate between IBM and disease controls and to provided recommendations on how to incorporate the pathological findings in IBM into future diagnostic criteria.

5.4 Methods

Cases were categorised according to clinical features and biopsy findings into five groups: IBM with rimmed vacuoles on muscle biopsy (IBM+RV) (*n*=15), IBM without rimmed vacuoles on muscle biopsy (IBM–RV) (*n*=9), steroid-responsive inflammatory myopathies (PM&DM) (*n*=11), protein accumulation myopathies with rimmed vacuoles on muscle biopsy (PAM+RV) (*n*=7) and normal muscle (*n*=6). Cases of IBM+RV were not used in Chapter 4. All biopsies were taken prior to any treatment. PM&DM cases showed a sustained and unequivocal clinical response to steroid treatment accompanied by normalisation of serum CK. PAM+RV cases included clinically and pathologically typical MFM with unidentified gene mutation (*n*=2), MFM with mutations in myotilin (*n*=2), hIBM with compound heterozygous mutations in GNE (*n*=1), inclusion body myopathy with Paget's disease and frontotemporal dementia (IBMPFD) with a mutation in VCP (*n*=1) and a BMD with deletion of exons 45-47 on the X-chromosome (*n*=1). Full clinical and pathological inclusion criteria are summarised in Chapter 2.

Tissue sections were stained with H&E, alkalinised Congo red, COX/SDH HC and IHC for p62, TDP-43, myotilin, ubiquitin, MHC Class I, T-cells (CD3), helper T-cells (CD4), cytotoxic T-cells (CD8), macrophages (CD68) and B-cells (CD20) was performed. Details of the staining protocols, antibodies and optimum conditions are summarised in Chapters 2 and 4. Tissue sections were analysed blinded to the clinical information. The distribution and intensity of the inflammatory infiltrate was assessed using the semi-quantitative inflammatory score tool validated in Chapter 4.

Criteria for a diagnostic test were either i) sensitivity of 95% and specificity of 75%; ii) sensitivity of 75% and specificity of 95%; iii) likelihood ratio (LR) of greater than 10; or iv) less than 0.1 (Pfeiffer, D, 1998)(Deeks and Altman, 2004). Intra-observer variability was calculated using Bland-Altman plots. Inter-observer reliability was calculated using Cohen's kappa statistic (κ), which is suitable for two assessors and multiple categories. Boundaries were: κ <0.4=poor, κ 0.4-0.75=fair to good and κ >0.75=excellent (Fleiss, 1981).

5.5 Results

5.5.1 Clinical characteristics

The clinical characteristics are shown in Table 5.1.

5.5.2 Quantitative assessment of protein aggregates and mitochondrial changes

5.5.2.1 Intra-observer and inter-observer reliability were good or excellent

Bland-Altman plots showed good intra-observer agreement between first and second counts, the difference between counts was 0.02 (±0.05). All counts and re-counts were within the 95% limits of agreement.

The presence or absence of partial invasion on H&E staining, p62, TDP-43, ubiquitin, myotilin immunoreactive aggregates and the grade of MHC Class I immunoreactivity in each biopsy was independently assessed by two observers blinded to the clinical details. In total 288 slides were assessed by both observers. Inter-observer agreement was good or excellent: partial invasion, κ=0.95; p62, κ=1.00; TDP-43, κ=0.70; ubiquitin, κ=0.95; Congo red, κ=1.00; myotilin, κ=0.88; and MHC Class I, κ=1.00.

5.5.2.2 Percentage of muscle fibres in IBM+RV containing protein aggregates and current diagnostic features IBM+RV

In agreement with the findings reported in Chapter 4, p62 immunoreactive aggregates were present

Table 5.1 Clinical characteristics

Characteristic	IBM+RV	IBM-RV	PM&DM	PAM+RV
Number of cases	15	9	11	7
Male:female ratio	2:1	4:5	4:7	4:3
Age at disease onset in years, median (IQR)	54 (48-67)	62 (44-68)	55 (34-65)	46 (24-54)
Age at muscle biopsy in years, median (IQR)	64 (59-71)	68 (47-74)	55 (34-65)	54 (29-59)
Duration of symptoms in years, median (IQR)	5 (4-7)	3 (2-8)	0 (0-0)	5 (3-9)
Creatine kinase in IU/l, mean (±SD)	1748 (±1348)	926 (±800)	6744 (±5875)	739 (±320)

IBM+RV = IBM with rimmed vacuoles on muscle biopsy; IBM-RV = IBM without rimmed vacuoles on muscle biopsy; PM&DM = Steroid-responsive inflammatory myopathies; PAM+RV = Protein accumulation myopathies with rimmed vacuoles on muscle biopsy; IQR = Interquartile range; SD = Standard deviation.

in a greater percentage of fibres than the current diagnostic pathological features ($p \leq 0.001$) and fibres containing myotilin and ubiquitin immunoreactive aggregates ($p \leq 0.0002$) (Figure 5.1).

5.5.2.3 Comparison of the pathological findings in IBM+RV, IBM–RV and disease controls

The percentage of fibres containing pathological features in the each group is summarised in Figure 5.2.

5.5.2.3.1 Comparison between IBM+RV and IBM-RV

p62, TDP-43, myotilin and ubiquitin immunoreactive aggregates and Congophilic deposits were present in a greater percentage of fibres in IBM+RV than IBM–RV. There was no difference in the percentage of COX-/SDH+ fibres between IBM+RV and IBM-RV.

5.5.2.3.2 Comparison between IBM+RV and PAM+RV

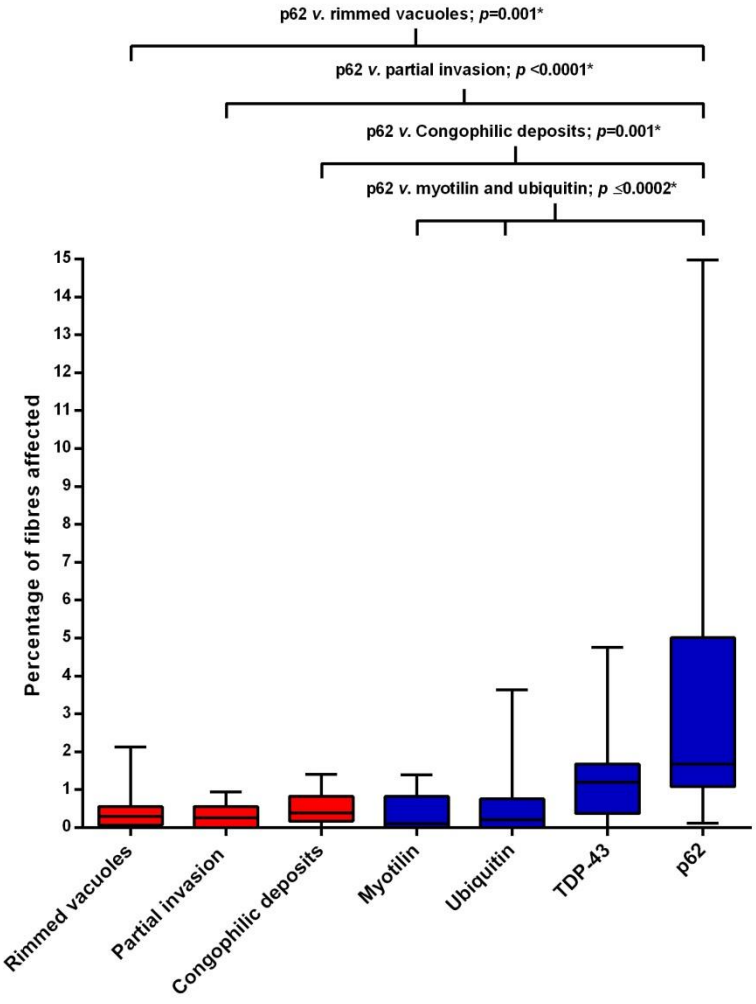
The percentage of fibres containing p62 and TDP-43 immunoreactive aggregates and COX-/SDH+ fibres were greater in IBM+RV than PAM+RV. There were no differences in the percentage of fibres containing rimmed vacuoles, myotilin or ubiquitin immunoreactive aggregates or Congophilic deposits.

5.5.2.3.3 Comparison between IBM–RV and PM&DM

Myotilin immunoreactive aggregates were present in a greater percentage of fibres in PM&DM than IBM–RV. The percentage of COX-/SDH+ fibres was greater in IBM-RV than PM&DM. Except for myotilin, all other immunoreactive aggregates were rare in IBM-RV and PM&DM and there were no differences in the percentage of fibres containing p62, TDP-43 or ubiquitin immunoreactive aggregates or Congophilic deposits between IBM-RV and PM&DM.

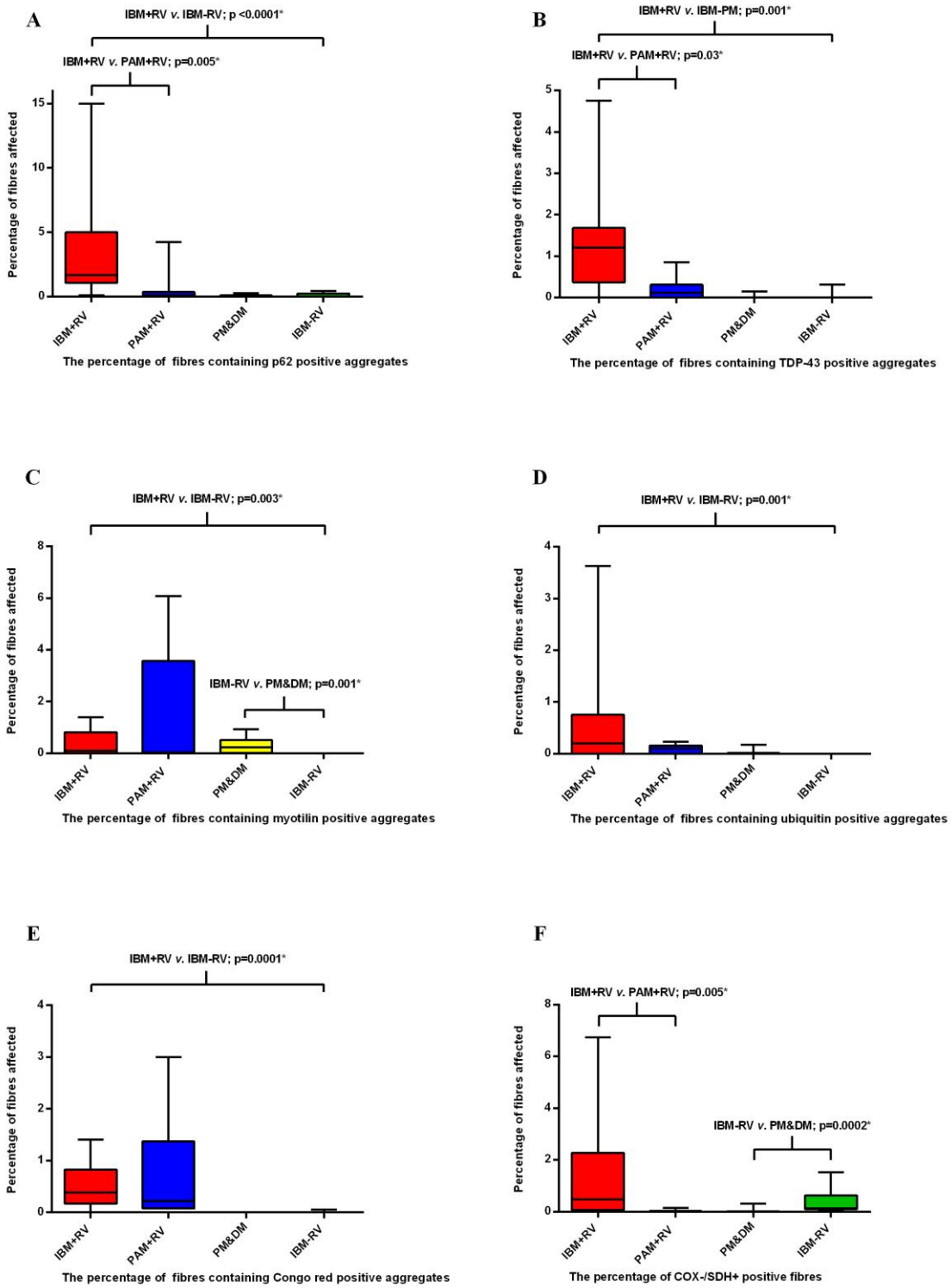
As PM is pathologically more similar to IBM-RV than DM a subgroup analysis was performed. The pathological findings in PM (excluding DM) were compared with IBM–RV and yielded the

Figure 5.1 Percentage of fibres containing protein aggregates and diagnostic pathological findings in IBM+RV



Box and whisker plot illustrating the percentage of fibres in IBM+RV containing pathological features. As reported in Chapter 4, only fibres containing p62 immunoreactive aggregates were more frequent than the fibres containing current diagnostic pathological features. Fibres containing p62 immunoreactive aggregates were more abundant than those containing ubiquitin and myotilin, but not TDP-43. No protein aggregates, fibres undergoing partial invasion, Congophilic deposits or rimmed vacuoles were observed in normal control biopsies.
IBM+RV = IBM with rimmed vacuoles on muscle biopsy; TDP-43 = Transactivation response DNA binding protein 43; p62 = Sequestosome 1. *Statistically significant results (p <0.05).

Figure 5.2 Percentage of fibres containing protein aggregates and COX-/SDH+ fibres in each group



Box and whisker plots illustrating the percentage of fibres containing p62 (A), TDP-43 (B), myotilin (C) and ubiquitin (D) immunoreactive aggregates, Congophilic deposits (E) and COX-/SDH+ fibres (F) in each group. Protein aggregates were present in a greater percentage of fibres in IBM+RV than in IBM–RV. However, there was no difference in the percentage of COX-/SDH+ muscle fibres between these groups. In IBM+RV, there were a greater percentage of fibres containing p62 (A) and TDP-43 (B) immunoreactive aggregates and COX-/SDH+ fibres (F) than PAM+RV. Pathological finding were similar in IBM-RV and PM&DM, with no differences in the percentage of fibres containing p62 (A), TDP-43 (B) and ubiquitin (D) immunoreactive aggregates or Congophilic deposits (E). However, there was a greater percentage of COX-/SDH+ fibres (F) in IBM–RV than PM&DM and a greater percentage of fibres containing myotilin immunoreactive aggregates (C) in PM&DM than IBM-RV.
p62 = Sequestosome 1; TDP-43 = Transactivation response DNA binding protein 43; IBM+RV = IBM with rimmed vacuoles on muscle biopsy; IBM–RV = IBM without rimmed vacuoles on muscle biopsy; PAM+RV = Protein accumulation myopathies with rimmed vacuoles on muscle biopsy; PM&DM = Steroid-responsive inflammatory myopathies; COX-/SDH+ = Cytochrome c oxidase negative/ succinate dehydrogenase positive. *Statistically significant results (p <0.05).

same results as IBM-RV *v.* PM&DM. COX-/SDH+ fibres were greater in IBM–RV than PM (0.13 *v.* 0.00; p=0.01), myotilin immunoreactive aggregates were more common in PM than IBM–RV (0.23 *v.* 0.00; p=0.01) and there were no differences in the percentage of fibres containing p62, TDP-43, ubiquitin immunoreactive aggregates or Congophilic deposits.

5.5.3 Diagnostic utility of protein aggregates and mitochondrial changes

5.5.3.1 Diagnostic utility determined using ROC curves

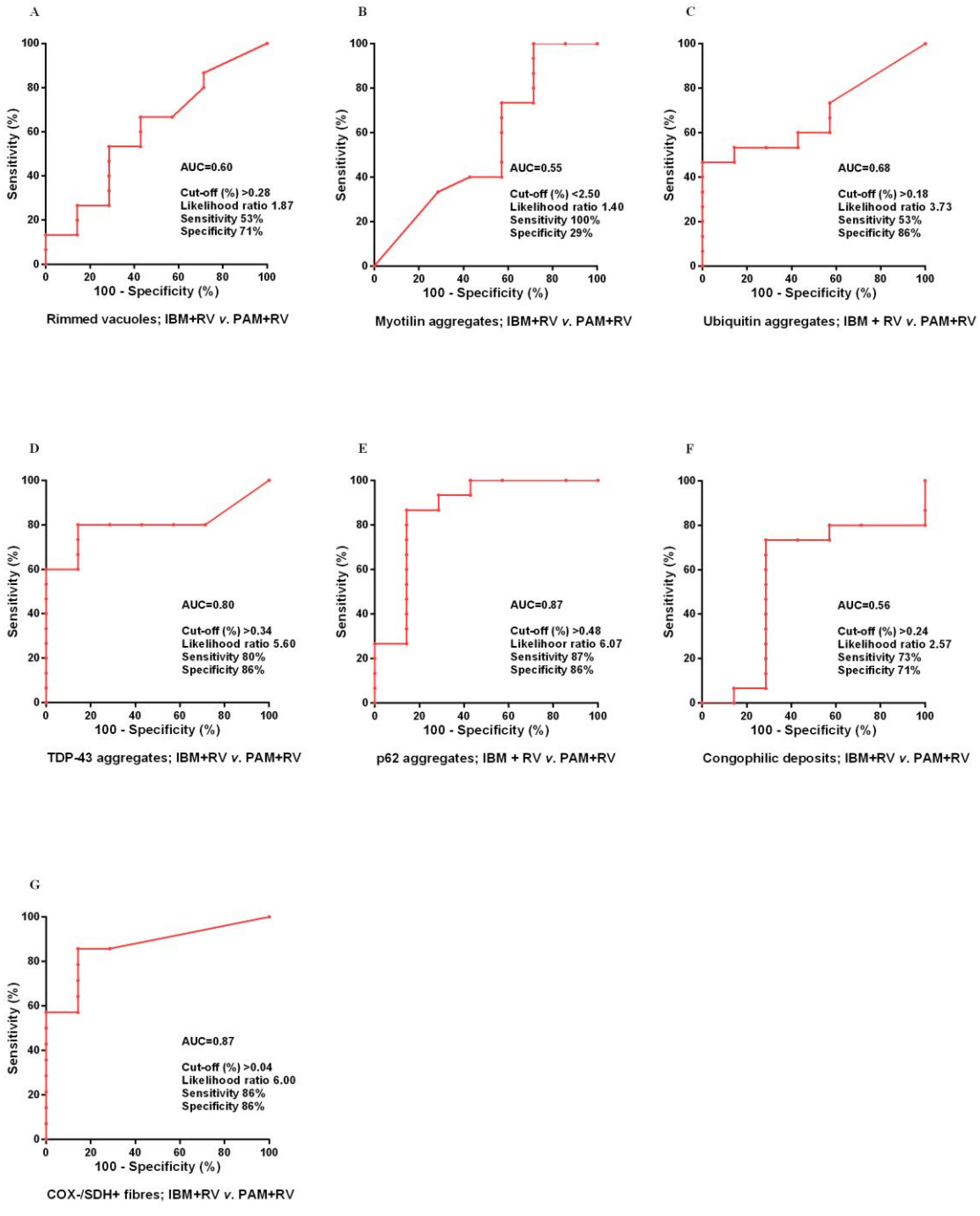
The potential for protein aggregates and mitochondrial changes to differentiate between IBM and disease controls was evaluated using ROC curves. To mimic the diagnostic difficulty encountered in clinical practice the vacuolated myopathies IBM+RV and PAM+RV were compared (Figure 5.3) and inflammatory myopathies lacking rimmed vacuoles IBM–RV and PM&DM were compared (Figure 5.4). ROC curves were plotted for each pathological feature.

In IBM–RV and PM&DM, only myotilin IHC reached the minimum criteria to be considered as a diagnostic test. Fibres containing myotilin immunoreactive aggregates were more abundant in PM&DM than IBM-RV, therefore if <0.01% of fibres containing myotilin aggregates were present this had a sensitivity of 100% and specificity of 82% for IBM-RV. COX/SDH HC staining was the most sensitive and specific test to differentiate IBM+RV and PAM+RV. However, none of the pathological finding reached the minimum criteria to differentiate between IBM+RV and PAM+RV.

5.5.3.2 Diagnostic utility determined by comparing the proportion of affected cases in each diagnostic group

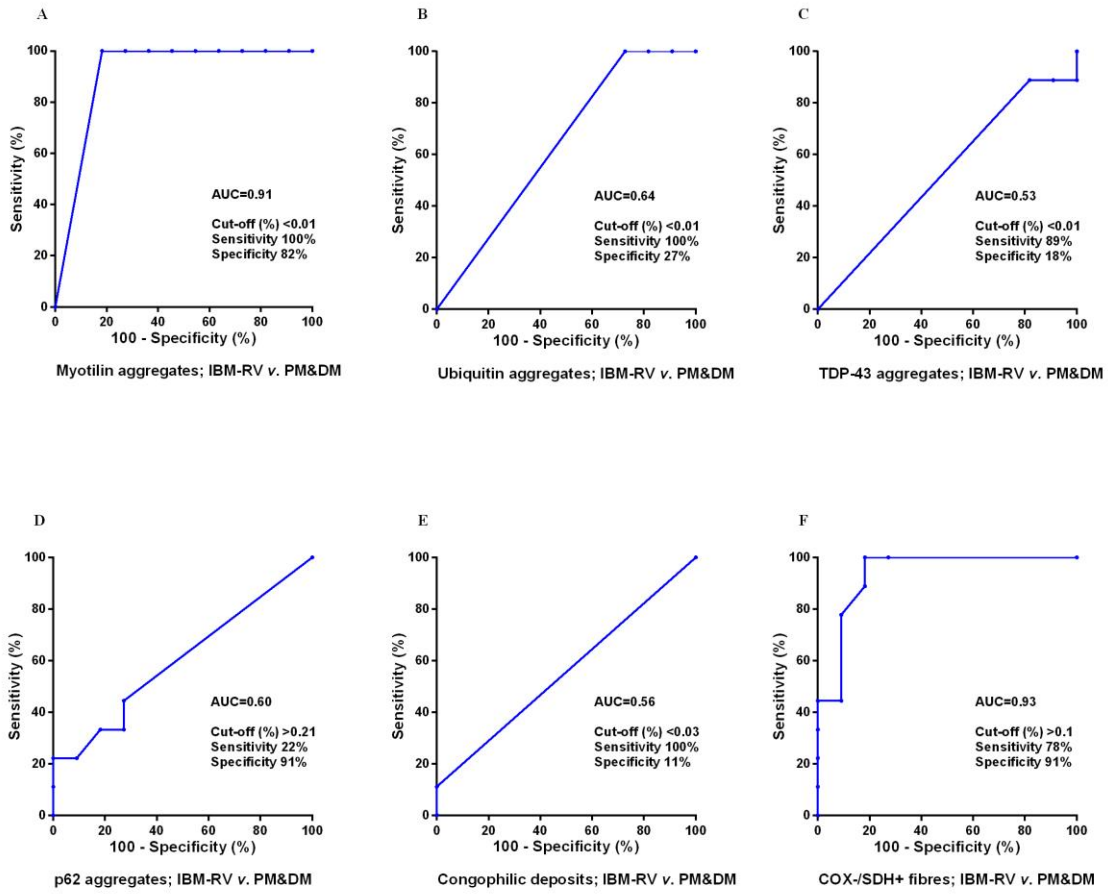
Although we have shown that the percentage of fibres containing p62 and TDP-43 immunoreactive aggregates and COX-/SDH+ fibres is different between IBM+RV and PAM+RV and that the

Figure 5.3 Optimum sensitivity and specificity of rimmed vacuoles, protein aggregates and COX-/SDH+ fibres in IBM+RV compared to PAM+RV



Receiver operating characteristic curves showing the area under the curve and the optimum cut-off with its associated likelihood ratio (LR), sensitivity and specificity for rimmed vacuoles (A), myotilin (B), ubiquitin (C), TDP-43 (D), p62 (E) immunoreactive deposits and Congophilic deposits (F) and COX-/SDH+ fibres (G). The more the curve approaches the top left corner the closer the AUC is to one and the more discriminative the test is. The sensitivity, specificity and LR associated with different cut-off points are then calculated. COX/SDH histochemical (HC) staining was the most discriminative test for differentiating IBM+RV and PAM+RV (G). However, there was little difference between COX/SDH HC staining, TDP-43and p62 immunohistochemistry and none were sufficiently discriminative to be considered diagnostic.
AUC = Area under the curve; IBM+RV = IBM with rimmed vacuoles on muscle biopsy; PAM+RV = Protein accumulation myopathy with rimmed vacuoles on muscle biopsy; p62 = Sequestosome 1; TDP-43 = Transactivation response DNA binding protein 43; COX/SDH = Cytochrome c oxidase/succinate dehydrogenase; COX-/SDH+ = Cytochrome c oxidase negative/ succinate dehydrogenase positive.

Figure 5.4 Optimum sensitivity and specificity of rimmed vacuoles, protein aggregates and COX-/SDH+ fibres in IBM-RV compared to PM&DM



Receiver operating characteristic curves showing the area under the curve and the optimum cut-off with its associated likelihood ratio, sensitivity and specificity for myotilin (A), ubiquitin (B), TDP-43 (C), p62 (D) immunoreactive aggregates and Congophilic deposits (E) and COX-/SDH+ fibres (F). Myotilin immunohistochemistry (G) was the most discriminative test for differentiating IBM-RV and PM&DM and the only one to fulfil criteria for a diagnostic test. Although it does not quite reach criteria for diagnostic use COX/SDH histochemical staining is close to diagnostic with a sensitivity of 78% and a specificity of 91%.
IBM–RV = IBM without rimmed vacuoles on muscle biopsy; PM&DM = Steroid-responsive inflammatory myopathies; p62 = Sequestosome 1; TDP-43 = Transactivation response DNA binding protein 43; COX-/SDH+ = Cytochrome c oxidase negative/succinate dehydrogenase positive; COX/SDH = Cytochrome c oxidase/succinate dehydrogenase.

percentage of fibres containing myotilin immunoreactive aggregates and COX-/SDH+ fibres is different between IBM-RV and PM&DM only myotilin immunoreactive aggregates met the criteria to be considered of diagnostic use. In addition, quantifying the biopsy in this manner is impractical for clinical use. It would be more practical to assess the presence or absence of individual pathological features. To determine if this method could be of diagnostic use the proportion of affected cases in each group were compared. Data are summarised in Table 5.2.

The results showed that none of the tests fulfilled the criteria for a diagnostic test (Table 5.2). The most discriminative was COX/SDH HC staining. To improve the discriminative value of COX/SDH HC staining different levels of the percentage of COX-/SDH+ fibres present in a biopsy were assessed e.g. >0.5% or >1% COX-/SDH+ fibres. This did not improve the specificity markedly and caused a significant reduction in sensitivity.

5.5.4 Qualitative assessment of protein aggregates

During the quantitative assessment of biopsies distinct patterns of p62 immunoreactive aggregates were noted. To assess whether the pattern of staining corresponded to a particular diagnosis, biopsies were grouped according the pattern of immunoreactivity blinded to the clinical details. Four patterns of p62 immunoreactivity were noted (patterns I-IV) (Figure 5.5). Categorising the pattern of immunoreactivity increased the discriminative value of p62 IHC from 14% to 57% for IBM+RV, with no loss of sensitivity (Table 5.3). There were no differences observed in TDP-43, myotilin and ubiquitin staining between biopsies (Figures 5.6).

On serial sections the same protein aggregates were not infrequently observed to stain with more than one antibody. In IBM+RV, aggregates were typically immunoreactive for TDP-43 and p62 with much weaker ubiquitin and myotilin immunoreactivity. In PAM+RV, aggregates were typically immunoreactive for myotilin and p62 and sometimes ubiquitin, but often lacked TDP-43

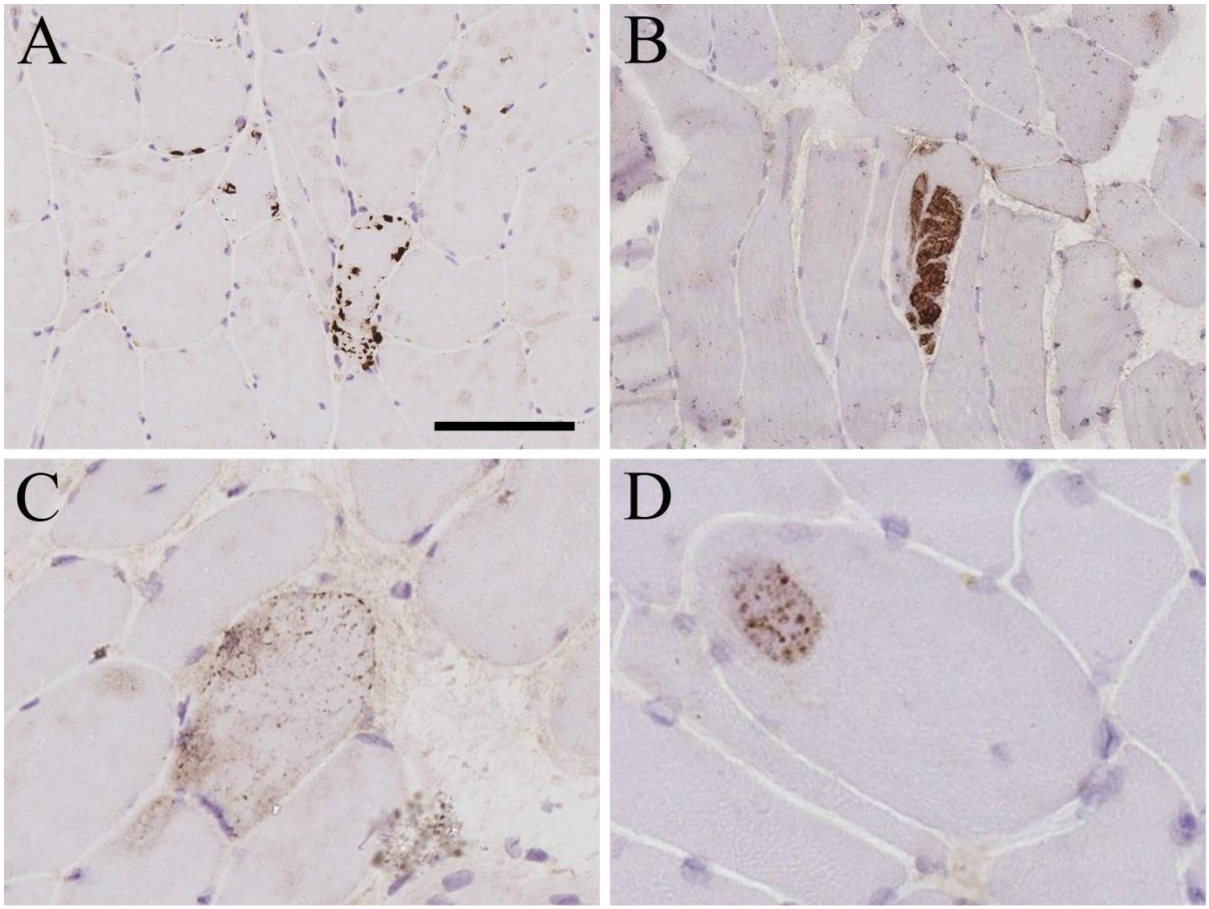
Table 5.2 Comparison of the proportion of positive cases in each group

Pathological findings	IBM+RV n (%)	PAM+RV n (%)	IBM+RV *v*. PAM+RV		IBM–RV n (%)	PM&DM n (%)	IBM-RV *v*. PM&DM		IBM+RV n (%)	IBM–RV n (%)	IBM+RV *v*. IBM-RV
			Sensitivity	Specificity			Sensitivity	Specificity			*p* value
Number of cases	15	7			9	11			15	9	
Aggregated proteins											
p62	15 (100)	6 (86)	1.00	0.14	4 (44)	3 (27)‡	0.4	0.72	15 (100)	4 (44)	0.003*
TDP-43	13 (87)	5 (71)	0.87	0.29	1 (11)	2 (18)‡	0.11	0.82	13 (87)	1 (11)	0.001*
Ubiquitin	11 (73)	4 (57)	0.73	0.43	0 (0)	3 (27)‡	0.00	0.73	11 (73)	0 (0)	0.001*
Myotilin	10 (67)	5 (71)	0.67	0.29	0 (0)	9 (82)	0.00	0.18	10 (67)	0 (0)	0.002*
Congophilic deposits	13 (87)	7 (100)	0.87	0.00	1 (11)	0 (0)	0.11	1.00	13 (87)	1 (11)	0.001*
COX-/SDH+ fibres†											
Any	12 (86)	2 (29)	0.86	0.71	9 (100)	3 (27)	1.00	0.73	12 (86)	9 (100)	0.50
>1%	7 (50)	0 (0)	0.47	1.00	2 (22)	0 (0)	0.22	1.00	7 (50)	2 (22)	0.23

Table shows the proportion of cases with pathological abnormalities in each diagnostic group and the diagnostic utility of individual tests. The high sensitivity of COX/SDH histochemical staining indicates that the absence of COX-/SDH+ fibres is strong evidence against the diagnosis of IBM. However, COX-/SDH+ fibres were not specific for IBM.

IBM+RV = IBM with rimmed vacuoles on muscle biopsy; IBM–RV = IBM without rimmed vacuoles on muscle biopsy; PAM+RV = Protein accumulation myopathies with rimmed vacuoles on muscle biopsy; PM&DM = Steroid-responsive inflammatory myopathies; p62 = Sequestosome 1; TDP-43 = Transactivation response DNA binding protein 43; COX-/SDH+ = Cytochrome c oxidase negative/ succinate dehydrogenase positive. †IBM+RV; n = 14. ‡p62, TDP-43 and ubiquitin immunoreactive aggregates were present in DM cases (n=5) and not in PM cases (n=6). *Statistically significant results (p <0.05).

Figure 5.5 Patterns of p62 immunoreactivity observed in IBM and disease controls



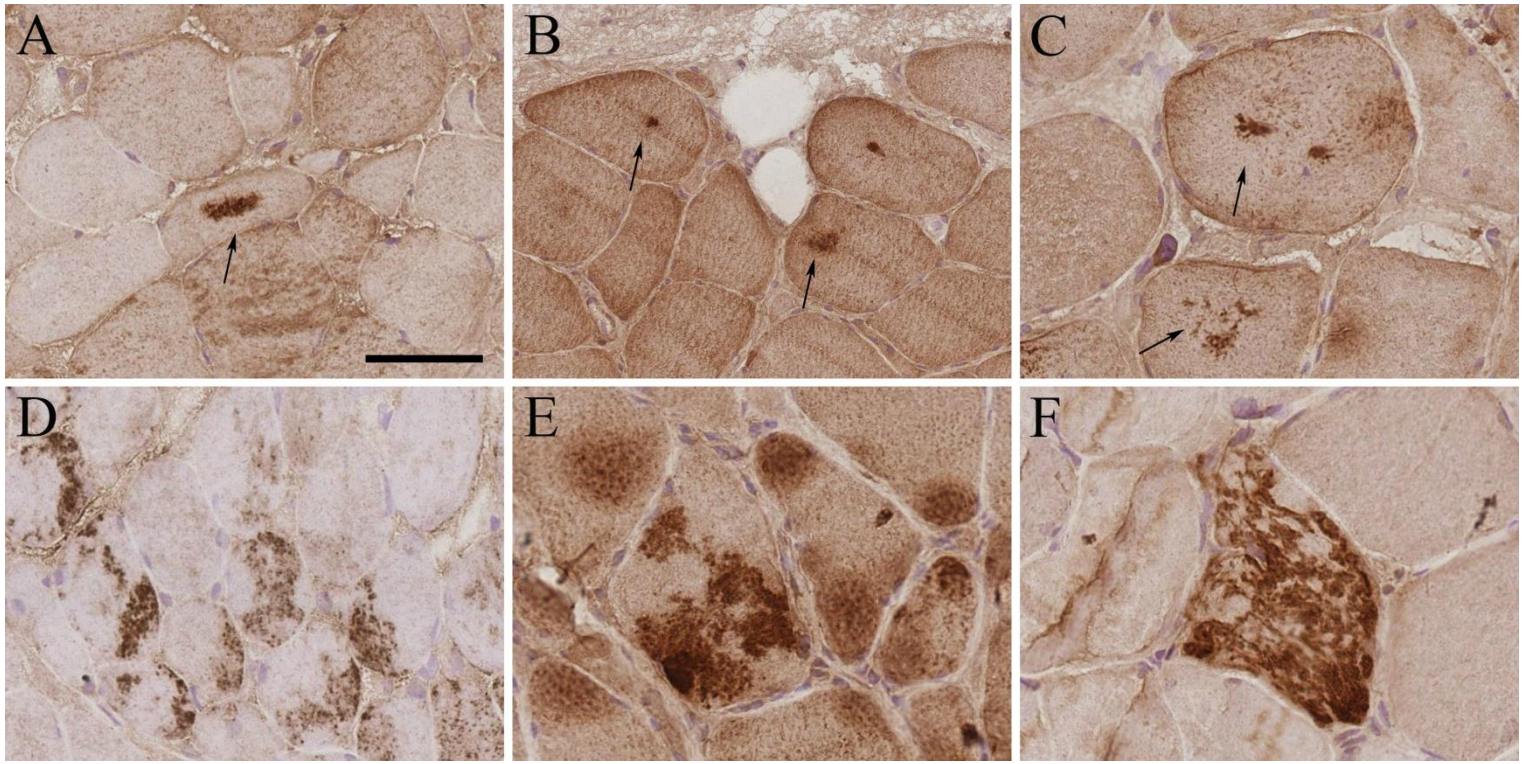
Eight µm thick sections stained for p62 using immunohistochemistry. Four patterns of p62 immunoreactivity were observed. Pattern I - strongly stained, discreet and clearly delineated, round or angular aggregates, variable in number and size within a muscle fibre but rarely filling it and predominantly in a subsarcolemmal location, but also perinuclear and adjacent to vacuoles (A). Pattern II - large aggregates of variable staining intensity (B). Pattern III - fine granular aggregates dispersed throughout the fibre (C). Pattern IV - fine granules and wisps of p62 immunoreactivity set within weakly basophilic inclusions (D). Scale bar in A represents 100 µm in A and B, 50 µm in C and 25 µm in D.
p62 = Sequestosome 1.

Table 5.3 Morphology of p62 aggregates in each group

Pathological findings	IBM+RV n (%)	PAM+RV n (%)	IBM+RV *v*. PAM+RV		IBM–RV n (%)	PM&DM n (%)	IBM-RV *v*. PM&DM		IBM+RV n (%)	IBM–RV n (%)	IBM+RV *v*. IBM-RV
			Sensitivity	Specificity			Sensitivity	Specificity			*p* value
Number of cases	15	7			9	11			15	9	
p62	15 (100)	6 (86)	1.00	0.14	4 (44)	3 (27)	0.40	0.72	15 (100)	4 (44)	0.003*
Pattern I	15 (100)	3 (43)	1.00	0.57	4 (44)	1 (9)	0.44	0.91	15 (100)	4 (44)	0.003*
Pattern II	0 (0)	2 (26)	0.00	0.71	0 (0)	0 (0)	0.00	1.00	0 (0)	0 (0)	1.00
Pattern III	0 (0)	0 (0)	0.00	1.00	0 (0)	2 (18)	0.00	0.82	0 (0)	0 (0)	1.00
Pattern IV	0 (0)	1 (14)	0.00	0.86	0 (0)	0 (0)	0.00	1.00	0 (0)	0 (0)	1.00
Intra-nuclear p62	0 (0)	1 (14)	0.00	0.86	2 (22)	1 (9)	0.22	0.91	0 (0)	2 (22)	0.13

In IBM+RV and IBM–RV, p62 immunoreactive aggregates were similar in morphology. Although, only pattern I p62 immunoreactive aggregates were observed in IBM they were not specific for IBM and did not differentiate between IBM and disease controls. However, pattern I p62 immunoreactive aggregates were observed in paraneoplastic DM but not PM and therefore, they may be helpful in differentiating between IBM–RV and PM.
IBM+RV = IBM with rimmed vacuoles on muscle biopsy; IBM–RV = IBM without rimmed vacuoles on muscle biopsy; PM&DM = Steroid-responsive inflammatory myopathies; PAM+RV = Protein accumulation myopathies with rimmed vacuoles on muscle biopsy; p62 = Sequestosome 1; PM = Polymyositis; DM = Dermatomyositis. *Statistically significant results (p <0.05).

Figure 5.6 Morphology of myotilin aggregates in IBM and disease controls



Eight µm thick stained sections showing the two patterns of myotilin immunoreactivity observed in PM&DM (A, D), IBM (B, E) and PAM+RV (C, F). Myotilin immunoreactive aggregates were either centrally located and small or medium in size (A, B and C) or large diffuse aggregates of variable staining intensity that occupied a significant portion of the sarcoplasm (D, E and F). Neither pattern was specific to a diagnosis. Scale bar in A represents 50 µm in A, B and D and 100 µm in C, E and F.

PM&DM = Steroid-responsive inflammatory myopathies; PAM+RV = Protein accumulation myopathies with rimmed vacuoles on muscle biopsy.

immunoreactivity. Although these observations may reflect differences in the underlying pathogenesis, they are unlikely to be of diagnostic use. As described in Chapter 4, Congophilic deposits were visible with fluorescent light but not polarised light (Figure 5.7). In IBM+RV, Congophilic deposits were almost exclusively found in vacuolated fibres. Typically, they were filamentous or granular and found within or next to vacuoles. In PAM+RV, they were present in fibres containing rimmed vacuoles and non-vacuolated fibres. Additionally, unlike those in IBM+RV, they were large and poorly defined in PAM+RV, often occupying a significant portion of the fibre, and corresponded to large eosinophilic areas visible on H&E staining.

5.5.5 Immunological characteristics of IBM

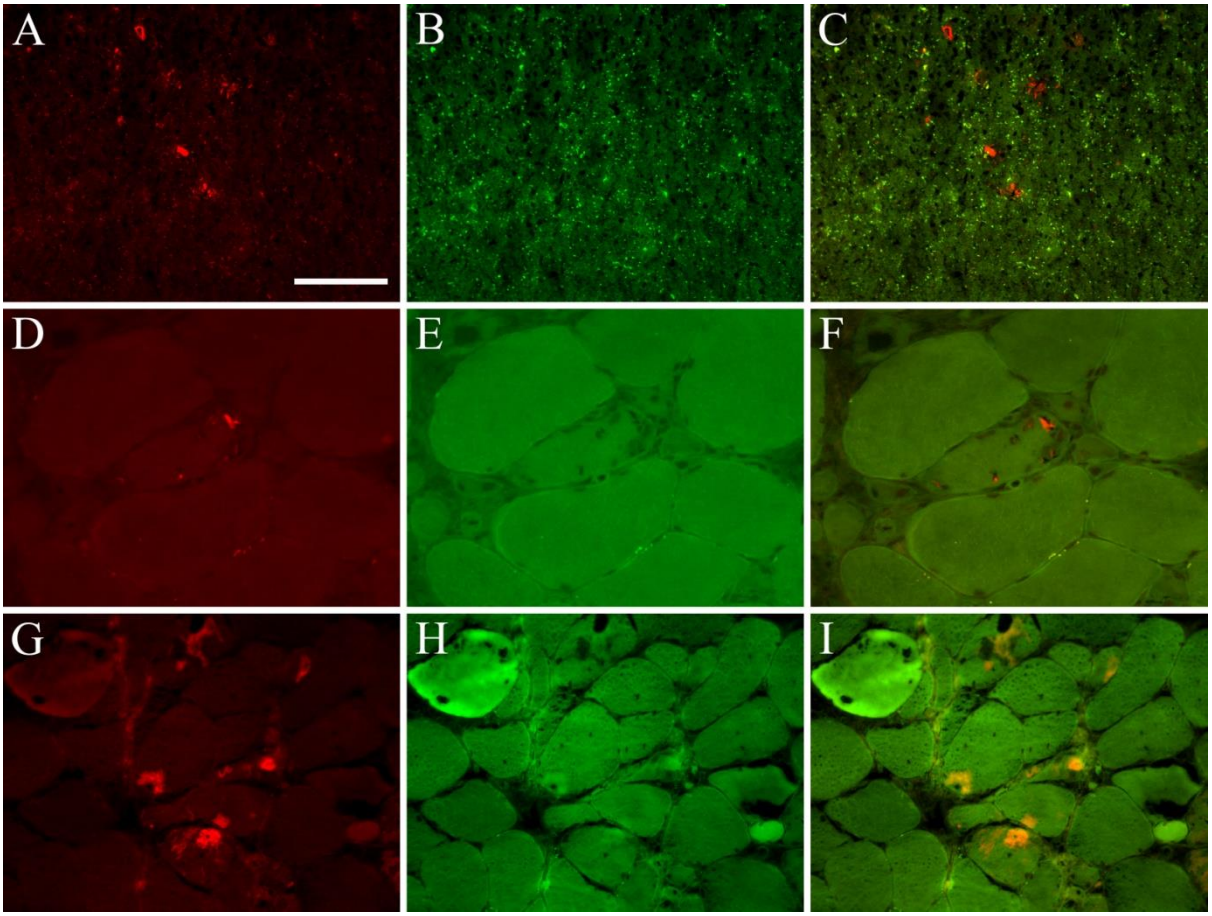
5.5.5.1 Inflammatory changes in normal control muscle

Sarcolemmal and sarcoplasmic MHC Class I staining was not increased in normal control muscle. Few inflammatory cells were observed in normal muscle. Using the semi-quantitative score tool the inflammatory scores in normal muscle were zero.

5.5.5.2 MHC Class I staining was independent of other pathological features in IBM and differentiated IBM from PAM+RV

Increased sarcolemmal and/or sarcoplasmic MHC Class I staining was observed in 15 (100%) cases of IBM+RV, 9 (100%) cases of IBM–RV, 11 (100%) cases of PM&DM and 3 (43%) cases of PAM+RV (Table 5.4). Increased MHC Class I staining therefore lacked specificity but the absence of MHC Class I staining was strong evidence against the diagnosis of IBM. However, three different patterns of MHC Class I staining were observed (patterns A-C) (Figure 5.8). The pattern of MHC Class I staining in each biopsy was re-assessed blind to the clinical details. Classifying the pattern of MHC Class I staining increased its diagnostic utility. Pattern C MHC Class I was highly specific for IBM+RV without significantly altering the sensitivity (Table 5.4).

Figure 5.7 Fluorescent Congophilic aggregates in IBM+RV and PAM+RV



Eight µm thick cryostat sections stained with alkalinised Congo red and visualised under fluorescent light. Positive control sections of AD brain (A-C), IBM+RV (D-F) and PAM+RV (G-I) visualised with rhodamine red filter (A, D and G), fluorescein isothiocyanate filter (B, E and H) and both images combined (C, F and I). Congophilic deposits in IBM+RV were typically filamentous or granular and exclusively found in vacuolated fibres. In PAM+RV they were larger, ill-defined and present in both vacuolated and non-vacuolated fibres. Scale bar in A represents 50 µm in A-I.

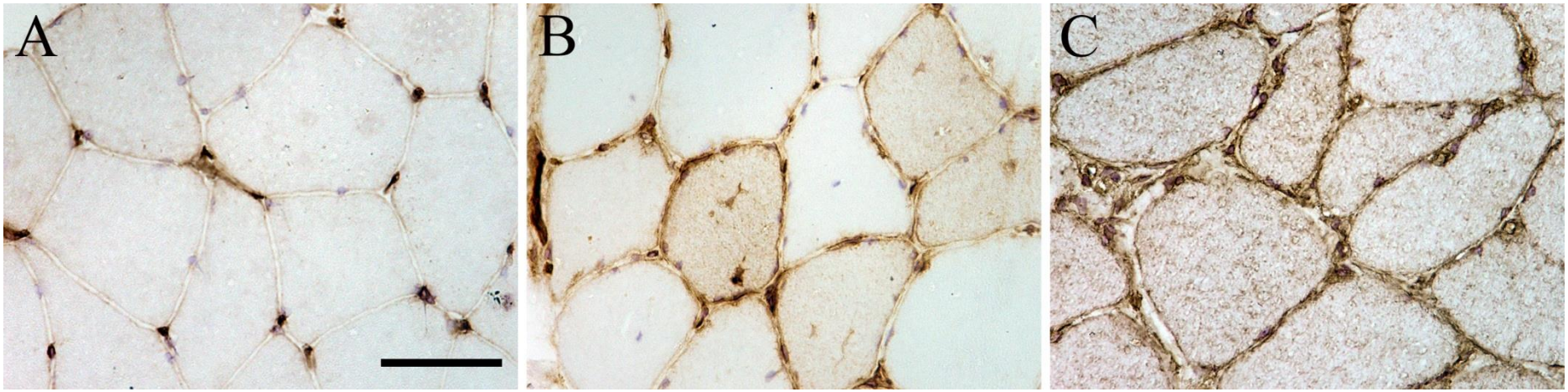
AD = Alzheimer's disease; IBM+RV = IBM with rimmed vacuoles on muscle biopsy; IBM–RV = IBM without rimmed vacuoles on muscle biopsy; PM&DM = Steroid-responsive inflammatory myopathies; PAM+RV = Protein accumulation myopathies with rimmed vacuoles on muscle biopsy.

Table 5.4 Patterns of MHC Class I staining in IBM, PM&DM and PAM+RV

Pathological findings	IBM+RV n (%)	PAM+RV n (%)	IBM+RV *v*. PAM+RV		IBM–RV n (%)	PM&DM n (%)	IBM-RV *v*. PM&DM		IBM+RV n (%)	IBM–RV n (%)	IBM+RV *v*. IBM-RV
			Sensitivity	Specificity			Sensitivity	Specificity			*p* value
Number of cases	15	7			9	11			15	9	
MHC Class I											
Normal	0 (0)	4 (57)	0.00	0.43	0 (0)	0 (0)	0.00	1.00	0 (0)	0 (0)	1.00
Increased	15 (100)	3 (43)	1.00	0.57	9 (100)	11 (100)	1.00	0.00	15 (100)	9 (100)	1.00
Pattern A	0 (0)	4 (57)	0.00	0.43	0 (0)	0 (0)	0.00	1.00	0 (0)	0 (0)	1.00
Pattern B	1 (7)	3 (43)	0.07	0.57	2 (22)	1 (9)	0.22	0.91	1 (7)	2 (22)	1.00
Pattern C	14 (93)	0 (0)	0.93	1.00	7 (78)	10 (91)	0.78	0.09	14 (93)	7 (78)	0.53

Table shows that increased MHC class I staining is sensitive, but not specific for IBM. However classifying the staining pattern enables IBM+RV to be reliably differentiated from PAM+RV.
IBM+RV = IBM with rimmed vacuoles on muscle biopsy; IBM–RV = IBM without rimmed vacuoles on muscle biopsy; PAM+RV = Protein accumulation myopathies with rimmed vacuoles on muscle biopsy; PM&DM = Steroid-responsive inflammatory myopathies; MHC Class I = Major histocompatibility complex class I. *Statistically significant results (p <0.05).

Figure 5.8 MHC Class I staining in normal muscle and IBM



Eight µm thick cryostat sections stained for MHC Class I using immunohistochemistry. Normal muscle (A) and IBM (B and C). Pattern A - in normal muscle, capillaries were positively stained without accompanying sarcolemmal or sarcoplasmic staining (A). Two distinct patterns of increased MHC Class I immunoreactivity were observed. Pattern B – mildly increased weak diffuse sarcolemmal staining and/or scattered muscle fibres with increased sarcolemmal and sarcoplasmic staining (B). Pattern C - strongly increased and widespread sarcoplasmic and sarcolemmal staining (C). Scale bar in A represents 50 µm in A, B and C.
MHC Class I = Major histocompatibility complex class I.

5.5.5.2.1 Comparison of the inflammatory infiltrate between diagnostic groups

The sum of the T-cell, B-cell and macrophage inflammatory scores in the endomysium, perimysium and perivascular areas in each group are shown in Figure 5.9. The number of cases in each diagnostic group affected by a particular inflammatory cell type, the degree of inflammation and site were compared and the results summarised in Table 5.5.

5.5.5.2.2 Inflammatory infiltrate is similar between IBM-RV and PM&DM

In IBM-RV and PM&DM the inflammatory infiltrate was very similar, although there were more perimysial T-cells, cytotoxic T-cells and endomysial B-cells in PM&DM than IBM–RV ($p \leq 0.02$). These findings were mirrored when the proportions of IBM–RV and PM&DM cases were compared (Table 5.5). There was no difference in the proportion of cases with fibres undergoing partial invasion between IBM–RV and PM&DM.

As in section 5.5.2.3.3, the inflammatory features in PM (n=6) and IBM-RV cases were compared without the inclusion of DM cases. These analyses yielded similar results as IBM-RV *v.* PM&DM.

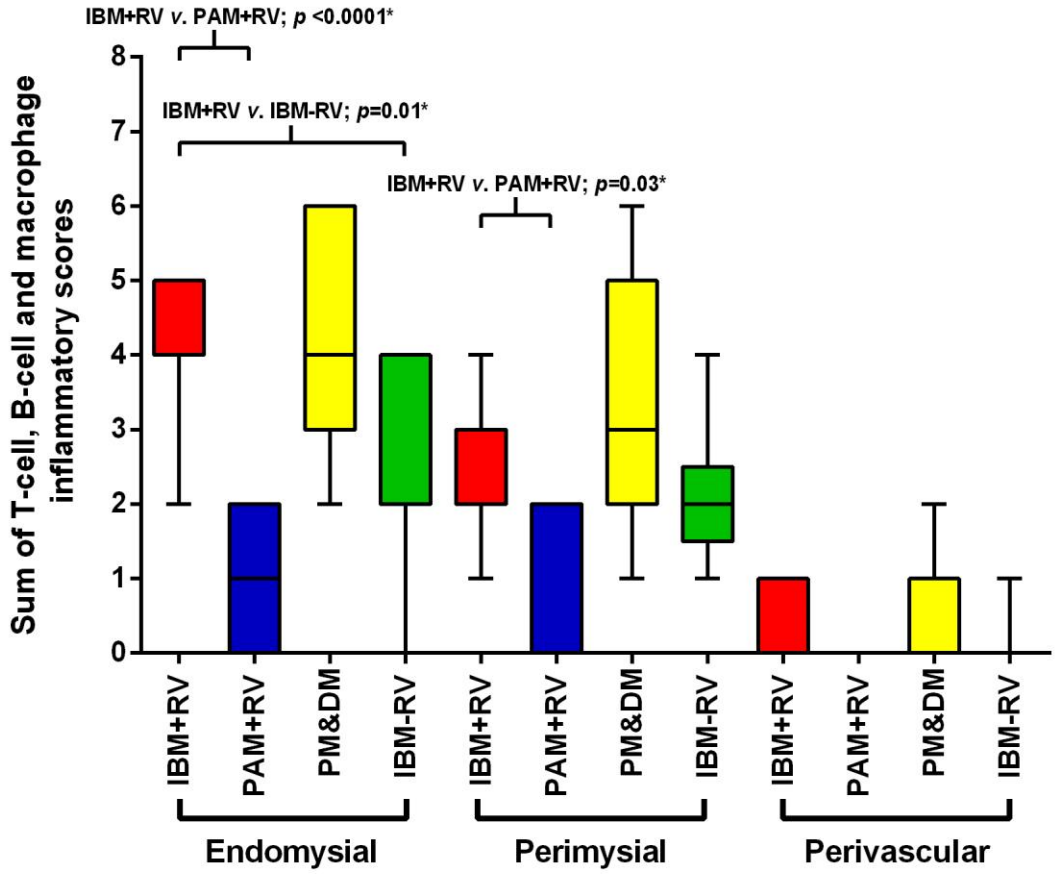
5.5.5.2.3 Inflammatory infiltrate is more prominent in IBM+RV than PAM+RV

Endomysial and perimysial inflammatory infiltrate was more pronounced in IBM+RV than PAM+RV. There were more endomysial T-cells, helper T-cells, cytotoxic T-cells and macrophages and also perimysial cytotoxic T-cells in IBM+RV than PAM+RV ($p \leq 0.01$). Partial invasion was observed in a greater number of IBM+RV cases than PAM+RV.

5.5.5.2.4 Endomysial inflammation is more prominent in IBM+RV than IBM-RV

The sum of the endomysial inflammatory scores (T-cells, B-cells and macrophages) was greater in IBM+RV than IBM-RV (p=0.01).Analysis of partial invasion and the location and severity of the inflammatory infiltrate assessed using the semi-quantitative score tool in each group revealed a greater density of inflammatory infiltrate in more cases in IBM+RV than IBM-RV, sometimes two

Figure 5.9 Severity and distribution of the inflammatory infiltrate



Box and whisker plot showing the burden of the inflammatory infiltrate in IBM+RV, IBM–RV and PM&DM was focussed upon the endomysial and perimysial areas. Fewer inflammatory cells were observed in the endomysium in IBM–RV than IBM+RV. There were no differences in the inflammatory infiltrate between PM&DM and IBM+RV or PM&DM and IBM–RV. The endomysial and perimysial inflammatory infiltrate present was much greater in IBM+RV than PAM+RV.

IBM+RV = IBM with rimmed vacuoles on muscle biopsy; IBM–RV = IBM without rimmed vacuoles on muscle biopsy; PM&DM = Steroid-responsive inflammatory myopathies; PAM+RV = Protein accumulation myopathies with rimmed vacuoles on muscle biopsy. *Statistically significant results (p <0.05).

Table 5.5 Location and severity of the inflammatory infiltrate assessed using the semi-quantitative score tool and the proportion of cases with fibres undergoing partial invasion

Inflammatory cell			IBM+RV	PAM+RV	IBM+RV *v.* PAM+RV		IBM–RV	PM&DM	IBM-RV *v.* PM&DM		IBM+RV *v.* IBM–RV
Type	Location	Degree	*n* (%)	*n* (%)	Sensitivity	Specificity	*n* (%)	*n* (%)	Sensitivity	Specificity	*p* value
PI†			10 (67)	0 (0)	0.67	1.00	3 (33)	2 (18)	0.33	0.82	0.21
CD3	E	>1	13 (87)	0 (0)	0.87	1.00	4 (44)	7 (64)	0.44	0.36	0.06
	E	>0	14 (93)	4 (57)	0.93	0.43	8 (89)	11 (100)	0.89	0.00	1.00
	P	>1	4 (27)	0 (0)	0.27	1.00	1 (11)	7 (64)	0.11	0.36	0.61
CD4	E	>1	12 (80)	0 (0)	0.80	1.00	2 (22)	5 (45)	0.22	0.46	0.01*
	E	>0	14 (93)	1 (14)	0.93	0.86	6 (67)	9 (82)	0.67	0.18	0.13
CD8	E	>1	13 (87)	0 (0)	0.87	1.00	4 (44)	5 (45)	0.44	0.54	0.06
	E	>0	14 (93)	0 (0)	0.93	1.00	7 (78)	9 (82)	0.78	0.18	0.53
	P	>0	11 (73)	0 (0)	0.73	1.00	3 (33)	10 (91)	0.33	0.09	0.09
CD68	E	>1	12 (80)	0 (0)	0.80	1.00	4 (44)	8 (73)	0.44	0.17	0.10
	E	>0	14 (93)	2 (29)	0.93	0.71	8 (89)	11 (100)	0.89	0.00	1.00
CD20	E	>0	5 (33)	0 (0)	0.33	1.00	0 (0)	6 (55)	0.00	0.45	0.12

Results are shown for those tests which were different between IBM+RV and PAM+RV or IBM–RV and PM&DM.
PI = Partial invasion; IBM+RV = IBM with rimmed vacuoles on muscle biopsy; IBM–RV = IBM without rimmed vacuoles on muscle biopsy; PAM+RV = Protein accumulation myopathies with rimmed vacuoles on muscle biopsy; PM&DM = Steroid-responsive inflammatory myopathies; CD3 = T-cells; CD4 = Helper T-cells; CD8 = Cytotoxic T-cells; CD68 = Macrophages; CD20 = B-cells; E = Endomysial; P = Perimysial. *Statistically significant results (p <0.05).
†Assessed on H&E stained tissue sections.

or threefold more; however, this difference was found to be statistically significant for endomysial helper T-cells >1 (p=0.01).

5.5.6 Clinicopathological correlation

In IBM+RV and IBM–RV, there were no correlations in individual biopsies between the following pathological features: the number of fibres containing rimmed vacuoles, Congophilic deposits or protein aggregates, the number of fibres undergoing partial invasion and the amount or distribution inflammatory infiltrate. Using linear regression analysis, no relationships were identified between the pathological findings and age at disease onset, age at time of biopsy, disease duration or CK. The same results were obtained when IBM+RV and IBM-RV were combined and analysed as one group.

5.6 Discussion

The diagnostic pathological features that have made IBM readily recognisable lack sensitivity (Chahin and Engel, 2008)(Benveniste et al., 2011). We found the required combination of pathological features is absent in the majority of patients with clinically typical IBM at presentation (Brady et al. 2013) and in agreement with other studies (Amato et al., 1996)(van der Meulen et al., 1998), we also found them to be undetectable in a number of cases despite repeated biopsy. However, the characteristic pattern of weakness associated with IBM is not always found at presentation. Therefore, there remains a need to document the spectrum of pathological features present in IBM and to determine which pathological features support the diagnosis.

As detailed in Chapter 1, many of the pathological features described in IBM and thought to be diagnostic are of unknown specificity and sensitivity. We have shown that p62, TDP-43, myotilin and ubiquitin immunoreactive aggregates were relatively more abundant in Griggs' pathologically definite IBM than some of the current diagnostic pathological features and were present in

morphologically normal fibres (Chapter 4). These observations suggest that protein aggregates may be useful diagnostic markers.

In this chapter, we investigated whether protein aggregates and immune changes, identified in Chapter 4, and other pathological features thought to commonly occur in IBM such as mitochondrial changes, are of sufficient specificity and sensitivity to complement the clinical features in the diagnosis of IBM. Our findings reveal firstly, that individually none of the pathological features assessed were sufficiently sensitive and specific for diagnostic purposes. However, in certain circumstances, e.g. differentiating between pathologically typical IBM and other myopathies with rimmed vacuoles, the pathological features may help support the diagnosis. Secondly, pathological features, namely endomysial inflammation, Congophilic deposits and protein aggregates, are more common when rimmed vacuoles are present suggesting that they are related to disease duration and explaining their poor sensitivity at disease presentation.

5.6.1 Previous studies

Many studies have reported on the pathological findings in pathologically definite IBM, but few have examined the diagnostic utility of these features using appropriate disease controls. Fewer still have investigated the pathological findings in clinically typical IBM lacking the diagnostic pathological features (Chahin and Engel, 2008)(Dubourg et al., 2011). In a detailed study, Van der Meulen *et al.* attempted to determine the diagnostic value of rimmed vacuoles on H&E stained sections and SMI-31 IHC for differentiating between IBM and PM. They found the optimal percentage of fibres containing rimmed vacuoles on the H&E stained sections for discriminating between IBM and PM was 0.3%. The sensitivity and specificity associated with finding ≥0.3% of fibres containing rimmed vacuoles and SM-31 staining were 83% and 100% respectively. However, exclusion criteria for PM included the presence of rimmed vacuoles in >0.3% of fibres and the presence of rimmed vacuoles in 47% of PM cases in this study suggests that the diagnosis of PM may have been incorrect in a number of cases. Although this study provided quantitative

data it did not address the fundamental difficulty facing pathologists and clinicians - how to differentiate IBM lacking the diagnostic pathological features from steroid-responsive inflammatory myopathies and pathologically typical IBM from other myopathies in which rimmed vacuoles are found. Chahin and Engel studied clinically typical cases of IBM lacking rimmed vacuoles (Chahin and Engel, 2008). They concluded that the absence of partial invasion and COX negative fibres was strong evidence against the diagnosis of IBM independent of the presence of rimmed vacuoles. Temiz *et al.* investigated the pathological differences between inflammatory myopathies with greater than one per cent COX negative fibres (referred to in the study as PM.Mito), IBM and PM (Temiz et al., 2009). Similarities in the pathological features between PM.Mito and IBM led them to surmise that these conditions were akin to one another. However, only limited conclusions can be drawn from this study as only a small area of each biopsy was assessed and 40% of PM.Mito cases lacked both finger flexion and knee extension weakness suggesting that the group was clinically heterogeneous. Finally, Dubourg *et al.* compared the pathological findings in definite IBM, possible IBM, PM and a variety of muscular dystrophies (Dubourg et al., 2011). They found that p62 and TDP-43 were sensitive for definite and possible IBM. However, the whole biopsy was not examined only a small area, inclusion criteria for definite and possible IBM overlapped (both groups containing fibres with rimmed vacuoles) and control cases were neither pathologically nor clinically similar to IBM.

To ensure the results of our study were clinically relevant the entirety of each muscle biopsy was analysed and control cases included were myopathies that are pathologically and clinically similar to IBM and often included in the differential diagnosis of IBM.

5.6.2 Diagnostic utility of pathological features in IBM

The spectrum of pathological findings in IBM meant that no individual tests could differentiate between IBM and disease controls. Therefore, mimicking the difficulty faced in clinical practice, we evaluated the ability of the each test to differentiate IBM with rimmed vacuoles from

myopathies with rimmed vacuoles and IBM without rimmed vacuoles from steroid-responsive inflammatory myopathies.

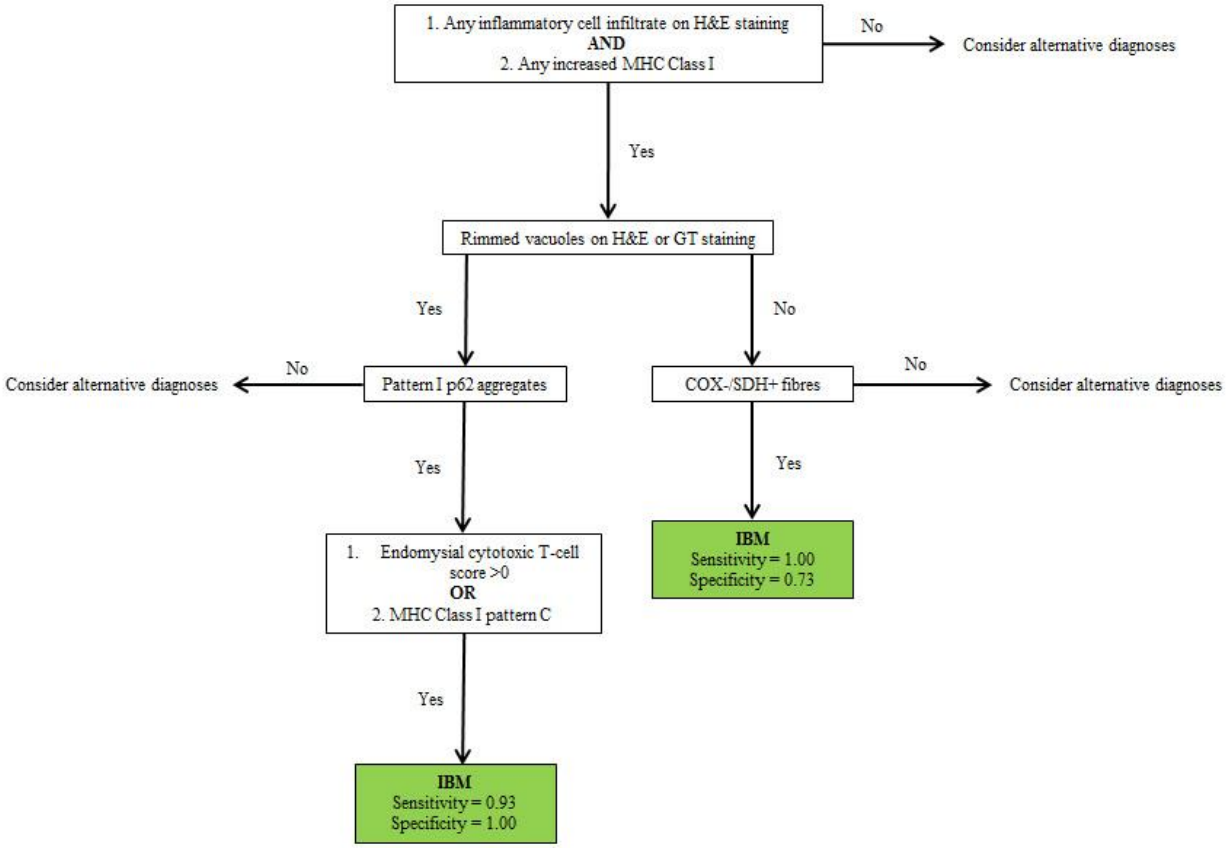
5.6.2.1 Sensitivity and specificity

Quantifying the percentage of affected fibres in each biopsy typically gave better sensitivities and specificities than defining a biopsy as positive or negative according to the presence or absence of pathological features. However, this method was impractical for routine clinical use and only myotilin IHC satisfied the criteria required of a diagnostic test. The simpler assessment, revealed that MHC Class I staining or CD8 IHC were best for differentiating between IBM+RV and PAM+RV; pattern C MHC Class I staining and a semi-quantitative endomysial cytotoxic T-cell inflammatory score >0 both had a sensitivity of 93% and specificity of 100%. Although type I p62 immunoreactive aggregates were highly sensitive, their absence ruling out a diagnosis of IBM+RV, they lacked specificity. The pathological findings were so similar between IBM–RV and PM&DM that none of the tests could reliability differentiate them. The most discriminative pathological feature was the presence of one or more COX-/SDH+ fibres. However, relying solely on the presence of an inflammatory cell infiltrate and one or more COX-/SDH+ fibres to reach a diagnosis of IBM-RV would result in the misdiagnosis of 27% of cases of treatable PM&DM as IBM-RV. This emphasises the need for clinicopathological correlation in making a diagnosis of IBM. Of note, there was no difference in the median age at biopsy between IBM-RV and PM&DM that could have contributed to the difference in COX-/SDH+ fibres. Combinations of pathological findings were tested, but did not lead to an increase in sensitivity and specificity. A diagnostic algorithm based on the pathological findings is proposed in Figure 5.10.

5.6.2.2 Likelihood ratios

Although, the sensitivity and specificity are one way of assessing a diagnostic test they describe how the presence or absence of abnormality predict the test result. However, in clinical practice, it is essential to know how a test result predicts the probability of having IBM. The LR summarises

Figure 5.10 Proposed diagnostic algorithm for IBM based on pathological findings



Flow diagram showing a proposed pathway for diagnosing IBM based on the pathological findings. Increased MHC Class I staining was observed in all cases of IBM and type I p62 aggregates in all cases of IBM+RV making them good initial screening tests. Their absence rules-out a diagnosis of IBM and IBM+RV respectively. The presence of an endomysial cytotoxic T-cell inflammatory infiltrate score >0 or MHC Class I pattern C in a biopsy with rimmed vacuoles and p62 aggregates secures a diagnosis of IBM+RV. Differentiating IBM-RV and PM&DM pathologically is more challenging. The presence of COX-/SDH+ fibres is not specific to IBM-RV. However, an absence of COX-/SDH+ fibres effectively rules out a diagnosis of IBM-RV.
H&E = Haematoxylin and eosin; MHC Class I = Major histocompatibility complex class I; p62 = Sequestosome I; COX-/SDH+ = Cytochrome c oxidase negative/ succinate dehydrogenase positive.

how much more or less likely patients with a particular disease are to have a negative or positive test result than those without the disease. LR greater than 10 or less than 0.1 is considered to be strong evidence for or against a diagnosis respectively (Deeks and Altman, 2004). In IBM–RV, finding Congophilic deposits or any COX-/SDH+ fibre has a LR greater than 10. However, unlike COX-/SDH+ fibres, Congophilic deposits were present in few cases of IBM–RV limiting their diagnostic use. Myotilin and ubiquitin immunoreactive aggregates and endomysial B-cells had a LR less than 0.1 and were therefore, strong evidence against a diagnosis of IBM–RV. However, myotilin aggregates and endomysial B-cells may be associated with the duration of disease as they were observed in IBM+RV and not IBM–RV, which may limit their diagnostic use. Also, ubiquitin immunoreactive deposits were observed in DM and not PM possibly limiting their diagnostic value in clinical practice. In agreement with our findings, Temiz *et al.* found that B-cells were present in a greater proportion of PM cases than IBM or PM.Mito (Temiz et al., 2008). In IBM+RV, COX-/SDH+ fibres, partial invasion and endomysial T-cells, cytotoxic T-cells, helper T-cells, macrophages and B-cells had a LR greater than 10.

5.6.3 Pathological findings in IBM+RV and IBM–RV indicate a common pathogenesis

p62 and TDP-43 immunoreactive aggregates, Congophilic deposits were observed in a greater percentage of fibres in IBM+RV than IBM–RV and the endomysial inflammatory cell infiltrate was greater in IBM+RV than IBM-RV. Ubiquitin and myotilin immunoreactive aggregates were present in IBM+RV, but not in IBM–RV. These differences may lead some to argue that IBM-RV and IBM+RV are two distinct diseases. However, we would suggest that opposed to this are the clinical and pathological similarities; in particular, there were no differences in the percentage of COX-/SDH+ fibres and the morphology of p62 immunoreactive aggregates and the pattern of MHC Class I up-regulation was identical in both. The pathological changes in IBM–RV were less marked than those in IBM+RV suggesting that, like rimmed vacuoles, protein aggregates, Congophilic deposits and the endomysial inflammatory infiltrate occur in chronologically more advanced disease. Widespread up-regulation of MHC Class I staining and mitochondrial changes

were present in nearly all IBM cases and were present in a greater number of biopsies than any other pathological feature. This indicates that they may be early pathological changes and therefore central to the pathogenesis of IBM, warranting greater scrutiny and investigation. The increase in pathological burden associated with rimmed vacuoles may contribute to the more rapid decline in function observed in IBM with rimmed vacuoles compared to cases without rimmed vacuoles (Temiz et al., 2009) and older patients with IBM compared to younger patients with IBM (Peng et al., 2000c)(Brady et al., 2013). However, we were unable to confirm that the pathological features correlated with the clinical findings and disease progression. This may be due to the small number of cases examined.

5.6.4 Study limitations

Limitations include the small number of cases and the retrospective study design. The number of cases allowed each marker to be systematically and quantitatively evaluated. This type of analysis would not have been possible with a larger number of cases. The small number of cases reflects the prevalence of these diseases in the UK and the scarcity of available muscle tissue, particularly of PAM+RV as once a genetic diagnosis is made in one family member others in the family tend to be diagnosed on genetic testing without a biopsy being performed. The retrospective nature of the study enabled the inclusion of patients whose diagnosis was confirmed after a response to therapy or with follow-up. The inclusion of only IBM patients with the characteristic pattern of weakness (described in Chapter 3) meant that the diagnosis was secure without the need for a further muscle biopsy to identify Griggs' pathological features.

5.6.5 Final comments

In conclusion, a valid clinicopathological definition of IBM is of paramount importance for selection and entry of patients into future clinical trials. The current pathological diagnostic criteria in IBM are too restrictive and the investigation of the pathogenesis of IBM in only those cases fulfilling the diagnostic criteria has probably led to incorrect conclusions being drawn about its

pathogenesis. The need and importance of demonstrating the presence of some of the pathological features included in the diagnostic criteria has long been debated (Sayers et al., 1992) and we have found that there is no additional diagnostic security in demonstrating all the features currently required by the pathologically focussed criteria. In addition, our findings suggest that protein aggregates, Congophilic deposits and rimmed vacuoles are indicative of chronologically more advanced disease and therefore, are of limited value in diagnosis. The most diagnostically useful features for differentiating IBM from pathologically similar myopathies were p62 immunoreactive aggregates, MHC Class I up-regulation and endomysial T-cells (CD3 and CD8) and COX-/SDH+ fibres and staining for these should be included in the histological assessment of IBM. This will enable the prospective evaluation of these diagnostic tests that is now required in patients suspected of having IBM. Finally, mitochondrial abnormalities and MHC Class I up-regulation appear to be early features of the disease and therefore may be more central to the pathogenesis. Further investigation and therapeutic intervention should be directed at these features.

Chapter 6

PROTEOMIC ANALYSIS OF IBM MUSCLE

6.1 Introduction

A number of abnormal proteins associated with neurodegenerative disease have been identified in IBM muscle fibres using IHC staining techniques; this has led to the hypothesis that neurodegenerative proteins, such as Aβ and tau, may be toxic to muscle fibres and cause muscle degeneration (Askanas and Engel, 2006). Subsequently, many more proteins have been described in IBM (Table 1.1). Those described are involved in a number of disparate cellular processes leading some authors to hypothesise that there is a general defect in protein handling in IBM involving either the ER, UPS or autophagy (Needham and Mastaglia, 2007)(Temiz et al., 2009). Other authors have suggested that myonuclear degeneration is an early and significant event in the pathogenesis of IBM (Greenberg, 2010). Support for this has come from early EM studies of IBM showing myonuclear abnormalities (Chou, 1967)(Carpenter et al., 1978), IHC demonstrating nuclear membrane proteins lamin in rimmed vacuoles (Greenberg et al., 2006) and more recently, the loss of myonuclear TDP-43 and its mislocalisation in sarcoplasmic aggregates (Salajegheh et al., 2009b). TDP-43 is a RNA binding protein, but its exact cellular functions are uncertain. Its loss from the myonucleus and accumulation in the sarcoplasm in IBM is hypothesised to cause impaired gene expression.

Almost all our understanding of IBM has come from IHC studies. However, as described in Chapter 1, many of the IHC findings may have been over-emphasised and studies using different methodologies to support the IHC findings are lacking. Relatively few studies have investigated protein or gene expression in IBM using immunoblotting and microarrays. Such studies utilised whole muscle homogenate with inclusion of other cell types namely inflammatory cells, blood vessels, fat and connective tissue in addition to muscle fibres (Mirabella et al., 1996)(Vattemi et al., 2001)(Vattemi et al., 2003)(Ferrer et al., 2004)(Maurage et al., 2004)(Fratta et al., 2005). The

inclusion of these other tissue components makes it very difficult to ascertain whether differences between IBM and controls are due to the addition of these contaminants or alterations within muscle fibres. Recently, proteomics has developed into a promising tool for the assessment of the protein expression in muscle. Four studies have investigated aspects of the proteome in IBM (Li et al., 2006)(Hutchinson and Jongbloed, 2008)(Parker et al., 2009a)(Doppler et al., 2011). However, these studies are limited by a number of factors including poor choice of control tissue, use of whole muscle homogenate and analysis of only the soluble fraction of the proteome.

6.2 Hypothesis

LCM and MS/MS proteomic analysis can be used to investigate the pathogenesis of IBM in uncontaminated muscle samples, therefore overcoming the limitations imposed by other techniques.

6.3 Aims

To identify proteins differentially expressed in abnormal fibres in IBM to gain insights into the pathogenesis of IBM, to identify possible diagnostic biomarkers and to verify the pathological findings documented in Chapters 4 and 5.

6.4 Methods and technical approaches

Six patients with IBM were identified, five from the National Hospital of Neurology and Neurosurgery and one from the Berufsgenossenschaftliches Universitätsklinikum Bergmannsheil, Bochum, Germany. Cryostat sections were cut and placed on PET membrane slides and stained with H&E and using IF for p62, LC3 and myotilin aggregates. Using a laser dissecting microscope, 250,000 μm^2 of muscle fibre sarcoplasm was dissected from each case for each sample. Samples were digested and separated with HPLC then analysed with MS/MS. Peptides unique to individual proteins were identified and their relative quantification was determined from the sum of the spectral counts. The protein lists produced were initially analysed for proteins believed to be

important in the pathogenesis of IBM and then in an unbiased manner by comparing proteins detected and examining those found to be differentially expressed. Bioinformatic analyses were also performed to identify overexpressed gene ontology (GO) terms.

Tissue staining and protein extraction were performed with Mrs A. Schreiner, and Miss A. Maerkens. Mass spectrometry was performed by the Department of Functional Proteomics, Medizinisches Proteom-Center, Ruhr-Universität Bochum, Bochum, Germany.

6.5 Results

6.5.1 Clinical characteristics of IBM patients

Demographic and clinical characteristics of the individual IBM cases are shown in Table 6.1.

6.5.2 Optimisation of PET membrane staining

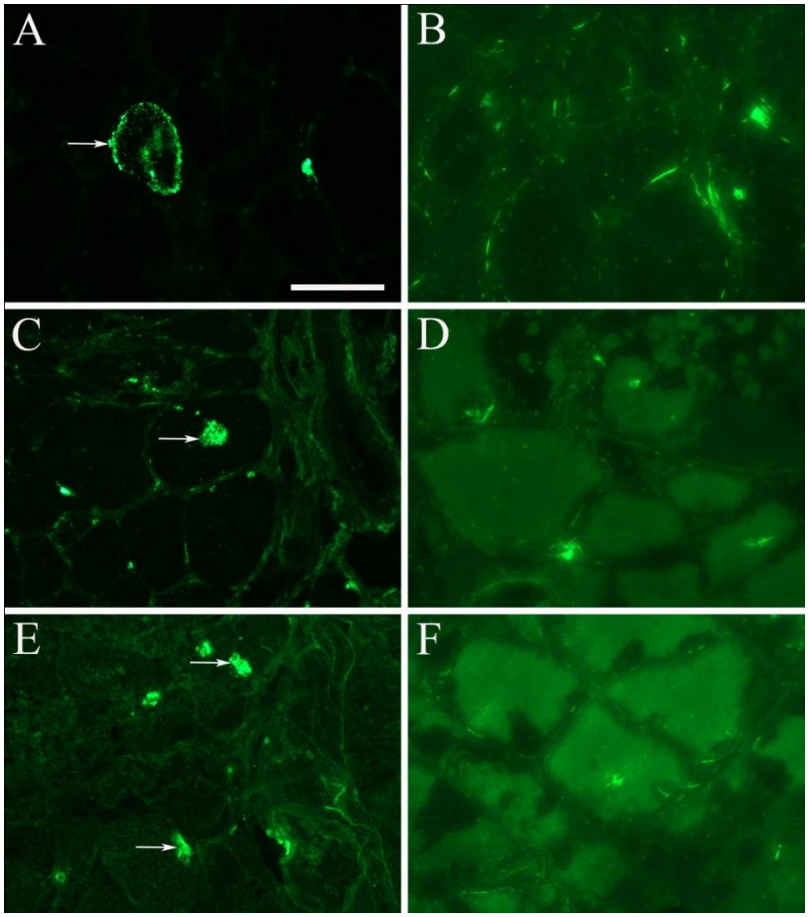
To identify abnormal muscle fibres, multiple ten µm thick frozen muscle tissue sections were placed on glass and PET membrane slides. Tissue sections were stained with H&E to identify rimmed vacuoles and with IF to identify p62, LC3 and myotilin immunoreactive aggregates. p62 immunoreactive aggregates were initially chosen as they were present in the greatest percentage of cases and muscle fibres in IBM and were easily identifiable. However, due to the characteristics of the PET membrane and the small size of many of the p62 immunoreactive aggregates, it was difficult to identify p62 immunoreactive deposits within fibres on PET membrane slides (Figure 6.1). As a surrogate marker for p62 immunoreactive deposits, IF staining was performed for LC3 immunoreactive deposits. LC3 is closely associated with p62 in the autophagic pathway and LC3 and p62 immunoreactive deposits have been shown to co-localise (Bjørkøy et al., 2005). In addition, LC3 immunoreactive deposits are reported to be a frequent in IBM (Temiz et al., 2009).

Table 6.1 Clinical characteristics of IBM patients

Sample	Gender	Ethnicity	Age at onset, years	Age at biopsy, years	CK (0-250 IU/L)*	Weakness
1	Male	Caucasian (UK)	56	60	446	FF and KE
2	Male	Caucasian (UK)	61	65	444	FF and KE
3	Female	Asian (UK)	58	62	500	FF and KE
4	Male	Caucasian (UK)	57	59	397	FF and KE
5	Male	Caucasian (UK)	71	76	323	FF and KE
6	Male	Caucasian (D)	65	68	427	FF and KE

CK = Creatine kinase; UK = United Kingdom; D = Germany; KE = Knee extensors; FF = Finger flexors. *At presentation.

Figure 6.1 IF staining of muscle tissue on standard glass and PET membrane slides to demonstrate protein aggregates



Ten µm thick sections of IBM muscle tissue sections stained using IF techniques with antibodies directed against p62 (A,B), LC3 (C,D) and myotilin (E,F) on standard glass slides (A,C,E) and PET membrane slides (B,D,F). Fluorescent aggregates were easily visible on glass slides (A, C, E arrows), but due to the small size of aggregates and distortions caused by dried deposits of PBS they could not be identified on PET membrane slides. Scale bar represents 100 µm in A-F.
p62 = Sequestosome I; LC3 = Microtubule-associated protein 1A/1B-light chain 3; PET = Polyethylene terephthalate; IF = Immunofluorescent.

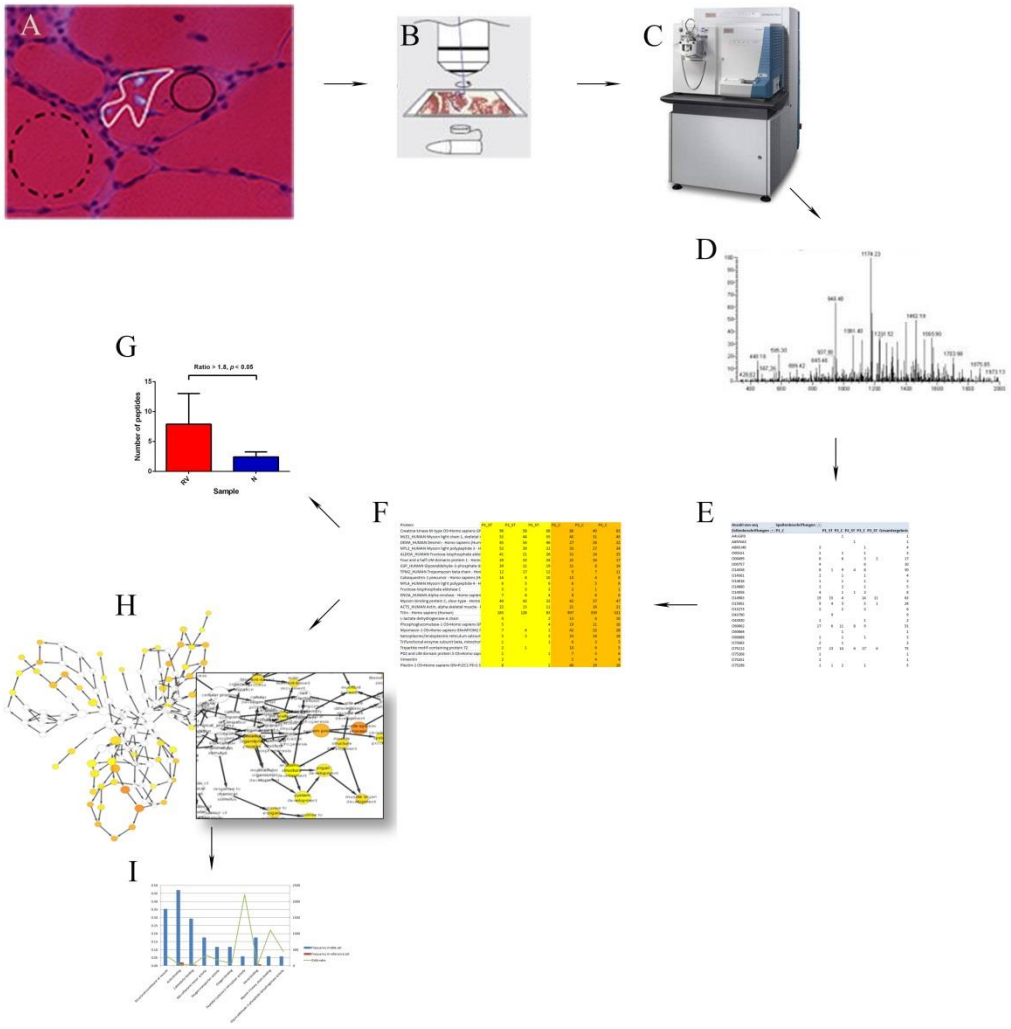
In addition to LC3 staining, IF staining for myotilin immunoreactive aggregates was performed because they were typically larger than p62 aggregates (Chapter 4) and therefore, easier to identify. However, IF staining for LC3 and myotilin was similarly unsuccessful (Figure 6.1). The difficulty in visualising IF aggregates was in part due to the formation of PBS crystals on the PET membrane distorting the staining. Because of the difficulty visualising the fluorescent aggregates on PET membrane slides, H&E stained tissue sections were used for this study. From H&E stained sections three areas were selected for study: i) rimmed vacuoles, their contents and the immediate surrounding sarcoplasm; ii) non-vacuolated sarcoplasm from fibres containing rimmed vacuoles; and iii) morphologically normal muscle fibres. These areas were individually collected using LCM therefore avoiding sample contamination with non-muscle cells.

6.5.3 Workflow

The workflow is detailed in Figure 6.2.

Samples were analysed consecutively, unique peptides within each sample were identified and the relative abundance – SI - of the corresponding proteins calculated. The mean relative quantity of each protein in each group - rimmed vacuoles, their contents and the immediate surrounding sarcoplasm (RV); non-vacuolated sarcoplasm from fibres containing rimmed vacuoles (ST); and morphologically normal muscle fibres (N) - was determined. Differentially expressed proteins between i) RV and N, ii) RV and ST and iii) ST and N samples were identified. A protein was accepted as increased if it was 1.8 times greater in one group than another and $p < 0.05$. A protein was defined as reduced if it was 0.55 times less in one group and $p < 0.05$. Optimum cut-off values for differentially expressed proteins have been determined through experience by the Department of Functional Proteomics, Medizinisches Proteom-Center, Ruhr-Universität Bochum, Bochum, Germany. Proteins reduced in RV samples were not analysed because comparable amounts of muscle tissue were not collected due to the absence of sarcoplasm within the vacuole.

Figure 6.2 Workflow applied to muscle samples



Three areas were selected for laser capture (A): rimmed vacuoles, their contents and the surrounding sarcoplasm (RV) (A, within the white line), non-vacuolated sarcoplasm from fibres containing rimmed vacuoles (ST) (A, within the black line) and sarcoplasm from morphologically normal fibres (N) (A, within the dotted black line). Two hundred and fifty thousand μm^2 of sarcoplasm from these areas was dissected (B). The samples were prepared and separated by high performance liquid chromatography. Label-free analysis was performed with tandem mass-spectrometry (C). The mass spectrometry spectra produced were assigned to peptides (D). Unique peptides were identified and assigned to their corresponding protein using Uniprot and Microsoft Excel. The amount of each protein present in a sample, known as the spectral index, was quantified (E). The protein lists produced were analysed in three ways (F-I). Firstly, they were searched for proteins of interest, those proteins believed to be of importance in the pathogenesis of IBM (F). Secondly, differentially expressed proteins were identified by comparing the mean spectral index between groups (G). Thirdly, differentially expressed proteins were analysed using bioinformatic programme such as Cytoscape to determine over-represented gene ontology (GO) terms. Cytoscape and a Biological Networks Gene Ontology plugin were used to produce a network diagram of the GO terms (H). From a network of GO terms a hierarchical chart was constructed.

The further down the hierarchy a term the more specific and therefore, the more informative it is thought to be. Statistically significant GO terms at the bottom of the hierarchy, referred to as ‘child-terms’, were identified and the odds ratio of their over-expression in the dataset calculated (I).

6.5.4 Protein composition of IBM samples is homogeneous

Protein samples were collected from 5 individuals (Table 6.1); sample 4 did not contain enough fibres with rimmed vacuoles to enable 250,000 μm^2 of rimmed vacuoles to be collected. The total number of peptides and type of proteins were similar in samples 1, 2 and 3, but samples 5 and 6 were distinct. In sample 5, a large number of peptides corresponding to proteins not present in muscle were detected indicating that it had become contaminated during sample preparation. Sample 5 was therefore excluded from further analyses. Sample 6 also stood apart from other samples. These differences led to a more detailed assessment of the patient which indicated that the diagnosis was more likely to be a hereditary limb-girdle muscular dystrophy. Therefore, sample 6 was excluded from all further analyses.

To determine the homogeneity of individual samples in each group, the top twenty proteins in each group - RV, ST and N in samples 1, 2 and 3 - were compared (Table 6.2). In RV, 13 proteins made up the top twenty proteins in all three samples. In ST, 12 proteins made up the top twenty proteins in all three samples. In N, 16 proteins made up the top twenty proteins in all three samples. This consistency between samples demonstrates a high level of the homogeneity between samples.

6.5.5 Greater variety of proteins are present in RV and N than ST

There were no statistical differences between the mean number of peptides present in RV, N and ST samples, which were 2732, 3153 and 1568 respectively. The protein with the greatest number of peptides identified in each sample corresponded to the massive sarcomeric protein titin. More proteins were detected in RV than ST (429 *v*. 99; $p < 0.004$) and N than ST (375 *v*. 99; $p < 0.01$).

6.5.6 Markers of ER stress are up-regulated in IBM

The first stage of our analysis focussed on those proteins believed to be important in the underlying pathogenesis of IBM. To examine some of the hypotheses surrounding the pathogenesis of IBM

Table 6.2 The number of proteins common to samples from each area

Area	No. of proteins common to samples 1,2 and 3	No. of proteins common to two samples	No. of proteins unique to one samples
RV	13	7	7
ST	12	8	8
N	16	3	6

The number of proteins common to RV, ST and N illustrates a high level of homogeneity between samples.
RV = Rimmed vacuoles, their contents and the surrounding sarcoplasm; ST = Non-vacuolated sarcoplasm from fibres containing rimmed vacuoles; N = Sarcoplasm from morphologically normal fibres.

which have been suggested from the IHC data, protein lists for RV, ST and N were interrogated for i) established markers of autophagy – p62, LC3, NBR1, atg 12 and beclin 1; ii) proteins classically associated with neurodegenerative diseases, such as AD, and proteins involved in their production – APP, Aβ, α-synuclein, PrP, β-secretases 1 (BACE 1) and 2 (BACE 2), α 1-antichymotrypsin, presenilin and tau; iii) ER stress - Grp78, endoplasmin, calnexin, calreticulin, X-box binding protein and C/EBP homologous protein, which is also pro-apoptotic.

Peptides corresponding to ER stress response proteins- endoplasmin, calnexin and Grp 78 were present in RV and N, but not ST samples. Peptides corresponding to p62 were present in all RV samples. There were no peptides associated with pro-apoptotic proteins or proteins associated with neurodegeneration, namely APP, Aβ, α synuclein, PrP, BACE 1, BACE 2, α 1-antichymotrypsin and presenilin 1 and 2. One peptide corresponding to tau was detected in a single sample. This approach yielded little information supporting the role of neurodegenerative proteins in the pathogenesis of IBM, but did reveal evidence of ER stress in fibres containing rimmed vacuoles and morphologically normal fibres in IBM.

6.5.7 Differentially expressed proteins between samples

Next we examined all proteins detected to compare the expression levels between groups. One hundred and eleven different proteins were increased in RV compared to ST, 13 in RV compared to N and 11 in ST compared to N. One hundred and eighteen proteins were decreased in ST compared to N. Differentially expressed proteins between groups are detailed in Tables 6.3-6.5. If more than 30 proteins were differentially expressed, only the top 30 are shown. Full lists of differentially expressed proteins identified are included in Appendix A.3.

6.5.7.1 Proteins increased in RV compared to N

Intermediate filaments – vimentin and nestin, ribosomal proteins, proteins involved in myogenesis, autophagy and nuclear proteins were found in greater quantity in RV than in N (Table 6.3).

Table 6.3 Proteins increased in RV compared to N

Accession number	Protein	Total number of unique peptides	RV (SI)	Control (SI)	Ratio	*p* value
P48681	Nestin	54	16.13	3.89	4.15	0.045
P02545	Lamin-A/C	45	10.91	4.13	2.64	0.01
P08670	Vimentin	42	10.52	4.63	2.27	0.03
Q09666	Neuroblast differentiation-associated protein	21	6.09	1.04	5.87	0.001
P09972	Fructose-bisphosphate aldolase C	13	3.40	1.23	2.76	0.02
P27816	Microtubule-associated protein 4	9	2.39	0.67	3.55	0.04
P62750	60S ribosomal protein L23a	7	2.26	0.24	9.40	0.01
Q5BKX8	Muscle-related coiled-coil protein	5	1.76	0.00	> 1.8	0.0002
P07900	Heat shock protein 90-alpha	5	1.43	0.24	5.96	0.03
O14949	Cytochrome b-c1 complex subunit 8	3	1.13	0.00	> 1.8	0.004
P62263	40S ribosomal protein	3	1.13	0.00	> 1.8	0.004
Q13501	p62	3	1.13	0.00	> 1.8	0.004
Q96MG2	Junctional sarcoplasmic reticulum protein 1	3	1.13	0.00	> 1.8	0.004

Intermediate filaments, autophagic and nuclear proteins were increased in RV compared to N. Proteins marked in yellow were increased in RV compared to N and ST. The proteins are ordered by RV SI from largest to smallest.
RV = Rimmed vacuoles, their contents and the surrounding sarcoplasm; N = Sarcoplasm from morphologically normal fibres; SI = Spectral index; p62 = Sequestosome 1.

Table 6.4 Proteins increased in RV compared to ST

Accession number	Protein	Total number of unique peptides	RV (SI)	ST (SI)	Ratio	*p* value
Q8WZ42	Titin	1971	408.76	176.97	2.31	0.003
P20929	Nebulin	257	58.06	13.88	4.18	0.001
Q15149	Plectin-1	114	26.48	3.97	6.67	0.004
P54296	Myomesin-2	85	18.56	5.64	3.29	0.01
P06576	ATP synthase subunit beta	68	16.39	3.55	4.62	0.01
P12111	Collagen alpha-3 (VI) chain	51	12.88	0.00	> 1.8	0.01
P48681	Nestin	45	11.80	0.00	> 1.8	0.001
P36871	Phosphoglucomutase-1	48	10.53	3.91	2.69	0.045
Q5VTT5	Myomesin-3	35	8.74	0.00	> 1.8	0.01
Q99798	Aconitate hydratase	32	7.94	1.25	6.33	0.01
P16615	SERCA 2	38	7.79	3.91	1.99	0.02
Q5VST9	Obscurin	33	7.70	0.73	10.52	0.02
P02545	Lamin-A/C	31	7.53	0.89	8.50	0.003
Q9UBF9	Myotilin	29	7.14	0.89	8.06	0.002
P08133	Annexin A6	28	7.12	0.00	> 1.8	0.001
P08670	Vimentin	26	6.65	0.73	9.08	0.01
P40939	Trifunctional enzyme subunit alpha	27	6.48	1.10	5.90	0.01
P35573	Glycogen debranching enzyme	20	5.40	0.00	> 1.8	0.004
Q6ZMU5	Tripartite motif-containing protein 72	22	5.01	1.25	3.99	0.04
P49748	Very-long-chain specific acyl-CoA dehydrogenase	19	4.95	0.00	> 1.8	0.003
Q14324	Myosin-binding protein C	23	4.91	1.77	2.77	0.03
P12109	Collagen alpha-1(VI) chain	20	4.91	0.00	> 1.8	0.04
O75923	Dysferlin	20	4.85	0.00	> 1.8	0.02
P21796	Voltage-dependent anion-selective channel protein 1	19	4.75	0.89	5.37	0.02
P08237	6-phosphofructokinase	19	4.25	1.25	3.40	0.02
P12277	Creatine kinase B-type	15	4.16	0.00	> 1.8	0.01
P17174	Aspartate aminotransferase	17	4.16	0.73	5.68	0.04
Q13423	NAD(P) transhydrogenase	17	4.14	0.37	11.30	0.04
P23109	AMP deaminase 1	16	3.83	0.37	10.45	0.01
Q09666	Neuroblast differentiation-associated protein	14	3.79	0.00	> 1.8	0.003

The top thirty proteins are included. Structural proteins were found in greater quantity in RV than ST. The proteins are ordered by RV SI from largest to smallest. Proteins marked in yellow are increased in RV compared to N and ST. RV = Rimmed vacuoles, their contents and the surrounding sarcoplasm; ST = Non-vacuolated sarcoplasm from fibres containing rimmed vacuoles; SI = Spectral index; ATP = Adenosine triphosphate; AMP = Adenosine monophosphate; NAD(P) = Nicotinamide adenine dinucleotide (phosphate); SERCA = Sarcoplasmic reticulum Ca^{2+}-ATPase.

Table 6.5 Proteins increased in ST compared to N

Accession number	Protein	Total number of unique peptides	ST (SI)	N (SI)	Ratio	*p* value
P06732	Creatine kinase	411	110.76	46.39	2.39	0.0004
P05976	Myosin light chain 1	272	77.60	30.80	2.52	0.01
P17661	Desmin	220	75.41	19.78	3.81	0.01
P08590	Myosin light polypeptide 3	216	61.03	24.32	2.51	0.002
P04075	Fructose-bisphosphate aldolase A	158	43.40	17.16	2.53	0.003
Q13642	Four and a half LIM domains protein 1	136	41.76	14.28	2.92	0.02
P04406	Glyceraldehyde-3-phosphate dehydrogenase	97	26.82	10.36	2.59	0.02
P07951	Tropomyosin beta chain	68	21.45	6.94	3.09	0.03
P31415	Calsequestrin-1 precursor	59	16.74	5.92	2.83	0.004
P12829	Myosin light polypeptide 4	34	8.71	4.41	1.98	0.01
P09972	Fructose-bisphosphate aldolase C	15	5.45	0.99	5.53	0.0001

Proteins involved in contraction and metabolism were increased in ST compared to N. The proteins are ordered by ST SI from largest to smallest.
ST = Non-vacuolated sarcoplasm from fibres containing rimmed vacuoles; N = Sarcoplasm from morphologically normal fibres; SI = Spectral index.

6.5.7.2 Proteins increased in RV compared to ST

Structural proteins were found in greater quantity in RV than ST, namely intermediate filaments - nebulin and nestin, Z-disc associated proteins – myotilin and plectin-1 and M-band proteins – myomesin-2 and myomesin-3 (Table 6.4).

Nine proteins were present in greater quantity in RV than N and ST. Of these nine proteins, four proteins reached the criteria for differential expression. These were intermediate filaments – nestin and vimentin, neuroblastoma differentiation-associated protein and nuclear membrane protein - lamin A/C.

6.5.7.3 Proteins increased in ST compared to N

Proteins involved in muscle contraction, carbohydrate metabolism and energy regulation were increased in ST compared to N (Table 6.5).

6.5.7.4 Proteins reduced in ST compared to N

Z-disc proteins, Z-disc associated proteins, intermediate filaments and M-band proteins were decreased in ST compared to N, namely titin, myomesin-1, vimentin, plectin-1, nebulin and myomesin-2.

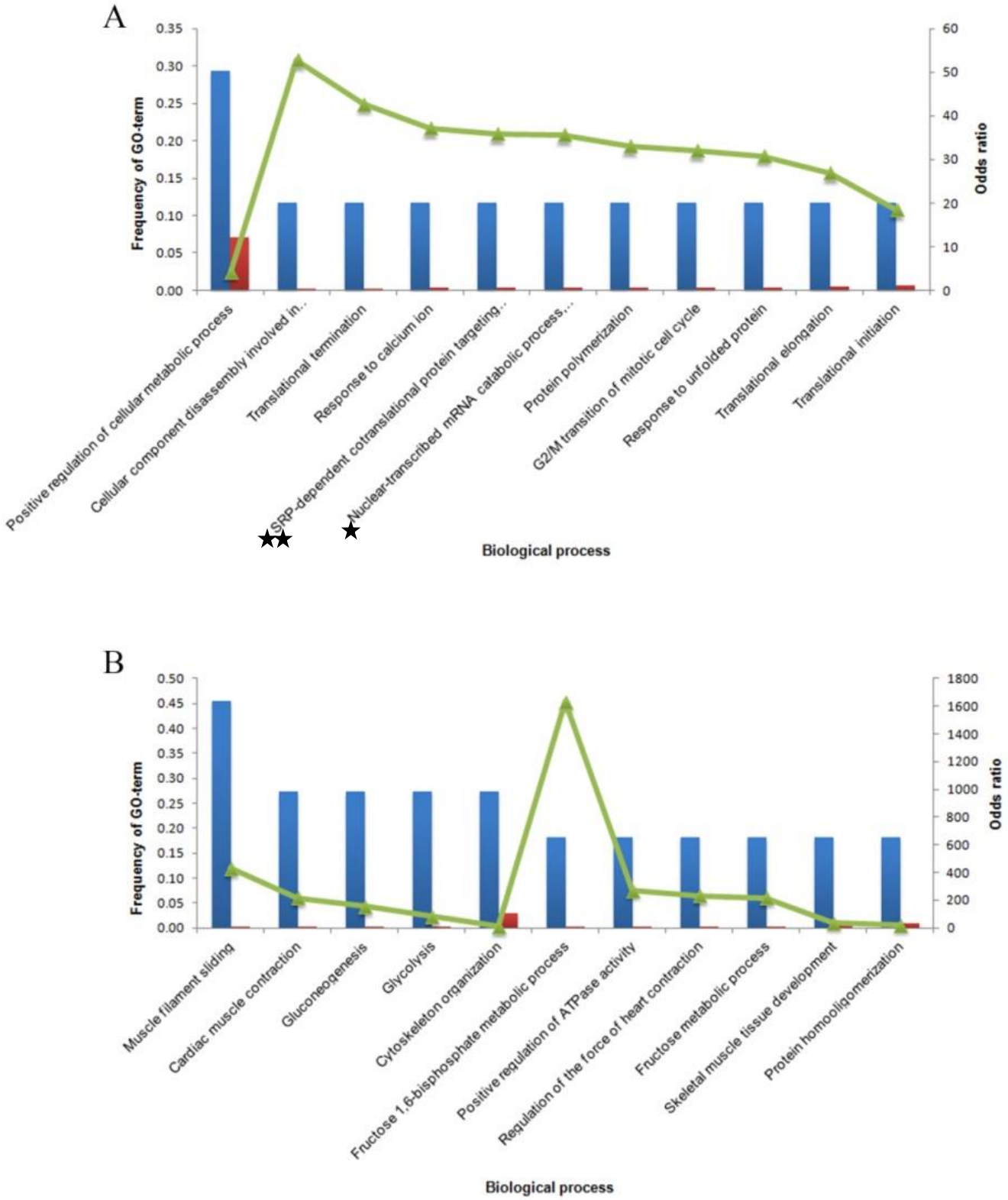
6.5.8 GO annotations analysis of proteomics data

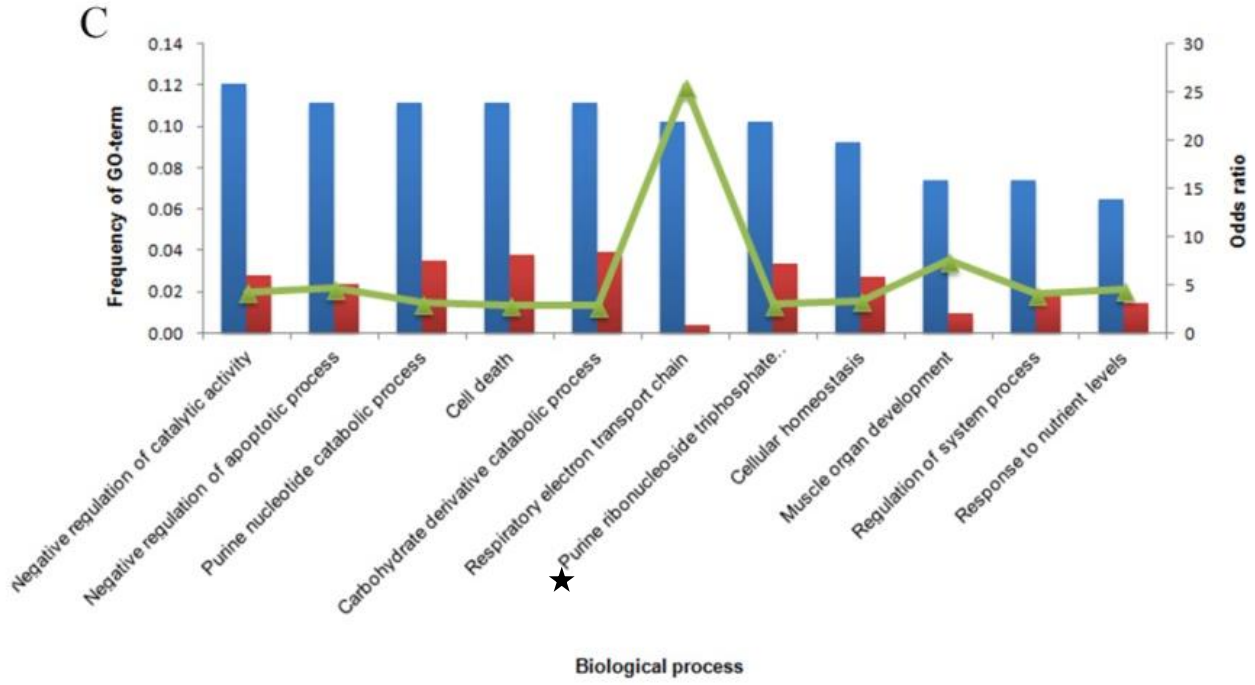
Lists of differentially expressed proteins can be useful when looking for specific changes in protein expression. However, functional relationships between proteins and protein interactions are difficult to glean from a list of proteins, not least because a single protein may have a number of functions. To analyse the biological effects of over- and under-represented proteins, GO analyses were performed. GO terms were developed to improve the analysis of large biological datasets produced from microarray and proteomic studies and to address the need for consistent description of the functions of individual genes and their products. GO terms describe three characteristics of

individual genes and their corresponding gene products: ‘molecular function’, ‘biological process’ and ‘cellular component’. Molecular function describes the activities of gene products at the molecular level e.g. catalytic or transportation. Biological process refers to the biological objectives to which a gene and its products contribute. A biological process is typically made up of one or more molecular function e.g. muscle contraction. Cellular component describes where in the cell the gene products are active e.g. nucleus. GO terms are assigned in a hierarchical fashion to these three characteristics. Terms further down the hierarchy are referred to as ‘child-terms’. The further down the hierarchy a child-term is the more specific and therefore, the more informative it is assumed to be.

Cytoscape 2.8.3 (NIGMS, America) with a BiNGO plugin was used to determine which biological processes were over-represented among differentially expressed proteins. Using Cytoscape and BiNGO, a network of over-represented GO terms could be visualised along with each term’s statistical significance (Figure 6.2) (Maere et al., 2005). This method enables the analysis of large protein lists. Therefore, in contrast to the previous analyses, all differentially expressed proteins that met the inclusion criteria were included. The odds ratio describing the over-representation in the dataset of a statistically significant term was also determined by calculating the ratio of the frequency of a term in the data set (differentially increased or decreased protein list) to its frequency in the reference set (Uniprot/Swissprot Gene Ontology Homo sapiens annotations file). The frequencies and odds ratios of the most significant terms in each data set are shown in Figure 6.3. GO terms corresponding to a particular theme such as protein synthesis are grouped together to show the distribution of over-represented terms (Figure 6.4).

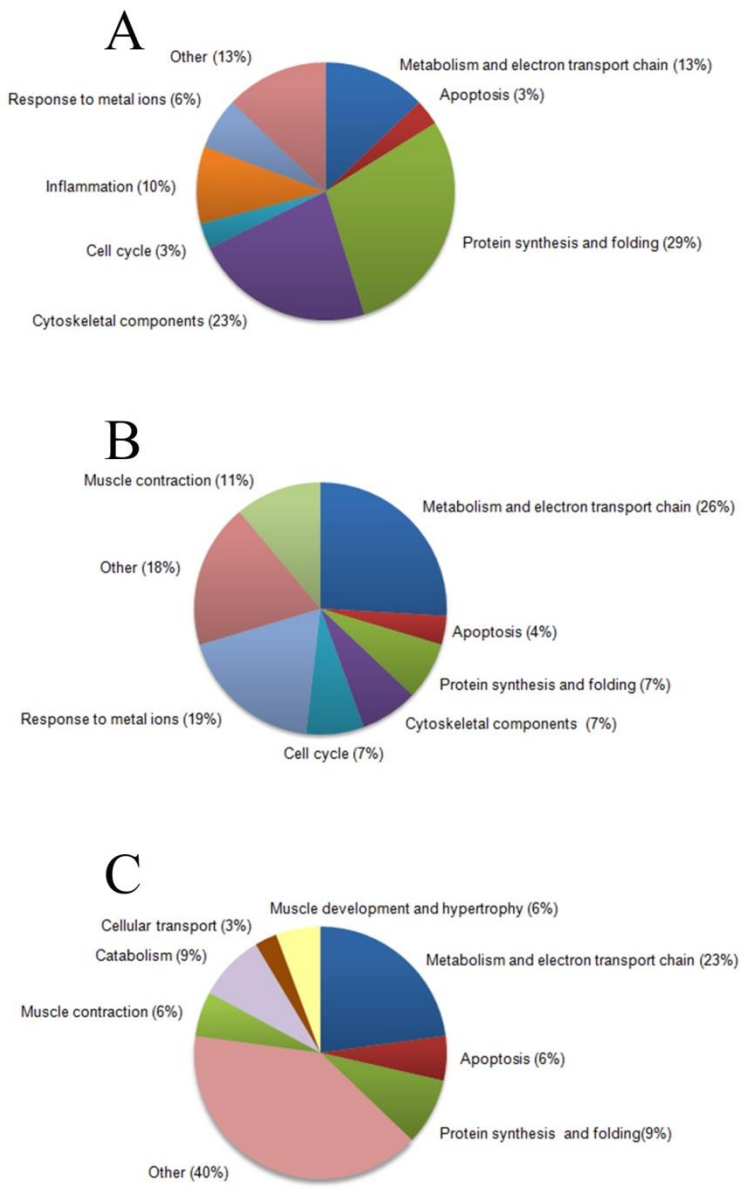
Figure 6.3 Up-regulated biological processes between samples





Bar charts show the top 11 over-represented biological process GO terms between RV and N (A), ST and N (B) and RV and ST (C) samples. The frequency of each GO-term in the data set is shown in blue and its frequency in the reference set is shown in red on the left *y*-axis. The odds ratio for each over-expressed GO-term is shown in green on the right *y*-axis.
RV = Rimmed vacuoles, their contents and the surrounding sarcoplasm; ST = Non-vacuolated sarcoplasm from fibres containing rimmed vacuoles; N = Sarcoplasm from morphologically normal fibres; GO terms = Gene ontology terms. *Cellular component disassembly involved in execution phase of apoptosis. **SRP-dependent cotranslational protein targeting to membrane and *Nuclear-transcribed mRNA catabolic process (nonsense-mediated decay) (A). *Purine ribonucleoside triphosphate catabolic process (C).

Figure 6.4 Over-represented biological processes between samples



Pie-charts showing the categories of over-represented GO terms between RV and N (A), ST and N (B) and RV and ST (C). All the statistically significant over-represented terms were categorised to emphasise the cellular functions that are over-represented between groups.
GO terms = Gene ontology terms; RV = Rimmed vacuoles, their contents and the surrounding sarcoplasm; ST = Non-vacuolated sarcoplasm from fibres containing rimmed vacuoles; N = Sarcoplasm from morphologically normal fibres

6.5.8.1 Over-represented biological process GO terms in RV compared to N show that protein translation and refolding is increased in RV

Analysis of the biological process terms revealed that those associated with protein synthesis and misfolded proteins including ‘protein refolding’ and ‘response to unfolded proteins’ were significantly over-represented in RV compared to N. Although GO terms associated with protein synthesis and misfolding did not have the highest statistical significance or odds ratio, they constituted the largest group of over-represented GO terms, making up nine (29%) over represented terms. GO terms associated with apoptosis were also over-represented in RV compared to N.

6.5.8.2 Over-represented biological process GO terms in ST compared to N shows that carbohydrate metabolism is increased in vacuolated fibres compared to normal sarcoplasm

Analysis of the ‘biological processes’ different between ST and N revealed that GO terms associated with carbohydrate metabolism and ATP were increased in ST compared to N. GO terms associated with metabolism were the most common differentially expressed GO terms and made up seven of 28 (29%) over-represented GO terms in ST compared to N. Similar to the analysis between RV and N, GO terms associated with apoptosis were found to be increased in ST compared to N.

6.5.8.3 Over-represented biological process GO terms in RV compared to ST shows that abnormal protein folding is increased around rimmed vacuoles

In agreement with the increased variety of proteins in RV samples compared to ST, a variety of biological processes were increased in RV samples compared to ST. Analysis of proteins differentially increased in RV compared to ST revealed that biological process GO terms ‘protein refolding’ and ‘protein signalling in the unfolded protein response’ were over-represented as was ‘cell-death’.

6.5.8.4 Over expressed cellular component GO terms show nuclear protein lamin is increased in RV compared to N

Analyses of the cellular component terms showed that GO terms associated with protein translation – 'cytosolic ribosomes' and 'ribosomal subunits' were the most statistically significant over-represented terms in RV compared to N. Other increased cellular component GO terms in RV compared to N were the nuclear 'lamin filament' and 'pre-autophagosomal structures'.

Cellular component analysis of differentially expressed proteins between RV and ST demonstrated that 'mitochondrial proteins' were the largest group of over-expressed GO terms followed by 'Z-disc', 'M-band' and nuclear membrane proteins in RV compared to ST.

6.6 Discussion

Studies supporting the IHC findings reported in IBM are lacking. To determine whether it is possible to analyse structural abnormalities in IBM and to verify our IHC findings we analysed rimmed vacuoles from three patients with clinicopathologically typical IBM with LCM and MS/MS. An interesting and potentially important finding was the similarity in protein expression between IBM cases. This would suggest that IBM is not just a 'promiscuous-proteinopathy' in which random proteins collect, but has a particular 'protein signature'. Classical neurodegenerative proteins were not found, supporting our earlier IHC findings and interpretation that they are unlikely to be involved in the pathogenesis of IBM. The presence of nuclear proteins in rimmed vacuole samples indicates, contrary to our IHC findings, that rimmed vacuoles may be derived from myonuclei and underlines the need to confirm experimental findings using a second independent method. The presence of intermediate filaments, microtubule proteins and p62 in RV samples suggests that rimmed vacuoles are surrounded by aggresomes.

6.6.1 Previous studies

Three studies have analysed the protein expression in IBM using proteomic techniques such as two dimensional gel electrophoresis (2DGE) and/or HPLC and MS (Li et al., 2006)(Hutchinson and Jongbloed, 2008)(Doppler et al., 2011), another study examined protein and gene expression in IBM (Parker et al., 2009a) and one further study analysed gene expression using microarray technology (Greenberg et al., 2002). Greenberg *et al.* reported that non-immune mRNA changes present in IBM are nonspecific and are present in other IIM, such as PM and DM, and therefore protein aggregates observed in IBM are due to post-translational events. Hutchison and Jongbloed also tried to answer this question using 2DGE to study whether protein aggregates in IBM are caused by uncontrolled transcription. They found no protein spots unique to IBM to support the hypothesis that widespread gene activation is responsible for the pathological changes observed in IBM. However, there was significant intra-sample variability limiting the value of their findings. Li *et al*. studied four cases of IBM and five non-IBM inflammatory myopathies with 2DGE and MS/MS. To avoid sample contamination muscle fibres were manually dissected from unstained sections. Of the six proteins decreased in IBM, five were contractile proteins. Sixteen proteins were increased; these were associated with protein folding, energy metabolism and amyloid. Parker *et al.* analysed IBM, PM, DM and normal muscle samples using HPLC separation followed by MS/MS. They found a preferential loss of type II fibre structural proteins and glycolytic enzymes and an increase in nuclear membrane proteins with preservation of the corresponding transcripts in IBM (Parker et al., 2009a). In the most recent study, Doppler *et al.* analysed muscle fibres surrounded by inflammatory cells and/or undergoing partial invasion in four IBM cases and found variable changes in basement membrane proteins, in addition to increased proline arginine-rich repeat protein and biglycan (Doppler et al., 2011). In these studies, samples were not matched for gender, age or muscle analysed which may have affected protein expression, obscuring important differences between samples. Other study limitations included blind or relatively blind (dissection from unstained tissue samples) microdissection of muscle fibres (Li et al., 2006), the use of whole tissue homogenate (Hutchinson and Jongbloed, 2008)(Parker et al., 2009a) and 2DGE. Analysis of

whole tissue homogenate or blind microdissection would have led to the inclusion of other cell types present in muscle tissue in addition to muscle fibres, which may have confounded results. Although 2DGE can be complimentary to MS informing on post-translational modifications and the presence of different isoforms some studies have shown significant intra-sample variation, poorly soluble proteins can be lost and resolution of certain proteins such as those with similar molecular weights and isoelectric points and basic proteins with an isoelectric point less than three is poor. To avoid these problems, we used LCM of stained tissue sections enabling direct visualisation of the tissue dissected and analysed the samples using HPLC and MS/MS.

6.6.2 Rimmed vacuoles contain nuclear membrane proteins

We found the nuclear membrane protein lamin A/C was differentially expressed in rimmed vacuoles compared to both the surrounding non-vacuolated sarcoplasm and sarcoplasm from morphologically normal fibres. This was in contrast to our IHC findings and those of others who were unable to find nuclear membrane proteins associated with rimmed vacuoles (Temiz et al., 2009), but agrees with reports by some researchers (Villanova et al., 1993) (Nalbantoglu et al., 1994)(Greenberg et al., 2006)(Nakano et al., 2008)(Nishii et al., 2011) and supports the hypothesis that rimmed vacuoles are derived from myonuclei. Lysosomal proteins have been identified in and around rimmed vacuoles using HC staining and IHC (Lotz et al., 1989) (Villanova et al., 1993) (Tsuruta et al., 2001) leading to the hypothesis that lysosomes are involved in the formation of rimmed vacuoles. However, we found no evidence of lysosomal proteins in rimmed vacuole samples to confirm that lysosomes involvement in their formation contrary to the findings of some IHC studies published (Villanova et al., 1993)(Tsuruta et al., 2001). This discrepancy between our study and others may be due to a difference in the antibody used, post-transcription alteration of lamin A/C or a progressive loss of lamin A/C from rimmed vacuoles over time. This difference underlines the importance of verifying results obtained through one experimental method with an alternative method, a practice which has been lacking in studies of IBM.

The presence of microtubule proteins, intermediate filaments and p62 in RV samples suggests that aggresomes are present around rimmed vacuoles. Aggresome formation is a third mechanism for cells to deal with abnormal proteins in addition to protein re-folding via molecular chaperones and protein degradation (Johnston et al., 1998). If a protein cannot be re-folded or degraded it is incorporated into an intracellular collection of thermodynamically stable proteins – an inclusion body. The sequestration of proteins into inclusion bodies is thought to reduce their cellular toxicity. Different types of aggresomal inclusion bodies are described in cells such as intracellular protein deposits and juxtanuclear quality control aggresomes (Kaganovich et al., 2008). Aggresomes are typically juxtanuclear structures to which abnormal proteins are targeted via microtubules using histone deacetylase 6 and dynein motors (Kawaguchi et al., 2003). In addition to aggregated proteins, aggresomes are composed of intermediate filaments, a core of mitochondria, proteasome subunits and molecular chaperones (García-Mata et al., 1999)(Wigley et al., 1999). Intermediate filaments, in particular vimentin, are the main structural component of aggresomes. When required intermediate filaments are re-distributed from around the cell to aggresomes where they are believed to provide structural support (Johnston et al., 1998). In addition to finding increased quantities of intermediate filaments and microtubule proteins in RV samples, analysis of the cellular components present revealed that mitochondrial components were significantly increased in rimmed vacuole samples. As aggresomes are commonly located at the microtubule organising centre next to the cell nucleus (Watanabe and Tanaka, 2011) these findings support the concept that rimmed vacuoles maybe derived from nuclei.

Typically, proteins sequestered in aggresomes were said to be ubiquitinated prior to transport to and inclusion in an aggresome (Kaganovich et al., 2008). We found rimmed vacuole samples to contain increased p62 but not ubiquitin. However, recent evidence suggests that neither ubiquitin nor p62 binding are required for aggresome formation. A number of studies have shown that aggresomes consisting of mutant superoxide dismutase, GFP250 and STAT5A_ΔE18 contained p62 but not ubiquitin (Johnston et al., 1998)(García-Mata et al., 1999)(Watanabe and Tanaka,

2011). Watanabe *et al.* also found that p62 knockdown cells are able to form aggresomes confirming that p62 is not necessary for aggresomes formation (Watanabe and Tanaka, 2011).

Two mechanisms may be responsible for the significant reduction in proteins observed in the non-vacuolated sarcoplasm in fibres containing rimmed vacuoles compared to morphologically normal fibres. GO-term analysis highlighted an increase in ER stress and UPR. UPR works to reduce ER stress by a number of mechanisms. One is to reduce protein synthesis, it achieves this by releasing protein kinase RNA-like endoplasmic reticulum kinase (PERK) from Grp78. PERK phosphorylates eukaryotic initiation factor 2α blocking it in its inactive form reducing protein translation leading to a decrease in the ER protein folding load (Harding et al., 1999)(Harding et al., 2000). However, this process is a transient measure. It has been suggested (Kopito, 2000) and is more likely that abnormal aggregate prone proteins act as a nidus and incorporate other proteins and reduce the number of soluble proteins within the muscle fibre. Another cause for the reduced protein numbers in the non-vacuolated sarcoplasm of vacuolated fibres may be the re-distribution of proteins such as vimentin to aggresomes (Johnston et al., 1998).

6.6.3 Increased protein expression leads to aggresome formation

It is estimated that over 30% of cellular proteins synthesised are abnormal and bound for degradation (Schubert et al., 2000). Inhibition of the cellular protein degradation mechanisms leads to the formation of protein aggregates (Watanabe and Tanaka, 2011). In addition to impaired degradation, physical cellular stresses, RNA modification and translational misincorporation of amino acids also promote the formation of protein aggregates. These abnormal unfolded and misfolded proteins cause ER stress and increased production of molecular chaperones that attempt to stabilise and refold them. Whether impaired protein degradation or increased production cause the formation of protein aggregates in IBM is unknown. We found an increase in GO terms associated with protein translation (initiation, elongation and termination) and transcription (ribosomal subunits) in RV samples suggesting an increase in protein expression may be

contributary. There was evidence of ER stress and a response to abnormally folded proteins such as the 'UPR', 'protein folding' and 'chaperone mediated protein folding'. These findings would support the hypothesis that abnormal protein synthesis rather than impaired protein degradation may play the major role in the formation of protein aggregates in IBM. An over-production of aggregate prone proteins in muscle fibres may be exacerbated by the decrease in protein degradation by autophagy that has been shown to occur with increasing age (Vittorini et al., 1999)(Cui et al., 2012). Changes in UPS function with aging are less clear. Studies have not shown an increase in RNA levels in IBM (Greenberg et al., 2002) to suggest that increased protein production leads to protein aggregation. Therefore it is likely that protein synthesis is altered post-translation leading to production of aggregate prone proteins which exceed the capacity of the cellular degradation mechanisms. Whether the mislocalisation of RNA binding proteins such as TDP-43 may be responsible is yet to be determined.

6.6.4 Proteomic studies support IHC findings

On the premise that IBM is a neurodegenerative disease akin to AD and PD, IHC analysis has been directed at identifying proteins that might support that view. Therefore, to validate our IHC findings we used LMD and label-free MS/MS, thus avoiding the restrictions imposed by hypothesis-driven IHC analysis. In agreement with our IHC findings, we found no evidence to support the role of neurodegenerative proteins including Aβ, α synuclein and PrP in IBM. In particular, there was no evidence of these proteins in fibres containing rimmed vacuoles, where they have been predominantly described. In addition, there was little to support a significant role for tau in the pathogenesis of IBM. Only one peptide corresponding to tau was found in a single sample. Although unlikely, this may be because these proteins were lost during processing or they may lack unique peptide sequences. In concordance with our IHC findings, both p62 and myotilin were increased in fibres containing rimmed vacuoles. As described earlier, in contrast to our IHC findings but in agreement with others, lamin A/C was present in rimmed vacuole samples.

6.6.5 Study limitations

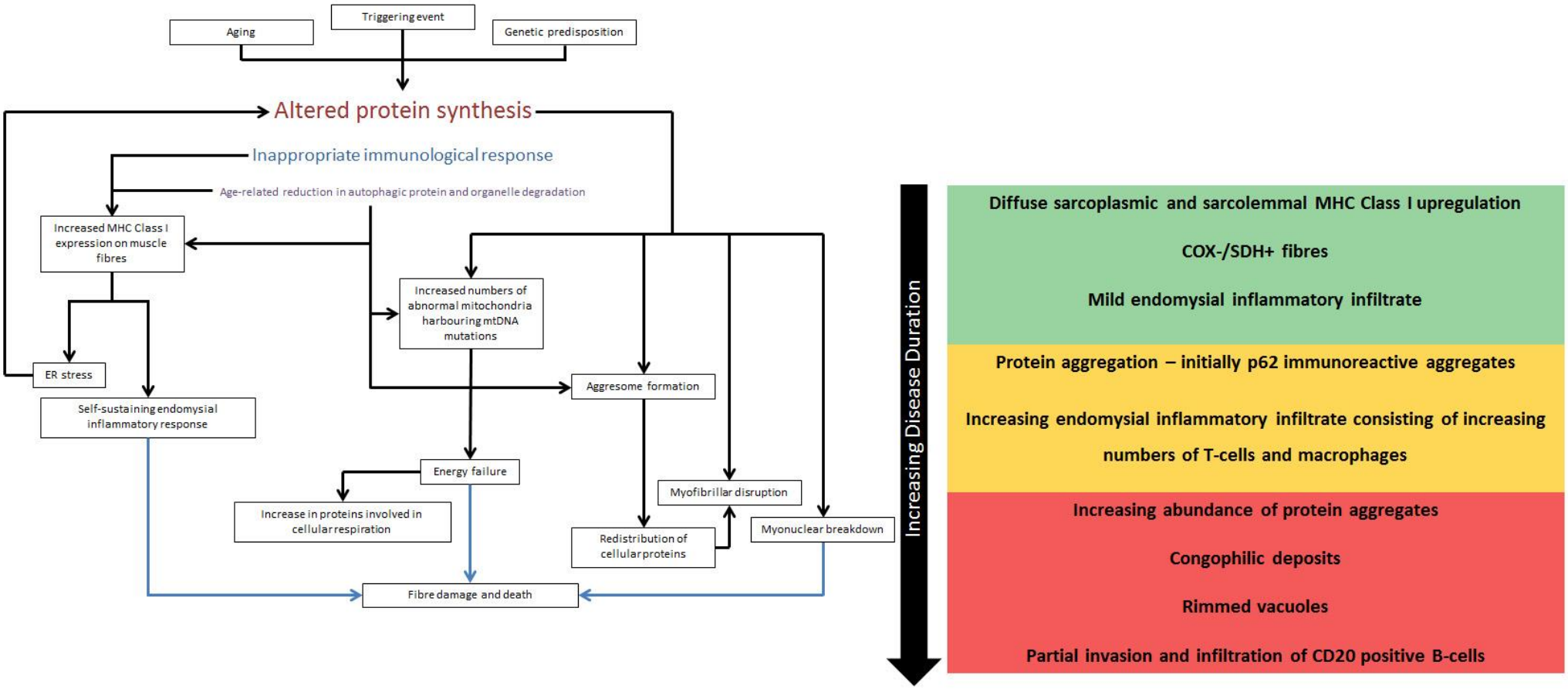
The small number of cases finally analysed in this study means that true differences between cases and controls may not reach statistical significance. A small number of cases were selected because of the large amount of tissue required for analysis and the time-constraints of performing LMD. However, we were able to show that it is possible to use LMD and MS/MS to analyse a relatively small and infrequent cellular structure such as a rimmed vacuole. This method avoids sample contamination with inflammatory cells, endothelium and connective tissue that occurs when using whole tissue homogenate. The best way to quantify the proteins present in a sample is debated (Nesvizhskii, Vitek, and Aebersold). We used a label free analysis and measured the abundance of proteins by spectral counting. Limitations of this method are that it is less accurate than stable isotope labelling, is unable to quantify low-abundance proteins and protein quantification is relative rather than absolute. However, it has been shown to be of practical use in a number of studies analysing the composition of structural abnormalities in muscle fibres (Schessl et al., 2008) (Kley et al., 2013) and sample preparation and data analysis are less complex and time-consuming. Some data is lost by the analysis of only unique peptides as identical peptide sequence can be present in different proteins (Nesvizhskii and Aebersold, 2005). However, shared peptides can lead to uncertainty in determining the identity and quantity of proteins within a sample. To avoid these ambiguities, only those peptides which were unique were included in the analysis making the results more reliable and any bias introduced by this method is limited as all samples were analysed in the same manner. We have shown that morphologically normal muscle fibres with H&E staining in IBM may lack rimmed vacuoles but are not normal. They express MHC Class I and may contain protein aggregates (Chapter 4). Therefore, using morphologically normal fibres from the same biopsy as the control may have hidden changes in protein expression that would have been observed if normal muscle samples were used. However, using intra-individual controls meant that samples were matched for factors that may have affected protein expression between biopsies. The advantage of an intra-individual control was to reduce these potential differences. Other limitations are not specific to this study but affect all proteomic studies. Proteins may not be

detected for a number of reasons. They may be insoluble, resistant to trypsin digestion or lost during separation. Additionally, they may not contain unique peptide sequences. Annotation databases are often incomplete. This influenced our choice of the available bioinformatic tools; with BiNGO, unlike a number of others, the latest International protein index (IPI) Homo sapiens GO annotations file can be downloaded and used and the IPI database is updated monthly and based upon Uni-prot/Swiss-prot which is updated fortnightly (Nesvizhskii and Aebersold, 2005).

6.6.6 Final comments

In conclusion, proteomic analysis of fibres containing rimmed vacuoles verified our IHC findings presented in Chapter 3, refuting the idea that neurodegenerative proteins of importance in AD and PD are central to the pathogenesis of IBM. In addition, proteomic analysis provided evidence to support the hypothesis that rimmed vacuoles are the remnants of myonuclei, something that was not identified in experiments using IHC techniques, emphasising the importance of validating experimental results. In addition, in fibres containing rimmed vacuoles, results suggested that there was increased protein synthesis accompanied by ER stress. These processes may contribute to the alteration in biological processes including energy metabolism and apoptosis observed in vacuolated fibres. The findings from Chapters 4, 5 and 6 are combined in Figure 6.5, which shows the possible pathogenic pathways in IBM and the resulting pathological features. Further work needs to be done on a larger cohort of samples and comparing morphologically normal fibres in IBM with muscle from age and biopsy site matched controls.

Figure 6.5 Proposed pathogenesis of IBM and the associated pathological features



The flow chart proposes a possible pathogenic pathway for IBM showing the interactions between different factors involved. The resulting pathological features that can be observed in IBM are shown to the right of the arrow which shows the evolution of the pathological features with time. Those thought to occur earlier in the disease are shown in the green box, those observed later in the orange box and later still in the red box.

Chapter 7

FINAL DISCUSSION AND FUTURE DIRECTIONS

IBM was first described as a distinct disease entity over 40 years ago. Despite much research over the ensuing period, our knowledge and understanding of IBM has progressed little. Arguably, one of the main limiting factors has been strict adherence to pathologically focussed diagnostic criteria which have remained largely unaltered since first proposed in 1987 (Calabrese et al., 1987). Despite recognition that the current diagnostic criteria are untested and based upon expert opinion rather than evidence, there has been anxiety and resistance over any changes to them. A persistent concern has been that changes would result in a loss of specificity and the inevitable misdiagnosis and inclusion of patients without IBM. This has meant that studies in IBM have tended to be small and may have led to erroneous conclusions being drawn.

The aims of this thesis were to characterise the clinical and pathological features of patients with IBM, enabling review of current diagnostic criteria and a providing a basis for the development of future criteria, and to investigate the pathogenesis of IBM in both pathologically typical and atypical patients utilising histological techniques and single fibre MS/MS protein analysis.

7.1 Overview of results

In characterising the clinical features and disease course of a large cohort of patients with IBM, I have confirmed that the characteristic pattern of weakness associated with IBM is present in the majority of patients at first presentation and this is independent of the pathological features. By contrast, the majority of our patients failed to fulfil the current pathologically focussed diagnostic criteria at presentation and we were able to show that typical pathological features associated with IBM are linked to disease duration. The only clinical difference between those with and without typical pathological findings at presentation was age at biopsy and therefore it would seem

reasonable to consider these patients as one group. These results support the addition of a clinically-defined category to current and future diagnostic criteria and a relaxation of the current pathological criteria. This should lead to a significant increase in the number of patients eligible for research studies.

One of the main concerns over the use of clinical criteria as a basis for diagnosis has been that they may lack specificity leading to the misdiagnosis of patients with myopathies that may mimic IBM such as steroid-responsive inflammatory myopathies and MFM. Further analyses comparing the clinical features of patients with IBM and disease controls revealed that this is unlikely, as no controls studied had the characteristic pattern of weakness that is the hallmark of IBM. Although diagnostic criteria are useful in defining homogenous cohorts for research they are often impractical for everyday clinical use. An important finding from our results was demonstrating that a diagnosis of IBM can be made with confidence in the majority of patients without the need for specialist histological techniques or muscle imaging. A further benefit of clinical diagnostic criteria is the ease with which they can be re-assessed compared to pathological criteria which require further tissue samples. Although the clinical features were found to be highly sensitive and specific, our results do not render the histological assessment of IBM redundant. A small number of patients did not possess the necessary clinical features at presentation and the diagnosis was made on the pathological features present on muscle biopsy.

Over the last two decades many abnormally aggregated proteins have been described in IBM but results have been conflicting and not always substantiated between laboratories (Greenberg, 2009). Studies often lacked robust inclusion criteria or quantitative data and employed different histological techniques, making individual studies difficult to compare. Despite this, the pathological findings described in IBM have driven a number of different theories on the likely pathogenesis. The most widely publicised is that derived from the 'neurodegenerative' theory which states that proteins such as Aβ and tau accumulate in and damage muscle fibres. Despite a

lack of supporting evidence, the presence of neurodegenerative proteins in fibres in IBM led to the development of cellular and animal disease models. We hypothesised that protein aggregates may be better diagnostic markers than the current pathological features necessary for a diagnosis of IBM, and thus we sought to determine in a systematic manner, using a well-defined cohort of patients with IBM, which proteins warranted further investigation to complement or replace currently recommended pathological diagnostic features. We found p62, TDP-43, myotilin, ubiquitin and α B-crystallin positive protein aggregates in addition to widespread MHC Class I up-regulation in clinicopathologically definite IBM, suggesting that they may be of diagnostic use. p62 and α B-crystallin positive protein aggregates were identified in a greater number of fibres than TDP-43, myotilin or ubiquitin staining and also highlighted more abnormal fibres than those with pathological features included in the Griggs diagnostic criteria. Importantly, we found no evidence of Aβ, α-synuclein, tau, hyperphosphorylated tau, VCP or FUS positive protein aggregates. Thus, our findings question the purported role of classical neurodegenerative proteins in IBM.

We went on to compare cases of pathologically typical and atypical IBM and pathologically similar disease controls. We found that there was a spectrum of pathological changes in IBM and none of the pathological features described above had the necessary sensitivity and specificity required of a diagnostic marker. However, we have shown that the absence of increased MHC Class I, endomysial T-lymphocytes or macrophages and mitochondrial changes were strong evidence against a diagnosis of IBM. We found that most pathological features, except for MHC Class I and mitochondrial changes, were predominantly found in cases in which rimmed vacuoles were present. Therefore these findings, like rimmed vacuoles, are likely to be markers of longstanding disease rather than any primary pathology. Our results urge caution in drawing conclusions about the pathogenesis of IBM from findings only noted in pathologically typical cases.

The majority of studies in IBM have used IHC staining techniques to test hypotheses regarding the pathogenesis. Studies utilising alternative techniques to support the IHC findings are lacking. Taking advantage of technological progress in microscopic subcellular dissection and MS/MS protein analysis, we analysed the protein constituents of fibres containing rimmed vacuoles in IBM. We found no evidence of the classical neurodegenerative proteins described in IBM, supporting our IHC findings and conclusions that they are unlikely to be involved in the pathogenesis of IBM. Contrary to our IHC findings, we demonstrated that nuclear membrane protein lamin A/C is associated with rimmed vacuoles suggesting that rimmed vacuoles are derived from myonuclei. In support of this finding was the presence of aggresomal proteins including intermediate filaments and p62 in tissue samples of rimmed vacuoles These findings emphasise the need to confirm experimental findings using a second independent method, a measure that is absent in much of the IBM literature. The similarity in protein expression between IBM cases was such that a non-IBM case could be identified. This indicates that IBM may not be a 'promiscuous-proteinopathy' in which random proteins accumulate, but rather that it is associated with a particular 'protein signature'. Therefore, it may be possible in the future that MS/MS could contribute to the diagnosis of IBM.

7.2 Future directions

The clinical and pathological findings reported here need to be validated in a prospective study to confirm our observations that clinical examination findings are more useful than pathological findings in the diagnosis of IBM at presentation and to assess the utility of our pathological findings in diagnostic Neuropathology laboratories. Further areas include investigation of the pathogenesis of IBM by analysis of morphologically normal fibres using MS/MS and determination of the role that protein degradation may play.

7.2.1 Elucidation of the protein composition of 'normal' fibres in IBM

The use of laser capture microscopy and label-free MS/MS to analyse small structural abnormalities in IBM revealed that the protein composition of samples was consistent across the small number of cases studied. An important next step is to establish whether these findings are consistent across a larger group of patients.

Analysis of the protein composition of muscle fibres in IBM may help uncover the pathogenic mechanisms at work. However, this would require a different approach to the one adopted here in which structurally normal fibres were compared with structurally abnormal fibres. As has been shown, morphologically normal fibres in IBM are not normal. They express increased sarcolemmal and sarcoplasmic MHC Class I and may contain immunoreactive deposits. Studying 'normal' fibres could give an insight into the early pathogenic changes occurring in IBM. This would require control samples from normal healthy individuals. However, the effects that age, gender and even muscle sampled have on protein expression are currently unknown. This needs to be determined first in order that appropriate controls could be selected.

7.2.2 Altered protein synthesis or disordered degradation

Events leading to the formation of protein aggregates in IBM are uncertain. Protein aggregation may be due to reduced protein degradation or an increase in protein expression exceeding the fibres degradative capacity or a combination of both. The presence of protein aggregates in IBM was initially taken as evidence of failing or dysfunctional protein degradation. This was supported by the presence of autophagy related proteins and constituents of the ubiquitin-proteasomal system (Fratta et al., 2005)(D'Agostino et al., 2011). However, an increase in autophagic proteins may represent an increase in degradation rather than failing autophagy. Could an increase in protein expression overwhelm the degradation pathways causing protein aggregation? Two studies have failed to show either an increase in RNA or protein expression in IBM that would support this theory (Hutchinson and Jongbloed, 2008)(Parker et al., 2009b). It may be that minor abnormalities

in both protein degradation and synthesis are prerequisites for developing IBM. A further explanation for the development of protein aggregates in IBM is the production of abnormal degradation-resistant aggregation-prone proteins. Investigating a dynamic process such as autophagy has been problematic. Autophagic proteins are both produced and degraded during autophagy and autophagic degradation occurs rapidly. Therefore evaluation of their absolute quantity may lead to misinterpretation. More recently, assays to measure autophagic flux have been developed. These may more readily enable the study of autophagy and help elucidate whether altered autophagy may play a role IBM.

7.3 Concluding remarks

This thesis describes our current knowledge of the clinical presentation and pathological features of IBM. It confirms that IBM has a typical clinical presentation and disease progression. IHC and proteomic results reveal that the pathological findings in IBM constitute a spectrum and that strict adherence to pathological criteria may have led to some erroneous conclusions about the pathogenesis of IBM. The data included here will lead to greater confidence in the clinical diagnosis and as a result inclusion of increased numbers of patients in future studies and a reassessment of our understanding of the pathogenesis of IBM.

REFERENCES

Albrecht, S., and Bilbao, J.M. (1993). Ubiquitin expression in inclusion body myositis. An immunohistochemical study. Arch. Pathol. Lab. Med. *117*, 789–793.

Amato, A.A., Barohn, R.J., Jackson, C.E., Pappert, E.J., Sahenk, Z., and Kissel, J.T. (1994). Inclusion body myositis: treatment with intravenous immunoglobulin. Neurology *44*, 1516–1518.

Amato, A.A., Gronseth, G.S., Jackson, C.E., Wolfe, G.I., Katz, J.S., Bryan, W.W., and Barohn, R.J. (1996). Inclusion body myositis: clinical and pathological boundaries. Ann. Neurol. *40*, 581–586.

Amemiya, K., Granger, R.P., and Dalakas, M.C. (2000). Clonal restriction of T-cell receptor expression by infiltrating lymphocytes in inclusion body myositis persists over time. Studies in repeated muscle biopsies. Brain *123*, 2030–2039.

Arahata, K., and Engel, A.G. (1984). Monoclonal antibody analysis of mononuclear cells in myopathies. I: Quantitation of subsets according to diagnosis and sites of accumulation and demonstration and counts of muscle fibers invaded by T cells. Ann. Neurol. *16*, 193–208.

Arahata, K., and Engel, A.G. (1986). Monoclonal antibody analysis of mononuclear cells in myopathies. III: Immunoelectron microscopy aspects of cell-mediated muscle fiber injury. Ann. Neurol. *19*, 112–125.

Arahata, K., and Engel, A.G. (1988a). Monoclonal antibody analysis of mononuclear cells in myopathies. IV: Cell-mediated cytotoxicity and muscle fiber necrosis. Ann. Neurol. *23*, 168–173.

Arahata, K., and Engel, A.G. (1988b). Monoclonal antibody analysis of mononuclear cells in myopathies. V: Identification and quantitation of T8+ cytotoxic and T8+ suppressor cells. Ann. Neurol. *23*, 493–499.

Askanas, V., and Engel, W.K. (2006). Inclusion-body myositis A myodegenerative conformational disorder associated with Aβ, protein misfolding, and proteasome inhibition. Neurology *66*, S39–S48.

Askanas, V., and Engel, W.K. (2008). Inclusion-body myositis: muscle-fiber molecular pathology and possible pathogenic significance of its similarity to Alzheimer's and Parkinson's disease brains. Acta Neuropathol. *116*, 583–595.

Askanas, V., Engel, W.K., and Alvarez, R.B. (1992a). Light and electron microscopic localization of beta-amyloid protein in muscle biopsies of patients with inclusion-body myositis. Am. J. Pathol. *141*, 31–36.

Askanas, V., Engel, W.K., Alvarez, R.B., and Glenner, G.G. (1992b). beta-Amyloid protein immunoreactivity in muscle of patients with inclusion-body myositis. Lancet *339*, 560–561.

Askanas, V., Engel, W.K., and Alvarez, R.B. (1992c). Strong immunoreactivity of beta-amyloid precursor protein, including the beta-amyloid protein sequence, at human neuromuscular junctions. Neurosci. Lett. *143*, 96–100.

Askanas, V., Serdaroglu, P., Engel, W.K., and Alvarez, R.B. (1992d). Immunocytochemical localization of ubiquitin in inclusion body myositis allows its light-microscopic distinction from polymyositis. Neurology *42*, 460–461.

Askanas, V., Bilak, M., Engel, W.K., Alvarez, R.B., Tomé, F., and Leclerc, A. (1993a). Prion protein is abnormally accumulated in inclusion-body myositis. Neuroreport *5*, 25–28.

Askanas, V., Engel, W.K., and Alvarez, R.B. (1993b). Enhanced detection of congo-red-positive amyloid deposits in muscle fibers of inclusion body myositis and brain of Alzheimer's disease using fluorescence technique. Neurology *43*, 1265–1267.

Askanas, V., Alvarez, R.B., and Engel, W.K. (1993c). beta-Amyloid precursor epitopes in muscle fibers of inclusion body myositis. Ann. Neurol. *34*, 551–560.

Askanas, V., Engel, W.K., Bilak, M., Alvarez, R.B., and Selkoe, D.J. (1994a). Twisted tubulofilaments of inclusion body myositis muscle resemble paired helical filaments of Alzheimer brain and contain hyperphosphorylated tau. Am. J. Pathol. *144*, 177–187.

Askanas, V., Engel, W.K., and Mirabella, M. (1994b). Idiopathic inflammatory myopathies: inclusion-body myositis, polymyositis, and dermatomyositis. Curr. Opin. Neurol. *7*, 448–456.

Askanas, V., Engel, W.K., Yang, C.C., Alvarez, R.B., Lee, V.M., and Wisniewski, T. (1998). Light and electron microscopic immunolocalization of presenilin 1 in abnormal muscle fibers of patients with sporadic inclusion-body myositis and autosomal-recessive inclusion-body myopathy. Am. J. Pathol. *152*, 889–895.

Askanas, V., Engel, W.K., Alvarez, R.B., McFerrin, J., and Broccolini, A. (2000). Novel immunolocalization of alpha-synuclein in human muscle of inclusion-body myositis, regenerating and necrotic muscle fibers, and at neuromuscular junctions. J. Neuropathol. Exp. Neurol. *59*, 592–598.

Ayala, Y.M., Misteli, T., and Baralle, F.E. (2008). TDP-43 regulates retinoblastoma protein phosphorylation through the repression of cyclin-dependent kinase 6 expression. Proc. Natl. Acad. Sci. U.S.A. *105*, 3785–3789.

Badrising, U.A., Maat-Schieman, M., van Duinen, S.G., et al. (2000). Epidemiology of inclusion body myositis in the Netherlands: a nationwide study. Neurology *55*, 1385–1387.

Badrising, U.A., Maat-Schieman, M.L.C., Ferrari, M.D., et al. (2002). Comparison of weakness progression in inclusion body myositis during treatment with methotrexate or placebo. Ann. Neurol. *51*, 369–372.

Badrising, U.A., Schreuder, G.M.T., Giphart, M.J., et al. (2004). Associations with autoimmune disorders and HLA class I and II antigens in inclusion body myositis. Neurology *63*, 2396–2398.

Badrising, U.A., Maat-Schieman, M.L.C., van Houwelingen, J.C., et al. (2005). Inclusion body myositis. Clinical features and clinical course of the disease in 64 patients. J. Neurol. *252*, 1448–1454.

Bancroft, J., Cook, H., and Turner, D. (1994). Manual of Histological Techniques and Their Diagnostic Application (Churchill Livingstone).

Banwell, B.L., and Engel, A.G. (2000). AlphaB-crystallin immunolocalization yields new insights into inclusion body myositis. Neurology *54*, 1033–1041.

Barohn, R.J., Amato, A.A., Sahenk, Z., Kissel, J.T., and Mendell, J.R. (1995). Inclusion body myositis: explanation for poor response to immunosuppressive therapy. Neurology *45*, 1302–1304.

Benjamin Larman, H., Salajegheh, M., Nazareno, R., et al. (2013). Cytosolic 5'-nucleotidase 1A autoimmunity in sporadic inclusion body myositis. Ann. Neurol. *73*, 408–418.

Benveniste, O., and Hilton-Jones, D. (2010). International Workshop on Inclusion Body Myositis held at the Institute of Myology, Paris, on 29 May 2009. Neuromuscular Disorders *20*, 414–421.

Benveniste, O., Guiguet, M., Freebody, J., et al. (2011). Long-term observational study of sporadic inclusion body myositis. Brain *134*, 3176–3184.

Beyenburg, S., Zierz, S., and Jerusalem, F. (1993). Inclusion body myositis: clinical and histopathological features of 36 patients. Clin. Investig. *71*, 351–361.

Bilak, M., Askanas, V., and Engel, W.K. (1993). Strong immunoreactivity of alpha 1-antichymotrypsin co-localizes with beta-amyloid protein and ubiquitin in vacuolated muscle fibers of inclusion-body myositis. Acta Neuropathol. *85*, 378–382.

Bjørkøy, G., Lamark, T., Brech, A., et al. (2005). p62/SQSTM1 forms protein aggregates degraded by autophagy and has a protective effect on huntingtin-induced cell death. J. Cell Biol. *171*, 603–614.

Blume, G., Pestronk, A., Frank, B., and Johns, D.R. (1997). Polymyositis with cytochrome oxidase negative muscle fibres. Early quadriceps weakness and poor response to immunosuppressive therapy. Brain *120*, 39–45.

Bohan, A., and Peter, J.B. (1975a). Polymyositis and dermatomyositis (first of two parts). N. Engl. J. Med. *292*, 344–347.

Bohan, A., and Peter, J.B. (1975b). Polymyositis and dermatomyositis (second of two parts). N. Engl. J. Med. *292*, 403–407.

Brady, S., Squier, W., and Hilton-Jones, D. (2013). Clinical assessment determines the diagnosis of inclusion body myositis independently of pathological features. J. Neurol. Neurosurg. Psychiatr. *84*, 1240-1246.

Calabrese, L.H., Mitsumoto, H., and Chou, S.M. (1987). Inclusion body myositis presenting as treatment-resistant polymyositis. Arthritis Rheum. *30*, 397–403.

Carpenter, S., Karpati, G., Heller, I., and Eisen, A. (1978). Inclusion body myositis: a distinct variety of idiopathic inflammatory myopathy. Neurology *28*, 8–17.

Chahin, N., and Engel, A.G. (2008). Correlation of muscle biopsy, clinical course, and outcome in PM and sporadic IBM. Neurology *70*, 418–424.

Chou, S.M. (1967). Myxovirus-like structures in a case of human chronic polymyositis. Science *158*, 1453–1455.

Chou, S.M. (1986). Inclusion body myositis: a chronic persistent mumps myositis? Hum. Pathol. *17*, 765–777.

Cui, J., Bai, X.-Y., Shi, S., Cui, S., Hong, Q., Cai, G., and Chen, X. (2012). Age-related changes in the function of autophagy in rat kidneys. Age *34*, 329–339.

D'Agostino, C., Nogalska, A., Engel, W.K., and Askanas, V. (2010). In sporadic inclusion-body myositis muscle fibres TDP-43-positive inclusions are less frequent and robust than p62-inclusions, and are not associated with paired helical filaments. Neuropathol. Appl. Neurobiol. *37*, 315-320.

D'Agostino, C., Nogalska, A., Cacciottolo, M., Engel, W.K., and Askanas, V. (2011). Abnormalities of NBR1, a novel autophagy-associated protein, in muscle fibers of sporadic inclusion-body myositis. Acta Neuropathol. *122*, 627–636.

Dahlbom, K., Lindberg, C., and Oldfors, A. (2002). Inclusion body myositis: morphological clues to correct diagnosis. Neuromuscul. Disord. *12*, 853–857.

Dalakas, M.C. (1991). Polymyositis, dermatomyositis and inclusion-body myositis. N. Engl. J. Med. *325*, 1487–1498.

Dalakas, M.C. (2006). Sporadic inclusion body myositis--diagnosis, pathogenesis and therapeutic strategies. Nat. Clin. Pract. Neurol. *2*, 437–447.

Dalakas, M.C., Sonies, B., Dambrosia, J., Sekul, E., Cupler, E., and Sivakumar, K. (1997). Treatment of inclusion-body myositis with IVIg: a double-blind, placebo-controlled study. Neurology *48*, 712–716.

Dalakas, M.C., Rakocevic, G., Schmidt, J., et al. (2009). Effect of Alemtuzumab (CAMPATH 1-H) in patients with inclusion-body myositis. Brain *132*, 1536–1544.

De Bleecker, J.L., Engel, A.G., and Ertl, B.B. (1996). Myofibrillar myopathy with abnormal foci of desmin positivity. II. Immunocytochemical analysis reveals accumulation of multiple other proteins. J. Neuropathol. Exp. Neurol. *55*, 563–577.

Deeks, J.J., and Altman, D.G. (2004). Diagnostic tests 4: likelihood ratios. BMJ *329*, 168–169.

De Paepe, B., Creus, K.K., and De Bleecker, J.L. (2008). Chemokines in idiopathic inflammatory myopathies. Front. Biosci. *13*, 2548–2577.

Ding, W.-X., Ni, H.-M., Gao, W., Yoshimori, T., Stolz, D.B., Ron, D., and Yin, X.-M. (2007). Linking of autophagy to ubiquitin-proteasome system is important for the regulation of endoplasmic reticulum stress and cell viability. Am. J. Pathol. *171*, 513–524.

Doppler, K., Lindner, A., Schütz, W., Schütz, M., and Bornemann, A. (2012). Gain and loss of extracellular molecules in sporadic inclusion body myositis and polymyositis - a proteomics-based study. Brain Pathol. *22*, 32-40.

Dubourg, O., Wanschitz, J., Maisonobe, T., Béhin, A., Allenbach, Y., Herson, S., and Benveniste, O. (2011). Diagnostic value of markers of muscle degeneration in sporadic inclusion body myositis. Acta. Myol. *30*, 103–108.

Emslie-Smith, A.M., Arahata, K., and Engel, A.G. (1989). Major histocompatibility complex class I antigen expression, immunolocalization of interferon subtypes, and T cell-mediated cytotoxicity in myopathies. Hum. Pathol. *20*, 224–231.

Engel, A.G., and Arahata, K. (1984). Monoclonal antibody analysis of mononuclear cells in myopathies. II: Phenotypes of autoinvasive cells in polymyositis and inclusion body myositis. Ann. Neurol. *16*, 209–215.

Felice, K.J., and North, W.A. (2001). Inclusion body myositis in Connecticut: observations in 35 patients during an 8-year period. Medicine *80*, 320–327.

Ferrer, I., Martín, B., Castaño, J.G., Lucas, J.J., Moreno, D., and Olivé, M. (2004). Proteasomal expression, induction of immunoproteasome subunits, and local MHC class I presentation in myofibrillar myopathy and inclusion body myositis. J. Neuropathol. Exp. Neurol. *63*, 484–498.

Fleiss, J.L. (1981). Statistical methods for rates and proportions (John Wiley).

Fratta, P., Engel, W.K., McFerrin, J., Davies, K.J.A., Lin, S.W., and Askanas, V. (2005). Proteasome inhibition and aggresome formation in sporadic inclusion-body myositis and in amyloid-beta precursor protein-overexpressing cultured human muscle fibers. Am. J. Pathol. *167*, 517–526.

García-Mata, R., Bebök, Z., Sorscher, E.J., and Sztul, E.S. (1999). Characterization and dynamics of aggresome formation by a cytosolic GFP-chimera. J. Cell Biol. *146*, 1239–1254.

Garlepp, M.J., Laing, B., Zilko, P.J., Ollier, W., and Mastaglia, F.L. (1994). HLA associations with inclusion body myositis. Clin. Exp. Immunol. *98*, 40–45.

Gayathri, N., Anisya-Vasanth, Veerendra Kumar, M., et al. (2000). Inclusion body myositis (IBM). Clin. Neuropathol. *19*, 13–20.

Greenberg, S.A. (2009). How citation distortions create unfounded authority: analysis of a citation network. BMJ *339*, b2680.

Greenberg, S.A. (2010). Theories of the Pathogenesis of Inclusion Body Myositis. Current Rheumatology Reports *12*, 221–228.

Greenberg, S.A., Sanoudou, D., Haslett, J.N., Kohane, I.S., Kunkel, L.M., Beggs, A.H., and Amato, A.A. (2002). Molecular profiles of inflammatory myopathies. Neurology *59*, 1170–1182.

Greenberg, S.A., Bradshaw, E.M., Pinkus, J.L., et al. (2005). Plasma cells in muscle in inclusion body myositis and polymyositis. Neurology *65*, 1782–1787.

Greenberg, S.A., Pinkus, J.L., and Amato, A.A. (2006). Nuclear membrane proteins are present within rimmed vacuoles in inclusion-body myositis. Muscle Nerve *34*, 406–416.

Griggs, R.C., Askanas, V., DiMauro, S., Engel, A., Karpati, G., Mendell, J.R., and Rowland, L.P. (1995). Inclusion body myositis and myopathies. Ann. Neurol. *38*, 705–713.

Grumati, P., Coletto, L., Sabatelli, P., et al. (2010). Autophagy is defective in collagen VI muscular dystrophies, and its reactivation rescues myofiber degeneration. Nat. Med. *16*, 1313–1320.

Harding, H.P., Zhang, Y., and Ron, D. (1999). Protein translation and folding are coupled by an endoplasmic-reticulum-resident kinase. Nature *397*, 271–274.

Harding, H.P., Zhang, Y., Bertolotti, A., Zeng, H., and Ron, D. (2000). Perk is essential for translational regulation and cell survival during the unfolded protein response. Mol. Cell *5*, 897–904.

Hengstman, G.J.D., and van Engelen, B.G.M. (2004). Polymyositis, invasion of non-necrotic muscle fibres, and the art of repetition. BMJ *329*, 1464–1467.

Hernandez Lain, A., Millecamps, S., Dubourg, O., et al. (2011). Abnormal TDP-43 and FUS proteins in muscles of sporadic IBM: similarities in a TARDBP-linked ALS patient. Journal of Neurology, Neurosurgery & Psychiatry *82*, 1414 –1416.

Hershko, A., and Ciechanover, A. (1998). The ubiquitin system. Annu. Rev. Biochem. *67*, 425–479.

Hilton-Jones, D., Miller, A., Parton, M., Holton, J., Sewry, C., and Hanna, M.G. (2010). Inclusion body myositis: MRC Centre for Neuromuscular Diseases, IBM workshop, London, 13 June 2008. Neuromuscul. Disord. *20*, 142–147.

Hughes, J.T., and Esiri, M.M. (1975). Ultrastructural studies in human polymyositis. Journal of the Neurological Sciences *25*, 347–360.

Hutchinson, D.O., and Jongbloed, B. (2008). Two-dimensional gel electrophoresis in inclusion body myositis. J. Clin. Neurosci. *15*, 440–444.

Isenberg, D.A., Rowe, D., Shearer, M., Novick, D., and Beverley, P.C. (1986). Localization of interferons and interleukin 2 in polymyositis and muscular dystrophy. Clin. Exp. Immunol. *63*, 450–458.

Jerusalem, F., Baumgartner, G., and Wyler, R. (1972). Virus-like inclusions in chronic neuromuscular disorders. Electronmicroscopic findings of 2 cases. Arch. Psychiatr. Nervenkr. *215*, 148–166.

Johnston, J.A., Ward, C.L., and Kopito, R.R. (1998). Aggresomes: a cellular response to misfolded proteins. J. Cell Biol. *143*, 1883–1898.

Kaganovich, D., Kopito, R., and Frydman, J. (2008). Misfolded proteins partition between two distinct quality control compartments. Nature *454*, 1088–1095.

Kannanayakal, T.J., Mendell, J.R., and Kuret, J. (2008). Casein kinase 1 alpha associates with the tau-bearing lesions of inclusion body myositis. Neurosci. Lett. *431*, 141–145.

Karpati, G., Pouliot, Y., and Carpenter, S. (1988). Expression of immunoreactive major histocompatibility complex products in human skeletal muscles. Ann. Neurol. *23*, 64–72.

Kawaguchi, Y., Kovacs, J.J., McLaurin, A., Vance, J.M., Ito, A., and Yao, T.P. (2003). The deacetylase HDAC6 regulates aggresome formation and cell viability in response to misfolded protein stress. Cell *115*, 727–738.

Kim, C., Srivastava, S., Rice, M., et al. (2011). Expression of human amyloid precursor protein in the skeletal muscles of Drosophila results in age- and activity-dependent muscle weakness. BMC Physiol. *11*, 7.

Kim, I., Rodriguez-Enriquez, S., and Lemasters, J.J. (2007). Selective degradation of mitochondria by mitophagy. Archives of Biochemistry and Biophysics *462*, 245–253.

Kitamoto, T., Ogomori, K., Tateishi, J., and Prusiner, S.B. (1987). Formic acid pretreatment enhances immunostaining of cerebral and systemic amyloids. Lab. Invest. *57*, 230–236.

Kitazawa, M., Trinh, D.N., and LaFerla, F.M. (2008). Inflammation induces tau pathology in inclusion body myositis model via glycogen synthase kinase-3beta. Ann. Neurol. *64*, 15–24.

Kley, R.A., Maerkens, A., Leber, Y., et al. (2013). A combined laser microdissection and mass spectrometry approach reveals new disease relevant proteins accumulating in aggregates of filaminopathy patients. Mol. Cell Proteomics *12*, 215–227.

Koffman, B.M., Sivakumar, K., Simonis, T., Stroncek, D., and Dalakas, M.C. (1998). HLA allele distribution distinguishes sporadic inclusion body myositis from hereditary inclusion body myopathies. J. Neuroimmunol. *84*, 139–142.

Kopito, R.R. (2000). Aggresomes, inclusion bodies and protein aggregation. Trends Cell Biol. *10*, 524–530.

Küsters, B., van Hoeve, B.J.A., Schelhaas, H.J., Ter Laak, H., van Engelen, B.G.M., and Lammens, M. (2009). TDP-43 accumulation is common in myopathies with rimmed vacuoles. Acta Neuropathol. *117*, 209–211.

Lampe, J.B., Gossrau, G., Kempe, A., et al. (2003). Analysis of HLA class I and II alleles in sporadic inclusion-body myositis. J. Neurol. *250*, 1313–1317.

Leff, R.L., Miller, F.W., Hicks, J., Fraser, D.D., and Plotz, P.H. (1993). The treatment of inclusion body myositis: a retrospective review and a randomized, prospective trial of immunosuppressive therapy. Medicine *72*, 225–235.

Li, B., Lei, Z., Lichty, B.D., Li, D., Zhang, G.-M., Feng, Z.-H., Wan, Y., and Huang, B. (2010). Autophagy facilitates major histocompatibility complex class I expression induced by IFN-γ in B16 melanoma cells. Cancer Immunol. Immunother. *59*, 313–321.

Li, J., Yin, C., Okamoto, H., et al. (2006). Proteomic analysis of inclusion body myositis. J. Neuropathol. Exp. Neurol. *65*, 826–833.

Lindberg, C., Persson, L.I., Björkander, J., and Oldfors, A. (1994). Inclusion body myositis: clinical, morphological, physiological and laboratory findings in 18 cases. Acta Neurol. Scand. *89*, 123–131.

Lindberg, C., Oldfors, A., and Tarkowski, A. (1995). Local T-cell proliferation and differentiation in inflammatory myopathies. Scand. J. Immunol. *41*, 421–426.

Lindberg, C., Trysberg, E., Tarkowski, A., and Oldfors, A. (2003). Anti-T-lymphocyte globulin treatment in inclusion body myositis: a randomized pilot study. Neurology *61*, 260–262.

Lotz, B.P., Engel, A.G., Nishino, H., Stevens, J.C., and Litchy, W.J. (1989). Inclusion body myositis. Observations in 40 patients. Brain *112 (Pt 3)*, 727–747.

Lübke, U., Six, J., Villanova, M., et al. (1994). Microtubule-associated protein tau epitopes are present in fiber lesions in diverse muscle disorders. Am. J. Pathol. *145*, 175–188.

Lundberg, I., Ulfgren, A.K., Nyberg, P., Andersson, U., and Klareskog, L. (1997). Cytokine production in muscle tissue of patients with idiopathic inflammatory myopathies. Arthritis Rheum. *40*, 865–874.

Lünemann, J.D., Schmidt, J., Schmid, D., Barthel, K., Wrede, A., Dalakas, M.C., and Münz, C. (2007). Beta-amyloid is a substrate of autophagy in sporadic inclusion body myositis. Ann. Neurol. *61*, 476–483.

Maere, S., Heymans, K., and Kuiper, M. (2005). BiNGO: a Cytoscape plugin to assess overrepresentation of Gene Ontology categories in Biological Networks. Bioinformatics *21*, 3448–3449.

Marconi, G., Ronchi, O., and Taiuti, R. (1982). Polymyositis with severe distal muscular involvement. Acta Neurol. *4*, 340–346.

Masiero, E., Agatea, L., Mammucari, C., et al. (2009). Autophagy is required to maintain muscle mass. Cell Metab. *10*, 507–515.

Matsubara, S., and Tanabe, H. (1982). Hereditary distal myopathy with filamentous inclusions. Acta Neurol. Scand. *65*, 363–368.

Maurage, C.-A., Bussière, T., Sergeant, N., et al. (2004). Tau aggregates are abnormally phosphorylated in inclusion body myositis and have an immunoelectrophoretic profile distinct from other tauopathies. Neuropathol. Appl. Neurobiol. *30*, 624–634.

Mendell, J.R., Sahenk, Z., Gales, T., and Paul, L. (1991). Amyloid filaments in inclusion body myositis. Novel findings provide insight into nature of filaments. Arch. Neurol. *48*, 1229–1234.

Mhiri, C., and Gherardi, R. (1990). Inclusion body myositis in French patients. A clinicopathological evaluation. Neuropathol. Appl. Neurobiol. *16*, 333–344.

Mirabella, M., Alvarez, R.B., Bilak, M., Engel, W.K., and Askanas, V. (1996). Difference in expression of phosphorylated tau epitopes between sporadic inclusion-body myositis and hereditary inclusion-body myopathies. J. Neuropathol. Exp. Neurol. *55*, 774–786.

Moraes, C.T., Ricci, E., Bonilla, E., DiMauro, S., and Schon, E.A. (1992). The mitochondrial tRNA(Leu(UUR)) mutation in mitochondrial encephalomyopathy, lactic acidosis, and strokelike episodes (MELAS): genetic, biochemical, and morphological correlations in skeletal muscle. Am. J. Hum. Genet. *50*, 934–949.

Moslemi, A.R., Lindberg, C., and Oldfors, A. (1997). Analysis of multiple mitochondrial DNA deletions in inclusion body myositis. Hum. Mutat. *10*, 381–386.

Murakami, N., Ihara, Y., and Nonaka, I. (1995). Muscle fiber degeneration in distal myopathy with rimmed vacuole formation. Acta Neuropathol. *89*, 29–34.

Muscle Study Group (2001). Randomized pilot trial of betaINF1a (Avonex) in patients with inclusion body myositis. Neurology *57*, 1566–1570.

Muscle Study Group (2004). Randomized pilot trial of high-dose betaINF-1a in patients with inclusion body myositis. Neurology *63*, 718–720.

Muth, I.E., Barthel, K., Bähr, M., Dalakas, M.C., and Schmidt, J. (2009). Proinflammatory cell stress in sporadic inclusion body myositis muscle: overexpression of alphaB-crystallin is associated with amyloid precursor protein and accumulation of beta-amyloid. J. Neurol. Neurosurg. Psychiatr. *80*, 1344–1349.

Nagaraju, K., Casciola-Rosen, L., Lundberg, I., et al. (2005). Activation of the endoplasmic reticulum stress response in autoimmune myositis: potential role in muscle fiber damage and dysfunction. Arthritis Rheum. *52*, 1824–1835.

Nakano, S., Shinde, A., Fujita, K., Ito, H., and Kusaka, H. (2008). Histone H1 is released from myonuclei and present in rimmed vacuoles with DNA in inclusion body myositis. Neuromuscul. Disord. *18*, 27–33.

Nalbantoglu, J., Karpati, G., and Carpenter, S. (1994). Conspicuous accumulation of a single-stranded DNA binding protein in skeletal muscle fibers in inclusion body myositis. Am. J. Pathol. *144*, 874–882.

Needham, M., and Mastaglia, F.L. (2007). Inclusion body myositis: current pathogenetic concepts and diagnostic and therapeutic approaches. Lancet Neurol. *6*, 620–631.

Needham, M., James, I., Corbett, A., Day, T., Christiansen, F., Phillips, B., and Mastaglia, F.L. (2008a). Sporadic inclusion body myositis: phenotypic variability and influence of HLA-DR3 in a cohort of 57 Australian cases. J. Neurol. Neurosurg. Psychiatr. *79*, 1056–1060.

Needham, M., Corbett, A., Day, T., Christiansen, F., Fabian, V., and Mastaglia, F.L. (2008b). Prevalence of sporadic inclusion body myositis and factors contributing to delayed diagnosis. J. Clin. Neurosci. *15*, 1350–1353.

Nesvizhskii, A.I., and Aebersold, R. (2005). Interpretation of Shotgun Proteomic Data The Protein Inference Problem. Mol. Cell Proteomics *4*, 1419–1440.

Neumann, M., Sampathu, D.M., Kwong, L.K., et al. (2006). Ubiquitinated TDP-43 in frontotemporal lobar degeneration and amyotrophic lateral sclerosis. Science *314*, 130–133.

Nishii, M., Nakano, S., Nakamura, S., Wate, R., Shinde, A., Kaneko, S., and Kusaka, H. (2011). Myonuclear breakdown in sporadic inclusion body myositis is accompanied by DNA double strand breaks. Neuromuscul. Disord. *21*, 345–352.

Nishino, H., Engel, A.G., and Rima, B.K. (1989). Inclusion body myositis: the mumps virus hypothesis. Ann. Neurol. *25*, 260–264.

Nogalska, A., Wojcik, S., King Engel, W., McFerrin, J., and Askanas, V. (2007). Endoplasmic reticulum stress induces myostatin precursor protein and NF-κB in cultured human muscle fibers: Relevance to inclusion body myositis. Experimental Neurology *204*, 610–618.

Nogalska, A., Terracciano, C., D'Agostino, C., King Engel, W., and Askanas, V. (2009). p62/SQSTM1 is overexpressed and prominently accumulated in inclusions of sporadic inclusion-body myositis muscle fibers, and can help differentiating it from polymyositis and dermatomyositis. Acta Neuropathol. *118*, 407–413.

Oldfors, A., Moslemi, A.R., Fyhr, I.M., Holme, E., Larsson, N.G., and Lindberg, C. (1995). Mitochondrial DNA deletions in muscle fibers in inclusion body myositis. J. Neuropathol. Exp. Neurol. *54*, 581–587.

Oldfors, A., Moslemi, A.R., Jonasson, L., Ohlsson, M., Kollberg, G., and Lindberg, C. (2006). Mitochondrial abnormalities in inclusion-body myositis. Neurology *66*, S49–S55.

Olivé, M., Goldfarb, L., Moreno, D., et al. (2004). Desmin-related myopathy: clinical, electrophysiological, radiological, neuropathological and genetic studies. J. Neurol. Sci. *219*, 125–137.

Olivé, M., Goldfarb, L.G., Shatunov, A., Fischer, D., and Ferrer, I. (2005). Myotilinopathy: refining the clinical and myopathological phenotype. Brain *128*, 2315–2326.

Olivé, M., van Leeuwen, F.W., Janué, A., Moreno, D., Torrejón-Escribano, B., and Ferrer, I. (2008). Expression of mutant ubiquitin (UBB+1) and p62 in myotilinopathies and desminopathies. Neuropathol. Appl. Neurobiol. *34*, 76–87.

Olivé, M., Janué, A., Moreno, D., Gámez, J., Torrejón-Escribano, B., and Ferrer, I. (2009). TAR DNA-Binding protein 43 accumulation in protein aggregate myopathies. J. Neuropathol. Exp. Neurol. *68*, 262–273.

Oteruelo, F.T. (1976). Intranuclear inclusions in a myopathy of late onset. Virchows Arch. B Cell Pathol. *20*, 319–324.

Pankiv, S., Clausen, T.H., Lamark, T., et al. (2007). p62/SQSTM1 binds directly to Atg8/LC3 to facilitate degradation of ubiquitinated protein aggregates by autophagy. J. Biol. Chem. *282*, 24131–24145.

Parker, K.C., Kong, S.W., Walsh, R.J., et al. (2009a). Fast-twitch sarcomeric and glycolytic enzyme protein loss in inclusion body myositis. Muscle Nerve *39*, 739–753.

Parker, K.C., Walsh, R.J., Salajegheh, M., Amato, A.A., Krastins, B., Sarracino, D.A., and Greenberg, S.A. (2009b). Characterization of human skeletal muscle biopsy samples using shotgun proteomics. J. Proteome Res. *8*, 3265–3277.

Patterson, N.L., and Mintern, J.D. (2012). Intersection of autophagy with pathways of antigen presentation. Protein Cell *3*, 911–920.

Peng, A., Koffman, B.M., Malley, J.D., and Dalakas, M.C. (2000a). Disease progression in sporadic inclusion body myositis: Observations in 78 patients. Neurology *55*, 296 –298.

Peng, A., Koffman, B.M., Malley, J.D., and Dalakas, M.C. (2000b). Disease progression in sporadic inclusion body myositis: observations in 78 patients. Neurology *55*, 296–298.

Peng, A., Koffman, B.M., Malley, J.D., and Dalakas, M.C. (2000c). Disease progression in sporadic inclusion body myositis: observations in 78 patients. Neurology *55*, 296–298.

Pfeiffer, D (1998). Veterinary Epidemiology. An Introduction. Institute of Veterinary, Animal and Biomedical Sciences (Massey University).

Phillips, B.A., Cala, L.A., Thickbroom, G.W., Melsom, A., Zilko, P.J., and Mastaglia, F.L. (2001). Patterns of muscle involvement in inclusion body myositis: clinical and magnetic resonance imaging study. Muscle Nerve *24*, 1526–1534.

Pluk, H., van Hoeve, B.J.A., van Dooren, S.H.J., et al. (2013). Autoantibodies to cytosolic 5'-nucleotidase 1A in inclusion body myositis. Ann. Neurol. *73*, 397–407.

Prayson, R.A., and Cohen, M.L. (1997). Ubiquitin immunostaining and inclusion body myositis: study of 30 patients with inclusion body myositis. Hum. Pathol. *28*, 887–892.

Price, P., Santoso, L., Mastaglia, F., Garlepp, M., Kok, C.C., Allcock, R., and Laing, N. (2004). Two major histocompatibility complex haplotypes influence susceptibility to sporadic inclusion body myositis: critical evaluation of an association with HLA-DR3. Tissue Antigens *64*, 575–580.

Pruitt, J.N., Showalter, C.J., and Engel, A.G. (1996). Sporadic inclusion body myositis: counts of different types of abnormal fibers. Ann. Neurol. *39*, 139–143.

Prusiner, S.B., McKinley, M.P., Bowman, K.A., Bolton, D.C., Bendheim, P.E., Groth, D.F., and Glenner, G.G. (1983). Scrapie prions aggregate to form amyloid-like birefringent rods. Cell *35*, 349–358.

Rajakulendran, S., Parton, M., Holton, J.L., and Hanna, M.G. (2011). Clinical and pathological heterogeneity in late-onset partial merosin deficiency. Muscle Nerve *44*, 590–593.

Raju, R., Vasconcelos, O., Granger, R., and Dalakas, M.C. (2003). Expression of IFN-gamma-inducible chemokines in inclusion body myositis. J. Neuroimmunol. *141*, 125–131.

Rebolledo, D.L., Aldunate, R., Kohn, R., Neira, I., Minniti, A.N., and Inestrosa, N.C. (2011). Copper reduces Aβ oligomeric species and ameliorates neuromuscular synaptic defects in a C. elegans model of inclusion body myositis. J. Neurosci. *31*, 10149–10158.

Ringel, S.P., Kenny, C.E., Neville, H.E., Giorno, R., and Carry, M.R. (1987). Spectrum of inclusion body myositis. Arch. Neurol. *44*, 1154–1157.

Rojana-Udomsart, A., Bundell, C., James, I., et al. (2012). Frequency of autoantibodies and correlation with HLA-DRB1 genotype in sporadic inclusion body myositis (s-IBM): a population control study. J. Neuroimmunol. *249*, 66–70.

Rose, M.R., McDermott, M.P., Thornton, C.A., Palenski, C., Martens, W.B., and Griggs, R.C. (2001). A prospective natural history study of inclusion body myositis: implications for clinical trials. Neurology *57*, 548–550.

Rutkove, S.B., Parker, R.A., Nardin, R.A., Connolly, C.E., Felice, K.J., and Raynor, E.M. (2002). A pilot randomized trial of oxandrolone in inclusion body myositis. Neurology *58*, 1081–1087.

Safdar, A., Bourgeois, J.M., Ogborn, D.I., et al. (2011). Endurance exercise rescues progeroid aging and induces systemic mitochondrial rejuvenation in mtDNA mutator mice. Proc. Natl. Acad. Sci. U.S.A. *108*, 4135–4140.

Salajegheh, M., Pinkus, J.L., Nazareno, R., Amato, A.A., Parker, K.C., and Greenberg, S.A. (2009a). Nature of "Tau" immunoreactivity in normal myonuclei and inclusion body myositis. Muscle Nerve *40*, 520–528.

Salajegheh, M., Pinkus, J.L., Taylor, J.P., Amato, A.A., Nazareno, R., Baloh, R.H., and Greenberg, S.A. (2009b). Sarcoplasmic redistribution of nuclear TDP-43 in inclusion body myositis. Muscle Nerve *40*, 19–31.

Santorelli, F.M., Sciacco, M., Tanji, K., et al. (1996). Multiple mitochondrial DNA deletions in sporadic inclusion body myositis: a study of 56 patients. Ann. Neurol. *39*, 789–795.

Sarkozi, E., Askanas, V., Johnson, S.A., Engel, W.K., and Alvarez, R.B. (1993). beta-Amyloid precursor protein mRNA is increased in inclusion-body myositis muscle. Neuroreport *4*, 815–818.

Sato, T., Walker, D.L., Peters, H.A., Resse, H.H., and Chou, S.M. (1971). Chronic polymyositis and myxovirus-like inclusions. Electron microscopic and viral studies. Arch. Neurol. *24*, 409–418.

Sawchak, J.A., Kula, R.W. (1988). Polymyositis and dermatomyositis. 112-131.

Sayers, M.E., Chou, S.M., and Calabrese, L.H. (1992). Inclusion body myositis: analysis of 32 cases. J. Rheumatol. *19*, 1385–1389.

Schessl, J., Zou, Y., McGrath, M.J., et al. (2008). Proteomic identification of FHL1 as the protein mutated in human reducing body myopathy. J. Clin. Invest. *118*, 904–912.

Schubert, U., Antón, L.C., Gibbs, J., Norbury, C.C., Yewdell, J.W., and Bennink, J.R. (2000). Rapid degradation of a large fraction of newly synthesized proteins by proteasomes. Nature *404*, 770–774.

Sekul, E.A., and Dalakas, M.C. (1993). Inclusion body myositis: new concepts. Semin. Neurol. *13*, 256–263.

Sekul, E.A., Chow, C., and Dalakas, M.C. (1997). Magnetic resonance imaging of the forearm as a diagnostic aid in patients with sporadic inclusion body myositis. Neurology *48*, 863–866.

Selcen, D. (2011). Myofibrillar myopathies. Neuromuscul. Disord. *21*, 161–171.

Selcen, D., and Engel, A.G. (2003). Myofibrillar myopathy caused by novel dominant negative alpha B-crystallin mutations. Ann. Neurol. *54*, 804–810.

Selcen, D., and Engel, A.G. (2004). Mutations in myotilin cause myofibrillar myopathy. Neurology *62*, 1363–1371.

Sherriff, F.E., Joachim, C.L., Squier, M.V., and Esiri, M.M. (1995). Ubiquitinated inclusions in inclusion-body myositis patients are immunoreactive for cathepsin D but not [beta]-amyloid. Neuroscience Letters *194*, 37–40.

Spuler, S., and Engel, A.G. (1997). SMI-31 immunoreactivity in inclusion body myositis. Ann. Neurol. *42*, 815.

Sugarman, M.C., Yamasaki, T.R., Oddo, S., et al. (2002). Inclusion body myositis-like phenotype induced by transgenic overexpression of beta APP in skeletal muscle. Proc. Natl. Acad. Sci. U.S.A. *99*, 6334–6339.

Sundaram, M.B., and Ashenhurst, E.M. (1981). Polymyositis presenting with distal and asymmetrical weakness. Can. J. Neurol. Sci. *8*, 147–149.

Tawil, R., and Griggs, R.C. (2002). Inclusion body myositis. Curr. Opin. Rheumatol. *14*, 653–657.

Temiz, P., Weihl, C.C., and Pestronk, A. (2009). Inflammatory myopathies with mitochondrial pathology and protein aggregates. J. Neurol. Sci *278*, 25–29.

Terracciano, C., Nogalska, A., Engel, W.K., and Askanas, V. (2010). In AbetaPP-overexpressing cultured human muscle fibers proteasome inhibition enhances phosphorylation of AbetaPP751 and GSK3beta activation: effects mitigated by lithium and apparently relevant to sporadic inclusion-body myositis. J. Neurochem. *112*, 389–396.

Tsuruta, Y., Furuta, A., Furuta, K., Yamada, T., Kira, J., and Iwaki, T. (2001). Expression of the lysosome-associated membrane proteins in myopathies with rimmed vacuoles. Acta Neuropathol. *101*, 579–584.

Uyama, E., Uchino, M., Chateau, D., and Tomé, F.M. (1998). Autosomal recessive oculopharyngodistal myopathy in light of distal myopathy with rimmed vacuoles and oculopharyngeal muscular dystrophy. Neuromuscul. Disord. *8*, 119–125.

Van Deerlin, V.M., Leverenz, J.B., Bekris, L.M., et al. (2008). TARDBP mutations in amyotrophic lateral sclerosis with TDP-43 neuropathology: a genetic and histopathological analysis. Lancet Neurol. *7*, 409–416.

Van der Meulen, M.F., Hoogendijk, J.E., Jansen, G.H., Veldman, H., and Wokke, J.H. (1998). Absence of characteristic features in two patients with inclusion body myositis. J. Neurol. Neurosurg. Psychiatr. *64*, 396–398.

Van der Meulen, M.F., Hoogendijk, J.E., Moons, K.G., Veldman, H., Badrising, U.A., and Wokke, J.H. (2001). Rimmed vacuoles and the added value of SMI-31 staining in diagnosing sporadic inclusion body myositis. Neuromuscul. Disord. *11*, 447–451.

Vattemi, G., Engel, W.K., McFerrin, J., Buxbaum, J.D., Pastorino, L., and Askanas, V. (2001). Presence of BACE1 and BACE2 in muscle fibres of patients with sporadic inclusion-body myositis. Lancet *358*, 1962–1964.

Vattemi, G., Engel, W.K., McFerrin, J., and Askanas, V. (2003). Cystatin C colocalizes with amyloid-beta and coimmunoprecipitates with amyloid-beta precursor protein in sporadic inclusion-body myositis muscles. J. Neurochem. *85*, 1539–1546.

Vattemi, G., Engel, W.K., McFerrin, J., and Askanas, V. (2004). Endoplasmic Reticulum Stress and Unfolded Protein Response in Inclusion Body Myositis Muscle. The American Journal of Pathology *164*, 1–7.

Vattemi, G., Nogalska, A., King Engel, W., D'Agostino, C., Checler, F., and Askanas, V. (2009). Amyloid-beta42 is preferentially accumulated in muscle fibers of patients with sporadic inclusion-body myositis. Acta Neuropathol. *117*, 569–574.

Vershuuren, J.J., Engelen, B.G.M. van, J van der Hoeven, and Hoogendijk, J. (1997). Inclusion Body Myositis. In Diagnostic Criteria for Neuromuscular Disorders, 81–84.

Villanova, M., Kawai, M., Lübke, U., et al. (1993). Rimmed vacuoles of inclusion body myositis and oculopharyngeal muscular dystrophy contain amyloid precursor protein and lysosomal markers. Brain Res. *603*, 343–347.

De Visser, M., Bakker, E., Defesche, J.C., Bolhuis, P.A., and van Ommen, G.J. (1990). An unusual variant of Becker muscular dystrophy. Ann. Neurol. *27*, 578–581.

Vittorini, S., Paradiso, C., Donati, A., et al. (1999). The age-related accumulation of protein carbonyl in rat liver correlates with the age-related decline in liver proteolytic activities. J. Gerontol. *54*, B318–323.

Walter, M.C., Lochmüller, H., Toepfer, M., et al. (2000). High-dose immunoglobulin therapy in sporadic inclusion body myositis: a double-blind, placebo-controlled study. J. Neurol. *247*, 22–28.

Wanschit, J., Nakano, S., Goudeau, B., et al. (2002). Myofibrillar (desmin-related) myopathy: clinico-pathological spectrum in 3 cases and review of the literature. Clin. Neuropathol. *21*, 220–231.

Watanabe, Y., and Tanaka, M. (2011). p62/SQSTM1 in autophagic clearance of a non-ubiquitylated substrate. J. Cell Sci. *124*, 2692–2701.

Wedderburn, L.R., Varsani, H., Li, C.K.C., et al. (2007). International consensus on a proposed score system for muscle biopsy evaluation in patients with juvenile dermatomyositis: a tool for potential use in clinical trials. Arthritis Rheum. *57*, 1192–1201.

Weihl, C.C., and Pestronk, A. (2010). Sporadic inclusion body myositis: possible pathogenesis inferred from biomarkers. Curr. Opin. Neurol. *23*, 482–488.

Weihl, C.C., Temiz, P., Miller, S.E., et al. (2008). TDP-43 accumulation in inclusion body myopathy muscle suggests a common pathogenic mechanism with frontotemporal dementia. J. Neurol. Neurosurg. Psychiatr. *79*, 1186–1189.

Wigley, W.C., Fabunmi, R.P., Lee, M.G., Marino, C.R., Muallem, S., DeMartino, G.N., and Thomas, P.J. (1999). Dynamic association of proteasomal machinery with the centrosome. J. Cell Biol. *145*, 481–490.

Wullschleger, S., Loewith, R., and Hall, M.N. (2006). TOR signaling in growth and metabolism. Cell *124*, 471–484.

Yang, C.C., Askanas, V., Engel, W.K., and Alvarez, R.B. (1998). Immunolocalization of transcription factor NF-kappaB in inclusion-body myositis muscle and at normal human neuromuscular junctions. Neurosci. Lett. *254*, 77–80.

Yunis, E.J., and Samaha, F.J. (1971). Inclusion body myositis. Lab. Invest. *25*, 240–248.

Zimmermann, K., Herget, T., Salbaum, J.M., et al. (1988). Localization of the putative precursor of Alzheimer's disease-specific amyloid at nuclear envelopes of adult human muscle. EMBO J *7*, 367–372.

APPENDICES

A.1 COX solution

COX solution: 10 ml [A] + 50 mg [B] + 10 mg [C]

[A] 0.1 M Tris(hydroxymethyl)aminomethane (TRIS) pH 9.0 buffer (25 ml of 2.42 g TRIS in 100 ml in distilled water added to 2.5 ml of 1.7 ml hydrochloric acid in 100 ml distilled water).

[B] DAB

[C] Cytochrome c

A.2 SDH solution

SDH solution: 15 ml [A] + 15 ml [B] + 30 mg [C]

[A] PBS

[B] 0.2 M Sodium succinate (1.08 g sodium succinate in 20 ml of distilled water)

[C] Nitroblue tetrazolium chloride.

A.3 Differentially expressed unique proteins between samples

A.3.1 Decreased proteins in ST compared to N

Accession number	Protein
Q5VTT5	Myomesin-3
P12111	Collagen alpha-3(VI) chain
P08133	Annexin A6
P35573	Glycogen debranching enzyme
P49748	Very-long-chain specific acyl-CoA dehydrogenase
P12109	Collagen alpha-1(VI) chain
Q9GZV1	Ankyrin repeat domain-containing protein 2
P24752	Acetyl-CoA acetyltransferase
P22695	Ubiquinol-cytochrome-c reductase complex core protein 2
Q9Y277	Voltage-dependent anion-selective channel protein 3
P12277	Creatine kinase B-type
P15259	Phosphoglycerate mutase 2
P13639	Elongation factor 2
P50461	Cysteine and glycine-rich protein 3
Q9NZQ9	Tropomodulin-4
P30044	Peroxiredoxin-5
Q9Y2J8	Protein-arginine deiminase type-2
P49411	Elongation factor Tu
Q16851	UTP-glucose-1-phosphate uridylyltransferase
Q9UHQ9	NADH-cytochrome b5 reductase 1
P12110	Collagen alpha-2(VI) chain precursor
P11021	78 kDa glucose-regulated protein
P30084	Enoyl-CoA hydratase
Q05639	Elongation factor 1-alpha 2
O75947	ATP synthase D chain
P08758	Annexin A5
P54652	Heat shock-related 70 kDa protein 2
P24539	ATP synthase subunit b
P09382	Galectin-1
P22314	Ubiquitin-like modifier-activating enzyme 1
P55822	SH3 domain-binding glutamic acid-rich protein
Q13011	Delta(3,5)-Delta(2,4)-dienoyl-CoA isomerase
Q9NZU5	LIM and cysteine-rich domains protein 1
P46976	Glycogenin-1
Q5VXT5	Synaptophysin-like protein 2
O15273	Telethonin
Q5D862	Filaggrin-2
O95817	BAG family molecular chaperone regulator 3
P07237	Protein disulfide-isomerase
P28161	Glutathione S-transferase Mu 2
O75489	NADH dehydrogenase [ubiquinone] iron-sulfur protein 3

P13807	Glycogen synthase
P18859	ATP synthase-coupling factor 6
P61981	14-3-3 protein gamma
Q9H7C9	UPF0366 protein C11orf67
P09211	Glutathione S-transferase P
P62937	Peptidyl-prolyl cis-trans isomerase A
P07355	Annexin A2
P09622	Dihydrolipoyl dehydrogenase
P13073	Cytochrome c oxidase subunit 4 isoform 1
O14880	Microsomal glutathione S-transferase 3
P07737	Profilin-1
P08238	Heat shock protein HSP 90-beta
P21912	Succinate dehydrogenase [ubiquinone] iron-sulfur subunit
P07954	Fumarate hydratase
P10606	Cytochrome c oxidase subunit 5B
P14927	Cytochrome b-c1 complex subunit 7
Q00325	Phosphate carrier protein
Q02978	Mitochondrial 2-oxoglutarate/malate carrier protein
P24310	Cytochrome c oxidase polypeptide VIIa-heart
Q99623	Prohibitin-2
O14561	Acyl carrier protein
O75915	PRA1 family protein 3
P04080	Cystatin-B
P05387	60S acidic ribosomal protein P2
P10768	S-formylglutathione hydrolase
P11047	Laminin subunit gamma-1
Q8NDY3	[Protein ADP-ribosylarginine] hydrolase-like protein 1
O00151	PDZ and LIM domain protein 1
O14818	Proteasome subunit alpha type-7
O60888	Protein CutA
O75964	ATP synthase subunit g
P03905	NADH-ubiquinone oxidoreductase chain 4
P10599	Thioredoxin
P13693	Translationally-controlled tumor protein
P23528	Cofilin-1
P26641	Elongation factor 1-gamma
P47985	Ubiquinol-cytochrome c reductase iron-sulfur subunit
P50914	60S ribosomal protein L14
P51884	Lumican
P61026	Ras-related protein Rab-10
P62424	60S ribosomal protein L7a
P62942	Peptidyl-prolyl cis-trans isomerase FKBP1A
P68371	Tubulin beta-2C chain
P78417	Glutathione S-transferase omega-1
Q8TDC0	Myozenin-3

Q99436	Proteasome subunit beta type-7
Q9BXS1	Isopentenyl-diphosphate Delta-isomerase 2
Q9HCP6	Glycerol uptake/transporter homolog
Q86TD4	Sarcalumenin precursor
Q13423	NAD(P) transhydrogenase
Q9Y235	Probable C->U-editing enzyme APOBEC-2
P23109	AMP deaminase 1
Q9Y281	Cofilin-2
P38646	Stress-70 protein
P06744	Glucose-6-phosphate isomerase
P45880	Voltage-dependent anion-selective channel protein 2
P08107	Heat shock 70 kDa protein 1
P17174	Aspartate aminotransferase
Q99497	Protein DJ-1
P62258	14-3-3 protein epsilon
P08670	Vimentin
Q9UBF9	Myotilin
P21796	Voltage-dependent anion-selective channel protein 1
Q96HC4	PDZ and LIM domain protein 5
P55084	Trifunctional enzyme subunit beta
P11142	Heat shock cognate 71 kDa protein
Q99798	Aconitate hydratase
Q6ZMU5	Tripartite motif-containing protein 72
P00338	L-lactate dehydrogenase A chain
P06576	ATP synthase subunit beta
P36871	Phosphoglucomutase-1
P16615	Sarcoplasmic/endoplasmic reticulum calcium ATPase 2
Q15149	Plectin-1
P54296	Myomesin-2
P52179	Myomesin-1
P20929	Nebulin
Q8WZ42	Titin

Proteins listed are listed from the smallest ST SI to the largest and are 1.8 x less in ST than N with a p <0.05.
ST = Non-vacuolated sarcoplasm from fibres containing rimmed vacuoles; N = Sarcoplasm from morphologically normal fibres; SI = Spectral index.

A.3.2 Increased proteins in RV compared to ST

Accession number	Protein
Q8WZ42	Titin
P20929	Nebulin
Q15149	Plectin-1
P54296	Myomesin-2
P06576	ATP synthase subunit beta
P12111	Collagen alpha-3(VI) chain
P48681	Nestin
P36871	Phosphoglucomutase-1
Q5VTT5	Myomesin-3
Q99798	Aconitate hydratase
P16615	Sarcoplasmic/endoplasmic reticulum calcium ATPase 2
Q5VST9	Obscurin
P02545	Lamin-A/C
Q9UBF9	Myotilin
P08133	Annexin A6
P08670	Vimentin
P40939	Trifunctional enzyme subunit alpha
P35573	Glycogen debranching enzyme
Q6ZMU5	Tripartite motif-containing protein 72
P49748	Very-long-chain specific acyl-CoA dehydrogenase
Q14324	Myosin-binding protein C
P12109	Collagen alpha-1(VI) chain
O75923	Dysferlin
P21796	Voltage-dependent anion-selective channel protein 1
P08237	6-phosphofructokinase
P12277	Creatine kinase B-type
P17174	Aspartate aminotransferase
Q13423	NAD(P) transhydrogenase
P23109	AMP deaminase 1
Q09666	Neuroblast differentiation-associated protein AHNAK
P11021	78 kDa glucose-regulated protein
P38646	Stress-70 protein, mitochondrial
Q9Y277	Voltage-dependent anion-selective channel protein 3
Q86TD4	Sarcalumenin precursor
P24752	Acetyl-CoA acetyltransferase
Q9NPC6	Myozenin-2
Q9GZV1	Ankyrin repeat domain-containing protein 2
P08107	Heat shock 70 kDa protein 1
P02794	Ferritin heavy chain
O14958	Calsequestrin-2
Q08554	Desmocollin-1

P04083	Annexin A1
P13639	Elongation factor 2
P50461	Cysteine and glycine-rich protein 3
P22695	Ubiquinol-cytochrome-c reductase complex core protein 2
P08758	Annexin A5
Q9UHQ9	NADH-cytochrome b5 reductase 1
P04040	Catalase
P01009	Alpha-1-antitrypsin
Q9Y2J8	Protein-arginine deiminase type-2
O95817	BAG family molecular chaperone regulator 3
O75947	ATP synthase D chain
P62937	Peptidyl-prolyl cis-trans isomerase A
P09382	Galectin-1
P12110	Collagen alpha-2(VI) chain precursor
Q08188	Protein-glutamine gamma-glutamyltransferase E
Q13011	Delta(3,5)-Delta(2,4)-dienoyl-CoA isomerase
P18206	Vinculin
Q96AQ6	Pre-B-cell leukemia transcription factor-interacting protein 1
P02647	Apolipoprotein A-I
P08238	Heat shock protein HSP 90-beta
P62750	60S ribosomal protein L23a
Q9Y281	Cofilin-2
P01024	Complement C3
P15259	Phosphoglycerate mutase 2
P27816	Microtubule-associated protein 4
P38117	Electron transfer flavoprotein subunit beta
P55786	Puromycin-sensitive aminopeptidase
Q9NZQ9	Tropomodulin-4
Q9NZU5	LIM and cysteine-rich domains protein 1
P07355	Annexin A2
P13073	Cytochrome c oxidase subunit 4 isoform 1
P61981	14-3-3 protein gamma
P02679	Fibrinogen gamma chain
P07602	Proactivator polypeptide
P02675	Fibrinogen beta chain
P07237	Protein disulfide-isomerase
P07737	Profilin-1
P10768	S-formylglutathione hydrolase
P21912	Succinate dehydrogenase [ubiquinone] iron-sulfur subunit
Q02978	Mitochondrial 2-oxoglutarate/malate carrier protein
Q5BKX8	Muscle-related coiled-coil protein
P61978	Heterogeneous nuclear ribonucleoprotein K
O75489	NADH dehydrogenase [ubiquinone] iron-sulfur protein 3
P06748	Nucleophosmin
P13489	Ribonuclease inhibitor

P36542	ATP synthase gamma chain
P43155	Carnitine O-acetyltransferase
P81605	Dermcidin
Q8N335	Glycerol-3-phosphate dehydrogenase 1-like protein
P07900	Heat shock protein HSP 90-alpha
P10599	Thioredoxin
O60664	Mannose-6-phosphate receptor-binding protein 1
O75964	ATP synthase subunit g
P01876	Ig alpha-1 chain C region
P02656	Apolipoprotein C-III
P13693	Translationally-controlled tumor protein
P18859	ATP synthase-coupling factor 6
P22061	Protein-L-isoaspartate(D-aspartate) O-methyltransferase
P23528	Cofilin-1
P35232	Prohibitin
P42765	3-ketoacyl-CoA thiolase
P47755	F-actin capping protein subunit alpha-2
P47985	Ubiquinol-cytochrome c reductase iron-sulfur subunit
Q00325	Phosphate carrier protein
Q12988	Heat shock protein beta-3
Q13501	Sequestosome-1
Q96IX5	Up-regulated during skeletal muscle growth protein 5
Q99735	Microsomal glutathione S-transferase 2
Q9HCP6	Glycerol uptake/transporter homolog

Proteins listed are listed from the largest RV SI to the smallest and are 1.8 x greater in RV than ST with a $p < 0.05$.
RV = Rimmed vacuoles, their contents and the surrounding sarcoplasm; ST = Non-vacuolated sarcoplasm from fibres containing rimmed vacuoles; SI = Spectral index.

ACKNOWLEDGEMENTS

Firstly, I would like to thank my supervisors, Dr David Hilton-Jones, Dr Janice L. Holton and Dr Waney Squier, and Prof. Caroline Sewry for their support, advice, training and expertise, all of which have been invaluable. I am extremely grateful to the Muscular Dystrophy Campaign and the Myositis Support Group who funded this research. I would like to thank my colleagues at the Queen Square Brain Bank, Department of Neuropathology at the John Radcliffe Hospital and the Institute of Neurology. In particular, I would like to thank Louise Young, Janis Carter, Samantha Cragg, Kate Strand and Yasmine Asi. I would also like to thank Dr Matthias Vorgerd and Dr Katrin Marcus for inviting me to join their group at the Berufsgenossenschaftliches Universitätsklinikum Bergmannsheil and the Department of Functional Proteomics, Medizinisches Proteom-Center, Ruhr-Universität, Bochum, Germany and for making me feel so very welcome. I would like to say a special thank you to Dr Joanna Kitley for introducing me to open water swimming and without her much of this would not have been possible. The final thank you is to my parents, for without their unwavering support and sacrifice I would never have made it this far.